UNIVERSIDADE FEDERAL DO RIO DE JANEIRO
ESCOLA DE QUÍMICA

BRENNO CASTRILLON MENEZES

DOCTORATE EXAM

QUANTITATIVE METHODS FOR STRATEGIC INVESTMENT PLANNING IN THE OIL-REFINING INDUSTRY

Advisers:
Prof. Ricardo de Andrade Medronho, TPQB/EQ/UFRJ
Prof. Fernando Pellegrini Pessoa, TPQB/EQ/UFRJ

Co-Adviser:
Eng. Lincoln Fernando Lautenschlager Moro, AB-RE/TR/PR/PETROBRAS

August, 2014

Brenno Castrillon Menezes

QUANTITATIVE METHODS FOR STRATEGIC INVESTMENT PLANNING IN THE OIL-REFINING INDUSTRY

Tese de Doutorado apresentada ao Programa em Tecnologia de Processos Químicos e Bioquímicos, Escola de Química, Universidade Federal do Rio de Janeiro, como requisito parcial à obtenção do título de Doutor em Tecnologia de Proc Químicos e Bioquímicos.

Advisers:
Prof. Ricardo de Andrade Medronho, TPQB/EQ/UFRJ
Prof. Fernando Pellegrini Pessoa, TPQB/EQ/UFRJ

Co-Adviser:
Eng. Lincoln Fernando Lautenschlager Moro, AB-RE/TR/PR PETROBRAS

Rio de Janeiro
2014

FICHA CATALOGRÁFICA

Menezes, Brenno Castrillon.

Quantitative methods for strategic investment planning in the oil-refining industry

Brenno Castrillon Menezes. – 2014.
xviii, 183 f.: 51 il.

Tese (Doutorado em Tecnologia de Processos Químicos e Bioquímicos) – Universidade Federal do Rio de Janeiro, Escola de Química, Rio de Janeiro, 2014.

Orientadores: Ricardo Andrade Medronho, Fernando Luiz Pellegrini Pessoa, Lincoln Fernando L. Moro.

1. Strategic Planning. 2. Capital Investment Planning. 3. Process Design Synthesis. 4. Oil-Refining Industry. 5. Capacity Expansion. 6. Net Present Value. 7. Quantitative Methods. 8. Brazilian Oil-Refining Investments. I. Medronho, Ricardo A.; Pessoa, Fernando L. P.; Moro, Lincoln F .L. II. Universidade Federal do Rio de Janeiro, Escola de Química. III. Título.

Brenno Castrillon Menezes

QUANTITATIVE METHODS FOR STRATEGIC INVESTMENT PLANNING IN THE OIL-REFINING INDUSTRY

Tese de Doutorado apresentada ao Programa em Tecnologia de Processos Químicos e Bioquímicos, Escola de Química, Universidade Federal do Rio de Janeiro, como requisito parcial à obtenção do título de Doutor em Tecnologia de Proc Químicos e Bioquímicos.

Aprovada em

_____

Prof. Ricardo de Andrade Medronho, Ph.D., EQ/UFRJ (orientador)

_____

Prof. Fernando Luiz Pellegrini Pessoa, D.Sc., EQ/UFRJ (orientador)

_____

Lincoln Fernando Lautenschlager Moro, D.Sc., PETROBRAS/AB-RE (orientador)

_____

Prof. Eduardo Mach Queiroz, D.Sc., EQ/UFRJ

_____

Fabio dos Santos Liporace, D.Sc., PETROBRAS/CENPES

_____

Prof. Jose Vitor Bomtempo, D. Sc., EQ/UFRJ

_____

Marcel Joly, D.Sc., PETROBRAS/RECAP

_____

Marcus Vinicius Oliveira Magalhães, Ph.D., PETROBRAS/AB-PQ

Acknowledgements

First and foremost, I would like to thank Professors Ricardo de Andrade Medronho and Fernando Pellegrini Pessoa for being my advisors. As well as my colleague and co-adviser Lincoln Fernando L Moro.

At the same time, I would like to thank my committee members – Marcus Vinicius Magalhaes, Marcel Joly, Fabio Liporace, Jose Vitor Bomtempo and Eduardo March for their valuable feedback and the effort they spent in evaluating this work.

I had the pleasure to work with very supportive collaborators from Industrial Algorithms, Jeffrey Kelly and Alkis Vazacopoulos, who I would like to thank for freed me their Industrial Modeling & Programming Language (IMPL) software.

Special thanks to Professor Ignacio Grossmann and Jeffrey Kelly for their valuable advices and their insightful feedback.

I would also like to thank my friends for just being there whenever I needed them: Humberto Mandaro, Andre Assaf, Whei Oh Lin.

Most importantly, I would like to thank my love and my parents, Rosangela and Gilberto (in memoriam), and my brother Brunno for their love and continuous support.

Finally, I would like to thank PETROBRAS for financial support.

MENEZES, Brenno Castrillon. **Quantitative Methods for Strategic Investment Planning in the Oil-Refining Industry**. Rio de Janeiro, 2014. Tese (Doutorado em Tecnologia de Processos Químicos e Bioquímicos – Escola de Química, Universidade Federal do Rio de Janeiro, Rio de Janeiro, 2014.

ABSTRACT

Although investment optimization in crude oil-refining can be difficult to handle in a quantitative manner, the large amount of financial capital involved and the hydrocarbon processing and logistics complexity force the constant development of high performance strategic planning methodologies, thus reducing structural bottlenecks and idling in capacity and capability of equipment within tactical and operational decision-making levels. Besides, the today's narrow oil refining margin has further increased the need to improve the expansion, extension or installation of equipment within a framework of multiperiod and multisite to guarantee the sustainability of oil refining companies. Unlike traditional process design scenario- or simulation-based methodologies to construct complex oil-refinery processing framework, discrete optimization approaches are proposed in this work to solve the capital investment planning problem also known as assets or facilities planning. The unit capacity increments (expansion or installation) per type of oil-refinery unit are predicted over time considering resources such as capital and raw/intermediate material, processing and blending capabilities, market demands, and project constraints. The strategic investment model is integrated with the operational model from where hydrocarbon processing and blending nonlinearities can give rise to non-convex mixed integer nonlinear problems if a full space model is solved for the strategic and the operational levels simultaneously. Different modeling strategies to tackle the large scale and complex oil-refining assets expansion problem are addressed such as (i) the multisite aggregate capacity approach, (ii) the generalized capital investment planning (GCIP) model with project stages using sequence-dependent changeover concepts from production scheduling, and (iii) the phenomenological decomposition heuristic (PDH) to separate the integer/discrete and nonlinear variables. In terms of oil processing, two new distillation methods in a planning and scheduling environment are proposed. The first is an improved swing-cut modeling, which uses an interfacial property-based linear interpolation to predict quality corrections for the light (upper) and heavy (lower) swing-cut streams using the crude-oil assay distribution curves in pseudocomponents, hypotheticals or micro-cuts discretized into 10ºC increments for example. The second is the distillation curve adjustment or shifting modeling to optimize distillate

stream temperature cutpoints using monotonic interpolation. As cases of studying, this work analyzes the Brazilian fuel market and the chosen strategies in the recent cycle of expansion of the national oil-refining assets and proposes different investment portfolio to supply all market needs within this decade. To demonstrate the effectiveness of the proposed models, several industrial and Brazilian actual data are provided throughout the work.

Keywords: Strategic Planning, Capital Investment Planning, Capacity Planning, Oil-Refining Industry, Brazilian Fuel Market, Process Synthesis Design, Quantitative Methods.

MENEZES, Brenno Castrillon. **Quantitative Methods for Strategic Investment Planning in the Oil-Refining Industry**. Rio de Janeiro, 2014. Tese (Doutorado em Tecnologia de Processos Químicos e Bioquímicos – Escola de Química, Universidade Federal do Rio de Janeiro, Rio de Janeiro, 2014.

RESUMO

Embora a otimização de investimentos no refino de petróleo seja difícil de tratar de modo quantitativo, a grande soma de capital financeiro envolvido e complexidade de processamento e logística de hidrocarbonetos forçam o constante desenvolvimento de modelos estratégicos de alta eficiência, reduzindo, portanto, gargalos e inatividades estruturais na capacidade e habilidade dos equipamentos nos níveis de tomada de decisão táctico e operacional. Além disso, hoje, a reduzida margem de refino aumentou ainda mais a necessidade de melhoria do planejamento da expansão, extensão ou instalação de equipamentos em múltiplos períodos de tempo e múltiplas plantas para garantir a sustentabilidade das empresas de refino de petróleo. Diferente das tradicionais metodologias baseadas em cenários ou simulação de esquemas de produção para construir a complexa estrutura de refino de petróleo, modelos de otimização discreta são propostos neste trabalho para resolver o problema de planejamento de investimento de capital também conhecido como planejamento de ativos ou de instalações. Incrementos na capacidade (expansão ou instalação) por tipo de unidade de processo são encontrados ao longo do tempo considerando recursos como capital, matéria-prima e insumos, transformações de processamento e mistura, demandas de mercado e restrições de projeto. O modelo estratégico de investimento é integrado com o modelo operacional cujas não linearidades do processamento e mistura de hidrocarbonetos podem levar a problemas misto-inteiros não lineares se o modelo completo é resolvido para os níveis estratégico e operacional simultaneamente. Diferentes estratégias de modelagem para lidar com a grande escala e complexidade do problema de expansão de ativos de refino de petróleo são introduzidos como (i) o modelo de capacidade agregada de múltiplas plantas, (ii) o modelo genérico para planejamento de investimentos de capital (GCIP) incluindo estágio dos projetos usando conceitos de transição e sequência dependentes da programação da produção, e (iii) a heurística de decomposição fenomenológica (PDH) para separar as variáveis inteiras/discretas e não lineares. Em termos de processamento de petróleo, dois novos métodos de destilação em ambiente de planejamento e programação da produção são propostos. O primeiro é o modelo swing-cut (“corte balançante”) aprimorado, o qual usa uma interpolação linear interfacial baseada na propriedade para prever correções na

qualidade das correntes leve (de cima) e pesada (de baixo) do swing-cut usando curvas de distribuição do petróleo em pseudo-componentes, hypotheticals ou micro-cortes (micro-cuts) segmentados a cada 10ºC. O segundo é a modelagem do ajuste ou deslocamento da curva de destilação para otimizar temperaturas de cortes de correntes destiladas usando interpolação monotônica. Como casos de estudos, este trabalho analisa o mercado de combustíveis brasileiro e as estratégias escolhidas no recente ciclo de expansão dos ativos de refino nacional e propõe diferente portfólio de investimento para suprir todas as necessidades de mercado dentro desta década. Para demostrar a efetividade dos modelos propostos, vários dados reais do Brasil e da indústria são fornecidos ao longo do trabalho.

Palavras-Chave: Planejamento Estratégico, Planejamento de Investimento de Capital, Planejamento de Capacidade, Indústria de Refino de Petróleo, Mercado de Combustíveis Brasileiro, Síntese de Esquemas de Produção, Métodos Quantitativos.

INDEX

INDEX OF FIGURES

INDEX OF TABLES

LIST OF ACRONYMS

Units

CDU	crude distillation unit
CLNHT	coker light naphtha hydrotreating
DC	delayed coker
DCA	delayed coker with atmospheric residue as feed
D1HT	diesel hydrotreating (medium severity)
D2HT	diesel hydrotreating (high severity)
FCC	fluid catalytic cracking
HCC	hydrocracking
KHT	kerosene hydrotreating
LCNHT	light cracked naphtha hydrotreating
PDA	propane deasphalting unit
REF	reformer
RFCC	residue fluid catalytic cracking
ST	Stabilizer
VDU	vacuum distillation unit
Imports	
ETH	ethanol
GLN_{imp}	gasoline A imported (pure gasoline)
JET_{imp}	jet fuel imported
LSD_{imp}	light-sulfur diesel imported
LPG_{imp}	liquid petroleum gas imported
Products	
C1C2	fuel gas (FG)
C3C4	liquid petroleum gas (LPG)
COKE	coke
GLN	gasoline C (with ethanol)
FG	fuel gas
FO	fuel oil
H2	hydrogen
HSD	high sulfur diesel (1800 wppm S)
JFUEL	jet fuel
LGP	liquid petroleum gas
LSD	low sulfur diesel (10 wppm S)
MSD	medium sulfur diesel (500 wppm S)
PQN	petrochemical naphtha
USD	ultra sulfur diesel (3500 wppm S)
Streams	
ASPR	asphaltic residue
ATR	atmospheric residue
C3	propane
C3=	propene
C4	butane
C4=	butane
C1C2	fuel gas

C3C4	liquid petroleum gas
CLN	coker light naphtha
CLGO	coker light gasoil
CHN	coker heavy naphtha
CMGO	coker medium gasoil
CHGO	coker heavy gasoil
DAO	deasphalted oil
DO	decanted oil
FG	fuels gas
FHD	final heavy diesel
FK	final kerosene
FLD	final light diesel
FN	final naphtha
FO	fuel oil
GLN	gasoline
GOST	diesel from ST
HCCD	hydrocraked diesel
HCCK	hydrocraked kerosene
HCCN	hydrocraked naphta
HCCO	hydrocraked gasoil
HCN	heavy cracked naphtha
HD	heavy diesel
HNST	heavy naphtha from ST
HTCLN	hydrotreated coker light naphtha
HTD	hydrotreated diesel
HTK	hydrotreated kerosene
HTLCN	hydrotreated light cracked naphtha
HSD	heavy sulfur diesel
HVGO	heavy vacuum gasoil
JET	jet fuel
K	kerosene
LCN	light cracked naphtha
LCO	light cycle oil
LD	light diesel
LNST	light naphtha from ST
LSD	light sulfur diesel
LVGO	light vacuum gasoil
MSD	medium sulfur diesel
N	naphtha
REFOR	reformate
SW1	swing-cut 1
SW2	swing-cut 2
SW3	swing-cut 3
SW1L	light swing-cut 1
SW1H	heavy swing-cut 1
SW2L	light swing-cut 2
SW2H	heavy swing-cut 2
SW3L	light swing-cut 1

SW3H	heavy swing-cut 3
VDU	vacuum distillation tower
VGO	vacuum gasoil
VR	vacuum residue

Subscripts

c	cuts
cr	crude
fc	final-cuts
h	heavier final-cut
HT	hydrotreaters
i,j,m	operation mode
imp	imports
ℓ	lighter final-cut
mc	micro-cuts
p	products
s	streams
sw	swing-cut
t	investment time period
t_0	operational time period
u	units

Parameters

$A_{cr,c}$	crude assay acidity for each cut
α_u	variable cost for investment in units
β_u	fixed cost for investment in units
CI_t	capital investment in *t*
D01	ASTM D86 temperature at 01% evaporation
D10	ASTM D86 temperature at 10% evaporation
D30	ASTM D86 temperature at 30% evaporation
D50	ASTM D86 temperature at 50% evaporation
D70	ASTM D86 temperature at 70% evaporation
D90	ASTM D86 temperature at 90% evaporation
D99	ASTM D86 temperature at 99% evaporation
Δ_{HT}	specific gravity reduction in hydrotreaters (not for KHT)
F_{t_0}	factor to annualize the daily profit
$G_{cr,c}$	crude assay specific gravity for each cut
$G_{cr,mc}$	micro-cut specific-gravity (volume-based)
ir	interested rate
$M_{cr,mc}$	micro-cut mass-based property
pr	prices
π_{sc}	probability of scenario *sc*
QE_u^L	expansion lower bound
QE_u^U	expansion upper bound
QI_u^L	installation lower bound
QI_u^U	installation upper bound
Ref_{cost}	operational cost
$S_{cr,c}$	crude assay sulfur content for each cut

tr	taxes rate
$Y_{cr,c}$	crude assay yield for each cut
$Y_{cr,mc}$	micro-cut volume yield from a crude-oil assay
Y_s	yields for other oil-refinery unit not CDU/VDU
$V_{cr,mc}$	micro-cut volume-based property

Variables

A_c	cut acidity
A_{fc}	final-cut acidity
ARO_s	aromatic concentration of stream *s* (fixed for some units)
ARO_V	volume-based aromatic concentration
ARO_{VQ}	quadratic volume-based aromatic concentration
$DYNT01$	yield delta at 01% evaporation
$DYNT99$	yield delta at 99% evaporation
G_c	cut specific gravity
$G_{c,fc}$	cut to final-cut specific-gravity property
G_{fc}	final-cut specific gravity
G_{HT}	hydrotreaters feed specific gravity (also for units)
J_s	sensitivity of stream *s* (fixed for some units)
J_V	volume-based sensitivity
MON_s	motor octane number of stream *s* (fixed for some units)
$MONv$	volume-based motor octane number
$MONVv$	motor octane number blending value
MP_c	cut mass-based property
$MP_{c,fc}$	cut to final-cut mass-based property
MP_{fc}	final-cut property in mass basis
$MPI_{c,\ell}$	interface mass-based property between adjacent lighter cut and cut
$MPI_{c,h}$	interface mass-based property between cut and adjacent heavier cut
$NT01$	new TBP temperature at 01% evaporation
$NT10$	new TBP temperature at 10% evaporation
$NT30$	new TBP temperature at 30% evaporation
$NT50$	new TBP temperature at 50% evaporation
$NT70$	new TBP temperature at 70% evaporation
$NT90$	new TBP temperature at 90% evaporation
$NT99$	new TBP temperature at 99% evaporation
$NY01$	normalized yield at 01% evaporation
$NY10$	normalized yield at 10% evaporation
$NY30$	normalized yield at 30% evaporation
$NY50$	normalized yield at 50% evaporation
$NY70$	normalized yield at 70% evaporation
$NY90$	normalized yield at 90% evaporation
$NY99$	normalized yield at 99% evaporation
$OT01$	old TBP temperature at 01% evaporation
$OT10$	old TBP temperature at 10% evaporation
$OT30$	old TBP temperature at 30% evaporation
$OT50$	old TBP temperature at 50% evaporation
$OT70$	old TBP temperature at 70% evaporation

$OT90$	old TBP temperature at 90% evaporation
$OT99$	old TBP temperature at 99% evaporation
OLE_s	olefinic concentration of stream *s* (fixed for some units)
OLE_V	volume-based olefinic concentration
$Q_{cr,CDU}$	crude-oil flow to CDU
$Q_{c,fc}$	cut to final-cut flow
$Q_{u',s,u}$	transfer stream *s* from *u'* to *u*
$QC_{u,t}$	unit capacity
$QE_{u,t}$	unit expansion in *t*
$QI_{u,t}$	unit installation in *t*
QF_u	unit throughput (also for products)
QF_u	unit throughput
$QS_{u,s}$	output stream (product) from unit *u*
$RONs$	research octane number of stream *s* (fixed for some units)
$RONv$	volume-based research octane number
$RONVv$	motor octane number blending value
S_c	cut sulfur content
S_{fc}	final-cut sulfur content
S_{HT}	hydrotreater feed sulfur content (also for units)
$S_{HT,s}$	hydrotreater output *s* (also for units)
VP_c	cut volume-based property
$VP_{c,fc}$	cut to final-cut volume-based property
VP_{fc}	final-cut property in volume basis
$VPI_{c,\ell}$	interface volume-based property between adjacent lighter cut and cut
$VPI_{c,h}$	interface volume-based property between cut and adjacent heavier cut
υ_{cr}	crude diet
$ye_{u,t}$	binary variable to setup the expansion of the unit *u* in *t*
$yi_{u,t}$	binary variable to setup the installation of the unit *u* in *t*
$YNT01$	yield at 01% evaporation
$YNT99$	yield at 99% evaporation
Υ_{HT}	severity in hydrotreaters (not for KHT)
Others	
HDI	heavy diesel interface between HD and SW3-Cut
KLI	kerosene interface between SW1-Cut and K
KHI	kerosene interface between K and SW2-Cut
LDLI	light diesel interface between SW2-Cut and LD
LDHI	light diesel interface between LD and SW3-Cut
NI	naphtha interface between N and SW1-Cut

Chapter 1

1. Introduction

In oil-refining industry, fuels production and crude and fuels distribution can be optimized in mathematical programming approaches to determine strategic, tactical and operational settings in supply chains mainly constituted by refinery and terminal sites. However, in the strategic investment planning optimization to construct oil-refineries or oil and gas facilities, most methodologies are based on simulation of numerous scenarios, thus reducing the models to linear (LP) and nonlinear (NLP) problems where the set of material flows and operating conditions are optimized regarding the selected production and logistics frameworks.

On the other hand, mixed integer linear (MILP) and mixed integer nonlinear (MINLP) models are able to optimize discrete decisions such as tasks in scheduling problems and process design frameworks in strategic investment planning, where the set of process units or equipment to be invested considering expansion/extension of existing assets and installation of new ones are set up. To model a full space process design synthesis example by including continuous and discrete decisions and by taking into account nonlinearities from processing and blending relations, a non-convex MINLP model arises, in which convergence problems and model size escalation are the main drawbacks due to limitations in MINLP solvers; hence, reducing the application of this type of models in industrial-sized problems. Different strategies or routes to possibly overcome these challenges can be proposed such as simplification in mathematical formulation, multisite aggregation in capacity, MILP approximations, warm-start phase to generate initial values, and tailored decomposition schemes.

The strategic and operational planning approaches to design production scenarios or frameworks for the oil-refining facilities expansion, extension or installation problem as proposed in this work deal with more rigorous formulation than those used in general in a high-level decision-making analysis by considering mixed-integer models, crude dieting, processing transformations, blending, project staging, and multiperiod and multisite problem. The need to improve the strategic and tactical decision-making levels in order to address issues in a quantitative manner rather than the usual qualitative approaches is acknowledged

as very relevant by the industry and still remains an active area of research (Shapiro, 2001, 2004).

From the literature on global supply chains, the use of high performance strategic and tactical supply chain models may result in cost savings within 5–10% (Goetschalckx et al., 2002). Hence, high performance strategic and tactical models are a paramount towards to the global supply chain margin improvement that is even more important in the narrow oil refining margin situation worldwide.

We discuss in section 1.1 the strategic, tactical and operational decision-making levels structure within the oil-refining industry to introduce the main objectives in each level and how the strategic investment planning problem is formulated in this work. In section 1.2, the thesis outline and objectives are presented as well as the current and future thesis related works in congress and journals (10 in total).

1.1. Strategic, Tactical, and Operational Decision-Making Levels Structure in the Oil-Refining Industry

In modern process industry, production planning and scheduling better predict business activities dealing with investment, production, distribution, sales and inventory within the different decision-making levels (Kallrath, 2002; Grossmann, 2005; Grossmann, 2012). Based on an economic point of view, planning problems deal with high level decisions such as investment in new facilities, supply chain service and production amounts within the sites. The main objective is to maximize profit by deducing, from the revenue to be obtained from products sale, the costs related to raw/intermediate material purchase, investment, maintenance/turnaround, and manufacturing/logistics operations. On the contrary, in scheduling problems the cost minimization of tasks is the common objective given that material resources (raw, inputs, and intermediate streams) and product delivery scenarios are practically unchanged within the short-term (weeks, days, or hours) or, at least, the material consumption and production can be held in inventories within a short period of time to maintain the process despite of changes in premises such as tanks and pipelines inoperability and delays in deliveries. In scheduling, the disaggregation of structure, time and space, so different of planning, implies considering lower level decisions such as sequencing of manufacturing and logistics operations to fulfill a given number of orders or required tasks in a feasible and if possible optimal scenario, therefore optimizing the performance of the

operations. Hence, economics tends to play a greater role in planning than in scheduling (Grossmann et al., 2002).

Within the process industry decision-making framework, the strategic planning defines the investments considering the business sustainability in line with future market demands. The investment portfolio optimization considers the available resources such as raw material, inputs, plant processing scheme, and capital throughout the operations to supply market demands. From the strategic decisions up to the product deliveries to clients, the decision process begins with the strategic choices such investment in production facilities within a long-term horizon of several years, in which goals are in general defined (without imports, new refinery for a specific crude oil, etc.). In the medium level, tactical planning considers the available resources for a mid-term planning (semesters, quarters, months) and gives guidance to operate corporate decision which are used to define production levels and supply chain services, all to fulfill in a short-term the operational planning and scheduling decisions among both production and distribution centers, from a month- to a week-, day-, or an hour-basis.

To increase supply chain productivity and improve business responsiveness there is a need for efficient integrated approaches to reduce capital and operating costs (Papageorgiou, 2009). This can be achieved by considering hierarchical coordination and collaboration between the different levels of management (Kelly and Zyngier, 2008). However, there can be numerous trade-offs between the levels due to their interdependency throughout the supply chain, so to achieve optimal solutions, ideally, the decisions from the different levels should be made all together, albeit solution strategies as decomposition may be necessary to solve industrial-sized models.

Maravelias and Sung (2009) classified the solution strategies for the integrated planning-scheduling problem into three categories: hierarchical, iterative, and full space. Although their definition was made for operational planning and scheduling integration, it can be extended for all decision-making levels. In the hierarchical and iterative strategies it is implied the need of decomposition methods to solve a master (high-level) problem and a slave (low-level) problem. The former determines production targets or investment setups as an input to the latter, in which the details of the operational level either in planning or scheduling environment are performed. When the information flows only from the master to the slave problem, the methods are considered hierarchical. If there is a do-loop from the lower-level back to the master problem as a feedback procedure, then the methods are iterative. As

opposed to the decomposed methods, the full-space methods solve the decision-making levels simultaneously. Figure 1.1 shows the structure of the strategic, tactical, and operational decision-making levels within the oil-refining industry in which is marked the processing inside the refineries as a domain of the iteration between the strategic and operational levels proposed in this work. Optimization within the purchasing and procurement, distribution, and marketing and sales branches is not being addressed. Instead, the calculation of the strategic investment analysis are enforced within processing domain, which relies on operational planning or pre-scheduling snapshots (in cubic meter per day) in order to improve the net present value accuracy, avoid production inconsistences and smooth the processing-related uncertainties in the strategic level by better assessing the production.

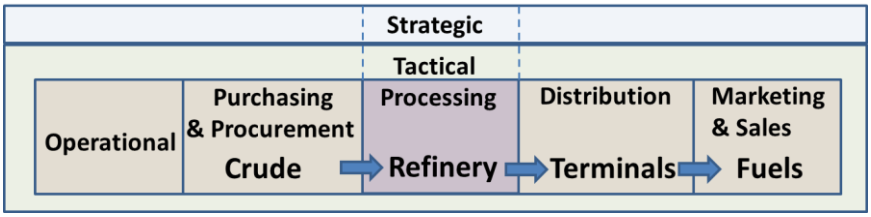

Figure 1.1. Strategic, tactical and operational decision-making levels within the oil-refining industry.

An optimal strategic formulation capable to incorporate the long-term investments in line with the mid- and short-term decisions needs to be developed upfront to achieve the expected performance within the lower levels. In a structural point of view, throughputs lower than the expanded/installed capacity, conversion lower than the extended capability and material balance bottlenecks must be avoided. Naturally, the integration among all levels by accounting for the spatial and temporal dimensions in a rigorous formulation leads to more precise models over the planning and scheduling decision in today's process. But, regards of model's size, rigor or integration, when the perfect equilibrium between accuracy and solvability is matched, its optimal formulation can be achieved.

The decision-making activities in crude oil and fuels supply chain within the downstream sector, when scaled in spatial and temporal dimensions and ranged in corporate and operational realms, can be outlined as in Figure 1.2. The off-line planning and scheduling tools used in PETROBRAS, the Brazilian state owned oil and energy company, is also presented to illustrate the portfolio of decision-making performed by one company. The level of details inside the models increases from the strategic to the operational level, since the trust in fulfilling the decisions becomes more critical due to the structural, time and/or spatial aggregation reduction. The size of the model is proportional to the integration degree among

the levels, uncertainty by considering scenarios, and spatial and temporal scales. Besides, it can be increased by the need to decompose the full space or monolithic model into separate or polylithic models to tackle industrial-sized problems in modeling and solution approaches in which mixed integer or non-convex nonlinear optimization problems are solved by tailor-made methods involving several models and/or algorithmic components, in which the solution of one model is input to another one (Kallrath, 2009, 2011).

In terms of modeling, the time representation generally is continuous when the model has to take decisions in a short time period, such as in real time optimization (RTO) and scheduling cases. In this direction, the level of details increases and the goals are set to the costs minimization highly constrained by fulfillment concerns. On the other hand, when the model takes into account the long-term strategic decisions, such as revamps, shutdowns, and framework modification, as those related to the capital investment planning, the time representation becomes discrete. A full review about the strategic, tactical and operational decision-making levels structure and considerations can be found in Shapiro (1998), Grossmann (2005), Stadtler (2005), Shah (2005) and Varma et al. (2007), and a strategic and tactical (and operational as our point of view) planning models review within the crude oil supply chain context was recently published by Sahebi et al. (2014).

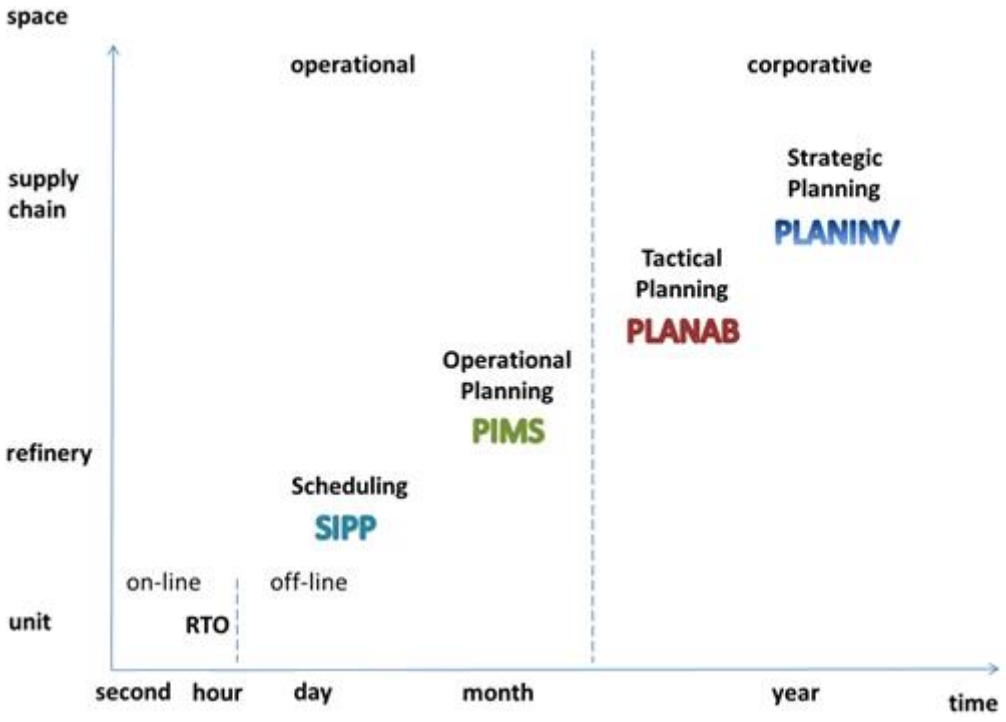

Figure 1.2. Supply chain activities in spatial and temporal dimensions.

The formulation adopted in this work, extracted from this crude oil and products supply chain, optimizes investment in oil-refinery frameworks to build new units and/or expand (capacity) and extend (capability) existing units considering nonlinearities from process unit transformations and material blending over a discrete time scaled in years. To find the best manner to deal with these mixed-integer nonlinear relations by means of one enterprise-wide optimization model, as the demanded for oil-refinery strategic planning, is a prominent pathway to increase the oil-refining margin as well as to operate in a responsive supply chain state.

A very detailed taxonomy to list the strategic, tactical and operational planning types of problems within the crude oil supply chain (COSC) can be found in Sahebi et al. (2014). They survey 54 papers related to COSC planning problems between 1988 and 2013, since the oil reserve and production problems until the fuel deliveries to the client models. In their review, the strategic decisions are classified as investment, facility location, facility relocation (e.g. capacity expansion and reduction), technology selection, upgrading, downgrading, and outsourcing. Besides, they categorized the supply chain structure as convergent, divergent, conjoined (convergent and divergent), and network. Upstream studies can be considered a convergent structure and a fuel blend-shop is a divergent one. A conjoined structure is when refineries, suppliers, terminals, and customers are configured. A network structure deals with processing units and interaction of them.

Considering the strategic decision classes defined in this COSC planning taxonomy, this work is a planning of investment (capital optimization), facility relocation (capacity expansion and reduction) and facility location (capacity installation). In terms of supply chain structure, the models handle very complex oil-refinery networks with yield, holdup and property variations along the processing and logistics operations. Other classifications indicated in the taxonomy involve handling of uncertainty, modeling approach, solution strategies, supply chain entity (upstream, refining, distribution, etc.), and shared information among the entities. The remaining qualification of the material developed in this thesis considering the mentioned classes will be given in section 1.2.

Scheduling was excluded from Sahebi et al. (2014) survey by considering this as an operational decision-making concern and they stated operational planning problems as tactical models such as the general operational planning of oil-refineries and terminals found in Neiro and Pinto (2004), in which three basic types of equipment (units, tanks, and pipelines) are

modeled considering their daily capacity as well as holdup and throughput limits. We disagree that only scheduling can be considered an operational level activity. The monthly, quarterly, weekly, per campaign, or per tank operational planning widely performed among the oil-refining companies' planning and scheduling grades determine the targets to be used within the scheduling in an operational point of view, because includes the overall amounts of products, operational modes, and the first-level inventory data (in an aggregated amount) to be explored in further scheduling or second-level inventory-detailed problems (in a non-aggregated amount), where the selection of discrete tasks is included.

Operational planning can be treated as preliminary scheduling for considering the production structure in space and time in a day- or an hour-basis without flow aggregation. It can be considered as a snapshot or an overall refinery intensive value of flows. It may even consider the true inventory in tanks as well as their maximum and minimum holdups, but disregards the logistics operations as in the operational scheduling. The operational planning problem addressed in this work provides the daily gains to the proposed strategic planning problem in a full space model (chapters 4 and 7) or in the proposed decomposition technique (chapter 8). The "microscopic" information of the profit within a daily operational planning or pre-scheduling perspective, as used in the strategic planning level problems of this work, reduces the possible bottlenecks or idling of the assets, which in a month to a year basis of material balances would be impossible to capture.

1.1.1. Current strategic investment planning structure in PETROBRAS

Figure 1.3 shows the current information flow of the strategic investment planning structure in PETROBRAS. From a possible strategy to invest in a capacity expansion of one unit to its final approval, the cascade of decisions can be segregated in:

1- Test several process designs for a local refinery (only one site) in a LP architecture;

2- Optimize the LP multisite problem for selected process design scenarios;

3- Regarding the capital resources and the required projects, select the best set of competing projects considering capital flow (gross margin - costs) balances.

Optimal process design scenarios are manually searched in the first step within one refinery site boundaries. The current modeling platform used to test several process networks is PIMS (Aspen Technology). After the selection of the more lucrative process frameworks

locally found, the new projects are configured one-by-one in the global investment planning supply chain model named PLANINV (PETROBRAS in-house developed tool) to determine the additional gains with the project inclusion. The cost calculation for each project is defined in parallel to the LP optimization problem and this amount must be lower than the additional gains found in PLANINV to approve the project for the next step.

The third and last step is related to the capital resource constraints to find the best set of competing investments regarding the total capital flow of each project. The PETROBRAS in-house developed model to perform this portfolio optimization is named SIPE and it is based on an MILP approach to maximize the NPV considering cash flow uncertainties in price, investment, project startup schedules, oil production curves, among others (Iachan, 2009). A risk measurement based on stochastic programming was implemented to handle with the risk generated by the uncertainties, where discrete random probabilities are represented in the model with scenarios.

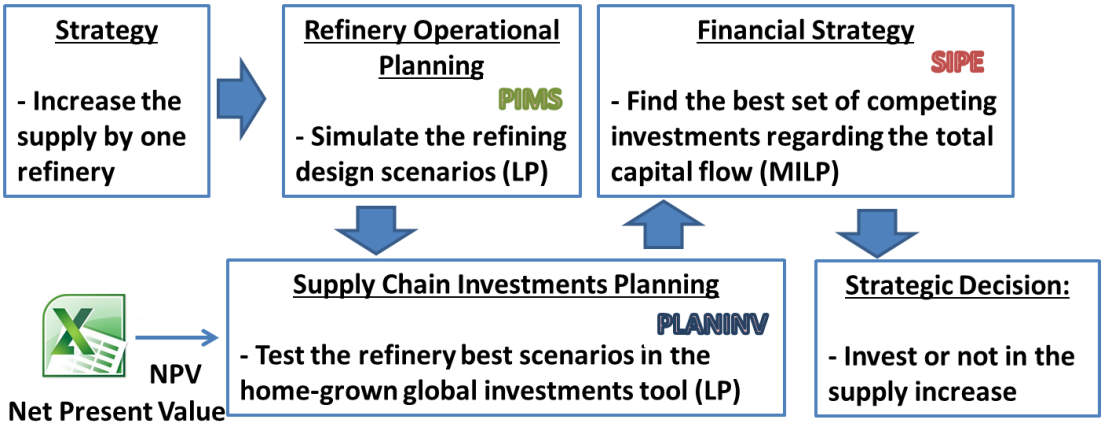

Figure 1.3. Current strategic investment planning procedure in PETROBRAS.

1.1.2. Proposed strategic investment planning structure in PETROBRAS

The model proposed in this work to improve the strategic investment planning accuracy in PETROBRAS or in any oil-refining company incorporates all of the three aforementioned steps as shown in Figure 1.4. The local manual search to determine possible expansions/extensions or installations of units inside one refinery is replaced by mixed-integer optimization by transforming the power-law capital cost correlations to linearized terms with a fixed cost related to the decision in investing or not in a certain project, a binary decision. More details about this linearization procedure will be given in chapters 4, 7 and 8 and in Appendix B. Also, the nonlinearities from processing and blending are introduced to rise above the simple linear approach in the investment planning problem, which are treated in an

MINLP full space model (chapter 4), in an MILP approach by including modes (chapter 7), or as decomposed solution (chapter 8) integrating the MILP strategic and the NLP operational problems. Finally, the capital resources constraints are included in the mixed-integer investment planning model and the financial strategies to address uncertainties in a risk-based approach are replaced by including only demand scenarios in a two-stage stochastic programming approach (chapter 8).

Uncertainty in yields is intended to decrease by more detailed formulation in the process transformations as a type of preventative uncertainty management. Uncertainty from material prices is out of the scope of this work, as the pricing uncertainty dynamics in the oil-refining field is not as critical as in the electrical systems, because the refineries "pricing" or storage (stocks) is not as real-time as in the electrical sector (without storage), so the crude-oil derivatives production is less market- or demand-driven than the electron production. Besides, the pricing control of hydrocarbon streams from geopolitical and economic frontiers is highly more influent at their prices. Another kind of uncertainty such as in project startup schedule, crude oil production, and investment resources are out of the scope of this work. The risk measurement as applied in the financial strategy studies in PETROBRAS today will be added in this work as future development.

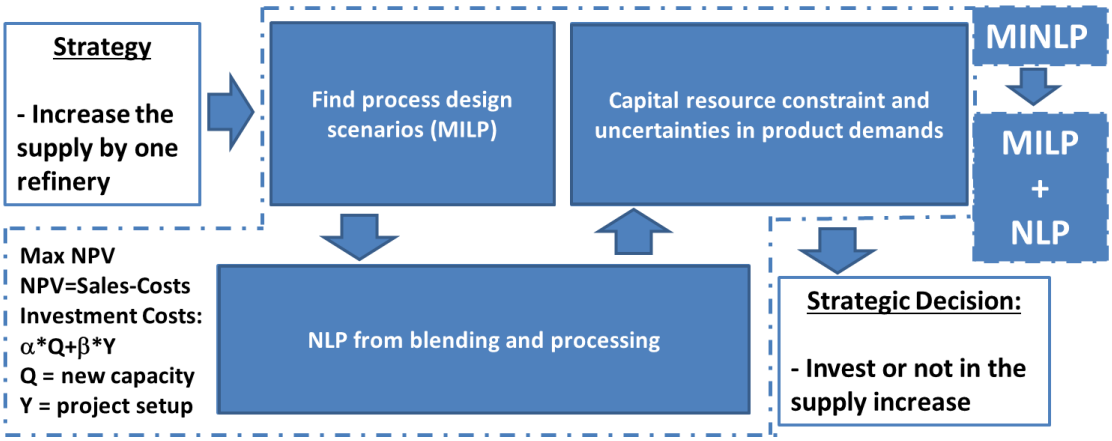

Figure 1.4. Proposed process design synthesis domain for the strategic investment planning modeling in this work.

1.2. Thesis Outline

Typically, as the strategic investment decisions are determined for a long-term horizon of multiple years (e.g. 10-25 years), and considering the uncertainties given by the demand scenarios, the resulting optimization problems are expected to be very large-scale, which

require tailored reformulations such as the multisite aggregate capacity and the phenomenological decomposition heuristic.

Hence, the objectives of this thesis are as follows:

1. Develop models for the optimal operational planning of oil-refinery processes as the operational level problem. (chapter 3)

2. Develop models for the optimal strategic planning of oil-refinery processes as the investment level problem. (chapters 4, 7, and 8)

3. Develop more accurate distillation models for planning and scheduling environment to better predict yield and property of the distillate streams. (chapters 5 and 6)

4. Develop models that address the multisite planning problem considering process capacity per type of unit (i) aggregated in hypothetical large refineries and (ii) their actual sizes. The case study is the Brazilian oil-refining industry. (chapters 3 and 4 for the multisite capacity-aggregated model; chapter 8 for the multisite model)

5. Develop a general capital investment planning to include stages of projects to cover correction, commission, and construction phases in, respectively, repair, retrofit, and revamp types of problems using sequence-dependent setups and considering capacity and capital as material flows as in a scheduling environment. (chapter 7)

6. Develop a decomposition algorithm with uncertainty in product demands that can solve the large scale mixed-integer nonlinear problem, which arises from the integration of strategic and operational decision-making levels. The tailor-made model considers quantity-quality phenomenological decomposition in logic or quantity-logic (QL) problem and quality or quantity-quality (QQ) problem. (chapter 8)

Figure 1.5 shows a brief overview of the chapters considering the levels of decision (strategic and operational) and the data (deterministic and stochastic).

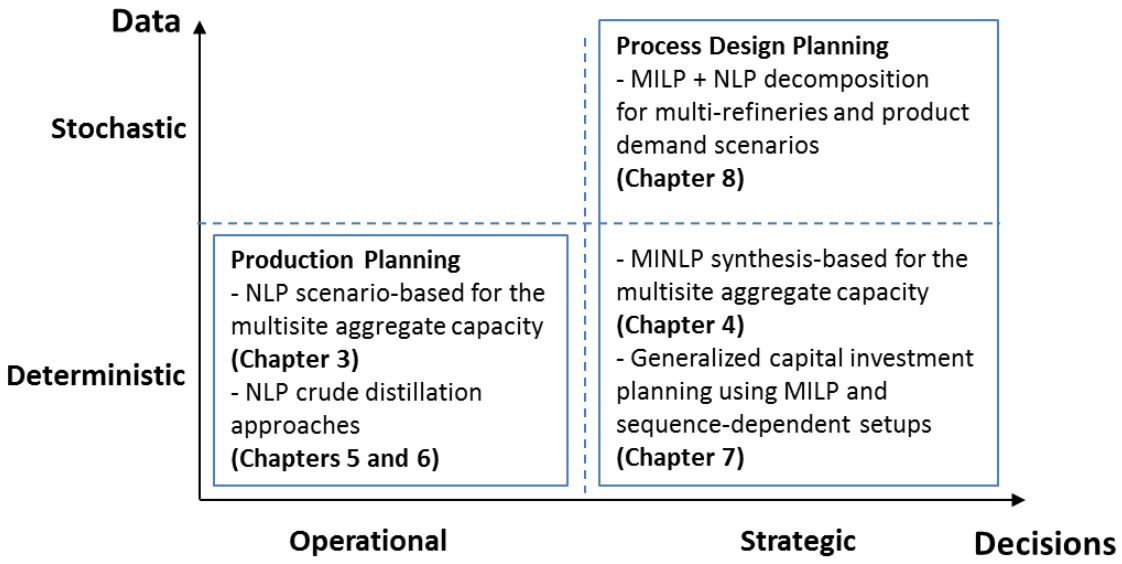

Figure 1.5. Overview of the thesis work.

In the following sections, an overview of the chapters is presented.

1.2.1. Chapter 2

In chapter 2, an overview about mathematical programming models, modelers and solvers is given. It is also presented a literature review on capital investment or facilities expansion planning and distillation models used in planning and scheduling problems.

1.2.2. Chapter 3

In chapter 3, it is developed a single-period NLP production planning model to simulate or test overall capacity of oil-refinery units in Brazil considering different fuel demands, customer preference between gasoline and ethanol, and planned investments by including the projects under construction and in conceptual phase. The chapter describes the oil-refinery configuration and the different constituents of the profit-based production planning model. The multisite reformulation aggregates capacity per type of oil-refinery unit considering the existing 12 refineries in 2013 as a baseline, where two grassroots refineries currently under construction and three new sites in conceptual phase are added, respectively, in 2016 and 2020, to outline future production and import amounts in the Brazilian oil-refining industry. New overall capacities are determined for eight demand and process design scenarios in 2020 to assist the current strategic decisions over the refineries in conceptual project, still in time to have modifications.

1.2.3. Chapter 4

In chapter 4, the single period production scenario-based model in chapter 3 is replaced by a multiperiod MINLP model to predict the process design scenario in terms of overall capacity per type of oil-refinery unit. The net present value (NPV) is maximized considering the potential portfolio of projects to match the future fuel market in Brazil in 2020. Unit capacity additions for the hypothetical large refinery are continuous variables lower and upper bounded by their respective project setup, representing the investment costs in the NPV objective function as varying (capacity addition) and fixed (project setup) terms. In the model, unit throughputs in the operational layer are upper bounded by their changeable capacity over time in the strategic layer. Better results indicate different processing outline in the capacity planning of the Brazilian oil-refining industry.

1.2.4. Chapter 5

In chapter 5, a new extension of the conventional swing-cut modeling is proposed to better predict quantities and qualities for the distillates or final cuts by taking into consideration that it is required corresponding light and heavy swing-cut fractions with appropriately varying qualities. By computing interpolated qualities relative to its light and heavy swing-cut quantities and considering the internal fractions (cuts and swing-cuts) distribution, it is shown an improvement in the accuracy of the blended or pooled final cut quality prediction. Additional nonlinear variables and constraints are necessary in the model, but it is shown that these are relatively easy to deal with in the nonlinear optimization.

1.2.5. Chapter 6

In chapter 6, a novel technique using monotonic interpolation to blend and cut distillation temperatures and evaporations for oil products in an optimization environment is proposed. Blending distillation temperatures is well known in simulation whereby cumulative evaporations at specific temperatures are mixed together then these data points are used in piece-wise cubic spline interpolations to revert back to the distillation temperatures. But, the method introduced here replaces the splines with monotonic splines to eliminate Runge's phenomenon (curve overshooting) (see Kruger, 2014) and to allow the distillation curve itself to be adjusted by optimizing its initial and final boiling points known as cutpoints. By optimizing both the recipes of the blended material and its blending component distillation

curves, very significant benefits can be achieved especially given the global push towards ultra low sulfur fuels (ULSF) due to the increase in natural gas plays reducing the demand for other oil distillates. Four examples are provided to highlight and demonstrate the technique.

1.2.6. Chapter 7

In chapter 7, a more tractable approach using MILP model and input-output (Leontief, 1986) models is proposed whereby the nonlinearities are approximated to linearized operations, activities, or modes in large-scaled flowsheet problems. To model the different types of capital investment planning known as revamping, retrofitting, and repairing, a unified modeling combines planning balances with the scheduling concepts of sequence-dependent changeovers to represent the construction, commission, and correction stages of the projects explicitly. Similar technique can be applied to process design synthesis, asset allocation and utilization, and turnaround and inspection scheduling, where two motivating examples, a small retrofit example and an oil-refinery investment planning are highlighted.

1.2.7. Chapter 8

In chapter 8, a phenomenological decomposition heuristic (PDH) method solves separately the quantity and logic variables in an MILP model, and the quantity and quality variables in a nonlinear NLP formulation. The goal is to maximize the NPV considering discrete investment decisions to install or expand oil-refinery units for process design synthesis of multisite refineries. Iteratively, multiperiod NLP models for the fuel demand scenarios are restricted by the multiperiod stochastic MILP results considering discrete probabilities for the demand scenarios. A motivating example and a multisite industrial-sized problem are highlighted to demonstrate the tailor-made decomposition strategy for the complex oil-refinery capital investment planning.

1.2.8. Chapter 9

Chapter 9 summarizes the contributions of the thesis and outlines future research. Furthermore, journals and conferences where the work developed in the thesis can be found as well as the current and future submissions are:

- Menezes, B.C.; Moro, L.F.L.; Grossmann, I.E.; Kelly, J.D. *A Nonlinear Integrated Model for Operational Planning of Multisite Refineries*. INFORMS Computer Science, 6-8 January, Santa Fe, NM. 2013.
- Menezes, B.C.; Kelly, J.D.; Grossmann, I.E. Improved Swing-Cut Modeling for Planning and Scheduling of Oil-Refinery Distillation Units. *Industrial & Engineering Chemistry Research*, 52: 18324-18333. 2013.
- Vazacopoulos, A.; Kelly, J.D.; Menezes, B.C.; Grossmann, I.E. *A General Approach for Capital Investment Planning using MILP and Sequence-Dependent Setups*. INFORMS Business & Analytics, 30 March – 01 April, Boston, MA. 2014.
- Menezes, B.C.; Moro, L.F.L.; Lin, W. O.; Medronho, R.A.; Pessoa, F.P. Nonlinear Production Planning of Oil-Refinery Units for the Future Fuel Market in Brazil: Process Design Scenario-Based Model. *Industrial & Engineering Chemistry Research*, 53: 4352-4365. 2014.
- Menezes, B.C.; Moro, L.F.L.; Lin, W.O.; Medronho, R.A.; Pessoa, F.P. Mixed-Integer Nonlinear Production Planning of Oil-Refinery Units for the Future Fuel Market in Brazil: Process Design Synthesis Model. *Industrial & Engineering Chemistry Research*, in submission.
- Menezes, B.C.; Moro, L.F.L.; Grossmann, I.E.; Kelly, J.D.; Medronho, R.A.; Pessoa, F.P. *Production Planning of Oil-Refinery Units for the Future Fuel Market in Brazil*. COBEQ, 19-22 October, Florianopolis, SC. 2014.
- Menezes, B.C.; Kelly, J.D.; Grossmann, I.E. *Distillation Curve Optimization using Monotonic Interpolation*. Aiche Annual Meeting, 16-21 November. Atlanta, GA. 2014.
- Kelly, J.D.; Menezes, B.C.; Grossmann, I.E. Distillation Blending and Cutpoint Temperature Optimization using Monotonic Interpolation *Industrial & Engineering Chemistry Research*, 53: 15146-15156. 2014.
- Menezes, B.C.; Kelly, J.D.; Grossmann, I.E.; Vazacopoulos, A. A General Approach for Capital Investment Planning using MILP and Sequence-Dependent Setups. *Computers & Chemical Engineering*, in submission.
- Menezes, B.C.; Kelly, J.D.; Grossmann, I.E. Phenomenological Decomposition Heuristic for Process Design Synthesis of Oil-Refinery Units. *Computers & Chemical Engineering*, to be submitted.

Chapter 2

2. Bibliographic Review

In section 2.1, a brief review about mathematical programming and the main types of models, modelers, and solvers is presented. In section 2.2, the background of capital investment planning for facilities expansion is given. The literature of distillation models in planning and scheduling problems to predict quantity and quality values of the distillate streams is presented in section 2.3. In section 2.4, the types of models covered in this thesis are depicted in a tridimensional cube formed by the projection of the quantity-quality interface (crude dieting, and processing and blending transformations) over the project selection in time (binary dimension).

2.1. Mathematical Programming Review

2.1.1. Modeling Platforms

Mathematical programming has been extensively used to model planning and scheduling problems in the oil-refining and process industries for decades (Symonds, 1955; Aronofsky et al., 1978; Pelham and Pharris, 1996). Although more accurate results may be obtained by using rigorous process models, their complexity, difficulty in formulating them as optimization problems, and the intractability of their solution prevent them from being used more extensively in practice (Li et al., 2005). Commercial planning software such as GRTMPS (Haverly), Aspen PIMS (Aspen Technology), and RPMS (Honeywell) somewhat overcome this problem by using simplified input-output types of process unit-operation models, which involve mostly linear, bilinear, and trilinear constraints and are solved using home-grown successive or sequential linear programming (SLP) algorithms, sometimes referred to as distributed recursion (DR) when less rigorous SLP algorithms are used. These purpose-specific commercial modelers are widely used among production planners because they are easy to handle given that the users usually only need to fill the data into specific spreadsheets in matrix form. The quality of the modeling used in current commercial planning software is limited by their simpler formulation and reduced solution strategies. More recently, PIMS-AO (Aspen Technology) permitted the modeling of NLP problems but still retains the simpler matrix modeling approach and relatively unsophisticated solution strategies to improve the objective function.

The alternative to improve the modeling quality is the development of optimization models expressed explicitly in algebraic form using algebraic modeling languages. They have the advantage of interfacing to many solver codes for solving the various types of problems and can perform automatic differentiation. The formulation and solution of major types of mathematical programming problems in algebraic form can be effectively performed in scalar-, set- or structure-based modeling platform systems. There are also stream-based languages which are more engineering domain-specific languages such as APMonitor, Ascend, Aspen Custom Modeler, gPROMS and Modelica which we do not discuss further but essentially connect, common, link or share sub-models together using variable to variable transfer equations. In the scalar-based tools such as Fortran and Matlab, the parameters, variables and constraints have their own identification explicitly named, so the equations should be formulated one by one, which for small-sized problems can be easily coded. However, for modeling medium to large scale problems, most modeling platforms use indexed labels to create constraints combined with the variables and parameter using sets, compound-sets, subsets, and index-sets, etc. The most common set-based modelers are AIMMS, AMPL, GAMS, LINGO, MOSEL, MPL and OPL. Despite these types of algebraic modelers for overcoming the management of large amounts of parameters, variables and constraints, to enable the construction of solution algorithms integrating successfully planning, scheduling, RTO and control decisions as well as managing data quality and management using statistical estimation techniques, it is required to be able to configure the network without coding.

Recently and to help overcome the above modeling barrier especially for less sophisticated end-users, a new modeling platform language was released to form a complex network using the unit-operation-port-state-superstructure (UOPSS) flowsheet representation (Kelly, 2004; Kelly and Zyngier, 2007; Zyngier and Kelly, 2012). In this new generation of modeling platform, the sets of the elements (e.g., units, tanks, and pipelines) and the material balances of the nodes are implicitly formed by the flowsheet/connectivity of the network (construction data). This kind of modeling language can be considered as a flowsheet or structure-based modeling where large-scale problems can be easily represented by coding indirectly the indexed constraints using the built-in flowsheet-oriented features found in the new modeling and solving platform called IMPL (Industrial Modeling & Programming Language).

In this generalized network optimization, not only are quantity variables created by the construction (flowsheet) and capacity data, but also logic (i.e., setups, startups, etc.) and quality (i.e., densities, properties, etc.) variables by populating them in specific frames or data lists from where the constraints are implicitly built to avoid the hands-on work of writing all the indexed constraints by the combination of sets and index-sets as in the set-based modeling platform languages. The only platform in the structure-based group (IMPL) covers most of the planning and scheduling relationships from the process industry. In the case of studies, both the GAMS and IMPL modeling languages are used. Comparing these two programming languages one can notice new modeling advancements in IMPL to facilitate the programming and data interfacing as well as proprietary techniques in nonlinear solution and computing derivatives automatically.

Table 2.1. GAMS and IMPL comparison.

	GAMS	IMPL
Modeling structure	set-based	structure-based
Built-in facilities	no	UOPSS flowsheet and frames
Sequencial Linear Programming (SLP)	no SLP	SLPQPE
Application Programmers Interface (API)	creates a file to exchange data	computer's memory
Interpolation derivative	given by the user	automatic

2.1.2. Types of models and solutions

Full dimensioned problems (*FDP*) for process design synthesis give rise to discrete and continuous optimization in multiperiod models considering the time period *t*, corresponding to an MINLP model as shown in *FDP* (Grossmann, 2002), where x_t are the continuous variables in X_t and y_t are the binary variables 0-1 in Y_t, linear $h_t(x_t)$ and nonlinear $g_t(x_t)$ constraints are differentiable functions in X_t, and a_t, b_t , c_t, d_t, A_t, B_t, D_t are vector or matrix of coefficients.

$$
\begin{aligned}
& min\, z = \sum_t \left(c_t x_t + {d_t}^T y_t \right) \\
& s.t. \quad g_t(x_t) + B_t y_t \le b_t \;\; \vee \; t \\
& \qquad h_t(x_t) = 0 \;\; \vee \; t \\
& \qquad A_t y_t \le a_t \;\; \vee \; t \\
& \qquad x_t \in X_t, y_t \in Y_t
\end{aligned}
\qquad (FDP)
$$

In most applications, the functions are linear in y_t. If all functions in *FDP* are linear the problem corresponds to an MILP. If there are binary variables, the *FDP* is reduced to an NLP if there is, at least, a single nonlinearity in the model, or an LP model if all functions are linear.

In the proposed process design synthesis models found in this thesis, linear constrains similar to $D_t x_t + B_t y_t \leq b_t$ are used in the financial capital resource and in the semi-continuous constraints relating new capacity increments x_t with their respective setup variables y_t. In the financial capital resource constraint, D_t and B_t are the varying and fixed costs and b_t are the amount of capital available. In the semi-continuous constraints relating new capacity increments, D_t is the identity and B_t can be lower or upper bounds and b_t is zero. If the project is selected ($y_t = 1$), the new capacity can vary between lower and upper bounds and the capital cost is active in the capital resource constraint and in the objective function, reducing both the amount of capital available and the objective function value. The linear transformations and the material flows are given by $h_t(x_t)$ and the $g_t(x_t)$ constraints are compounded by the nonlinear processing transformations and blending formulas, mostly non-convex constraints. The proposed approaches in this thesis are solved by NLP (chapters 3, 5, and 8), MILP (chapters 7 and 8) and MINLP (chapters 4 and 8) solvers. Also, the examples in chapter 6 and the motivating example in chapter 8 are solved by the proprietary SLP technique (SLPQPE) found in the IMPL modeler, which embed LP/MILP solvers such as CPLEX, COINMP, LPSOLVE, GLPK, etc.

2.1.2.1. LP and MILP

LP and MILP have been widely used in planning and scheduling problems (Sahinidis et al., 1989; Iyer and Grossmann, 1996; Pinedo, 2002; Floudas and Lin, 2004; Mendez et al., 2006; Pochet and Wolsey, 2006; Kelly and Zyngier, 2007; Mitra et al., 2014a, 2014b), and supply chain optimization (Grossmann, 2005, Ryu and Pistikopoulos, 2005; Sousa et al., 2008). The LP problems solution relies basically on the simplex algorithm (Dantzig, 1963), although for polynomial complexity of industries-sized problems, the interior-point algorithm (Karmarkar, 1984) are more indicated to avoid the incessant search along the polyhedral vertices when using the simplex algorithm for cases with millions of variables.

From advances in LP, the MILP simplex LP-based branch and bound (B&B) methods (Nemhauser and Wolsey, 1988; Wolsey et al., 1998) consist of a tree enumeration in which the LP sub problems are solved at each node and eliminated based on bounding properties. In

the B&B algorithms, the solution of a linear relaxation (where binary variables are treated as continuous) establishes a lower bound in a minimization problem and an upper bound in a maximization problem. The B&B solution fix the binary variables in 0 or 1 one-by-one within a tree search and solve the LP sub problems to obtain upper or lower bounds and then rounding to the nearest integer solution until it matches the current solution bound at least within a gap. During the search, the branches of the tree are cut by the bounds of the solutions from each node continuously searched until the convergence (Land and Doig, 1960; Nemhauser and Wolsey, 1988). The B&B method is improved through cutting plane techniques, which produce tighter bounds.

Remarkable progress in the ability to solve MILP models has been made in recent years mainly due to (Harjunkoski et al., 2014): (i) advances in CPU speed and memory which reduced the solution time of a medium-sized problem from roughly 1000 s in 1993 to less than 1 s in 2003, and (ii) algorithm improvements such as pre-processing methods, heuristics within the B&B search, cutting planes generation at pre-processing and during the search, and parallel computing. Commercial solvers for complex MILP models with solution in a reasonable CPU time such as CPLEX, XPRESS and GUROBI incorporated the mentioned algorithm (Johnsnon et al., 2000; Bixby, 2002; Bixby and Rothberg, 2007) and computing advances, and only since one decade from now, these solvers can handle effectively large-scale LP and MILP problems. The LP and MILP free solvers such as LPSOLVE, GLPK, COINMP, and SCIP have limited ability to solve large problems effectively.

The MILP problems are NP-complete, which means that the set of all decision solutions, each one verified in a polynomial time at each node, can lead to an exponential execution time for the whole solution. Therefore, an industrial-sized problem can become intractable when solving problems with large number of 0-1 variables, especially if the integrality gap is large, so decomposition strategies (Iyer and Grossmann, 1998; You et al., 2011; Corsano et al., 2014; Mitra et al., 2014a, 2014b) and approximation/reformulation algorithms such as aggregated models are the common strategies to handle with such complicated problems.

2.1.2.2. NLP and MINLP

The main commercial NLP solvers are CONOPT (Drud, 1985), that uses reduced gradient method, KNITRO (Byrd et al., 1999), which uses the interior point methods, and SNOPT (Gill et al., 2002), based on successive quadratic programming. The main free NLP

solver is IPOPT (Wächter and Biegler, 2006), which uses the interior point methods. These NLP solvers are sensitive to initial points because they are based on Newton's methods and the global optimum is guaranteed only if the problem is convex (i.e. convex objective function and constraints). When the NLP problem is non-convex, as those found in this thesis due to the processing transformations and blending, the global optimum is not guaranteed, so potentially can lead to local solutions.

Alternatively to the NLP solvers, nonlinearities can be solved by using successive or sequential linear programming (SLP) algorithms. This method solves a sequence of linearization of the nonlinear terms transformed in Taylor series truncated at the first-order approximation. Some estimate of the optimal solution is, as a rule, required in order to provide good initial points. Besides, as the linear approximations need not to be bounded, restricted step or trust region methods are required to attain convergence to some solution (Bazaraa, Sheraly, and Shetty, 1993).

Nonlinearities integrated with binary models are solved in MINLP methods which includes standard branch and bound methods (BB) and decomposition algorithms such as generalized Benders decomposition (GBD) (Geoffrion, 1972), outer-approximation (OA) (Duran and Grossmann, 1986), and the Extended Cutting Plane Method (ECP) (Westerlund and Pettersson, 1995), in which, in the last, the NLP sub problem is replaced by function evaluations reducing the algorithm to a successive MILP method (Harjunkoski et al., 2014). Within the MINLP solution, NLP solvers (e.g. reduced gradient, successive quadratic programming, or interior point method) are performed at each node, in BB methods, or solve a separate problem in GBD and OA, in which an iterative sequence of master problem and slave sub problem (with fixed 0-1) yield lower and upper bounds for the objective function until the convergence is achieved within a specified tolerance. In a minimization case, the NLP sub problems yield upper bounds, while the MILP master problems yield lower bounds. In a maximization case, the MILP master problems yield upper bounds and the NLP sub problems lower bounds. The GBD and OA methods difference relies on the definition of the MILP master problem. While the OA method utilizes accumulated linearizations of the functions, GBD uses accumulated Lagrangian functions parametric in the 0-1 variables (Grossmann et al., 1999). In order to avoid the full search within the nodes, branch and cut methods can be applied to prevent the repeated sequence of MILP master problems by updating the linear approximations with solution of NLP sub problems at selected nodes.

Solvers implementing MINLP problems include DICOPT (Viswanathan and Grossmann, 1990), SBB (Standard Branch and Bound), among others. Non-convexities can be handled in non-rigorous methods such as the equality relaxation algorithm and the augmented penalty. The derivation of the most methods for MINLP assumes that the functions f and g are convex. Global optimization solvers like BARON (Sahinidis, 1996) use spatial branch and bound method to rigorously guarantee the global optimum in non-convex NLP problems, although can handle only with small-sized models.

2.2. Capital investment planning approaches within the process industry

Discrete investment decisions based on net present value (NPV) formulations were discussed by Sahinidis et al. (1989) considering a multi-period MILP model for the overall mass balance to predict expansions of existing units over time. Different strategies were proposed such as normal branch and bound, cutting planes, Benders decomposition (Benders, 1962) and heuristics. A combination of integer cuts, cutting planes and branch and bound was the most promising strategy for solving mixed-integer problems. Other approaches using polyhedral projection and strong cutting planes proved to be faster and more robust than the conventional mixed-integer formulation for large scale problems with long time horizons (Liu and Sahinidis, 1996).

Following these works, Iyer and Grosmann (1998) proposed a bi-level decomposition by separately solving the design and the operational models. The bi-level approach is based on the idea that some complicating variables e.g., investment decisions or assignment variables, are withdrawn to solve an easier sub-model and then included in a further step fixing some results from the previous model. In their NPV-based capital investment planning example with two set of binary variables (selection and expansion of process unit), the design master problem does not contain binary variables associated with capacity expansion decisions. It only contains binary variables representing the selection of a process over the entire planning horizon, so the high-level or design problem is combinatorially less complex and selects a subset of processes for design. Following the algorithm, the lower level planning problem is solved for the selected set of processes to define the capacity expansion. Bounding information is used over the algorithm based on specific relaxations that under- and over-estimate the investment costs in the NPV maximization. For very small problems, the method is no faster than the full space branch and bound method. For medium-sized problems that can

be solved to optimality, the bi-level method proved to be faster. For large problems, solutions with 10% higher NPV were obtained when compared to the suboptimal solution from the full space MILP model.

Van den Heever and Grossmann (1999) proposed disjunctive outer-approximation (Duran and Grossmann, 1986) and bi-level decomposition (Iyer and Grosmann, 1998) strategies for design and planning of process industry networks, incorporating design, operation planning and capacity expansion in the same model for both MILP and MINLP problems. Their work addresses the problem of the computational effort in solving the MILP step, which is often the bottleneck in the computations of multi-period optimization problems when the number of period increases.

Jackson and Grossmann (2002) proposed a high-level MILP model to address the retrofit design of process networks to allow multiple types of modifications in each time period. Examples illustrate the robustness of the generalized disjunctive programming (Raman and Grossmann, 1994) approach with convex hull formulation (Balas, 1985), which gives a tight LP relaxation and leads to faster solution times when compared to the big-M constraints.

Large scale process industry problems found in the capital investment planning literature include multi-entity relationship by integrating the production and distribution supply chain problems. You et al. (2011) proposed a multiperiod capacity, production and distribution planning model for multisite networks consisting of several production trains for families of products to adjust the capacities of production. The MILP model takes into account multiple trades-offs and simultaneously predicts the optimal capacity adjustment plan, production levels, and sale profiles. A bi-level decomposition method (Iyer and Grossmann, 1998) and a spatial decomposition scheme based on Lagrangean decomposition (Guignard and Kim, 1987) were developed to avoid solving the resulting large-scale multiperiod MILP problem simultaneously. Numerical results showed that the bi-level decomposition requires smaller computational times for all the examples, leading to solutions that are much closer to the global optimum when compared to the full space solution and to Lagrangean decomposition.

Corsano et al. (2014) has recently addressed the simultaneous design of batch plants and production sites allocation inside supply chains, taking into account an MILP that calculates different hierarchical levels decisions (i.e., single site and multisite design tasks) for three decomposition algorithms (bi-level decomposition (Iyer and Grossmann, 1998),

Lagrangean (Guignard and Kim, 1987) and their hybrid). The bi-level decomposition is the best method in terms of quality of the final solution produced, i.e., the global optimum, and time spent in its generation, the fast to close the optimality gap. This finding is consistent with other results published in literature (You et al., 2011).

Integrating planning and scheduling activities, a quantitative approach for designing responsive supply chains under demand uncertainty was presented by You and Grossmann (2008), in which the strategic, tactical and operational decisions (e.g. installation of plants, selection of suppliers, manufacturing sites, distribution centers and transportation links) are integrated with the scheduling decisions (e.g. product transitions and changeovers) for the multisite and multi-echelon process supply chain network. The expected lead time was proposed as a measure of process supply chain responsiveness. A multiperiod mixed integer nonlinear (MINLP) model was developed for the bi-criterion optimization of economics and responsiveness, while considering customer demand uncertainty.

Many authors (Sahinidis et al., 1989; Liu and Sahinidis, 1996; Iyer and Grosmann, 1998; Jackson and Grossmann, 2002) deal with capacity or design planning problems applied to chemical or petrochemical processes, which compared to oil-refining have simpler mass/volume balances and, in general, without quality optimization. Moreover, these models addressed simple processing transformations and less complex raw materials than crude-oil. The oil-refinery complexity and scale prevent the solution of more accurate industrial-sized models in planning and scheduling problems (Li et al., 2005), thereby stimulating the research of quantitative methods in terms of more rigorous models. The proposed strategic capital investment planning model for oil-refinery framework synthesis deals with mixed-integer problems (chapters 4, 7, and 8), crude dieting (chapters 3, 4, 5, 6, and 8), processing transformations (chapters 3, 4, 5, 6, and 8), pooling (chapters 3, 4, 5, 6, and 8), project scheduling and staging (chapter 7), and multisite domain (chapter 8), significantly more rigorous than those formulations generally used in a strategic decision-making level.

The quantitative methods to improve the accuracy of the binary search of unit expansion and installation projects as proposed in chapter 8 consider multisite, multiperiod, multi-scenario, and quantity-quality formulation, thus the model gives rise to large scale MINLP problems in which the purpose-designed phenomenological decomposition heuristic to solve the process design synthesis of oil-refinery framework is outlined for solving industrial-sized optimization.

Further to these conventional approaches to solve the capital investment planning problem (CIP) is the novel model presented in chapter 7, in which the CIP problem is reformulated using sequence-dependent setups (Kelly and Zyngier, 2007) to handle with project execution phase and the capital and capacity are regarded as flows or amounts as in a scheduling environment. In this work, units or equipment expansion and installation are modeled in a non-aggregated framework, i.e., in an actual or real plant model. In this case, considering also a multi-period formulation, the model size gives rise to large scale MINLP problems in which the input-output Leontief approximation using sequence-dependent setups modeling is proposed for solving industrial-sized problems in a MILP model.

2.3. Distillation models in planning and scheduling environment

Distillation or fractionation models for planning and scheduling activities play an important role in all decision-making problems within the oil-refining sector. As the distillation units separate the crude-oil into various cuts or distillates and then distribute these to downstream transforming and treating units, all efforts to improve their quantity and quality predictions to avoid potential inconsistencies in the targets for scheduling and/or control applications is always worth pursuing. The driving force in most separation processes found in oil refining is the volatility difference between multiple light and heavy crude-oil components, which are of course temperature and pressure dependent. Rigorous engineering calculations to represent the details of most oil-refining processes can be found in commercial simulators such as Aspen-Plus and Hysys (Aspen Techology), Petro-SIM (KBC), PRO-II (Invensys), and UniSim (Honeywell). These tools provide extensive capabilities to model, on a molar basis, material, energy, kinetic, and equilibrium relationships along with embedding several physical and thermodynamic property packages.

However, distillation models in planning and scheduling problems rely on essentially mass and/or volume-basis material balances, where the crude oils are decomposed into several cuts based on what are known as true boiling point (TBP) temperature distribution curves for how yields and other qualities are distributed as a function of TBP temperature. In this way, variations in material flows and property profile from these distillation processes can be modeled considering the column's known temperature distribution.

Previous work embedding distillation process models into oil-refining planning problems somewhat improved the simple fixed yield and properties model by considering

different operational modes (Brooks, 1999). Moro et al. (1998), Pinto et al. (2000) and Neiro and Pinto (2004) proposed a nonlinear planning model considering the furnace outlet temperature as an operational or process variable, and then by experimental or through process simulations, fit delta or shift coefficients for the intermediate or final-cuts or stream flows and quality values with variations. Zhang et al. (2001) highlighted the conventional swing-cut model considering the existence of fractions with the same qualities swinging between adjacent cuts using a volume ratio on crude-oil feed. Li et al. (2005) proposed improvements in the swing-cut model based on weighted-average cumulative yield variations of the crude-oil assay considering "weight transfer ratios" of each product-cut. The upper and lower bounds for the yields are defined by the union of different operational modes in the distillation tower. Their approach also included empirical models similar to those from Watkins (1979) to predict distillate properties. In addition, Guerra and Le Roux (2011a, 2011b) applied this modified swing-cut model to improve the overall oil-refinery planning modeling for a medium-scale case with several process units and product blends. Although these previous works try to improve the distillation model's accuracy without overloading the formulation, they do not deal with the issue that the swing-cut properties vary inside the light and heavy portions or fractions of the swing-cut. Instead, they use empirical correlations based on the crude-oil assay TBP curves alone without adjusting the swing-cut qualities directly, as proposed in this work.

More recent and complex distillation models applied to planning and scheduling problems have been published that use nonlinear relations, as well as molar and energy balances with temperature cut-points as variables. Alattas et al. (2011) applied nonlinear programming for a single-period refinery operational planning problem to predict yields using the well-known fractionation-index (Geddes, 1980) showing profit increases by stressing the accuracy in the distillation process. In their work, the distillation column is considered as a sequence of flashes using pre-determined temperatures, and with both rectifying and stripping fractionation indices (FI) in each section. The nonlinear Heaviside function is used to model the fractionation-index pair within the molar balance of each flash. Extending this work, Alattas et al. (2012) addresses the multiperiod operational planning problem by replacing the Heaviside function to manage the FI pair with mixed-integer constraints using convex hull and big-M formulations. In both FI models, some simplification, such as constant pressure throughout the column, is assumed. Another issue in their paper is the exponential polynomial

in the equation (22), which calculates the vapor pressure as a function of reduced temperature and is highly nonlinear. This can be a source of instability during the solution process.

Mahalec and Sanchez (2012) proposed an inferential monitoring and optimization of distillation columns via hybrid models, i.e., combining first-principles and statistical empirical correlations together. They also use molar and energy balances for the TBP changes in a tray-by-tray formulation. Their technique uses actual data from the column's operation, and/or data from a rigorous process simulator of the column to fit parameters in both the first-principles and empirical correlations. This of course requires continuous calibration to keep the models sufficiently accurate. In addition, their approach is mainly concerned with the yield or fraction of each product-cut fractionated at the initial and final TBP temperatures, and unfortunately does not consider the variations in other qualities or properties as a function of temperature.

Two novel distillation methods for planning and scheduling environment are proposed in this work. The first is the improved swing-cut modeling (chapter 5), which uses property-based linear interpolation to predict quality corrections for the light and heavy swing-cut streams. A focus is adopted on improving the conventional swing-cut formulation instead of reformulating it using more detailed temperature cut-points along with short-cut molar, energy, and equilibrium relationships used by the previous researchers. The proposed method is still flow-based (either volume or mass) and encompasses a straightforward enhancement to the swing-cut formulation by correcting or adjusting the qualities of both the light (top) and heavy (bottom) swing-cut fractions, thus improving the quality predictions of the blended or pooled distillate streams as it will be shown later.

The second distillation method is the distillation curve adjustment or shifting modeling to optimize temperature cutpoints for distillate streams using monotonic interpolation (chapter 6). In this novel formulation, the distillation curve of the final distillate (naphtha, kerosene, diesel, etc.) is defined in three different regions (front-end, middle, and back-end) with linear approach in each one. The model proposes adjustments throughout the distillation curves considering the front- and back-ends shifts or deltas. A thorough description of this technique is found in chapter 6.

2.4. Types of models from the thesis

Fig. 1 shows the linear (LP) and nonlinear (NLP) models to be considered through the variation of the logic (L) variables (binary variables) over time. The quantity-quality (QQ) interface is formed by processing transformation and blending constraints.

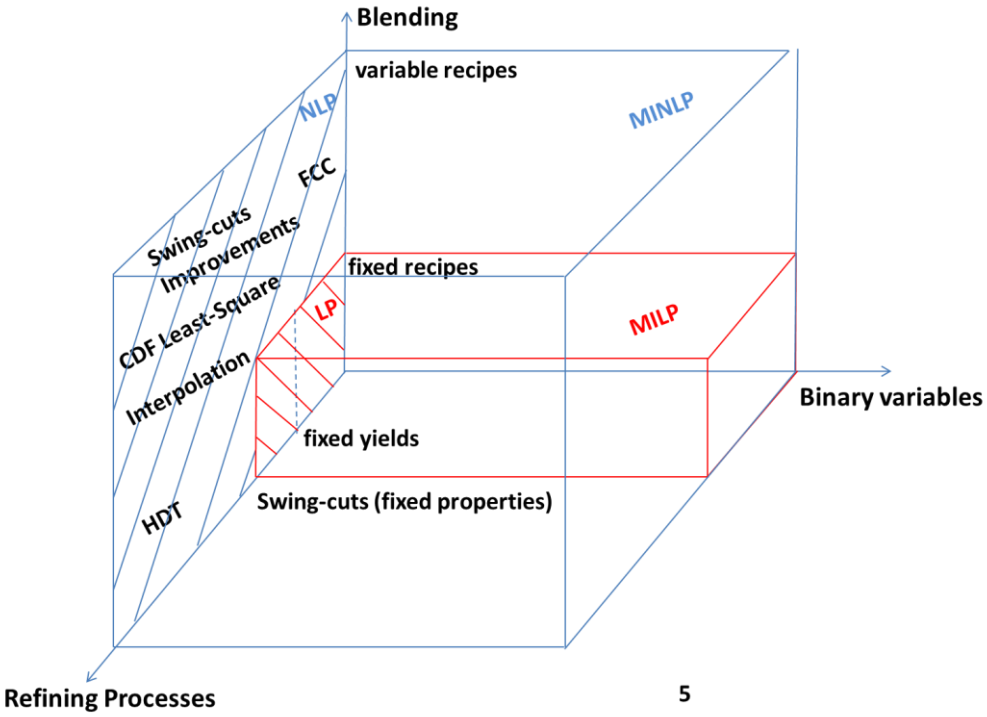

Figure 2.1. Three dimensional set of variables in the QLQ problem.

Chapter 3

in Menezes, B.C.; Moro, L.F.L.; Lin, W.O.; Medronho, R.A.; Pessoa, F.P. Nonlinear Production Planning of Oil-Refinery Units for the Future Fuel Market in Brazil: Process Design Scenario-Based Model. *Industrial & Engineering Chemistry Research*, 53: 4352-4365. 2014.

3. NLP Production Planning of Oil-Refinery Units for the Future Fuel Market in Brazil: Process Design Scenario-Based Model

In this chapter and in the following one (chapter 4), the Brazilian refineries are aggregated in one hypothetical large refinery to calculate demanded capital expenditures, additional processing capacities and overall crude and oil products balances in terms of both quantity and quality. This approximation can be considered satisfactory for a national/corporate strategic planning perspective to defined overall material balances (production and imports) and prevents the solution of very large models that include all the refineries. The straightforward approach for strategic planning analysis considers a single-period NLP operational planning problem to test or simulate possible production design to avoid mixed-integer linear or nonlinear models as will be seen in this chapter. As usual, company's profitability is an important investment qualifier, and is considered as a quick and easy way to judge the overall production performance.

A second option to design production scenarios is to consider discrete formulations capable of predicting capacity addition of process units. In this case binary variables for expansion of existing units and installation of new ones create a combinatorial enumeration for a selection of projects to be explored by branch-and-bound methods. These can be combined with continuous variables to evaluate the size of the capacity additions as seen in chapter 4, in which the size of the proposed full space MINLP model for the multisite aggregate capacity approach is reduced considering the hypothetical large refinery. This strategic planning model demands a small number of setup variables, which, regarding the considerations presented in chapter 4, is good enough for the overall crude diet, process unit capacities and fuel balances planning for a whole country, and can overcome the drawbacks related with model size escalation and tractability in more rigorous formulations.

In section 3.1, the Brazilian oil-refining industry investments are outlined. The NLP operational planning model proposed for all Brazilian fuel market demand scenarios is presented in section 3.2. Section 3.3 describes the Brazilian oil-refining industry with a

review of the national data considered. In section 3.4, the daily operational profit objective and the scenario tree for all cases are presented. Crude and fuel balances for all scenarios and unit demanded throughputs for the 2020 cases are shown in section 3.5. Finally, conclusions are discussed in section 3.6.

3.1. Introduction

This chapter proposes a scenario-based production planning model for the Brazilian oil-refining industry to supply oil products needs within this decade. Today, as seen in Figure 3.1 the national oil-refining asset expansion includes two grassroots refineries currently under construction and three additional sites currently in the conceptual project phase to prevent a fuel deficit of around 30% in 2020, according to recent forecasts in the country (PETROBRAS, 2013). National planned investments project an increase of 1595 kbpd in crude distillation capacity, which only includes refineries of the national oil and energy company known as PETROBRAS, which accounted for 98% of the total crude distillation capacity in 2013 (ANP, 2013).

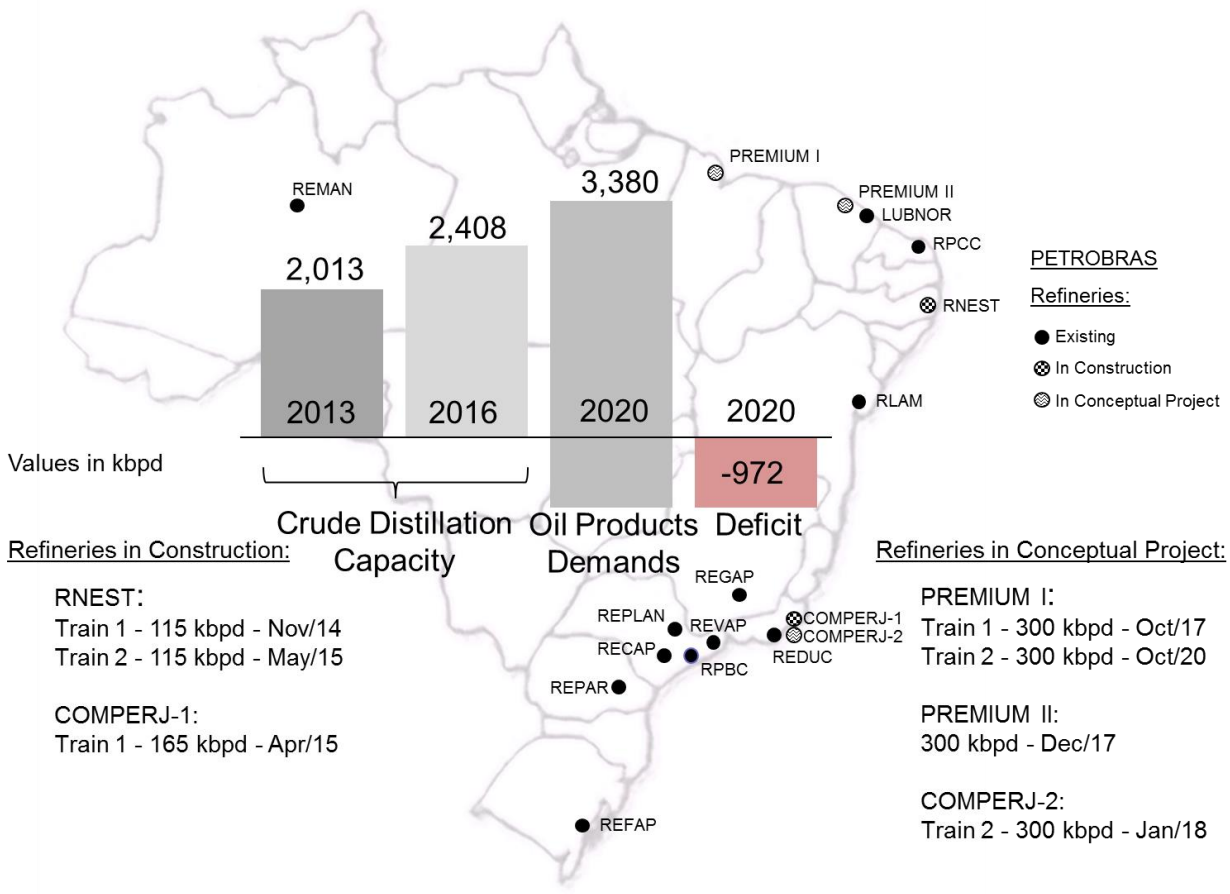

Figure 3.1. Oil product deficit of 30% without the refineries in conceptual project phase.

The proposed approach predicts the overall capacity of oil-refinery units considering the current Brazilian refineries aggregated in one hypothetical refinery called REBRA to approximate the national overall capacity for several types of units. The single-period nonlinear programming (NLP) operational planning model for REBRA defines the national crude diet, unit throughputs, fuel production, and import amounts, taking into account profit maximization in 2013, 2016, and 2020. Regarding the expected and proposed fuel market scenarios for the conceptual projects in 2020, with planned overall capacities higher than their demanded throughputs, the projects require refitting.

Different fuel market scenarios, including the gasoline-ethanol customer preference, are proposed to cover all limiting demands. The final overall capacity planning results may indicate project alteration once the refineries currently in the conceptual phase can still be modified to find the best investment portfolio considering the future official and proposed market scenarios defined in this work. A full review on the investment strategies for the future fuel market in Brazil can be found in Appendix A.

3.2. NLP Operational Planning Model

Production and market scenarios are tested considering the NLP operational planning model presented in this section. Figure 3.2 shows the oil-refinery unit framework considered. For the cases under analysis, the hydrocracker (HCC) is excluded from the hypothetical refinery for the current scenario in 2013 as well as the ability to process atmospheric residuum (ATR) in a delayed coker unit (DC). For the 2016 and 2020 scenarios, both options are considered.

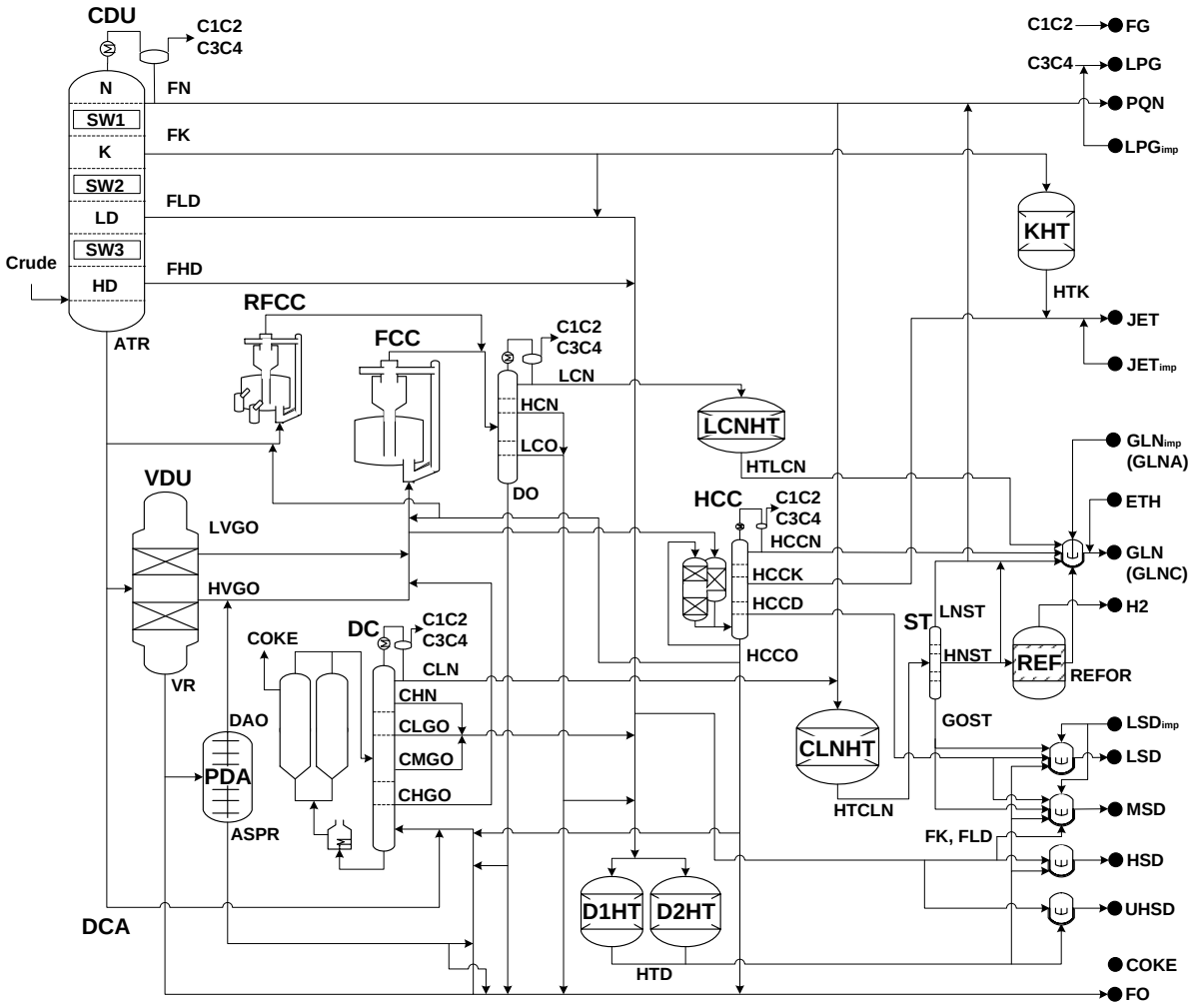

Figure 3.2. Hypothetical refinery REBRA.

3.2.1. Swing-Cut distillation modeling

Distillation units are often modeled into several operational modes, such as maximum gasoline, kerosene, or diesel (Brooks, 1999). Each mode is based on a set of temperature cutpoints defined by previous experience, experimental data, or process simulators, so that intermediate fractions can be managed to both adjacent distillates, creating swing cuts, which can be included in a distillation model instead of considering the final distillates with fixed yields and fixed properties based only on the pooled crude-oil feed. Thus, the swing-cut modeling approximates the temperature cut-point variation without the need to recut the crude assay (Di Vita, 2009)

The swing-cut approximation models the consequence of the thermodynamic variation inside the distillation column, which, driven by pressure and temperature, allows some hydrocarbon fractionation by creating internal cut swinging, which can be expressed as a

volume ratio on crude feed, as a certain boiling temperature range, or as volume/mass transfer ratios. Zhang et al. (2001) used 5% and 7% volume ratios on crude feed as the sizes of the naphtha/kerosene and kerosene/diesel swing cuts, respectively. Li et al. (2005) considers that the swing cuts ranges are bounded by the union of three operational modes in the CDU (crude distillation unit) taking into account maximization of naphtha, light diesel and heavy diesel to find mass transfer ratios for the swing cuts. Despite the CDU processing-variance consideration by the swing cuts modeling, these authors considered a fixed crude diet for their cases, which reduces decision-making in planning and scheduling cases, and used Watkins (1979) correlations based on yields to predict the final distillate properties and not the crude-oil assay property data.

Unlike previous researchers, in this work the mixed crude oil given by the CDU feed diet found in the model defines the blended fractions inside the distillation towers (cuts, including the swing-cuts), and then a new pooling occurs to get the final distillate yield and properties for an optimal volume yielding distribution given by the exchangeable cuts. These swing cuts are split into light and heavy fractions, the former representing the swing-cut part flowing to the light distillate and the latter representing the one flowing into the heavy distillate. Optimization involving quantity variables for the light and heavy swing cuts and quality variables for the whole swing-cut as presented in this work is found in commercial planning platforms such as GRTMPS (Haverly), Aspen PIMS (Aspen Technology), and RPMS (Honeywell). Their solutions include the crude diet and final distillate quality optimization, both related to the cut and swing-cut internal blending modeling, by employing home-grown successive linear programming algorithms to solve the nonlinearities. The mentioned authors do not consider properties for the swing-cuts (Zhang et al., 2001) or calculate the final distillates properties by empirical correlations based on distillate yields (Li et al., 2005), nor do they consider crude-oil assay data as in this work, in which a typical 30-40ºC true boiling temperature (TBP) range is set to the swing-cut fractions, which is already expressed in the given crude-oil assay yields and properties.

Figure 3.3 shows the material flow for cuts *c* and final-cuts *fc* of the CDU. The light and heavy swing-cut fractions mix with their upper (light) and lower (heavy) cuts, respectively, internally to the tower and not as schematically presented.

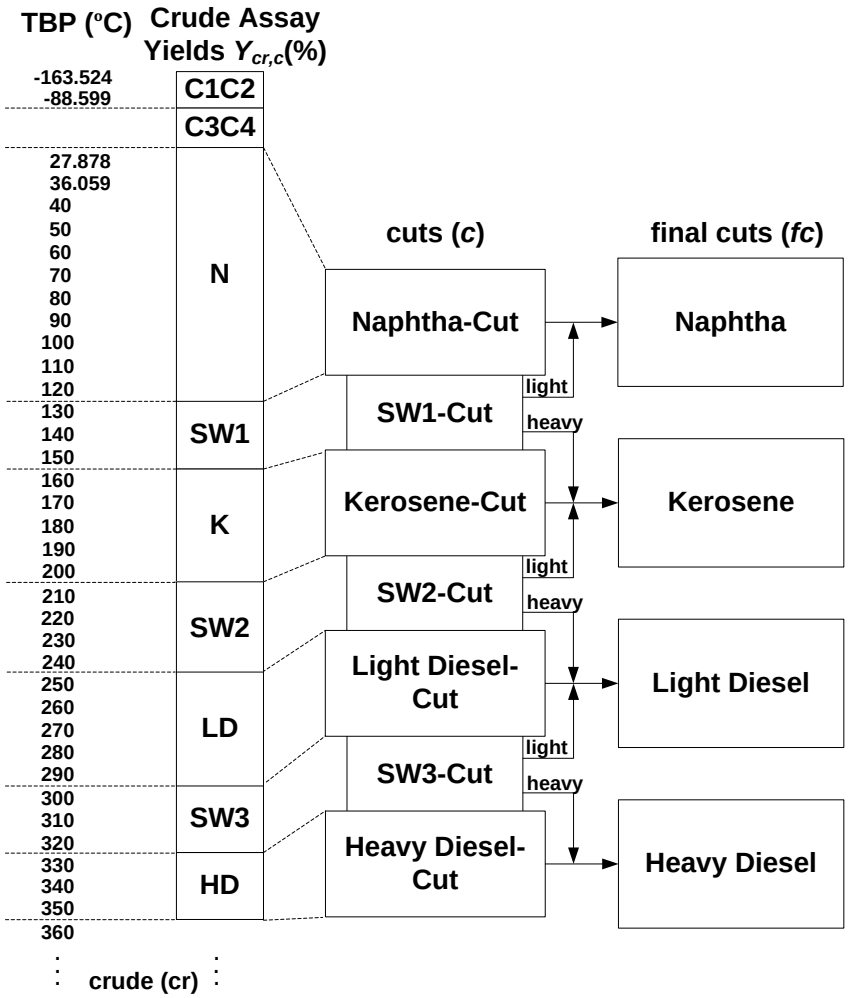

Figure 3.3. Cut and swing-cut material flow modeling for CDU yields.

Given the CDU and VDU (vacuum distillation unit) configurations in Figure 3.2, the crude is separated into different internal cut; some of them can swing (SW1, SW2, SW3) between their adjacent final-cuts or final distillates as seen in Figure 3.3. Each crude *cr* to be processed $Q_{cr,CDU}$ is defined as a CDU throughput QF_{CDU} volume ratio υ_{cr} as in Equation 3.1, whose sum is calculated by Equation 3.2.

$$Q_{cr,CDU} = \upsilon_{cr} QF_{CDU} \quad \forall\, cr \tag{3.1}$$

$$\sum_{cr} \upsilon_{cr} = 1 \quad \forall\, CDU \tag{3.2}$$

The quantity of CDU/VDU internal cuts *c* flowing to the final-cuts *fc* $Q_{c,fc}$ is given by crude-oil assay data in Table S3.1 (see the Supporting Information) and crude feed. $Y_{cr,c}$ represents the yields for the CDU and VDU cuts (with some as swing-cuts) based on the crude assay. Only the swing cuts flow to both adjacent final-cuts. For other cuts, the first sum

in Equation 3.3 has only one term, because the no-swing cuts flow only to their respective final-cuts as represented in Figure 3.3.

$$\sum_{fc} Q_{c,fc} = \sum_{cr} Q_{cr,CDU} Y_{cr,c} \quad \forall\, c \tag{3.3}$$

$G_{cr,c}$, $S_{cr,c}$, and $A_{cr,c}$ in Table S3.2 to Table S3.4 (see the Supporting Information) represent the specific gravity, sulfur content, and acidity of each cut in the crude assays. G_c and S_c in Equations 3.4 and 3.5 are the specific gravity and sulfur content values for each internal cut considering the CDU crude diet pool found in the model. The acidity value for each cut A_c, which is not represented, is a mass-based property like sulfur content.

$$G_c = \frac{\sum_{cr} G_{cr,c} Q_{cr,CDU} Y_{cr,c}}{\sum_{cr} Q_{cr,CDU} Y_{cr,c}} \quad \forall\, c \tag{3.4}$$

$$S_c = \frac{\sum_{cr} S_{cr,c} Q_{cr,CDU} G_{cr,c} Y_{cr,c}}{\sum_{cr} Q_{cr,CDU} G_{cr,c} Y_{cr,c}} \quad \forall\, c \tag{3.5}$$

After the CDU feed defines the quantity of cuts flowing to the final-cut pools $Q_{c,fc}$, as in Equation 3.3 and cut qualities, as in Equations 3.4 and 3.5, another blending occurs to find the final-cuts *fc* quantities and qualities, Equations 3.6-3.8. Only in the final-cuts with swing-cuts in between can the qualities G_{fc}, S_{fc}, and A_{fc} change. All VDU final-cut qualities are equal to those of their respective cuts, calculated by Equations 3.4 and 3.5.

$$QS_{fc} = \sum_{c} Q_{c,fc} \quad \forall\, fc \tag{3.6}$$

$$G_{fc} = \frac{\sum_{c} G_c Q_{c,fc}}{\sum_{c} Q_{c,fc}} \quad \forall\, fc \tag{3.7}$$

$$S_{fc} = \frac{\sum_{c} S_c G_c Q_{c,fc}}{\sum_{c} G_c Q_{c,fc}} \quad \forall\, fc \tag{3.8}$$

The final-cut acidity A_{fc} is calculated as shown for S_{fc}. As noticed, the properties G_c, S_c, and A_c for each swing-cut, based on the crude diet and assay, are the same in both adjacent final-cuts. This is the main simplification in the swing-cut model, which considers that the light and heavy swing-cut fractions have the same qualities. If the swing-cut flows to its

adjacent lighter distillate it carries heavy ends, which will influence properties such as sulfur content and gravity of the lighter distillate. Similarly, moving the swing-cut to its adjacent heavier distillate will bring light ends, particularly affecting properties such as the viscosity and flash point, which are more sensitive to light ends (Li et al., 2005). In the context of this work, this simplification is quite acceptable for strategic plans, and an improved swing-cut model addressing quality variations for both light and heavy swing-cut streams will be seen in Chapter 5. A similar approach to that of the swing-cut model described in this work is used by the Energy Information Agency (EIA) to plan fuel balance in the United States (Divita, 2009); however, it considers average fixed qualities for the final distillates, as it is being treated here for other unit output stream properties.

We consider the yield and property variations to predict distillation tower outputs by permitting crude-oil diet and final-cut variation, a big step toward improve the planning results in a high-level decision-making model in the oil-refining industry. Despite model improvements by considering nonlinearities, which in turn tend to be ill-conditioned when size increases, global optimal solutions are not a guarantee in non-convex models. Initial value randomization and do/loop searching can find better results iteratively.

3.2.2. Other oil-refinery units

As mentioned, product yields and properties for other oil-refinery units are considered averaged fixed values. The yield $Y_{u,s}$ for each stream s is given as a unit throughput ratio forming the output or stream flows $QS_{u,s}$, as seen in Equation 3.9. All necessary data are given in Table S3.5 (see the Supporting Information).

$$QS_{u,s} = Y_{u,s} QF_u \quad \forall \; u, s \tag{3.9}$$

Moro et al. (1998), Pinto et al. (2000), and Neiro and Pinto (2004) modeled operational planning and scheduling cases for refining process units considering a network whose streams are linked to them by mixers and splitters as shown in Equations 3.10 and 3.11; the former concentrates streams from upstream unit u' ($u' \in up$) into the unit u, and the latter distributes the unit streams or outputs to downstream unit u' ($u' \in do$). The units are connected considering the framework shown in Figure 3.2.

$$\sum_{u' \in up} Q_{u',s',u} = QF_u \quad \forall \; u \tag{3.10}$$

$$QS_{u,s} = \sum_{u' \in do} Q_{u,s,u'} \quad \forall \; u,s \tag{3.11}$$

As specific gravity and sulfur content are included in the model to allow variations in the final product qualities based on crude diet and swing-cut variations, it is important to consider modification of properties in hydrotreaters (HT). The unit removes sources of molecular instability and contamination such as sulfur, nitrogen, metals, and unsaturated hydrocarbons. As the unit operates at high pressure and temperature, some molecular cracking inevitably occurs; thus, some properties such as specific gravity and octane number change. In this work, sulfur reduction promoted by the hydrotreaters is modeled as a variable $\Upsilon_{HT,t}$, as seen in Equation 3.12. The lower and upper bounds for the medium and high severity hydrotreaters for diesel are $0.800 \leq \Upsilon_{D1HT} \leq 0.980$ and $0.960 \leq \Upsilon_{D2HT} \leq 0.998$, respectively. For gasoline hydrotreaters (LCNHT and CLNHT) are $0.500 \leq \Upsilon_{LCNHT/CLNHT} \leq 0.990$. Severity in kerosene hydrotreater (KHT) is not being considered. The specific gravity reduction factor Δ_{HT} promoted by residual molecular cracking is treated as a fixed value for all hydrotreaters like in Equation 3.13 and its value in this work is 0.99.

$$S_{HT,s} = S_{HT}(1 - \Upsilon_{HT}) \quad \forall \; HT,s \tag{3.12}$$

$$G_{HT,s} = G_{HT}\Delta_{HT} \quad \forall \; HT,s \tag{3.13}$$

Specific gravity G_{HT} and sulfur content S_{HT} in hydrotreater feed are volume- and mass-based properties calculated by Equations 3.7 and 3.8, respectively, considering the final distillates or final-cuts *fc* as a unit feed mix (mixer) and the cut properties (G_c and S_c) as the properties of each upstream flowing to the unit. The properties for the blended crude-oil processed and intermediate and final products are found in the same way. Mixing and splitting involving oil-refinery units, other blending rules and properties, and other processing transformations can be found in mentioned authors (Moro et al., 1998; Pinto et al., 2000; and Neiro and Pinto, 2004).

3.2.3. Octane number calculation: Ethyl equation

The octane number calculations presented in Equations 3.14 and 3.15 are the ethyl formulations to predict the research octane number *RON* and motor octane number *MON* needed to determine the retail gasoline recipe. The octane rating or number is a gasoline property related to the combustion efficiency in Otto cycle engines in which the maximum compression ratio is intended at the ignition spark, avoiding spontaneous ignition under high-pressure conditions.

The blending correlation for *RON* and *MON* is highly nonlinear and depends on the recipe components to be calculated, because it considers molecular interactions based on the aromatic *ARO* and olefin *OLE* contents. $RONV_s$ and $MONV_s$ represent blending values for *RON* and *MON* of each component in the gasoline pool, whose final *RON* and *MON* values are volume-based properties considering blending values $RONV_s$ and $MONV_s$ as the component properties. The blending value of a blending component changes with the molecular composition and recipe; thus, it is different for every blend (Barsamian, 2007).

RON_s, MON_s, OLE_s and ARO_s represent properties for each stream *s*, component of the gasoline formulation as shown in Figure 3.2. They are fixed for the streams in Table S3.5 (see the Supporting Information) and calculated as a blend for coker light naphtha hydrotreater (CLNHT) output and for the gasoline C (GLNC) blender stream. J_s is the octane number sensibility defined as RON_s-MON_s. J_V (RON_V-MON_V), RON_V, MON_V, OLE_V, and ARO_V are volume-based properties. ARO_{VQ} is the volume-based property for ARO^2. The coefficients *a* to *g* are given in Table S3.6 (see the Supporting Information), but they can be determined experimentally. *RON* and *MON* decrease by values of 1.2 and 1 after hydrotreating units.

$$\begin{aligned} RONV_s = {} & RON_s + a[(RON_s - RON_V)(J_s - J_V)] + b(ARO_s - ARO_V)^2 \\ & + c(OLE_s - OLE_V)^2 \\ & + d[(ARO_s - ARO_V)(OLE_s - OLE_V)] \quad \forall\, s \end{aligned} \tag{3.14}$$

$$\begin{aligned} MONV_s = {} & MON_s + e[(MON_s - MON_V)(J_s - J_V)] + f(ARO_s - ARO_V)^2 \\ & + g\left[2(OLE_s - OLE_V)^2\left(ARO_{VQ} - {ARO_V}^2\right)\right. \\ & \left. - \left(ARO_{VQ} - {ARO_V}^2\right)^2\right] \quad \forall\, s \end{aligned} \tag{3.15}$$

3.3. Problem Statement: The Brazilian Oil Industry Scenario

Using the proposed NLP operational planning model, it is analyzed the national fuel balance of each scenario taking into account the situation in 2013 and the planned investments and different product demands in 2016 and 2020. Data from several official sources were considered to represent the situation in 2013 that is the baseline on which the other ones were drawn. The national fuel production and processed crude results are used to validate the scenario in 2013. In the next subsections the available data on the Brazilian oil-refining industry and the production and market scenarios are presented.

3.3.1. Fuels demands and production

Figure 3.4 shows the national fuel production and demands during the period 2000-2012 and the future demands considering the 2009-2012 boost in fuel demands in the country. In the work it is proposed future fuel market scenarios considering (1) 4.2% p.a. (per year) for all fuels, based on the Brazilian GDP forecast (ANP, 2013) and (2) 2009-2012 trends for each fuel as in Figure 3.4 considering GLNC and $GLNC_{ETH}$ scenarios for gasoline.

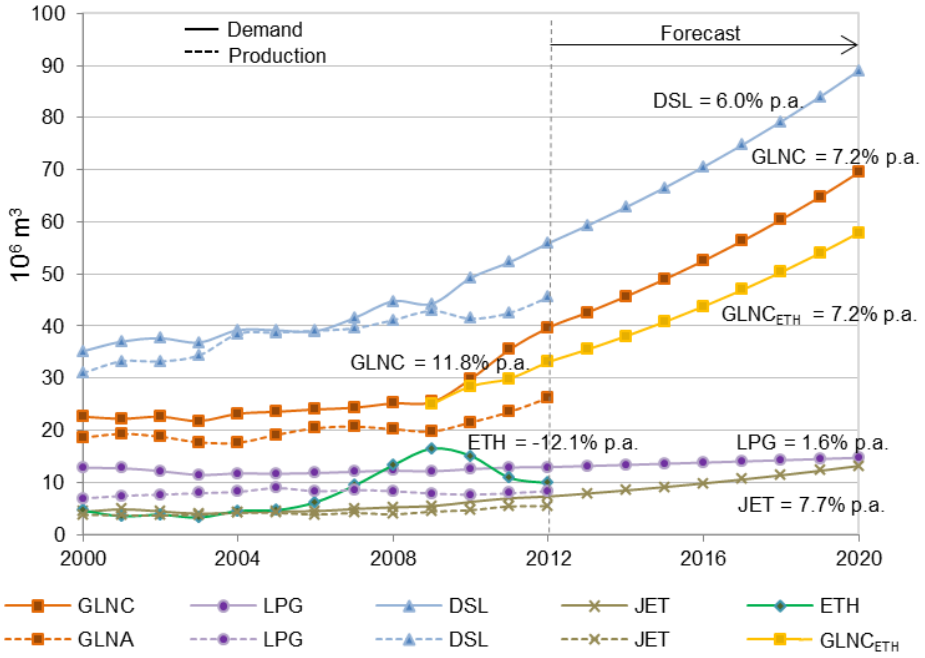

Figure 3.4. Demand and production levels and forecast considering the 2009-2012 trends.

The boost in national fuel demands after the 2008-2009 global crisis is considered a representative alternative for the future market scenarios. This situation is a consequence of the economic growth in the country and is still expected to rise even with the economic and

political instability in Brazil that emerged in 2013 and the 2008-2009 economic crisis uprising return worldwide.

3.3.2. Gasoline-Ethanol mix and ethanol for fueling

Ethanol commercialization presents particular dynamics for small and medium cars fleets in Brazil. It can be part of the retailed gasoline and up to 100% fuel in flex-fuel fleets. The ethanol content in the retailed gasoline varies between 25 to 18% in volume, a proportion controlled by the ethanol market demand and prices. During periods when the country needed to import ethanol to blend into gasoline A (pure gasoline, without ethanol), the ethanol content was 18%. The value considered in this work is 25% which is the current situation without any influence from the ethanol market, a preferred condition due to the gasoline deficit in the country. Retailed gasoline (GLNC) is a mix of gasoline A (GLNA) and ethanol permitted by the blended volume range (25 to 18% in volume). Ethanol content higher than 25% in gasoline can negatively affect the performance of a non-flex-fuel automobile and intensify corrosion problems inside the motor. Today in Brazil, flex-fuel fleet sales represent 90% of the market in both the small- and medium-car categories, and it is expected that the total flex-fuel fleet in these categories, currently at around 60%, will reach 80% within the next 5 years.

In addition to the normal demand increase in fuels, the GLNC demand increase in the period 2009-2012 (11.8% p.a.) was influenced by the ethanol for fueling (ETH) to GLNC consumer preference shift. This occurred because of the ethanol price surge, which was an effect of nationwide sugar cane harvesting problems in 2009 and of the escalation of sugar demand overseas, both of which shaped the current ETH-GLNC fuel preference. Besides, the widening demand for retailed gasoline maintains the ethanol demand and price growth once ethanol is included in its formulation. As a consequence, the relative price between ethanol for fueling and retailed gasoline remains higher than 0.7, so that gasoline is more attractive for fueling. Considering the heats of combustion and engine efficiency of both fuels, when ETH prices are higher than 70% of the GLNC it is considered more profitable to fuel the car. For values lower than 70%, ETH is preferred. This fact is well-known to the consumer who compares the ETH/GLNC relative price and decides which fuel to buy.

Considering the gasoline/ethanol market stabilization, the retailed gasoline demand growth considered in Figure 3.4 is 7.2%, which is its increase discounting the ethanol for

fueling demand decrease during 2009-2012, hence excluding the influence of the ETH (100% ethanol) shift. As shown, the ETH shift to GLNC reached its steady state in 2012, and on the bases of this fact, we consider that the range of demand for retailed gasoline plotted in the graph represents the equilibrium between GLNC and ETH driven by the consumer of the flex-fuel fleet. GLNC is the current situation considering the ETH shift stabilization, and $GLNC_{ETH}$ is the situation where the ETH demand decrease is discounted from the retailed gasoline demand increase between 2009 and 2012.

3.3.3. Future fuels demands

This work simulates the production and market scenarios in an operational planning manner to find the best operational setting, so the future fuel demands are given in a daily flow considering the demand scenarios shown in Table 3.1. Table 3.2 shows the diesel grade evolution for the next several years (MPF, 2009), which is taken into consideration when future diesel demands are defined.

Table 3.1. Demand forecast for 2016 and 2020.

				2009-2012 trends		4.2% p.a.	
product			2013*	2016	2020	2016	2020
liquid petroleum gas		LPG	36.2	38.6	41.2	42.6	50.2
gasoline C		GLNC	112.4	148.8	196.8	132.5	156.2
gasoline C – ethanol ↓		$GLNC_{ETH}$	90.6	119.9	158.6	106.8	125.9
jet fuel		JET	19.7	26.4	35.5	23.2	27.3
diesel	10 wppm	DSL	16.0	60.6	153.0	56.6	133.5
	500 wppm		80.1	90.9	51.0	84.9	44.5
	1800 wppm		56.0	40.4	45.9	37.7	40.1
	3500 wppm		8.0	10.1	5.1	9.4	4.5
Diesel Total			160.1	202.0	254.9	188.7	222.5

* past 12 months until October, 2013 (ANP, 2013)

Table 3.2. Diesel grades market.

	2013	2016	2020
10 wppm S	10%	30%	60%
500 wppm S	50%	45%	20%
1800 wppm S	35%	20%	18%
3500 wppm S	5%	5%	2%

3.3.4. Current and planned capacities in 2013, 2016 and 2020

The refinery configuration considered in the work is shown in Figure 3.2. Table 3.3 shows the capacities of the units for the three production scenarios aforementioned. All data regarding the overall oil-refinery units capacities considered for the productive scenarios are presented in Perrissé (2008). In the cases of study, the minimum feed allowed for the units is 68% of their overall capacity, excepted in the units showed with a mark * in Table 3.3 and in the propane deasphalting unit (PDA), which is 30%.

Table 3.3. Overall refining processes capacities for the three production scenarios (k m^3/d), excluding lubricant plants.

	2013	2016	2020
crude distillation unit (CDU)	310*	372*	536
vacuum distillation unit (VDU)	140*	153*	260
residue fluid catalytic cracking (RFCC)	22	22	22
fluid catalytic cracking (FCC)	76	76	76
hydrocracking (HCC)		10	74
propane deasphalting (PDA)	10	10	10
delayed coker (DC)	42	50	100
delayed coker with atmosferic residue as feed (DCA)		24*	24*
light cracked naphtha hydrotreater (LCNHT)	54	54	54
coker light naphtha hydrotreater (CLNHT)	22	34	62
stabilizer (ST)	22	34	62
kerosene hydrotreater (KHT)	15*	15*	15*
diesel hydrotreater (medium severity) (D1HT)	60*	60*	60*
diesel hydrotreater (high severity) (D2HT)	30*	68*	135
reformer (REF)	7	12	20**

* upper and lower bounds are the same to avoid local solution

** added 8 k m^3/d arbitrarily (different from conceptual project) to yield feasible results

3.3.5. National and imported crude oils

Figure 3.5 shows crude-oil amounts considering national production, imports, and processing as well as the export and import prices. As shown, since 2008 the country has been self-sufficient in equivalent oil but still needs ultralight oil imports to increase medium distillate (jet fuel and diesel) production and paraffinic oil for lubricants.

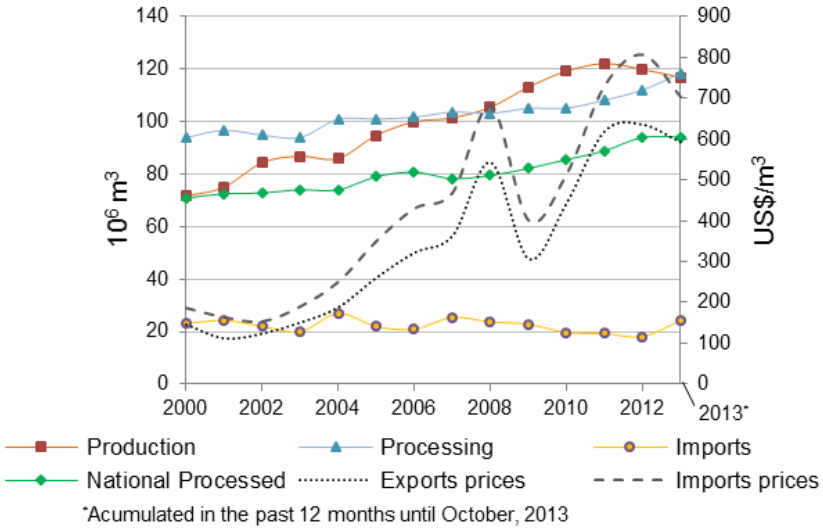

Figure 3.5. Crude-oil produced, imported and processed and imports and export prices (ANP, 2013).

In Figure 3.6, the national oil production is distributed in four ºAPI ranges (ultralight, light, medium, heavy) and the average ºAPI and sulfur content of each group are shown as well as the national average values (24.36 ºAPI and 0.536 % S).

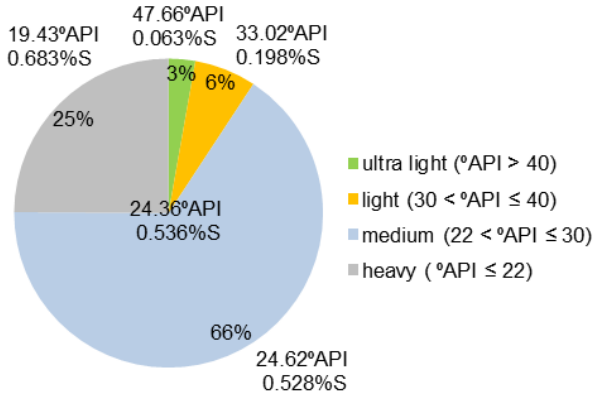

Figure 3.6. National crude-oil production in 2012 (ANP, 2013).

In this work five different crude oils are considered to represent the national and importd groups. The national medium crude is split into presalt and medium. The presalt crude is considered medium-light to light oil and represented 14% of the entire national production in 2012. Ultralight crude is given to represent the imports to achieve the optimal ºAPI for the crude blend to be processed in the Brazilian fuel market and production scenarios. The crude oils considered are shown in Table 3.4 and the crude diet upper bounds υ_{max} of the national crude to be processed are defined by their production in 2012 as seen in Figure 3.6. For the 2016 and 2020 scenarios, the presalt crude is predicted to increase to 22% and 33%, respectively, as expected by PETROBRAS (PETROBRAS, 2013a), and the

medium upper bound ratio is reduced to maintain medium and presalt crude sum in 66% as considered in Figure 3.6.

Table 3.4. Crude oils considered in this work.

crude		ºAPI	G (g/cm^3)	S (%)	A (mgKOH/g)	υ_{max}
national	light	33.2	0.859	0.091	0.226	0.09
	presalt	29.7	0.878	0.344	0.255	0.14
	medium	25.2	0.903	0.519	0.196	0.52
	heavy	20.5	0.931	0.608	1.007	0.25
imported	ultra light	45.2	0.801	0.049	0.096	

3.3.6. Crude and fuel prices

Crude and fuel prices and their sources are shown in Table 3.5. The price baseline is considered that in 2013 with a growing rate of 4.2% per year (p.a.) as expected for the GDP rate considered in this work. Crude prices per m^3 of US$ 702 for the imported oil and US$ 587 for the exported oil are considered (average value in the past 12 months until October, 2013) (ANP, 2013). The country exports unprocessed heavy and medium crude, and considering the national heavy crude price of US$ 570 and the exported crude composed by 30% medium and 70% heavy (in volume), the medium oil price estimate is US$ 592. For the national light and presalt crude, prices take an intermediate value between national medium and Brent oils, closer to the medium, because they are national crude and heavier than the Brent. The standard crude-oil Brent (38 ºAPI, 0.45 % S) price considered is US$ 687 (US$ 109.2 per barrel) in the North Sea port (EIA, 2013). Fuel prices are defined by the retail prices in the past 12 months until October 2013 (ANP, 2013; UNICA, 2013) and the producer percentages shown in Figure 3.7. The imported prices consider the U.S. Gulf Coast region (EIA, 2013), adding transport expenses and taxes.

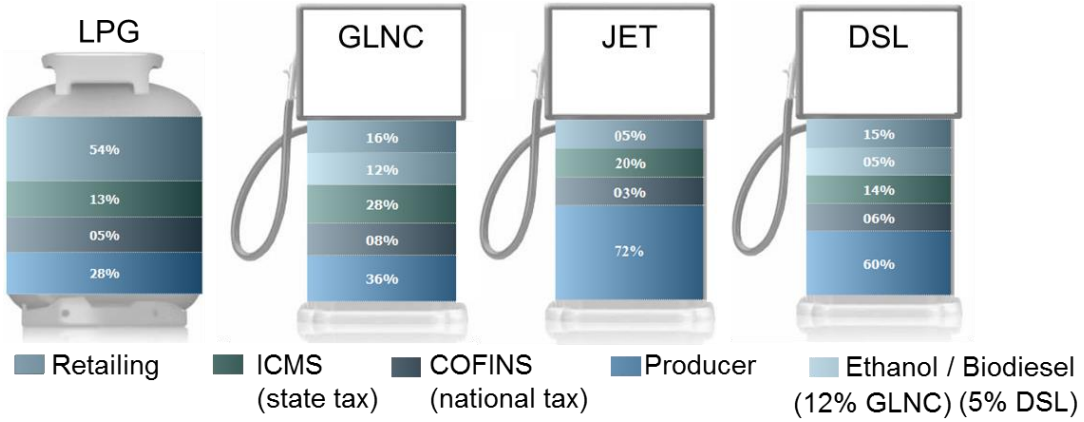

Figure 3.7. Fuels prices percentage (PETROBRAS, 2013b; Agencia T1, 2013).

Table 3.5. Prices (US$/m^3) of crude, products, and imports in Brazil grow at a rate 4.2% p.a.

			2013	2016	2020
crude*	national	light	600.0	678.8	800.2
		presalt	595.0	673.2	793.6
		medium	592.0	669.8	789.6
		heavy	570.0	644.9	760.2
	imported	ultralight	702.0	794.2	936.3
products*	FG				
	LPG		380.0	429.9	506.8
	naphtha		545.0	616.6	726.9
	gasoline C		618.3	699.5	824.7
	jet fuel		760.0	859.8	1013.6
	diesel	10 wppm S	662.0	749.0	882.9
		500 wppm S	636.0	719.5	848.3
		1800 wppm S	623.3	705.2	831.3
		3500 wppm S	610.8	691.1	814.7
	FO		416.0	470.6	554.8
	coke		530.0	599.6	706.9
ethanol§			590.0	667.5	786.9
imports†	LPG		398.2	450.5	531.1
	gasoline A		762.3	862.4	1016.7
	jet fuel		860.0	973.0	1147.0
	diesel	15 wppm S	834.1	943.7	1112.5

*ANP (2013) §UNICA (2013) †EIA (2013)

3.3.7. Crude and fuel quality specifications

Upper and lower bounds of the CDU feed properties and the specifications of final product properties are shown in Table 3.6.

Table 3.6. CDU feed and final products property specifications.

		G_{min}	G_{max}	S_{max}	A_{max}	MON_{min}	RON_{min}
CDU feed		0.850	0.950	0.800	0.60		
GLN (GLNC)		0.720	0.775	0.005		82	88
JET		0.771	0.836	0.300			
DSL	10 wppm S	0.820	0.850	0.001			
	500 wppm S	0.820	0.865	0.050			
	1800 wppm S	0.820	0.880	0.180			
	3500 wppm S	0.820	0.880	0.350			

G [=] g/cm^3 S [=] % A [=] mgKOH/g

3.3.8. Other relations

Two other constraints are related to (i) the current official ethanol content in the retailed gasoline pool (GLN), Equation 3.16, and (ii) the maximum concentration of coker light naphtha (CLN) from delayed coker units (DC or DCA) in the coker light naphtha hydrotreater (CLNHT) feed, Equation 3.17. This upper bound for CLN streams protects the catalyst bed from high metal concentration poisoning.

$$QF_{ETH} = 0.25QF_{GLN} \tag{3.16}$$

$$Q_{DC/DCA,CLN,CLNHT} \leq 0.30QF_{CLNHT} \tag{3.17}$$

3.4. Operational Planning Objective: Daily Operational Profit

Eight future scenarios in 2020 are illustrated in Figure 3.8. At the first, consumer preference between ethanol for fueling and retail gasoline is taken as a starting point by discounting and not the ethanol shift proposed previously (see Figure 3.4). The second choice is the demand increase rate considering 2009-2012 trends for each fuel and 4.2% p.a. for all, and the last option is to consider the refineries in conceptual design to be built or not in 2020 in order to avoid a deficit of 30% in oil products. Crossover over the time is not permitted; so that once a scenario option is selected it is true for the following scenarios.

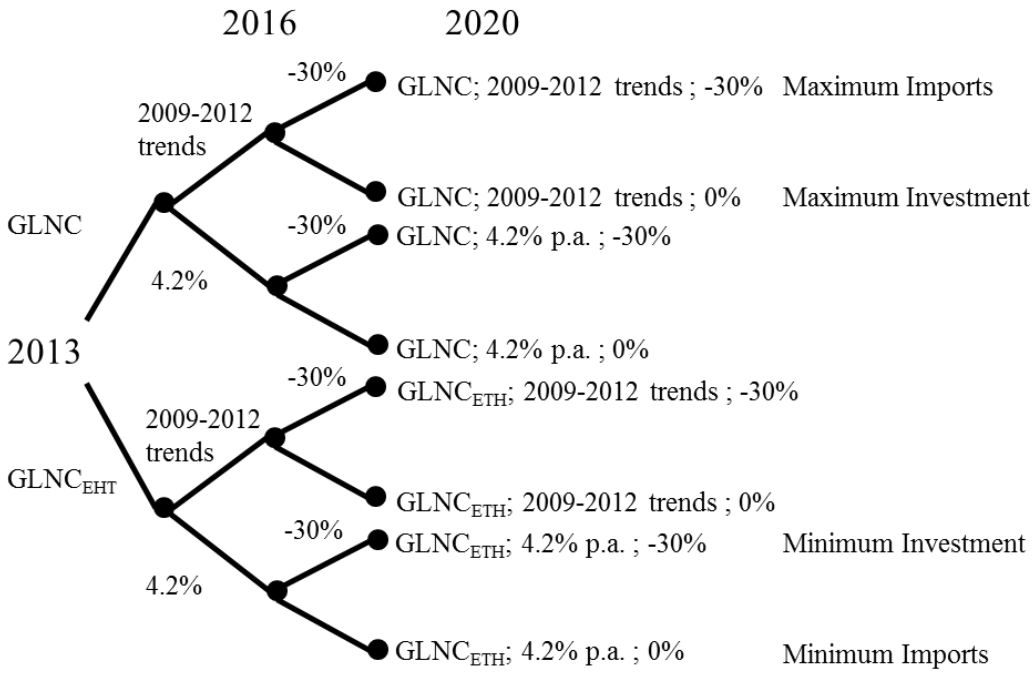

Figure 3.8. Initial, intermediate, and final scenarios considered.

The single-period objective function in millions of U.S dollars per day is summarized in Equation 3.18. Operational costs from inventory, utilities (steam, water, hydrogen, nitrogen, fuel gas, electricity), and materials like catalysts and chemicals are not directly considered in the model. Ref_{cost} approximates the overall refining costs in US$ 4.5 per barrel of product (US$ 28.3/m^3) for a standard production cost at American refineries (EIA, 2013). Additionally, to avoid sulfur content giveaway when we have different grades of diesel, it is a good practice is to consider hypothetical blender for each grade and HT operational costs defined as a function of its feed flow QF_{HT} similar to a penalty in the objective function. The taxes are discounted from the profit considering a fixed tax ratio *tr* of 25%, what is a practice in Brazil for companies' profit taxes.

The operational planning model includes Equations 3.1-3.18. The crude amounts $QF_{cr,CDU}$ are determined by prices *pr*, product demands, processing structure, and product specifications like specific gravity, octane number, sulfur content and acidity. Products amounts QF_p supplying demands are set to be only 1% apart, avoiding surplus of any fuel.

$$\max\ profit = (1 - tr)\left(\sum_{p}(pr_p - Ref_{cost})QF_p - \sum_{cr} pr_{cr}QF_{cr,CDU} - \sum_{imp} pr_{imp}QF_{imp} - \sum_{HT} QF_{HT}\right) \quad (3.18)$$

Seasonal variations regarding demands can be considered by verifying the level of flexibility for the refining framework for gasoline and diesel maximization modes. Annual average demand data of 2013 are used as the baseline for the cases in analysis, so these seasonal variations are not being included in the scope of this work.

3.5. Results and Discussion

The national refining framework and fuel market demands in October 2013 are the baselines to find the intermediate scenarios for 2016 and the eight scenarios for 2020 as previously defined. For the 2020 cases with the projects in the conceptual phase performed, if the unit throughput is lower than the planned capacity, which in the model is the throughput upper bound $QF^{U}_{u,t}$, the country's capacity planning for 2020 needs refitting. All case studies were implemented in the GAMS modeling system (Brook et al., 2002), version 23.9.3, on an Intel Core 2 Duo (3.00 GHz, 16.0 GB of RAM) and used as starting points unit capacities,

output standard values for flows and given specifications for calculated properties. The overall data given in this work can be used to find initial values. The NLP problems are solved by nonlinear general-purpose optimizers such as CONOPT, which is based on the reduced gradient method, IPOPT, which utilizes interior point methods, and the solver SNOPT, which is based on successive quadratic programming.

3.5.1. Pricing policy in 2013

Table 3.7 shows the profit obtained to match country's demands in the 2013 GLNC baseline scenario (Table 3.1) considering different pricing policies. As indicated, the current refining activity in Brazil is not profitable on a stand-alone view. This is a well-known condition due to the lower national producer prices of gasoline and diesel in comparison with import prices. If prices in U.S. Gulf are considered for gasoline and diesel 15 wppm S (682.43 and 760.89 US$/m^3, respectively), the national-international (Brazil-US) loss difference (-16.761 million US$/d) is close to the estimate of the Brazilian Center of Infrastructure (OGLOBO, 2013), which evaluated losses from January to May, 2013 of 2.2 billion US$ (-14.379 million US$/d). The prices for other grades of diesel have the same price relation found in Table 3.5. As the country needs to import gasoline and diesel to supply the market, the price difference between domestic market and imports is bore by the national oil and energy company PETROBRAS. Although the country needs to import LPG and jet fuel, these fuels do not damage the company's profitability because of the state LPG subsidies and the jet fuel uncontrolled prices. Currency variation along the year is not being considered and it is fixed in 2.2 R$/US$.

The new pricing policy announced Nov 29, 2013 increased the producer price of retail gasoline by 4% and diesel by 8%, but this move was not sufficient to overcome the daily refining losses in the country (-13.786 million US$/d). In this work it is considered price increases of 15% for retail gasoline and 20% for diesel in its different grades to yield a positive gain (1.068 million US$/d). This price rise is evaluated by the market as the demanded pricing policy to avoid losses and get a minimal margin return (of around US$ 0.5/barrel). This obtain positive gain policy is considered to calculate future scenarios in the daily single-period NPL operational planning model for fixed production frameworks in 2013, 2016, and 2020.

Table 3.7. REBRA profit for the different gasoline and diesel pricing policies.

million US$/d		last 12 months until October		November 29th Policy	Demanded Policy
		Brazil	US Gulf	Brazil	Brazil
profit		-21.951	-5.190	-13.786	1.068
sales		228.901	251.249	239.788	259.594
crude costs		186.213	186.213	186.213	186.213
imports costs		60.518	60.518	60.518	60.518
operational costs		11.289	11.289	11.289	11.289
HTs costs		0.150	0.150	0.150	0.150
profit / crude	US$/m^3	-70.81	-16.74	-44.47	3.45
	US$/barrel	-11.26	-2.66	-7.07	0.55
no. of equations		406			
no. of variables		460			
no. of non zero elements		1772			
no. of non linear elements		1061			
CPU (s)	CONOPT	0.328	0.421	0.452	0.359
	IPOPT	0.952	1.123	0.827	2.012
	SNOPT	0.125	0.063	0.062	0.156

Table 3.8 shows the 2013 scenarios and all possible intermediate scenarios until 2016. The limit demands for retail gasoline are represented by GLNC and $GLNC_{ETH}$. The former is the current market and production scenario in which the ethanol to GLNC shift reached its steady state. $GLNC_{ETH}$ discounts the ethanol consumption decrease since its price surge in 2009. The current scenario in 2013 (GLNC) is compared with the national actual data for fuel production and crude-oil processed as shown in Table 3.9.

The calculated data presented reasonable accuracy when compared with the national results in Table 3.9. The imported crude represented 19% of all processed crude by the country in the past 12 months until October 2013 (ANP, 2013), but discounting the distillation for lubricants, which are not considered in this work, the national imported crude for fuel production is around 12.2%, which is very close to the value found in the proposed model (11.9%). Also the °API calculated for the processed crude presented good adherence. When compared with the national crude oil production (average of 24.36 °API), it became clear the need for importing light or ultralight crude for the processed crude-oil blend in the current refining assets.

Table 3.8. 2013 and 2016 production and market scenarios (thousand cubic meter per day [=] k m^3/d).

			2013		2016			
					2009-2012 trends		4.2% p.a.	
			GLNC	$GLNC_{ETH}$	GLNC	$GLNC_{ETH}$	GLNC	$GLNC_{ETH}$
crude diet	national	light	9.0	9.0	9.0	9.0	9.0	9.0
(% vol)		presalt	14.0	14.0	22.0	22.0	22.0	22.0
		medium	40.1	40.1	33.6	33.6	33.6	30.9
		heavy	25.0	25.0	25.0	25.0	25.0	25.0
	imported	ultralight	11.9	11.9	10.4	10.4	10.4	13.1
LPG	national		16.8	16.3	20.7	20.7	20.7	20.3
	imported		19.3	19.9	17.9	17.9	21.9	22.3
	sales		36.2	36.2	38.6	38.6	42.6	42.6
gasoline C	national	GLNA	72.1	68.0	84.0	83.6	83.8	80.1
(GLNC)	imported	GLNA	12.3		27.6	6.3	15.6	
		Ethanol	28.1	22.7	37.2	30.0	33.1	26.7
	sales	GLNC	112.4	90.6	148.8	119.9	132.5	106.8
jet fuel	national		15.0	15.0	16.8	16.8	16.8	16.8
(JET)	imported		4.7	4.7	9.6	9.6	6.4	6.4
	sales		19.7	19.7	26.4	26.4	23.2	23.2
diesel	national	10 wppm S	16.0	16.0	60.6	60.6	56.6	56.6
(DSL)		500 wppm S	52.6	51.1	56.9	56.9	64.2	65.3
		1800 wppm S	56.0	56.0	40.4	40.4	37.7	37.7
		3500 wppm S	8.0	8.0	10.1	10.1	9.4	9.4
	imported	15 wppm S	27.4	29.0	34.0	34.0	20.7	19.7
	sales		160.1	160.1	202.0	202.0	188.7	188.7

Table 3.9. Actual and calculated data for the current scenario (GLNC) in 2013.

Processed Crude			Fuel Production (k m^3/d)		
actual*		calculated	actual*	product	calculated
27.9	°API	27.6	22.2	LPG	16.8
12.2	imported (%)	11.9	76.4	GLNA	72.1
			15.3	JET	15.0
			133.3	DSL	132.7

*past 12 months until October, 2013 (ANP, 2013)

The calculated data presented reasonable accuracy when compared with the national results in Table 3.9. The imported crude represented 19% of all processed crude by the country in the past 12 months until October 2013 (ANP, 2013), but discounting the distillation for lubricants, which are not considered in this work, the national imported crude for fuel production is around 12.2%, which is very close to the value found in the proposed model (11.9%). Also the °API calculated for the processed crude presented good adherence. When compared with the national crude oil production (average of 24.36 °API), it became clear the need for importing light or ultralight crude for the processed crude-oil blend in the current refining assets.

Considering the main fuel production, the lower LPG found is expected since the model excludes LPG from CDU for lubricants, lubricant plants, and production from liquid natural gas plants and condensates. The lower GLNA obtained is a result of the production from non-PETROBRAS refineries excluded in this model, whose daily gasoline A production reaches around 4 k m^3/d. For JET and DSL the model presented good match compared with the actual data.

The $GLNC_{ETH}$ case in 2013 shows that, without the ethanol to gasoline market shift after 2009, the country would be able to cease gasoline imports, as in the period before the current flex-fuel fleet consumer preference setup between retail gasoline and ethanol for fueling. The $GLNC_{ETH}$ scenario lower profit in 2013 (see Table 3.10) is due to the lower FCC throughput and CDU stream differences comparing with the GLNC counterpart. It occurs to avoid fuel surplus, in this case for gasoline, and the outcome is higher LPG and diesel imports in the $GLNC_{ETH}$ scenario (see Table 3.8). Besides, the lower ethanol price (US$ 590/m^3) mixed at 25% in volume with refined gasoline (GLNA) to produce GLNC (US$ 711/m^3) contributes for higher profits in the GLCN scenario.

In the 2016 (2009-2012 trends) scenarios, the GLCN case presented lower profit. Crude diet, LPG, kerosene and diesel imports are similar in both GLNC and $GLCN_{ETH}$ scenarios (see Table 3.8), and only the costs related to gasoline and ethanol imports and the operational costs are varying in the profit calculation comparing both gasoline scenarios. As the GLCN-$GLCN_{ETH}$ deltas for sale amounts and import costs are practically equivalents, the higher operational costs in the GLNC pair (of 0.924 million US$/d) explain its lower profit.

In the 2016 (4.2% p.a.) scenarios, the $GLCN_{ETH}$ pair presented lower profit. In this case, the GLCN-$GLCN_{ETH}$ deltas for sale amounts, import costs, and operational costs are practically equivalents, but the crude diet in the $GLCN_{ETH}$ scenario uses more ultralight oil (see Table 3.8), which has higher prices.

The size of the models is shown in Table 3.10. For the 2016 and 2020 scenarios HCC was added and, as defined for the RNEST refinery, a new DC receiving ATR (DCA) as feed with a capacity equal to 24 k m^3/d is added. All three solvers (CONOPT, IPOPT, SNOPT) can solve the problems in less than 1 second and converge to the same result (profit) in each of the six scenarios in Table 3.10.

Table 3.10. Economic and model data for the 2013 and 2016 scenarios.

million US$/d		2013		2016			
				2009-2012 trends		4.2% p.a.	
		GLNC	$GLNC_{ETH}$	GLNC	$GLNC_{ETH}$	GLNC	$GLNC_{ETH}$
profit		1.068	0.161	3.529	4.177	5.150	4.482
sales		259.594	246.861	371.013	347.801	345.381	326.415
crude costs		186.213	186.213	252.249	252.249	252.249	253.475
imports costs		60.518	49.445	98.063	74.911	71.189	52.625
operational costs		11.289	10.843	15.797	14.873	14.878	14.145
HTs costs		0.150	0.146	0.199	0.199	0.199	0.195
profit / crude	US$/$m^3$	3.45	0.52	9.49	11.23	13.84	12.05
	US$/barrel	0.55	0.08	1.51	1.79	2.20	1.92
no. of equations		406		466			
no. of variables		460		532			
no. of non zero elements		1772		2115			
no. of non linear elements		1061		1276			
CPU (s)	CONOPT	0.515	0.374	0.655	0.453	0.608	0.514
	IPOPT	0.469	1.591	0.826	0.702	0.639	0.874
	SNOPT	0.078	0.078	0.156	0.125	0.110	0.140

3.5.2. Conceptual project scenarios in 2020

The proposed scenarios in 2020 take into account the projects in conceptual phase and whether they are executed for the four market scenarios; hence, eight cases are presented, as shown in Figure 3.8, with maximum and minimum investment and import cases. As shown in Table 3.11, in the four cases with projects in conceptual phase executed in 2020 (0% deficit) as planned, the unit throughput results indicate different overall capacity in all market demand cases, so the set of units to be expanded or installed needs refitting. In the 0% deficit cases is in real permitted fuel imports. It is only labeled 0% to contrast with the -30% deficit if the projects in conceptual phase were not executed.

The scenarios for 2020 in which the projects under conceptual phase were not executed lead to significant fuel import amounts, resulting in unacceptable high expenditures, trade deficit, and external dependence at critical levels. For the cases with the projects executed, only in the lower demand scenarios (4.2% and $GLNC_{ETH}$) can the country be free of gasoline, jet fuel, and diesel imports. For the cases that cannot count on the investments in the conceptual phase, the crude import remains at 9.8 and 7.6% for the 2009-2012 trends and 4.2% p.a., respectively, even with the presalt crude level at 33%. For the cases with investments, only in the scenario with maximum demands is it necessary to continue with crude import, but at a slight level (5.8%). In the other three cases, the country becomes free of

oil imports. In Table 3.12 the economic data for the scenarios in 2020 are shown. As expected, all cases with investments are more profitable because of lower fuel imports.

Additionally, to explore the comparison between the required and the planned capacities for 2020, GLNA, JET, and DSL imports were set to zero. But the results got feasible only in the minimum demands scenario (4.2% and $GLNC_{ETH}$). Table 3.11 shows the results for this case at the last column. The unit throughputs got higher upper bounds than its counterpart with relaxed fuel imports requirements. However, as shown in Table 3.12, the profit in this case was lower because of the additional crude expenses to feed the CDU, which is higher than the import costs decrease. When the refineries in conceptual project were defined before 2009, the strategic decisions considered were to be free of main fuel imports (GLNA, JET, and DSL) in 2020 and the gasoline ethanol market shift was not in mind at that time. In this way, the last column of Table 3.11 and Table 3.12 represents roughly the official scenario in the country used to plan unit capacity expansions for 2020. In this work, an overall 4.2% p.a. demand increase was adopted for the low fuel demand cases, as described in PETROBRAS business plan 2013-2017 (PETROBRAS, 2013a), which in real should have a different distribution growth rate throughout the different fuels. In the fuels production charts presented in the next subsection, the official scenario in 2020 (4.2% p.a. and $GLNC_{ETH}$) without GLNA, JET, and DSL import is considered.

Finally, considering the cases with projects in conceptual phase executed, the profit obtained ~15−20 million US$/d demonstrated the gasoline and diesel pricing policy adopted, desired to avoid losses today, can be flexible in the future. It happens because of the lower or zero import amounts in 2020.

Table 3.11. Production and market scenarios in 2020 (thousand cubic meter per day [=] k m^3/d).

			2009-2012 trends				4.2% p.a.				
			GLNC		$GLNC_{ETH}$		GLNC		$GLNC_{ETH}$		
			-30%	0%	-30%	0%	-30%	0%	-30%	0%	0%*
crude diet	national	light	9.0	9.0	9.0	9.0	9.0	9.0	9.0	9.0	9.0
(% vol)		presalt	33.0	33.0	33.0	33.0	33.0	33.0	33.0	33.0	33.0
		medium	23.2	27.2	23.2	33.0	25.4	33.0	25.4	33.0	33.0
		heavy	25.0	25.0	25.0	25.0	25.0	25.0	25.0	25.0	25.0
	imported	ultralight	9.8	5.8	9.8		7.6		7.6		
LPG	national		20.7	29.6	20.7	27.7	20.5	27.2	20.5	25.0	25.4
	imported		20.5	11.6	20.5	13.5	29.8	23.1	29.8	25.2	24.9
	sales		41.2	41.2	41.2	41.2	50.2	50.2	50.2	50.2	50.2
gasoline C	national	GLNA	84.7	111.7	84.1	105.3	84.1	104.6	83.7	94.5	94.5
(GLNC)	imported	GLNA	63.0	35.9	34.8	13.7	33.1	12.6	10.7		
		Ethanol	49.2	49.2	39.7	39.7	39.1	39.1	31.5	31.5	31.5
	sales	GLNC	196.8	196.8	158.6	158.6	156.2	156.2	125.9	125.9	125.9
jet fuel	national		16.8	28.3	16.8	28.3	16.8	27.3	16.8	27.3	27.3
(JET)	imported		18.7	7.1	18.7	7.1	10.5		10.5		
	sales		35.5	35.5	35.5	35.5	27.3	27.3	27.3	27.3	27.3
diesel	national	10 wppm S	67.8	141.5	67.8	127.0	73.1	133.5	73.1	115.2	133.5
(DSL)		500 wppm S	49.1	51.0	49.1	51.0	44.5	44.5	44.5	44.5	44.5
		1800 wppm S	45.9	45.9	45.9	45.9	40.1	40.1	40.1	40.1	40.1
		3500 wppm S	5.1	5.1	5.1	5.1	4.5	4.5	4.5	4.5	4.5
	imported	15 wppm S	87.2	11.4	87.2	26.0	60.4		60.4	18.3	
	sales		255.0	254.9	255.0	254.9	222.6	222.6	222.6	222.6	222.6
capacity	CDU	536		505.1		498.1		483.7		446.0	497.9
refitting	VDU	260		227.9		235.7		227.1		206.2	257.6
	HCC	74						68.4		68.4	68.4
	DC+DCA	124		117.6		106.5		103.8		94.2	94.2
	D2HT	135		114.7		103.2		106.6		92.6	104.8
	CLNHT	62		55.6		48.5		48.7		43.9	43.9
	ST	62		55.6		48.5		48.7		43.9	43.9
	REF	12		20.0		20.0		20.0		20.0	20.0

* GLNA, JET and DSL imports set to zero

Table 3.12. Economic and model data for the 2020 scenarios.

million US$/d		2009-2012 trends				4.2% p.a.				
		GLNC		$GLNC_{ETH}$		GLNC		$GLNC_{ETH}$		
		-30%	0%	-30%	0%	-30%	0%	-30%	0%	0%*
profit		-0.588	20.383	0.412	17.540	2.488	20.051	3.286	17.161	15.216
sales		551.475	553.397	515.270	526.105	479.397	483.168	450.653	450.967	469.756
crude costs		297.167	400.501	297.167	390.780	295.998	379.643	295.998	349.918	390.609
imports costs		232.004	102.329	195.906	89.391	159.483	55.744	130.814	58.533	37.989
operational costs		22.886	23.111	21.444	22.287	20.387	20.782	19.243	19.394	20.630
HTs costs		0.203	0.279	0.203	0.261	0.212	0.265	0.217	0.240	0.240
profit / crude	US$/$m^3$	-1.58	40.36	1.11	35.21	6.69	41.45	8.83	38.47	30.56
	US$/barrel	-0.25	6.42	0.18	5.60	1.06	6.59	1.40	6.12	4.86
no. of equations					466					
no. of variables					532					
no. of non zero elements					2115					
no. of non linear elements					1276					
CPU (s)	CONOPT	0.951	0.655	0.780	0.670	0.796	0.530	0.717	1.248	0.936
	IPOPT	0.874	1.467	1.139	0.639	1.045	0.983	0.655	2.386	1.700
	SNOPT	0.156	0.219	0.141	0.125	0.109	0.218	0.171	0.172	0.094
profit (local solution)										
	IPOPT		18.081		16.828		18.864		12.844	13.993
	SNOPT					2.421				

* GLNA, JET and DSL imports set to zero

3.5.3. Scenario-based fuel production charts

Demand, national production, and import amounts are plotted in Figure 3.9 to Figure 3.12 for LPG, GLNC, $GLNC_{ETH}$, JET, and total DSL. In Figure 3.9, the LPG production declined after 2012 because the model only considers LPG from refineries, excluding the production from other sources. Hence, the LPG production is higher than presented, and the imports are lower.

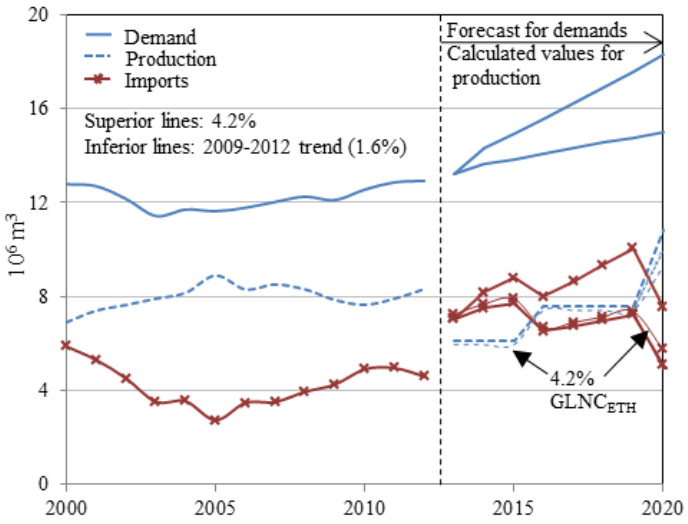

Figure 3.9. Demands and production amounts for LPG.

The short decline for GLNA production in Figure 3.10 is a consequence of the small production from non-PETROBRAS refineries, which are not included in the model. For GLNC in both considerations, with and without the ethanol shift, the imports and production refer to GLNA, the pure gasoline without ethanol. As seen in Figure 3.10, there is a smaller GLNA production in the $GLNC_{ETH}$ cases, which is represented by the inferior blue dotted line. In this case, the lower gasoline demands decreased FCC, RFCC and DC throughputs implying in lower refined gasoline (GLNA). As shown in Figure 3.9, some intermediate cases for imports (4.2% p.a. and $GLNC_{ETH}$) are found due to the lower throughputs in some units, but they are not drawn in the Figure 3.10 to Figure 3.12.

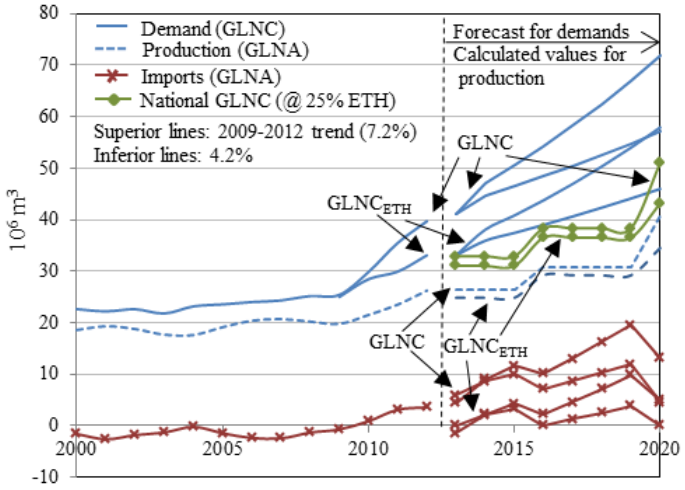

Figure 3.10. Demands and production amounts for GLNC and $GLNC_{ETH}$.

In Figure 3.11, jet fuel production only increased due to the inclusion of the HCC unit and not because of kerosene hydrotreaters (KHTs). The kerosene increase from the CDU capacity expansion goes to diesel production. As seen throughout the figures, only in the total DSL projections may the imports reduce to zero, as illustrated in Figure 3.12. For retail gasoline, its import can cease only in the lower demand case (4.2% p.a and $GLNC_{ETH}$). For jet fuel, its import can be reduced to zero in both 4.2% p.a. cases.

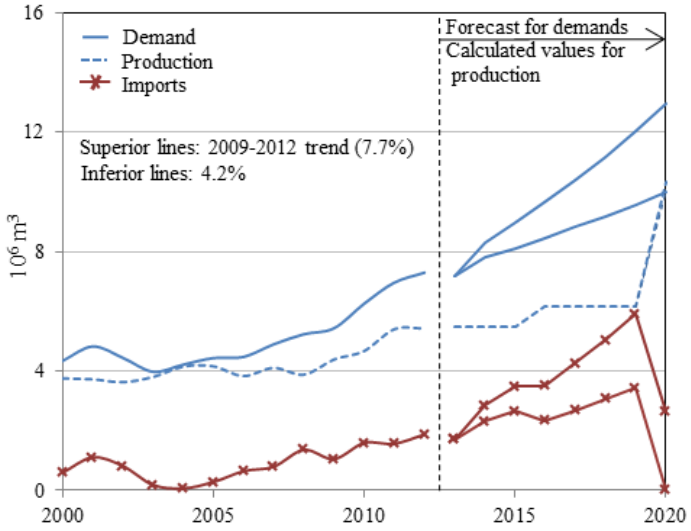

Figure 3.11. Demands and production amounts for jet fuel (JET).

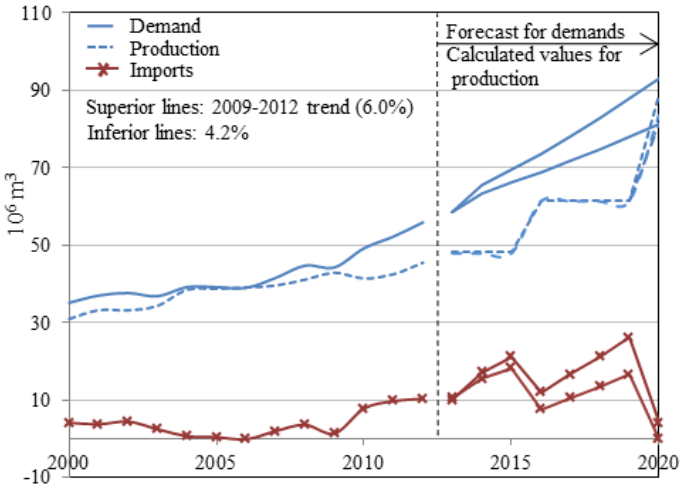

Figure 3.12. Demands and production amounts for diesel (DSL).

3.6. Conclusion

The results for the 2020 scenarios indicate strategic decisions reevaluation to supply fuel market needs in Brazil taking into account the possible variation in future fuel demands. In the lower demand cases (4.2% p.a.) with investments in 2020, jet fuel and diesel imports are reduced to zero. For gasoline, the external dependence was eliminated in the investment cases with the projects in conceptual phase performed with refitting only in the minimum import scenario (4.2% p.a. and $GLNC_{ETH}$). In the other 2020 scenarios with investment, gasoline, jet fuel, and diesel imports are needed. Comparatively, in all cases with jet fuel and diesel imports, jet fuel presents higher relative difference between demand and production, which becomes jet fuel supply and contingency plans more critical than diesel. Clearly, in the proposed process design for the refineries in conceptual project, diesel production was privileged as in the refineries under construction. In all cases of analysis, to avoid a fuel deficit of ~30%, which means performing the projects in conceptual phase, the overall capacity of the main units needs refitting. In terms of CDU capacity, in the four cases with projects, the demanded throughputs were ~30−40 k m^3/d lower than the planned overall capacity (536 k m^3/d). This suggests that a medium to large refinery is not used. Selecting possible investments in Figure 3.1, one future project can be postponed like as the first or second trains in the refinery PREMIUM I, or even the whole project in PREMIUM II or COMPERJ-2. The future perspectives over the capacity expansion in Brazil's oil-refining assets do not release fuel imports in the short term, and doubts remain regarding the long-term scenario due to market variation and delays in planned projects under execution and in

conceptual phase. These, in turn, are leading to project reanalyzes directly related to the new fuel market demand and indirectly influenced by the production increase of the national presalt crude. Besides, the economic logic may lead the country to postpone the investments in downstream (refining and segments linked to it) to invest in higher return projects in upstream (oil exploration and production). To find the best set of investments conjugated with import and export equilibrium should be the goal inside any thoughtful investment plan.

Chapter 4

4. MINLP Production Planning of Oil-Refinery Units for the Future Fuel Market in Brazil: Process Design Synthesis Model

In the previous chapter, a single-period NLP model for operational planning of oil-refinery units outlines overall unit throughputs considering different fuel markets. In this paper, the single period scenario-based model is modified to a multi-period mixed-integer nonlinear programming model, where unit throughputs, calculated in the operational layer, are upper bounded by unit capacities, updated in the strategic layer over time. The approach maximizes net present value considering the potential portfolio of projects to match the future fuel market in the country, where unit capacity additions are continuous variables lower and upper bounded by the respective project setup, representing the investment costs in the objective function as varying (capacity addition) and fixed (project setup) terms. Better results indicate different processing outline for overall capacity planning in the Brazilian oil refining industry.

4.1. Introduction

A strategic investment decision-making problem for overall capacity expansion of oil-refining units proposes investment alternatives for the future fuel market in Brazil. The problem maximizes net present value (NPV) for investing in capacity expansion of units, discrete decisions modeled as binary variables, taking into account processing and blending nonlinearities; hence, giving rise to an MINLP model. All required data of the Brazilian oil-refining industry such as prices, overall capacity of the units, fuel demands, national crude production and the nonlinear formulation used in this work can be found in the process design scenario-based model in chapter 3.

The national overall capacity of the oil-refinery units considers the existing oil-refining assets in 2016, because after this year the refineries currently under construction will be considered on-stream. A full review about the planned projects in the Brazilian oil-refining industry can be found in chapter 3 and Appendix A. In section 4.2, the process design synthesis model is presented. The four different fuel market scenarios covering all limiting demands is shown in section 4.3, where the problem statement and objective function are also

defined. In section 4.4, the overall capacity planning results indicate alterations in terms of additional capacity and capital investment throughout the projects. These indications are supposed to be in time to be effective, once the refineries currently in conceptual phase, as shown in Figure 3.1, can still be modified to find the best investment portfolio considering the proposed market scenarios defined in this work.

Additionally, the process design scenario-based NLP operational planning model results are compared with the proposed optimization-based MINLP investment planning model, the process synthesis design approach, considering that the capacity expansion needs to match the future fuel demands in the scenario-based model are found by the difference between the unit throughputs in 2020 and their capacities in 2016. In this case, the unit throughput upper bounds are considered a large number as will be seen. Finally, the results and future work are discussed in section 4.5.

4.2. Production Model for Oil-Refinery Units Refit

4.2.1. MINLP production planning for process design synthesis of oil-refinery units

The proposed production synthesis modeling is segregated into strategic (investment) and operational layers as shown in Figure 4.1. The investment layer manages the capacity increase for each unit *u* along the investment time *t*. When an investment is set up ($y_{u,t}$ = 1), the capacity expansion $QE_{u,t}$ takes place. Along each investment time period, the link constraint between both layers is given by Equation 4.1, in which unit throughput $QF_{u,t}$ modeled in the operational layer problem must be lower than its current capacity $QC_{u,t}$ updated in the strategic investment layer over time.

$$QF_{u,t} \leq QC_{u,t} \quad \forall\ u,t \tag{4.1}$$

Only in the following investment time periods are the capacities currently in expansion considered on-stream, but the production from the existing units is not being affected because of their expansions that occur during these time periods. A mixed-integer linear programming (MILP) formulation is proposed for the investment layer, while the operational layer is a nonlinear programming (NLP) problem, which forms the scenario-based approach proposed in chapter 3. When both layers are included, as in the process synthesis design or framework optimization-based approach proposed in this chapter, the model becomes a full space MINLP model.

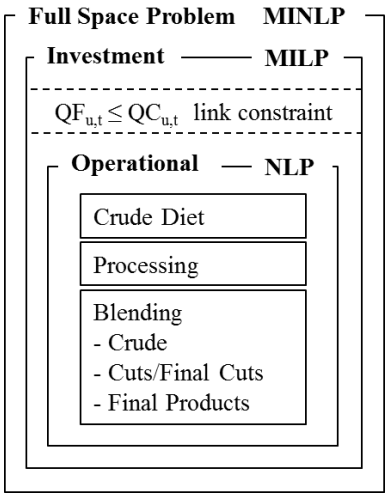

Figure 4.1. Investment and operational layers structure.

The possible expansions in the MILP layer could result in additional capacity for the different process units in Figure 3.2, which represents the hypothetical refinery REBRA (the multisite aggregate approximation) without distinguishing between expansion of existing units and the installation of new ones. In this work, the binary selection for expansions of propane deasphalting (PDA), delayed coker fed by atmospheric residuum (DCA) and medium hydrotreater (D1HT) units is deactivated, meaning that such expansions are not allowed. In the model, the binary setup possibilities comprise 12 expansions over each time period with investment under consideration, without including the last period t_{end}. The project execution of the capacity expansion is considered as the length of the time period Δt_1 and the fuel demands to be matched occurs at the beginning of the time period t_2. The details and considerations related to the evaluation of the objective function are shown in section 4.3. Figure 4.3.

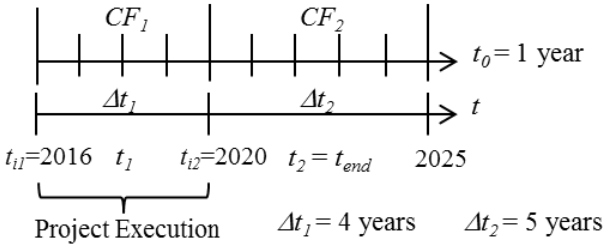

Figure 4.2. Investment and operational time periods.

In the operational layer, the formulation predicts distillation tower yields and distillate stream properties based on the crude diet determined in the model considering the conventional swing-cuts distillation modeling inside the crude distillation unit (CDU) as defined previously in chapter 3. The products of the remaining refining units have fixed yields

and fixed properties, with the exception of the hydrotreaters, which remove sulfur from their feeds and secondarily reduce the specific gravity and octane number of their streams. Properties like specific gravity, octane number, acidity and sulfur content are calculated to achieve the quality specification for the crude-oil and intermediate streams to be processed and final products to be sold. The operational layer model can be found in the scenario-based approach (chapter 3), in which the single-period NLP operational planning results for the present, intermediate, and for the proposed production and market scenarios in 2020 are presented considering daily profit as goal. In this case, for the results with unit throughputs lower than their planned capacity or, as in operational planning model, the unit throughput upper bound, the country's planned overall capacity expansion for the unit *u* in 2020 needs refitting.

In the MINLP investment planning based on NPV formula the synthesis of capacity expansion for each unit determines production scenarios for 2020 considering four different fuel market scenarios and the binary superstructure for the possible capacity expansion setups, 12 per time period with investment under consideration ($t<t_{end}$). Figure 4.3 shows the flowchart for both approaches and their cases. The NLP operational planning model can be used to simulate or test the current and the proposed production scenarios as planned in the Brazilian investment portfolio (process design scenario-based approach in chapter 3), and to generate initial values for the MINLP investment planning as a warm-start phase. In this case, better initial values to the MINLP problem result in lower execution time and avoids local solution and infeasibilities as will be seen.

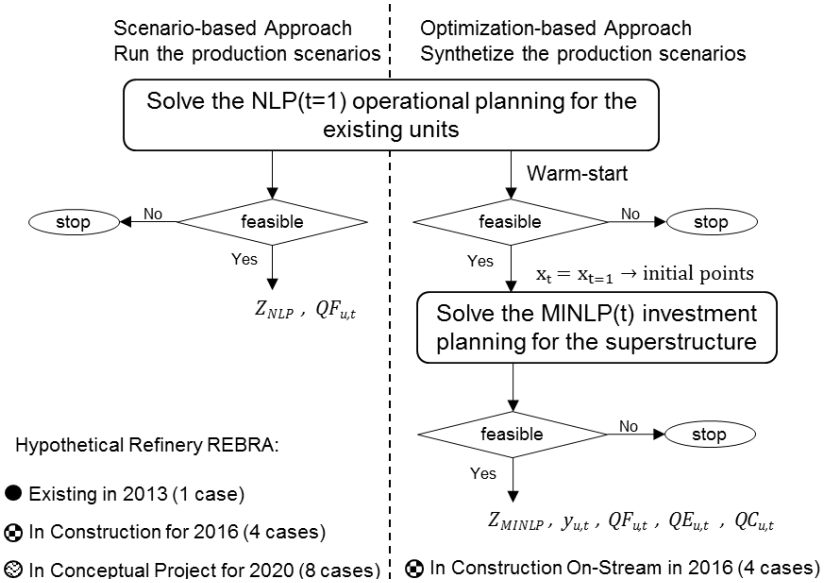

Figure 4.3. Simulation- and optimization-based approaches to find overall capacity of units.

The following subsection presents the MILP formulation related to the investment layer. The operational layer formulation is completely found in chapter 3.

4.2.2. MILP investment layer for expansion of process units

The capacity expansion $QE_{u,t}$ for a given unit *u* in a certain time *t* is limited or lower and upper bounded by the constraints in Equation 4.2.

$$y_{u,t}QE_u^L \leq QE_{u,t} \leq y_{u,t}QE_u^U \quad \forall\ u, t < t_{end} \tag{4.2}$$

As the proposed expansion does not distinguish between an actual revamp and a new unit installation, the lower (QE_u^L) and upper (QE_u^U) bounds for the overall capacity expansions are defined as $QE_u^L = 0.15QC_{u,t=1}$ and $QE_u^U = 10QC_{u,t=1}$, where $QC_{u,t=1}$ is the existing capacity. In effect, when an oil-refinery unit is revamped the reasonable capacity expansion is at least around 10% of its existing capacity. On the other hand, the maximum value can reach about 50%, depending on the unit complexity. If higher values are necessary, a new unit has to be installed. During the first investment time period, the operational gains result exclusively from the existing capacities. After the expansions, a new capacity $QE_{u,t}$ can be added to the unit as shown in Equation 4.3, so an additional production is obtained in the following time period in the operational layer.

$$QC_{u,t+1} = QC_{u,t} + QE_{u,t} \quad \forall\ u, t < t_{end} \tag{4.3}$$

This work does not limit the number of expansions permitted in a unit. In practice, an oil-refinery unit can be revamped at reasonable levels once during its lifetime, excluding distillation towers, which can be expanded several times by adding side towers and pre-flashes, and by changing mass transfer internals and heat transfer in the heat exchanges battery, condensers and reboilers. In any case, constraints for a maximum number of expansions in each unit can be included if necessary. Small projects to repair or debottleneck the units are not being considered in this work.

The unit throughputs $QF_{u,t}$ in the operational layer are bounded by their capacities $QC_{u,t}$ at every investment period *t*, as seen in Equation 4.1, which are updated after the expansions to obtain the gains from the possible operational activities within the following periods and, subsequently, the discrete decision to approve the projects at the beginning of each investment period can be made. The total expenses with the projects are upper bounded by the capital

available in each investment time CI_t, as shown in Equation 4.4. The parameter α_u represents the unit variable investment cost related to its size and β_u the fixed cost related to the decision to invest or no in its capacity expansion at a certain time.

$$\sum_{u}(\alpha_{u,t}QE_{u,t} + \beta_{u,t}y_{u,t}) \leq CI_t \quad \forall\ t < t_{end} \tag{4.4}$$

Process design synthesis constraints similar to Equations 4.1-4.4 can be found in mentioned authors (Sahinidis et al., 1989; Liu and Sahinidis, 1996; Iyer and Grosmann, 1998; Van den Heever and Grossmann, 1999; and Jackson and Grossmann, 2002), but without considering the project execution length time as used in this work.

4.3. Problem Statement: The Brazilian Oil-Industry Investment Scenario

Considering the overall capacity of the units and the fuel market scenarios in 2016, this work predicts overall capacity of the units in 2020 found as a result of selection of investment projects. Data from several official sources were considered to represent the situation in 2016, as found in chapter 3. The capital planned for investments in the next years, the fuel market scenarios and the NPV objective function are shown in the following subsections.

4.3.1. Brazilian oil industry investments after 1997

After 1997 the end of the oil industry monopoly resulted in a surge in oil investments with PETROBRAS expanding its investment levels from US$ 5 to approximately US$ 45 billion per year in the past 10 years as shown in Figure 4.4 (PETROBRAS, 2014), which can be considered a capital growing amount for investments never-before-seen in any company worldwide. For the next 5 years (2014-2018) PETROBRAS plans to invest US$ 220.6 billion, an average of US$ 44.12 billion per year with 70% in upstream and 18% in downstream (PETROBRAS, 2014). Despite the current and probably even with the future fuel deficit in the country, the upstream sector emerges as a definitive priority in the investment portfolio due to the lack of enough capital to be invested in all necessary projects throughout all sectors and also due to the fact that the upstream margins are considerably higher than the downstream ones. A historical review of the investments in PETROBRAS with capital amount statistics since the first year after its foundation in 1953 can be found in Appendix A,

where the Brazilian oil-refining industry current and future scenarios are shown in terms of investments, oil-refining assets and fuel demands in quantity (sharp increase) and quality (new specifications).

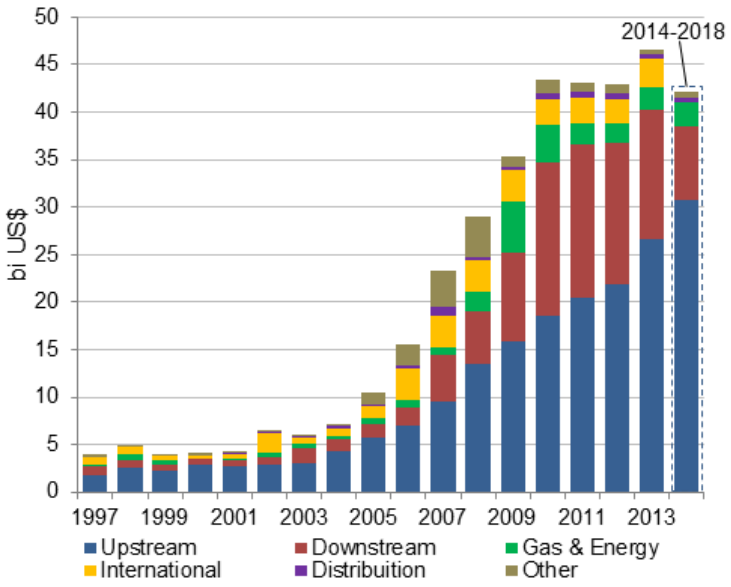

Figure 4.4. Investments in PETROBRAS after the flexibilization of the market.

The Brazil's planned investment in oil-refining assets is given in Figure 4.5 . From the total capital destined for the whole downstream sector (38.7 billions of U.S. dollars) during the 5 years period (2014-2018), those related to the capacity increase taken into account in this work are the refining asset expansion and the new market specifications. The former includes capacity expansion of separation, conversion and cracking processes to yield more fuels, and the latter accounts for the investment to match gasoline and diesel specifications such as octane number in gasoline and sulfur content in gasoline and diesel. The investments in upgrading oil-refining assets account for 22.3 billions of U.S. dollars, yielding 4.46 billions of U.S. dollars per year.

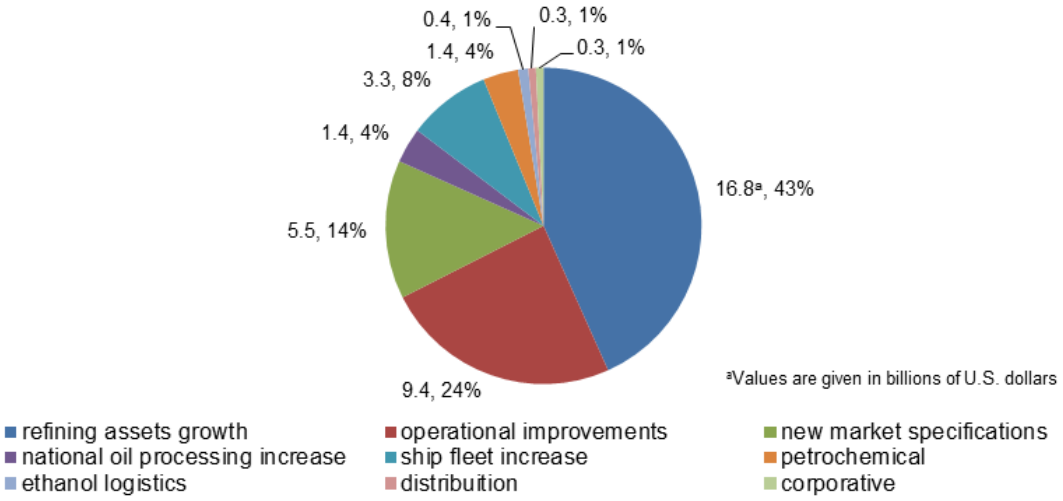

Figure 4.5. Downstream investments per segment in PETROBRAS (PETROBRAS, 2014)

4.3.2. Fuel demand scenario tree and investment costs

The proposed multi-period MINLP model predicts overall oil-refinery unit framework in 2020 taking into account the different market scenarios proposed in this work. As shown in Figure 4.6 four fuel demand scenarios in 2016 are proposed including both gasoline options (without and with discounting the ethanol-fuel market shift, GLNC and $GLNC_{ETH}$, respectively) and the 2009-2012 demand ratio increment for each fuel as an alternative to the 4.2% p.a. forecast for the Brazilian GDP (ANP, 2012). The full review about the fuel market considerations can be found in chapter 3.

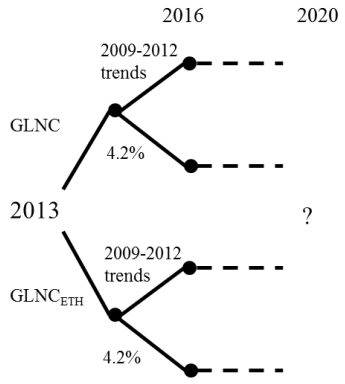

Figure 4.6. Four fuel market scenarios in 2016 considered to project the overall refining process scenario in 2020.

The underway projects of the RNEST and COMPERJ-1 refineries are considered to come on-stream by the beginning of 2016. This is the baseline upon which the refining units can submit expansion proposals that are represented by binary variables, where the investments costs related to each unit are defined by variable (α_u) and fixed (β_u) terms. Table

4.1 shows the investment parameters for the installation of new units considered in the model. These values already include expenses with power, utility, and off-site assets and also other considerations for regional cost in Brazil. Costs for expansion of existing units are lower than those for installation of new units, but this work uses only values for new units. A full review and data about investment costs for oil-refinery units can be found in Kaiser and Gary (2007), in which capital costs of oil-refinery units are specified as a function of capacity and scaled using the power-law relation $capacity/capacity^o = (cost/cost^o)^{0.6}$, considering standard capacity and cost ($capacity^o$ and $cost^o$) of a previous project. In this work, these nonlinear curves were linearized to find α_u and β_u, in which the parameter β_u is the binary variable $y_{u,t}$ coefficient in millions of U.S. dollars and the slope α_u is the expansion continuous variable $QE_{u,t}$ coefficient in millions of U.S. dollars per 1000 m^3, as shown for CDU and VDU in Figure 4.7.

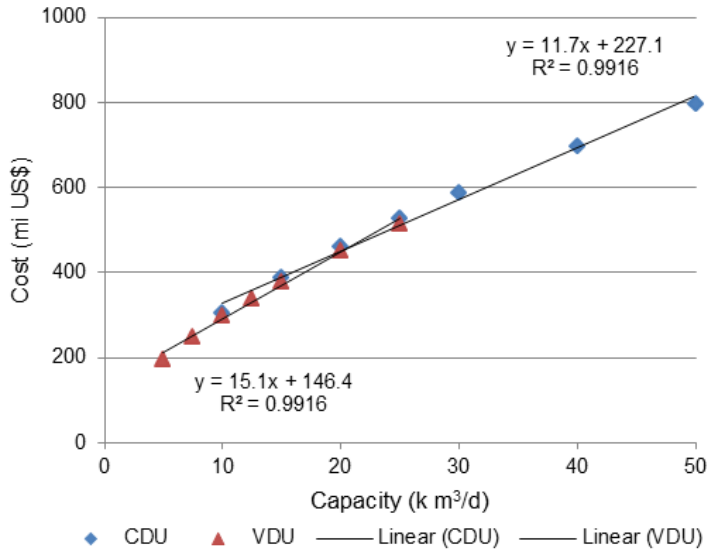

Figure 4.7. CDU and VDU plots to find their fixed and variable investment costs.

Table 4.1. Fixed and variable investment costs.

Unit (u)	α_u (mi US$ per 1000 m^3)	β_u (mi US$)
CDU	11.7	227.1
VDU	15.1	146.4
FCC	57.5	241.2
HCC	150.6	747.6
RFCC	70.2	588.8
DC	108.9	456.5
KHT	21.8	115.9
DHT	29.6	162.6
LCNHT / CLNHT	14.0	69.3
ST	11.5	193.9
REF	46.0	80.0

4.3.3. NPV for expansion of existing units

NPV maximization is the main objective in strategic investment planning. This is based on company's cash flows and reveals possible incomes (cash inflows) and expenses (cash outflows) along the horizon under evaluation. It can be estimated according to the applicable rules (depreciation), legislation (taxes), market expectations, monetary policy, company's specifics, etc., but these specifics and deductions related to depreciation and salvage value and the working capital necessary to operate the facilities are not considered in this chapter.

The NPV calculation involves the summation of the cash flow balances CF_t in each time interval evaluated at the current time, i.e., the future cash amounts (gains, costs or investments) are deflated by an interest rate *ir*. This future-to-present correction or deflated value is equivalent to how much savings are needed in the present to reach one certain capital amount in the future if the cash was invested at a fixed interest rate. The interest rate considered for Brazil in this work is 10% (Trade Economic, 2013).

The objective function is summarized in Equation 4.5. The calculation of daily operational gains from the scenario-based model, which is inside the first big bracket, is simply multiplied by a factor F_{t_0} to generate the annual income (F_{t_0}=365). The values are deflated using the future-to-present discount rate and a general price and costs increase rate of 4.2% p.a. is considered, as considered in this work for the Brazilian prices increase. The time horizon comprises investment and operational time periods as can be seen in Figure 4.3. . The investment interval *t* considers the time necessary to complete the projects construction, while the production from the current assets is simultaneously maintained fixed within each fixed interval, varying at t_0 = 1 year.

$$\max NPV = \sum_{t}\left[(1-tr)F_{t_0}\sum_{t_0}\frac{1}{(1+ir)^{t_0}}\left(\sum_{p}(pr_{p,t_0}-Ref_{cost_{t_0}})QF_{p,t}-\sum_{cr}pr_{cr,t_0}QF_{cr,CDU}-\sum_{imp}pr_{imp,t_0}QF_{imp,t}-\sum_{HT}QF_{HT,t}\right)-\left(\frac{1}{(1+ir)^{t_{it}}}\sum_{u}(\alpha_{u,t}QE_{u,t}+\beta_{u,t}y_{u,t})\right)_{t<t_{end}}\right] \quad (4.5)$$

In order to simplify the solution, CDU throughput $QF_{CDU,t}$, crude diet $\upsilon_{cr,t}$, severity and feed of the hydrotreaters ($\Upsilon_{HT,t}$ and $QF_{HT,t}$, respectively), production $QF_{p,t}$ and imports $QF_{imp,t}$ are kept constant within the investment time period t, so that price and demand increments along the operational time period t_0 are not used to update the operational setting within each time period t. The overall material flow from refining production is kept unchanged within the operational layer until a process design modification is implemented. Any additional amounts necessary to supply the yearly market demands inside the interval t are supplied by imports, so that the international market acts as a buffer controlled by the production and demand equilibrium and may point out logistics bottlenecks inside the supply chain. In Equation 4.5 the demands are actually given by the product amounts over time.

From a process synthesis perspective, the daily profit used here can be considered as an intensive variable, i.e., a snapshot of the daily process gains from the current assets conditions extrapolated to a whole year. Annual variations in prices change the income weights in the NPV objective at every t_0 step, although the MINLP model is performed at every step t. The expenses with extra imports to match the yearly market demands are supposed to be equivalent to the increment in annual fuel sales. Fortunately, these annual extra imports have little or no influence in the NPV-based decision. Crude variations within the investment period are also disregarded. Any optimization resulting from crude diet modification is residual in the strategic decisions. Naturally, in scheduling problems such crude variations over a short time period would be vital because they significantly influence the process and logistics operations of a refinery.

4.4. Results and Discussion

4.4.1. NPV-based results from the MINLP process design synthesis problem

The overall capacity of oil-refinery units considering different fuel market demands in Brazil is presented. All cases of study were implemented in the GAMS modeling language (Brooke et al., 1992) version 23.9.3 on an Intel Core 2 Duo (3.00 GHz, 16.0 GB of RAM). In the warm-start phase, the single-period NLP operational planning problem uses unit capacities and product yields to determine starting points for material flows. For calculated properties, given specifications are used. In the MINLP problem, the cases without the warm-start phase use the same initial values as mentioned before. When the warm-start phase is included in the

solution, the starting points in the MINLP problem are the warm-start results (NLP problem), considering them equal over all periods.

The model considers only 12 discrete variables, which are defined in the first investment time period t_1. The unit capacity increase is modeled in Equations 4.2-4.4 until the next-to-last investment time period ($t < t_{end}$), in this case t_1. The last time period t_2 does not include the possibility to have investment decision because the execution time length of the projects is considered as the size of the investment time period in which the setup decision occurs. Operational variables such as CDU throughput $QF_{CDU,t}$, crude diet $\upsilon_{cr,t}$, feed of the hydrotreaters $QF_{HT,t}$, and all other variables shown in the NLP scenario-based approach (operational layer), are being evaluated until the last period ($t_2 = t_{end}$), when the projects set up in t_1 are considered on-stream. The model is comprised of 12 discrete variables, 1127 continuous variables, 1019 equations, 4463 nonzero elements and 2552 nonlinear elements.

The NLP sub-problems are solved by non-linear general-purpose optimizers such as CONOPT (reduced gradient method), IPOPT (interior point methods) and the solver SNOPT (sequential quadratic programming). The MILP solver used in all cases is CPLEX. As shown in Table 4.2, the solution is faster using DICOPT as an MINLP solver, which uses extensions of the outer-approximation (Raman and Grossmann, 1994) algorithm for the equality relaxation strategy, in which a decomposed method solves a sequence of MILP and NLP sub problems until a stopping criteria convergence is reached. The examples use the augmented penalty heuristics as stopping criteria. SBB, based on standard branch and bound, in which an NLP solution is executed at each node, showed results similar to DICOPT in some cases, but in larger execution time. Other MINLP solvers such as AlphaECP and BARON did not yield any result.

The results with the warm-start phase included (execution time within 1 s) presented lower processing time in all cases, excepted in the 2009-2012 trends/GLNC case (using DICOPT/SNOPT combination as solvers) and in 2009-2012 trends/$GLNC_{ETH}$ case, in which the local solution was bypassed by the warm-start addition. The warm-start phase avoided infeasibilities and local solution in some cases, but in the 2009-2012 trends/GLNC yielded local solution when it was included. The best solution set is showed in Table 4.2 for each fuel demand scenario.

Table 4.2. MINLP problem results for different MINLP and NLP solvers.

		2009-2012 trends				4.2% p.a.			
		GLNC		$GLNC_{ETH}$		GLNC		$GLNC_{ETH}$	
MINLP solver	NLP solver	NPV[a]	CPU[b]	NPV	CPU	NPV	CPU	NPV	CPU
DICOPT	CONOPT	8.3867	3.511	infeasible		11.6236	3.120	6.4503	3.180
	IPOPT	8.8189	9.718	5.2465	3.900	11.6236	5.694	6.4503	4.520
	SNOPT	8.8189	0.826	5.1746	1.356	infeasible		6.4279	1.150
+warm-start	CONOPT	8.3867	1.060	5.2465	1.746	11.6236	1.080	6.4503	0.734
	IPOPT	8.3459	4.476	5.5455	7.377	11.6236	6.926	6.4503	3.010
	SNOPT	8.3855	1.262	5.2169	1.155	11.4447	1.015	6.6886	0.936
SBB	CONOPT	8.3867	4.165	infeasible		11.6236	6.050	6.4503	3.635
	IPOPT	8.8189	64.554	infeasible		11.6236	40.358	6.4503	19.984
	SNOPT	8.3865	3.307	infeasible		11.5902	5.930	infeasible	
+warm-start	CONOPT	8.3867	1.919	infeasible		11.6236	2.280	6.4503	1.014
	IPOPT	8.3867	52.307	infeasible		11.6236	37.331	6.4503	18.174
	SNOPT	infeasible		infeasible		11.6009	4.090	6.3855	1.260
best solution (higher profit and lower solution time)									
DICOPT	SNOPT	8.8189	0.826						
DICOPT	IPOPT+warm-start			5.5455	7.377				
DICOPT	CONOPT+warm-start					11.6236	1.080		
DICOPT	SNOPT+warm-start							6.6886	0.936

[a]NPV is given in billions of U.S. dollars

[b]CPU is given in seconds.

The cash inflows and outflows realized, used to calculate the NPV, are shown in Table 4.3, as well as the gains at each investment time corrected annually by the prices as previously described, which was extracted from a post-optimization analysis. The model considers two periods, the first t_1 of 4 years and the second t_2 of 5 years, as shown in Figure 4.3. . In terms of capital expenditure, the computed investment represents the capital needed at the beginning of each investment period to build the required portfolio of projects. The realized and real investment costs are the same only in the first period, because the investment capital is supposed to be withdrawn immediately at the beginning of each period that, in the present case, is only in t_{i1}. Gasoline, jet fuel and diesel imports in t_{i2} are set to zero, so that the capacity expansion sizes are those necessary to match the fuel demands at this point. Their imports are allowed in t_1, and LGN imports are free over all periods. Additionally, demand of LPG, gasoline, jet fuel and diesel is set to be 1% apart, avoiding surplus of these fuels. These considerations are based on the investment needs to match fuel demands in the country in 2020 in order to compare with the planned capacity expansion with the inclusion of more three oil refining sites as shown in Figure 4.3. .

Table 4.3. NPV value and operational and investment cash flows for the demanded capacity expansion and investment per type of unit (in billions of U.S. dollars).

		2009-2012 trends		4.2% p.a.	
		GLNC	$GLNC_{ETH}$	GLNC	$GLNC_{ETH}$
realized value in the NPV					
NPV (2016-2025)		8.8189	5.5455	11.6236	6.6885
operational gains (+)	t_1	4.5255	5.3542	6.5964	5.7408
	t_2	29.2934	24.6992	24.1971	22.1185
investment costs (-)	t_1	25.0000	24.5079	19.1699	21.1708
real value along each interval					
operational gains (+)	t_1	5.7398	6.7906	8.3658	7.2809
	t_2	57.0174	48.0752	47.0979	43.0519
capacity expansion[a]					
CDU		218.5	181.3	120.0	95.2
VDU		51.5	113.9	52.5	65.2
FCC			14.9		
HCC		43.2	65.6	44.0	83.4
RFCC		83.5		26.8	
DC		29.8	42.8	30.5	25.6
KHT		10.9	3.9	2.6	
D2HT		57.3	49.3	43.0	28.1
LCNHT		44.0	8.1	13.4	
CLNHT		14.7	21.2	15.1	12.6
ST		14.7	21.2	15.1	12.6
REF		6.1	12.6	8.4	10.7
investment costs per type of unit					
CDU		2.7834	2.3478	1.6315	1.3413
VDU		0.9234	1.8658	0.9385	1.1312
FCC			1.0952		
HCC		7.2488	10.6209	7.3707	13.3041
RFCC		6.4479		2.4694	
DC		3.7021	5.1127	3.7828	3.244
KHT		0.3529	0.2000	0.1722	
D2HT		1.8592	1.6229	1.4350	0.995
LCNHT		0.6831	0.1823	0.2561	
CLNHT		0.2744	0.3648	0.2796	0.2451
ST		0.3630	0.4375	0.3672	0.3388
REF		0.3617	0.6580	0.4669	0.5713
total		25.0000	24.5079	19.1699	21.1708

[a]capacity expansion is given in k m^3/d.

The investment amount for each unit presented in Table 4.3 should be unwrapped to evaluate a real case when, for instance, instead of installing one CDU of 100 k m^3/d (US$ 1.3949 billion), that is technically unrealistic, the portfolio should indicate two CDU units with 50 k m^3/d (US$ 0.8121 billion) each, representing an increase of 20% in the real case.

From a post-optimization analysis, the comparison of the daily profit and the refining margins as they are realized at the moment of decision with their real value is shown in Table

4.4. The realized NPV and real values consider annual variation over prices and costs. Also Table 4.4 shows that the real values of profit and margin considering prices at the beginning of the investment interval are lower than those considering their annual variation. For t_1 they are equal to the scenarios in 2016 as shown in the scenario-based model (chapter 3), because the gain at the first period (2016-2020) is constant within the whole interval.

Table 4.4. Daily profit and margin in t_1 and t_2.

	2009-2012 trends				4.2% p.a.			
	GLNC		$GLNC_{ETH}$		GLNC		$GLNC_{ETH}$	
	t_1	t_2	t_1	t_2	t_1	t_2	t_1	t_2
realized value at moment of decision								
profit[a]	3.100	16.051	3.667	13.534	4.518	13.259	3.932	12.120
margin[b]	1.32	4.32	1.57	3.89	1.93	4.28	1.68	4.12
real value along each investment interval								
profit	3.931	31.242	4.651	26.343	5.730	25.807	4.987	23.590
margin	1.68	8.41	1.99	7.57	2.45	8.34	2.13	8.03
real value at periods beginning								
profit	3.529	27.539	4.177	23.219	5.150	22.747	4.480	20.795
margin	1.51	7.42	1.79	6.67	2.20	7.35	1.91	7.08

[a]profit is given in millions of U.S. dollars per day

[b]margin is given in U.S. dollars per barrel

Table 4.5 shows the results of the overall capacity of the units for 2020 considering the four fuel market demands as previously defined. By adding the projects under construction, considered on-stream in 2016, to the country's current oil-refining assets, we obtained the lower bounds of the unit capacities for 2020, as shown in the second column of Table 4.5. Adding to this the planned capacities currently in conceptual phase from the three new oil refining sites, the last column of Table 4.5 is obtained. As the capital investment needed in both 4.2% p.a. resulting scenarios (GLNC and $GLNC_{ETH}$) is lower than the planned investments for 2020, it clearly indicates the necessity of a portfolio reevaluation considering that the official assumptions of the country's demands are similar to the $GLNC_{ETH}$ scenario or at least are in between the GLNC and $GLNC_{ETH}$ scenarios.

The available capital in all cases is considered 25 billions of U.S. dollars, because it is the minimal amount found to get results in the maximum fuel demand case (2009-2012 trends/GLNC). Table 4.5 also presents the profitability index, which attempts to identify the relationship between the investment costs and gains after the project portfolio implementation. In the case, the calculation is the difference between the operational gains in t_2 and t_1 divided by the investment amount. A ratio of 1.0 is the lowest acceptable measure,

and any value lower than 1.0 indicates that project gains are lower than the initial investment, i.e., without financial attractiveness. In the GLNC cases, with gasoline to ethanol market shift, the profitability index is higher because of the lower ethanol price, which is mixed at 25% in volume with refined gasoline (GLNA), to produce GLNC. As the considered GLNC price (711 US$/m^3) is higher than the blended ethanol (590 US$/m^3), higher profits in the GLNC scenarios are expected. Considering the profitability index of the real value along the interval *t* is higher than 1.0, the four cases are attractive to invest.

Table 4.5. Required capacity (k m^3/d) in 2020 to match fuel market demands.

		2020 (Results)				2020 (Planned)
		2009-2012 trends		4.2% p.a.		(Conceptual
unit (u)	2016	GLNC	$GLNC_{ETH}$	GLNC	$GLNC_{ETH}$	Project)
CDU	372	590.5	553.3	492.0	467.2	536
VDU	153	204.5	266.9	205.5	218.2	260
FCC	76	76.0	90.9	76.0	76.0	76
HCC	10	53.2	75.6	54.0	93.4	73
RFCC	22	105.5	22.0	48.8	22.0	22
DC	50	79.8	92.8	80.5	75.6	100
KHT	15	25.9	18.9	17.6	15.0	15
D2HT	68	125.3	117.3	111.0	96.1	135
LCNHT	54	98.0	62.1	67.4	54.0	54
CLNHT	34	48.7	55.2	49.1	46.6	62
ST	34	48.7	55.2	49.1	46.6	62
REF	12	18.1	24.6	20.4	22.7	10
capital investment needed[a]		25.0000	24.5079	19.1699	21.1708	23.1563
profitability index						
realized value at moment of decision		0.99	0.79	0.92	0.77	
real value along the period		2.05	1.68	2.02	1.69	

[a]values are given in billions of U.S. dollars

As mentioned, the real capital investment is around 20% lower than that in the multisite aggregate approximation results in Table 4.5, so that considering the planned capital for the refining assets growth and new fuel specifications in Figure 4.4, only in the 4.2% p.a. fuel demand scenarios (both GNLC and $GLNC_{ETH}$) the capital available (25 billions of U.S. dollars) would be enough. Comparing the capital needs in the 4.2% p.a. demand cases with the initial planned investment for the conceptual phase projects shown in Figure 3.1, it is clear that the country's new proposal presented in the PETROBRAS Business Plan in February 2014 already includes some capacity planning refitting considering the original strategic planning.

4.4.2. Profit- and NPV-based results from the NLP and MINLP production planning problems

In order to compare the NLP scenario-based and the MINLP optimization-based production planning approaches, the first found in chapter 3 and the second as shown in this chapter, the unit throughput upper bounds in the NLP scenario-based model is considered a large number (1000 k m^3/d). As the upper and lower bounds for LPG, gasoline, kerosene, and diesel demands are 1% set apart to avoid surplus of these fuels, the unit throughputs will be those to match these demands considering the problem with zero fuel imports (except for ethanol and LPG) at the beginning of 2020. Additionally, crude-oil imports are considered zero in order to compare with the MINLP results, as in all 2020 cases the country is free of ultralight oil imports.

In Table 4.6 and Table 4.7 the results of the NLP operational planning problem are shown. If it is considered lower bounds of the unit capacities in 2016 (see Table 3.3), FCC and RFCC throughputs in 2020 are lower than the 2016 capacity of these two units, and the results are labeled as NLP in Table 4.6 and Table 4.7. This outcome is a result of more profitable HCC cracking, because this process does not need to include hydrotreaters to reduce sulfur content in gasoline and diesel fractions. The process cracks large hydrocarbon chains to yield smaller molecules, hydrotreating them at the same time. But, as the NLP model does not include the investment constraints, the large amount of investment to expand HCC capacity cannot be evaluated, so another case with FCC and RFCC lower bounds equal to their capacities in 2016 are proposed to compare with the MINLP results. In all cases, the crude-oil diet is similar to the MINLP counterpart. In Table 4.7 the negative sign in the FCC/RFCC capacities means that their throughputs in 2020 are lower than their capacities in 2016.

Table 4.6. Required overall throughput (k m^3/d) to match fuel demands at zero crude and fuel imports (except for LPG and ethanol) in the NLP problem.

		NLP				NLP (FCC / RFCC lower bound = capacity)			
		2009-2012 trends		4.2% p.a.		2009-2012 trends		4.2% p.a.	
unit (u)	2016	GLNC	$GLNC_{ETH}$	GLNC	$GLNC_{ETH}$	GLNC	$GLNC_{ETH}$	GLNC	$GLNC_{ETH}$
CDU	372	544.0	538.8	482.7	491.2	549.1	550.0	482.4	507.3
VDU	153	202.2	265.7	233.9	253.8	242.8	265.0	226.8	246.7
FCC	76	51.7	67.7	83.0	64.3	76.0	76.0	79.2	76.0
HCC	10	96.4	113.7	68.4	68.4	91.5	98.3	68.4	68.4
RFCC	22	81.5	15.0	15.0	15.0	43.7	22.0	22.0	22.0
DC	50	127.2	118.5	110.1	80.4	146.2	104.7	106.0	56.3
KHT	15	18.1	15.0	15.0	15.0	19.0	17.8	15.0	15.0
D2HT	68	121.6	117.1	109.3	105.6	122.4	120.0	109.4	97.2
LCNHT	54	71.9	44.7	52.9	42.8	64.6	52.9	54.6	52.9
CLNHT	34	72.4	68.0	63.9	49.0	81.9	60.8	61.8	37.0
ST	34	72.4	68.0	63.9	49.0	81.9	60.8	61.8	37.0
REF	12	32.6	33.1	28.7	22.6	37.2	28.6	27.7	16.4
profit[a]									
	CONOPT	38.992	33.376	27.431	18.507	38.491	29.081	27.384	16.046
	IPOPT	38.992	21.844	27.352	5.524	38.489	28.854	26.614	16.038
	SNOPT	Infeasible	31.339	27.389	18.479	Infeasible	Infeasible	27.378	16.285
CPU[b]									
	CONOPT	0.280	0.358	0.406	0.500	0.561	0.375	0.530	0.484
	IPOPT	4.930	1.139	1.857	1.560	2.122	2.450	3.136	1.700
	SNOPT	Infeasible	0.140	0.093	0.063	Infeasible	Infeasible	0.078	0.140

[a]profit is given in millions of U.S. dollars per day.

[b]CPU is given in seconds.

Table 4.7. Required capacity expansion and investment costs per type of oil-refinery unit to match fuel demands at zero crude and fuel imports (except for LPG and ethanol) in the NLP problem (values from post-optimization analysis).

	NLP				NLP (FCC / RFCC lower bound = capacity)			
	2009-2012 trends		4.2% p.a.		2009-2012 trends		4.2% p.a.	
unit (u)	GLNC	$GLNC_{ETH}$	GLNC	$GLNC_{ETH}$	GLNC	$GLNC_{ETH}$	GLNC	$GLNC_{ETH}$
capacity expansion[a]								
CDU	172.0	166.8	110.7	119.2	177.1	178.0	110.4	135.3
VDU	49.2	112.7	80.9	100.8	89.8	112.0	73.8	93.7
FCC	-24.3	-8.3	7.0	-11.7			3.2	
HCC	86.4	103.7	58.4	58.4	81.5	88.3	58.4	58.4
RFCC	59.5	-7.0	-7.0	-7.0	21.7			
DC	77.2	68.5	60.1	30.4	96.2	54.7	56.0	6.3
KHT	3.1				4.0	2.8		
D2HT	53.6	49.1	41.3	37.6	54.4	52.0	41.4	29.2
LCNHT	17.9	-9.3	-1.1	-11.2	10.6	-1.1	0.6	-1.1
CLNHT	38.4	34.0	29.9	15.0	47.9	26.8	27.8	3.0
ST	38.4	34.0	29.9	15.0	47.9	26.8	27.8	3.0
REF	20.6	21.1	16.7	10.6	25.2	16.6	15.7	4.4
investment costs per type of unit[b]								
CDU	2.2355	2.1747	1.5193	1.6189	2.2950	2.3060	1.5163	1.8075
VDU	0.8868	1.8435	1.3655	1.6641	1.4988	1.8338	1.2579	1.5576
FCC			0.6433				0.4253	0.2412
HCC	13.7600	16.3598	9.5421	9.5421	13.0182	14.0481	9.5421	9.5421
RFCC	4.7650				2.1137			
DC	8.8628	7.9119	7.0008	3.7641	10.9317	6.4150	6.5513	
KHT	0.1836				0.2028	0.1760		
D2HT	1.7506	1.6163	1.3853	1.2767	1.7744	1.7009	1.3881	1.0259
LCNHT	0.3192				0.2178		0.0783	
CLNHT	0.6051	0.5437	0.4858	0.2784	0.7377	0.4438	0.4570	0.1105
ST	0.6355	0.5849	0.5372	0.3663	0.7448	0.5025	0.5134	0.2278
REF	1.0287	1.0491	0.8482	0.5665	1.2380	0.8453	0.8002	0.2842
total	35.0329	32.0839	23.3277	19.0770	34.7730	28.2714	22.5300	14.7968

[a]capacity expansion is given in k m^3/d

[b]investment costs are given in billions of U.S. dollars

Finally, Table 4.8 shows the NLP and the MINLP cases in terms of overall capacity, capital investment needs and profit. Comparing the NLP and MINLP solutions, it is clear that in the 2009-2012 trends for both GNLC and $GLNC_{ETH}$ scenarios the overall unit throughputs of the NLP cases present more efficient design with lower CDU utilization and higher HCC and DC utilization, which cracks gasoil (e.g., LVGO) and vacuum residue (VR) streams, respectively. However, this production scenario demands more investments as can be seen comparing the capital investment needs in both NLP and MINLP 2009-2012 trend scenarios. The 4.2% p.a./GLNC scenario presented the same logic.

In the 4.2% p.a./$GLNC_{ETH}$ fuel demand scenarios, the CDU capacity in the NLP case was higher than the MINLP counterpart. Although in this demand scenario the NLP case

yielded lower capital investment, its lower profit discharge this framework capacity. This is a result of higher expenses with crude due to its higher CDU capacity. Analyzing these results, the fuel oil (FO) production was (~ 20%) of the CDU feed that shows this NLP scenario is not realistic or desired production design.

Table 4.8. NLP and MINLP results.

		2020 (Results)								2020 (Planned)
		NLP (FCC / RFCC lower bound = capacity)				MINLP				(Conceptual Project)
		2009-2012 trends		4.2% p.a.		2009-2012 trends		4.2% p.a.		
unit (u)	2016	GLNC	$GLNC_{ETH}$	GLNC	$GLNC_{ETH}$	GLNC	$GLNC_{ETH}$	GLNC	$GLNC_{ETH}$	
CDU	372	549.1	550.0	482.4	507.3	590.5	553.3	492.0	467.2	536
VDU	153	242.8	265.0	226.8	246.7	204.5	266.9	205.5	218.2	260
FCC	76	76.0	76.0	79.2	76.0	76.0	90.9	76.0	76.0	76
HCC	10	91.5	98.3	68.4	68.4	53.2	75.6	54.0	93.4	73
RFCC	22	43.7	22.0	22.0	22.0	105.5	22.0	48.8	22.0	22
DC	50	146.2	104.7	106.0	56.3	79.8	92.8	80.5	75.6	100
KHT	15	19.0	17.8	15.0	15.0	25.9	18.9	17.6	15.0	15
D2HT	68	122.4	120.0	109.4	97.2	125.3	117.3	111.0	96.1	135
LCNHT	54	64.6	52.9	54.6	52.9	98.0	62.1	67.4	54.0	54
CLNHT	34	81.9	60.8	61.8	37.0	48.7	55.2	49.1	46.6	62
FRAC3	34	81.9	60.8	61.8	37.0	48.7	55.2	49.1	46.6	62
REF	12	37.2	28.6	27.7	16.4	18.1	24.6	20.4	22.7	12
capital investment[a]		34.7730	28.2714	22.5300	14.7968	25.0000	24.5079	19.1699	21.1708	23.1563
profit[b]		38.491	29.081	27.384	16.046	27.123	23.100	22.747	20.701	
no. of equations				406				1019		
no. of continuous variables				460				1127		
no. of discrete variables				-				12		
no. of non zero elements				1772				4463		
no. of non linear elements				1061				2552		
CPU (s)		0.561	0.375	0.530	0.484	0.826	7.377	1.080	0.936	

[a]values are given in billions of U.S. dollars

[b]profit is given in millions of U.S. dollars per day.

4.5. Conclusion

Process design synthesis is essential to predict capital expenditure to fully supply an increase in final goods market. Despite the importance, most methodologies used to decide whether to implement a capacity expansion rely on trial-and-error procedures, as presented in the scenario-based approach, where an NLP model for several scenarios was proposed considering demands variations for fixed process design. Alternatively, in the optimization-based approach presented in this chapter, a discrete optimization model is used to find the best process design by investing in expansion of existing units.

The results for the 2020 scenarios, when the refineries under conceptual phase are considered on-stream, indicate the necessity to reevaluate the strategic decisions to supply fuel market needs taking into account the possible variation on future fuel demands. This optimization-based model gives a better scenario about the capital needs within the next cycle of investments in the downstream sector in Brazil because the results obtained with the

proposed MINLP model presented higher profit and margin and lower capital investment needs when compared with the official scenarios.

In terms of modeling, the effect of taking into account the prices varying annually in the NPV-based objective instead of taking them at beginning of periods increased the gains around 10% as seen in Table 3.1 for the first period. On the other hand, the profit and margin found in t_1 without considering the annual prices variation is the same for the equivalent demand scenario in the scenario-based approach in the 2016 design. Comparing the results obtained with both the NLP and the MINLP methodologies, the former is incomplete because does not take into account the investment constraints which in turn leaded to very expensive and unrealistic design by decrease the capacity of separation units (CDU and VDU) and by increase the capacity of cracking units (HCC and DC).

Chapter 5

in Menezes, B.C.; Kelly, J.D.; Grossmann, I.E. Improved Swing-Cut Modeling for Planning and Scheduling of Oil-Refinery Distillation Units. *Industrial & Engineering Chemistry Research*, 52: 18324-18333. 2013.

5. Improved Swing-Cut Modeling for Planning and Scheduling of Oil-Refinery Distillation Units

When swing-cuts are introduced in planning and scheduling problems to determine distillation unit products, these are used to model the fact that the temperature profile can be manipulated, controlled or optimized to produce more or less amounts of adjacent light and heavy intermediate swing-cuts before being blended into a final distillate or product-cut, which is dispatched downstream. Unfortunately this approach, albeit simple to implement in planning and scheduling models, has a serious drawback in the sense that the properties for the light and heavy swing-cut flows are assumed to be the same, which is not true.

In this chapter it is proposed a novel swing-cut model enhancement, which mitigates this issue by correcting the light and heavy swing-cut properties using a set of simple flow-weighted interpolations at their interfaces which will be described in detail. Two examples are presented, one with a crude-oil distillation unit using actual data, and the second is a planning case with different grades of diesel, where both provide a comparison between the conventional and the improved swing-cut models. In section 5.1, the conventional swing-cut model is rewrote differently from chapter 3 by considering small fractions of crude oil as micro-cuts *mc* (hypotheticals or pseudocomponents) to model the quantity and quality variation of the distillate streams or final-cuts *fc*. The proposed improvement in the swing-cut modeling given by quality corrections of the light and heavy swing-cut streams, within the interfacial property-related interpolation between the bulk properties of the whole swing-cut and its upper (light) and lower (heavy) interfaces, is shown in section 5.2. The problem statement of the two examples is highlighted in section 5.3. The first is a simulation case and the second is an optimization one. The results and conclusion are in sections 5.4 and 5.5 respectively.

5.1. Micro-Cut Crude-Oil Assays and Conventional Swing-Cut Modeling

Crude-oil and vacuum distillation units (CDU/VDU) at the planning and scheduling levels, are typically modeled by decomposing or separating each of its crude-oil feedstocks into what are known as hypothetical or pseudocomponents, also referred to here as micro-cuts. Each micro-cut has a predefined TBP temperature interval of approximately 5-25ºC ranging across the entire crude-oil, which usually has an overall temperature range from the boiling point of methane to 850ºC (Kelly, 2004). Together with the volume and/or weight yields, and a set of relevant qualities including specific gravity for each micro-cut, this forms what is called the crude-oil assay. Further information regarding the crude-oil assay data and the conventional swing-cut modeling can also be found in Li et al. (2005). The micro-cut TBP temperature interval used in this work is 10ºC. The assay data for each crude oil were generated using the process simulator PetroSIM. Volume yields, specific gravity, and sulfur content for a single crude oil is shown in Figure 5.1.

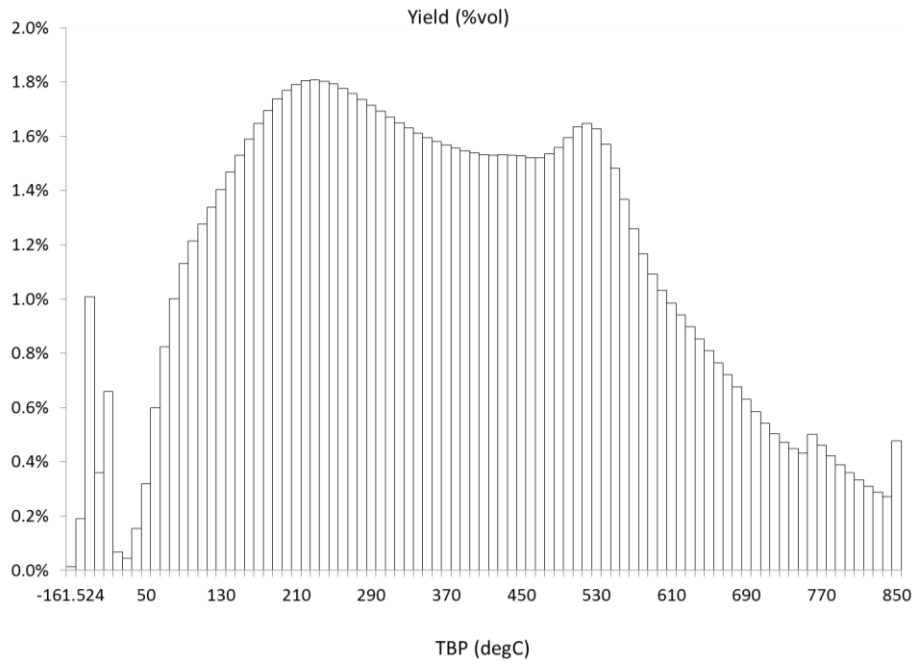

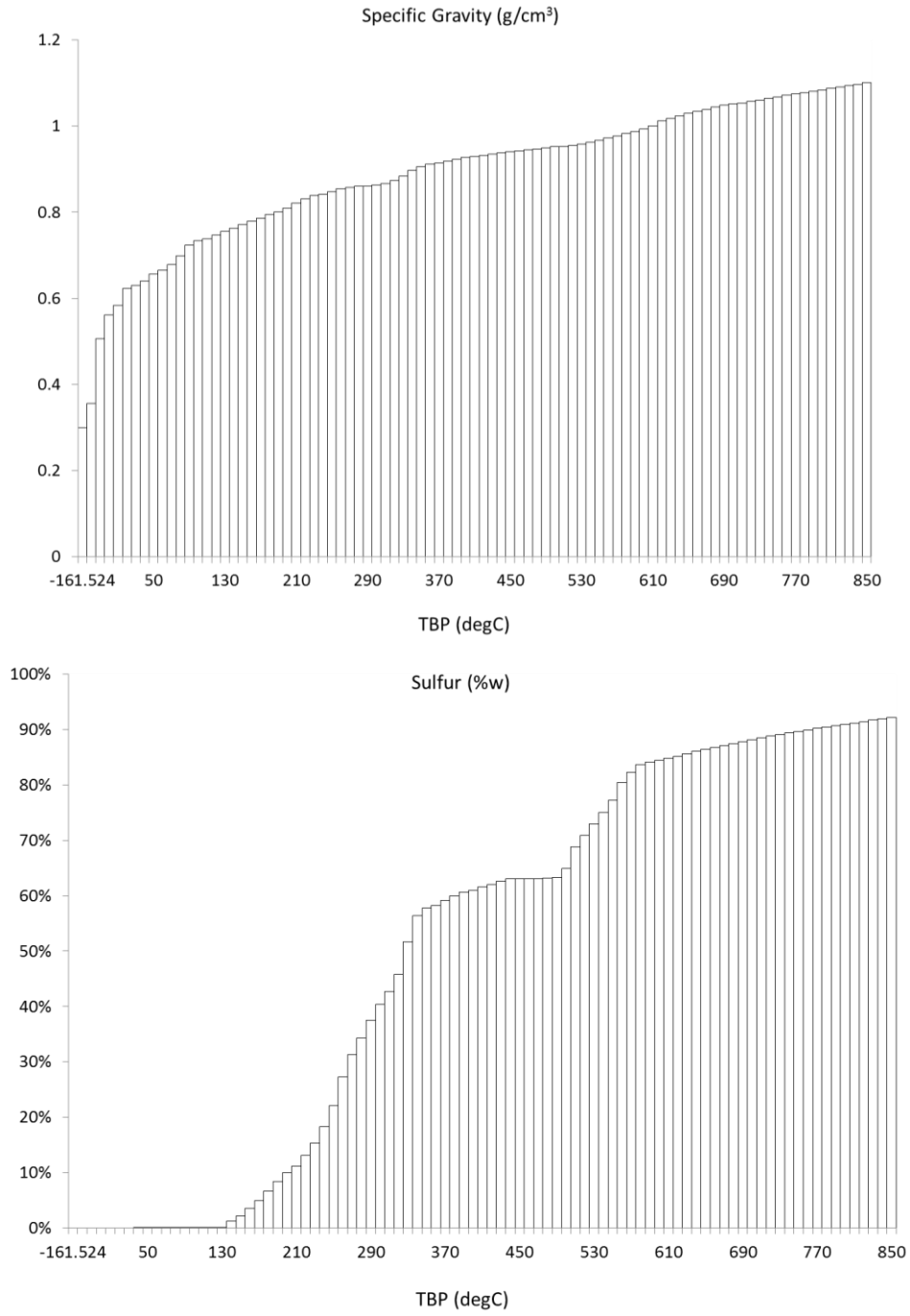

Figure 5.1. Example crude-oil assay data with eighty-nine 10ºC micro-cuts for yield, specific gravity and sulfur.

Micro-cut or pseudo-component yields and qualities, as well as empirically derived molecular weight, accentric factor and critical temperature and pressure, can be used by rigorous distillation models for detailed process simulation and optimization to characterize each crude oil fractionated in the distillation towers. However, for the purpose herein, first-principles column fractionation is not being considered. Instead, as is typical for planning and

scheduling modeling, the yields and qualities for the cuts or streams leaving the distillation process are determined by mixing, blending, or pooling a predefined set of micro-cuts for each cut or distillate, weighted by the composition of each crude oil feeding the tower similar to a blend recipe.

The conventional swing-cut model proposed in this work uses micro-cuts *mc* to define the crude oil, instead of simply cuts *c* used in previous approaches where final-cuts *fc* are introduced to represent the mixing or blending of the cuts and any swing-cuts to form the final product leaving the fractionator as shown in Figure 5.2. The naphtha-cut, for example, is formed by blending any pure components such as isopentane (IC5) and the micro-cuts mc40-mc120. The first swing-cut, SW1-cut, is formed by mixing mc130, mc140, and mc150. Kerosene-cut includes mc160- mc200, and SW2-cut is formed by mc210, mc220, mc230 and mc240. The other cuts shown, light diesel-cut, SW3-cut, and heavy diesel-cut are modeled in a similar way. The four final-cuts or product-cuts, naphtha, kerosene, light, and heavy diesel, are then pools of the cuts shown. The special lines in Figure 5.2 with the labels "light" and "heavy" are the swing-cut split streams and will be described in more detail later.

The CDU configuration, which may have one or more crude-oil feedstocks and three swing-cuts, is shown in Figure 5.3. As can be seen, the swing-cuts are essentially internal modeling constructs, and they are not necessarily present physically in the tower, although they can be related to what are known as side-draw trays. The three quantity flow variables shown are taken from the general framework found in Neiro and Pinto (2004).

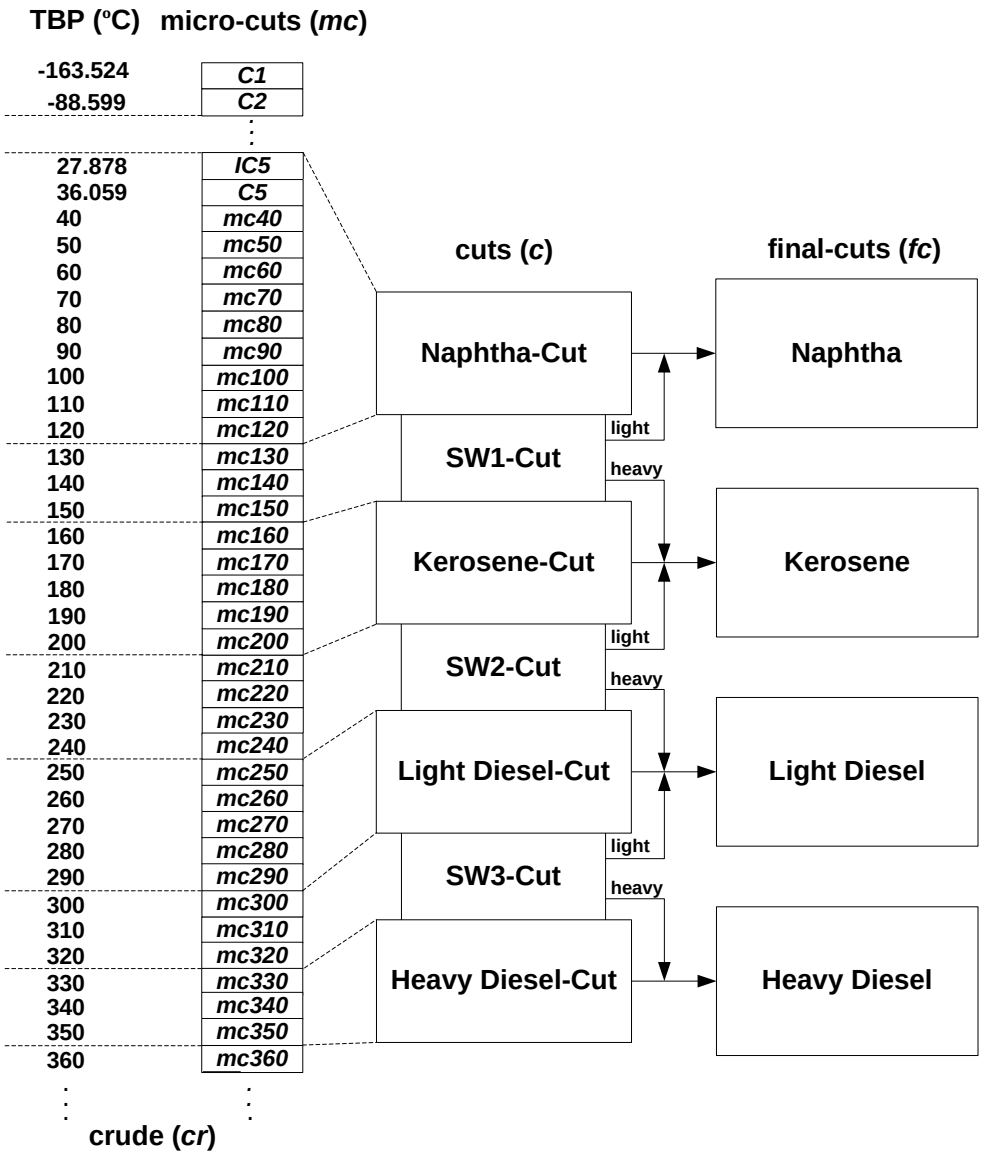

Figure 5.2. Micro-cuts, cuts, swing-cuts and final-cuts.

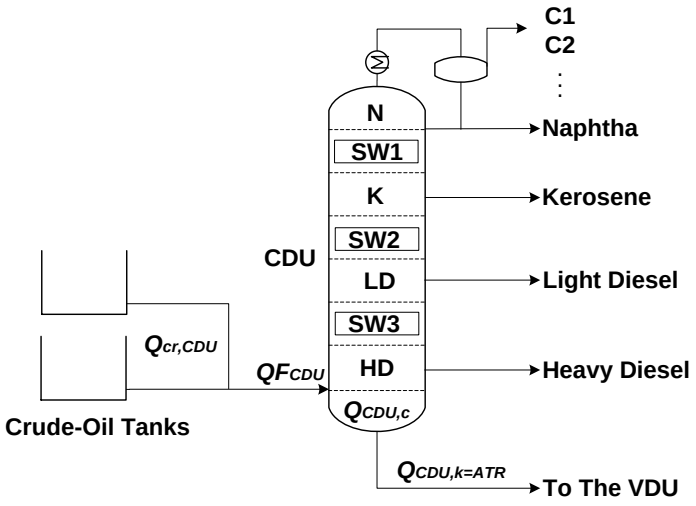

Figure 5.3. Multiple crude-oils, cuts and final-cuts for the CDU.

The mathematical model using multiple crude oils, micro-cuts, cuts and final-cuts in terms of how they are combined together to model the CDU in Figure 5.3 is as follows. Equation 5.1 takes the flows for each crude oil *cr* and sums them together to form a total or overall feed flow to the CDU.

$$QF_{CDU} = \sum_{cr} Q_{cr,CDU} \tag{5.1}$$

Each cut flow inside the CDU is represented by Equation 5.2 as the sum over all crude-oils, times the sum over of each micro-cut's yield from its initial micro-cut (*mci(c)*) to its final micro-cut (*mcf(c)*) given by the temperature cut-points. When cut *c* is a swing-cut *sw*, it is split into a light and a heavy stream where their sum is constrained and given by Equation 5.3. Their values are variables that can be changed by variations on the final distillates quantities and qualities to match the final products demands and specifications.

$$Q_{CDU,c} = \sum_{cr} Q_{cr,CDU} \sum_{mc=mci(c)}^{mcf(c)} Y_{cr,mc} \quad \forall\ c \tag{5.2}$$

$$Q_{CDU,c} = Q_{c,fc=\ell} + Q_{c,fc=h} \quad \forall\ c = sw \tag{5.3}$$

Similar to the CDU cut flows, in Equations 5.4 and 5.5 we model the volume and mass properties or qualities, respectively. An example of a volume property VP_c is specific gravity, and an example of a mass property MP_c is sulfur content. For the mass property density, specific gravity is required to provide the volume to mass conversion inside.

$$VP_c = \frac{\sum_{cr} Q_{cr,CDU} \sum_{mc=mci(c)}^{mcf(c)} V_{cr,mc} Y_{cr,mc}}{\sum_{cr} Q_{cr,CDU} \sum_{mc=mci(c)}^{mcf(c)} Y_{cr,mc}} \quad \forall\ c \tag{5.4}$$

$$MP_c = \frac{\sum_{cr} Q_{cr,CDU} \sum_{mc=mci(c)}^{mcf(c)} M_{cr,mc} G_{cr,mc} Y_{cr,mc}}{\sum_{cr} Q_{cr,CDU} \sum_{mc=mci(c)}^{mcf(c)} G_{cr,mc} Y_{cr,mc}} \quad \forall\ c \tag{5.5}$$

Now that individual cut flows and properties are defined, it is possible to form the final-cuts or product stream flows and properties leaving the CDU, shown in Figure 5.3 as the arrows to the right of the CDU. Equation 5.6 simply sums together the nonzero cut to final-cut

flows $Q_{c,fc}$. Typically, cuts that are not swing-cuts are mapped or allocated one to one with its corresponding final-cut, i.e., naphtha-cut only goes to the naphtha final-cut. Whereas swing-cuts such as SW3-cut have light and heavy cut flows, where the light flow is included in the light diesel final-cut and the heavy flow mixes with the heavy diesel final-cut. Equations 5.6-5.8, similar to Equations 3.6-3.8 from the conventional swing-cut modeling in chapter 3, are used to find final-cuts quantities, outputs or flows $Q_{CDU,fc}$ being produced from the CDU unit and their qualities, the volume-based property VP_{fc} and the mass-based property MP_{fc}, all considering the tuples of cuts and swing-cuts forming the final-cuts as defined in Figure 5.2.

$$Q_{CDU,fc} = \sum_{c} Q_{c,fc} \quad \forall \; fc \tag{5.6}$$

The final-cut volume and mass properties are calculated in Equations 5.7 and 5.8 similar to the other property calculations. It is worth mentioning that the specific gravity property G_c is also a volume property and can also be computed via Equation 5.7.

$$VP_{fc} = \frac{\sum_{c} VP_c Q_{c,fc}}{\sum_{c} Q_{c,fc}} \quad \forall \; fc \tag{5.7}$$

$$MP_{fc} = \frac{\sum_{c} MP_c G_c Q_{c,fc}}{\sum_{c} G_c Q_{c,fc}} \quad \forall \; fc \tag{5.8}$$

In addition, properties that do not obey ideal blending, can be easily precalculated for each micro-cut property using well-known blending indexes or ad-hoc blending transforms. These transformed properties then behave ideally as volume- or mass-based properties. This is also true for the blending or pooling of the final-cuts. In the following section, it is described the improvement to the conventional swing-cut modeling approach just described.

5.2. Improved Swing-Cut Modeling

Taking into consideration that the swing-cut can be split into two internal streams, the light going to the lighter final-cut and the heavy moving to the heavier final-cut, in the new formulation each of these internal streams has their own qualities. In contrast, the conventional swing-cut model has the same quality value for both the light and heavy streams,

which are the bulk or whole swing-cut properties VP_c, G_c and MP_c. In this work, it is proposed a new swing-cut model that adds a set of interpolations to better predict the pooled qualities of the final-cuts or products leaving the CDU or VDU. As mentioned before, it is considered that both the light and heavy swing-cut streams have their own qualities, and are computed as a function of their flows, and vary linearly or proportionately between the properties at their adjacent hypothetical interfaces and the whole property of the swing-cut.

The properties of the adjacent hypothetical interfaces, between the swing-cuts and their lighter and heavier cuts, can be easily calculated using the adjacent micro-cut pairs in the initial and final boiling point temperatures of each swing-cut, taking into account CDU's crude diet to determine the micro-cut values. For instance, SW1-Cut in Figure 5.2 has its light interface property variables as $VPI_{c=\text{SW1-Cut},\ell}$ and $MPI_{c=\text{SW1-Cut},\ell}$, which are determined by blending the mc120 and mc130 properties identical to Equations 5.4 and 5.5. Similarly, the heavy interface properties $VPI_{c=\text{SW1-Cut},h}$ and $MPI_{c=\text{SW1-Cut},h}$ are computed using the micro-cuts mc150 and mc160. This implies that the TBP temperature range for SW1-Cut has an initial point of 130ºC and a final point of 160ºC, i.e., contains micro-cuts mc130, mc140, and mc150.

As shown in Figure 5.4, the light and heavy swing-cut portions labeled SWL and SWH have their properties varying between their adjacent hypothetical interface properties, and its whole swing-cut property where the properties shown are volume-based but are the same for mass-based. If the whole swing-cut flows entirely to the lighter final-cut then $VP_{c=sw,fc=\ell}$ is equal to the swing-cut bulk property $VP_{c=sw}$. And, if all of the swing-cut flow goes entirely to the heavier final-cut, then $VP_{c=sw,fc=h} = VP_{c=sw}$. In the cases where the swing-cut is split to both the lighter and heavier product-cuts, then the properties are of course different but related to the whole swing-cut property and have simple inequality constraints bounding them, which may or may not be explicitly included in the model formulation.

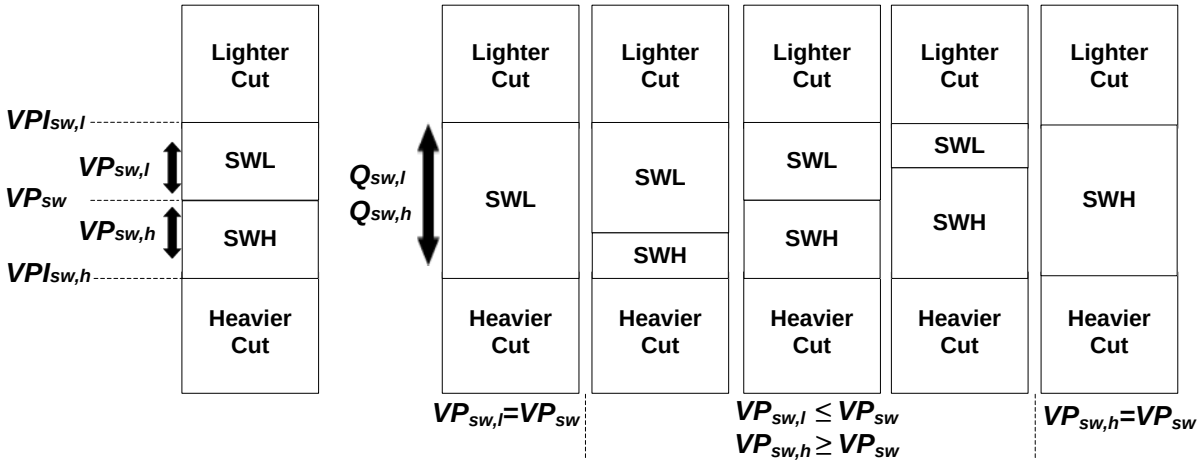

Figure 5.4. Swing-cut properties as a function of light and heavy swing-cut flows.

Equations 5.9 and 5.10 are the equality constraints that allow to compute the light and heavy swing-cut volume-based properties going to the light and heavy final-cuts, respectively, where Equations 5.11 and 5.12 are for the mass properties using the specific-gravity variables.

$$VP_{c=sw,fc=\ell} = VPI_{c=sw,\ell} + \frac{VP_{c=sw} - VPI_{c=sw,\ell}}{Q_{CDU,c=sw}} Q_{c=sw,fc=\ell} \tag{5.9}$$

$$VP_{c=sw,fc=h} = VPI_{c=sw,h} - \frac{VPI_{c=sw,h} - VP_{c=sw}}{Q_{CDU,c=sw}} Q_{c=sw,fc=h} \tag{5.10}$$

and

$$MP_{c=sw,fc=\ell} = MPI_{c=sw,\ell} + \frac{MP_{c=sw} - MPI_{c=sw,\ell}}{G_{c=sw} Q_{CDU,c=sw}} G_{c=sw,fc=\ell} Q_{c=sw,fc=\ell} \tag{5.11}$$

$$MP_{c=sw,fc=h} = MPI_{c=sw,h} - \frac{MPI_{c=sw,h} - MP_{c=sw}}{G_{c=sw} Q_{CDU,c=sw}} G_{c=sw,fc=h} Q_{c=sw,fc=h} \tag{5.12}$$

With these equations, whole swing-cut properties $VP_{c=sw}$ and $MP_{c=sw}$ that can be calculated by Equations 3.7 and 3.8 are replaced by $VP_{c=sw,fc=\ell}$, $VP_{c=sw,fc=h}$, $MP_{c=sw,fc=\ell}$ and $MP_{c=sw,fc=h}$ which enables to predict more accurate mixed or pooled properties for the final distillates. As shown in Figure 5.2, each swing-cut has light and heavy streams, and therefore their properties can be corrected by this new improvement. Compared to the conventional swing-cut method for the volume-based properties, four new variables are required $VPI_{c=sw,fc=\ell}$, $VPI_{c=sw,fc=h}$, $VP_{c=sw,fc=\ell}$ and $VP_{c=sw,fc=h}$, and two new equality constraints,

Equations 5.9 and 5.10. For the mass-properties, six new variables are required that include specific gravity and two new equality constrains, Equations 5.11 and 5.12.

5.3. Examples

Two examples are presented, one with a crude distillation unit using actual data and the second is a planning case with different grades of diesel where all provide a comparison between the conventional and the improved swing-cut models. The objective is to maximize the profit obtained by sales of final products *p* to match their demands QF_p discounting the crude *cr* purchasing and hydrotreaters (HT) operation costs, as shown in Equation 5.13.

$$\max profit = \sum_{p} pr_p QF_p - \sum_{cr} pr_{cr} Q_{cr,CDU} - \sum_{HT} Y_{HT} \tag{5.13}$$

The hydrotreaters severity Y_{HT} is considered the sulfur reduction percentage, and its operational costs in the objective function are needed to avoid property giveaways when we have different grades of one product, as in the second example. Also, a good practice is to consider a hypothetical blender for each grade; both were used in the planning example. The CDU feed and final product specifications used in this work are given in Table 5.1.

Table 5.1. CDU feed and final product specifications.

	SG (g/cm^3)		sulfur (w%)
	min	max	max
CDU	0.700	0.900	0.800
JET	0.780	0.836	0.030
LSD	0.820	0.850	0.001
MSD	0.820	0.865	0.050
HSD	0.820	0.880	0.180

The calculations were performed using GAMS version 23.9.3 as the modeling system on an Intel Core 2 Duo (3.00 GHz, 16.0 GB of RAM), and the NLP solvers used in this work are CONOPT, IPOPT and SNOPT.

5.4. Results

5.4.1. Example 1: CDU with three swing-cuts

This example involves an actual CDU operation with a capacity of approximately 35 k m^3 per day, and processes eighteen different crude oils, and their compositions are known and fixed as shown in Table 5.2. The CDU configuration is shown in Figure 5.3 and has three swing-cuts (SW1-Cut, SW2-Cut, and SW3-Cut) and four final-cuts (naphtha, kerosene, light, and heavy diesel) of interest.

Table 5.2. Crude-oil diet with volume compositions.

crude	° API	SG (g/cm^3)	sulfur (%w)	volume flow (m^3/d)	volume rate (%)
Agbami	45.20	0.801	0.049	133	0.004
Akpo	44.96	0.802	0.066	2,444	0.069
Alcabora leste	20.26	0.932	0.562	3,624	0.102
Baz	28.54	0.884	0.271	2,428	0.068
Golfinho	26.91	0.893	0.152	339	0.010
Marlim leste jabuti	28.20	0.889	0.494	2,745	0.077
Marlim leste P-53	22.01	0.922	0.560	878	0.025
Marlim P-32	19.76	0.936	0.767	230	0.006
Marlim P-37	23.21	0.915	0.681	765	0.022
Marlim sul FPSO mls	23.59	0.912	0.599	13,569	0.383
Marlim sul P-40	22.98	0.916	0.638	168	0.005
Marlim sul P-51	21.05	0.928	0.639	986	0.028
Marlim sul P-56	18.01	0.946	0.727	565	0.016
Okono	40.61	0.822	0.057	1,556	0.044
Pennington	33.17	0.859	0.091	827	0.023
Roncador P-52	28.30	0.885	0.580	2,162	0.061
Roncador P-54	17.05	0.953	0.686	1,802	0.051
Saharan blend	43.47	0.809	0.071	237	0.007
total				35,458	1.000

In Figure 5.5 and Figure 5.6, we plot the specific gravity and sulfur profiles for each CDU cut mentioned, where specific gravity is an example of a volume-based property. The conventional swing-cut (CSW) calculations are displayed as the solid line with triangular sample points (–▲–), whereas the improved swing-cut (ISW) values are displayed as the dashed line with square sample points (–■–). As expected, with the conventional method, the light and heavy swing-cut properties are the same, which show as flat-lines for each swing-cut pair. As proposed by the new and improved swing-cut method, the light and heavy swing-cut

properties are different from its whole or bulk swing-cut property and obey the varying proportions shown in Figure 5.4.

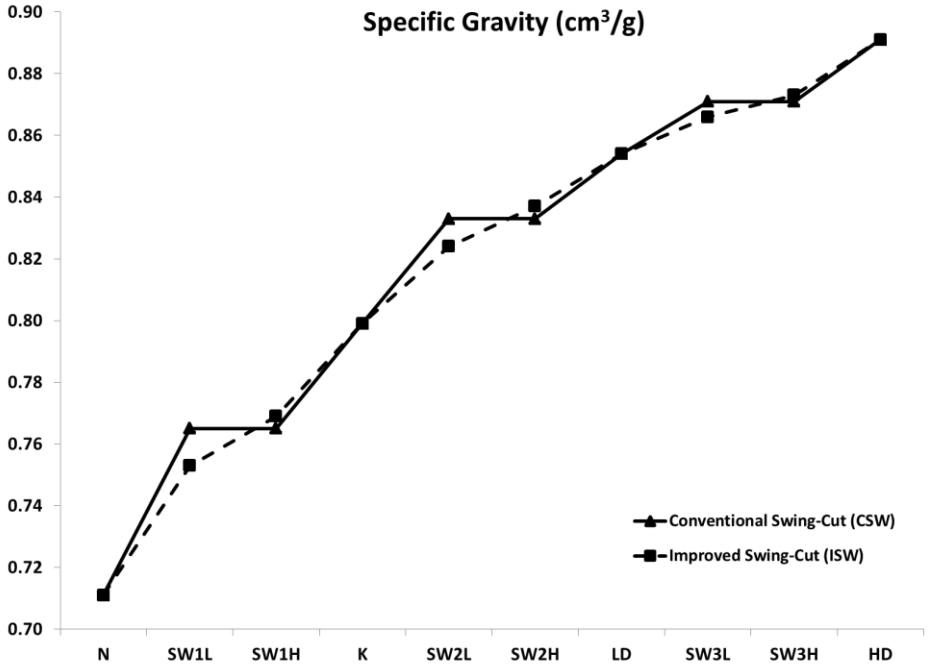

Figure 5.5. Specific gravity for each CDU cut including the swing-cuts.

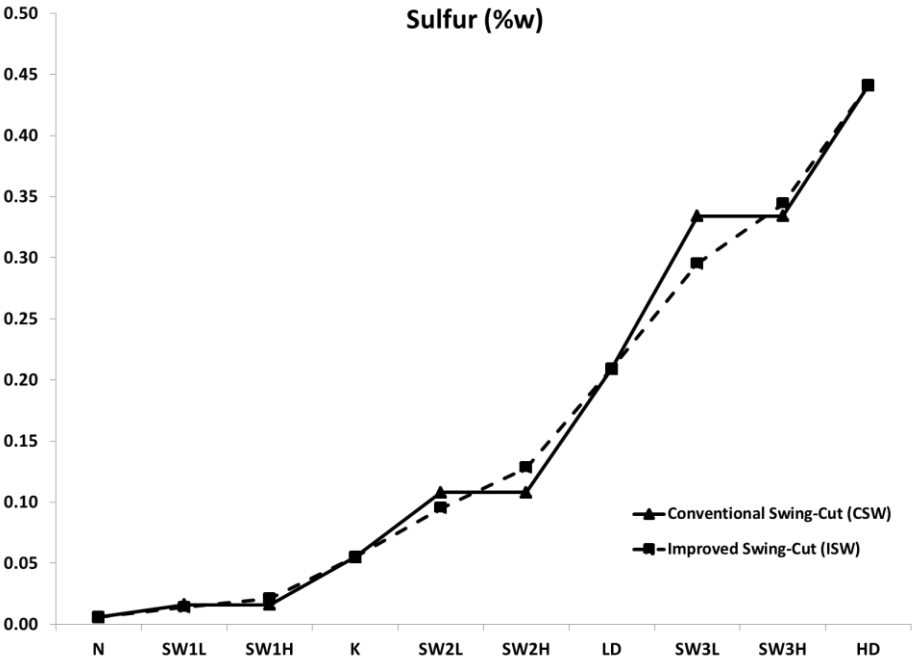

Figure 5.6. Sulfur content for each CDU cut including the swing-cuts.

Table 5.3 presents the CDU cuts volume flows determined when the throughput and crude-oil diet are fixed as the final-cut amounts for naphtha (N), kerosene (K), and light diesel (LD), which in this case are their final product demands, whereas Table 5.4 shows the

calculated specific gravity and sulfur property values for both the conventional and improved swing-cut methods. Heavy diesel (HD) amounts are not fixed

Table 5.3. Flows for CDU cuts calculated and the given final-cuts used for both swing-cut methods.

cuts	final-cuts	flow (k m^3/d)	
		cuts	final-cuts
N	N	2.762	3.208
SW1L		0.446	
SW1H	K	0.957	4.441
K		2.457	
SW2L		1.027	
SW2H	LD	1.218	4.597
LD		2.444	
SW3L		0.935	
SW3H	HD	1.564	-
HD		2.498	

Table 5.4. Specific-gravity and sulfur concentration for naphtha to heavy diesel cuts.

		SG (g/cm^3)		sulfur (%w)	
		CSW	ISW	CSW	ISW
N	naphtha-cut	0.711		0.006	
NI	naphtha interface	0.747		0.009	
SW1-cut	swing-cut 1	0.765	0.753	0.016	0.014
		0.765	0.769	0.016	0.021
KLI	kerosene light interface	0.777		0.024	
K	kerosene-cut	0.799		0.055	
KHI	kerosene heavy interface	0.817		0.068	
SW2-cut	swing-cut 2	0.833	0.824	0.108	0.095
		0.833	0.837	0.108	0.127
LDLI	light diesel light interface	0.842		0.127	
LD	light diesel-cut	0.852		0.195	
LDHI	light diesel heavy interface	0.860		0.220	
SW3-cut	swing-cut 3	0.869	0.866	0.316	0.278
		0.869	0.873	0.316	0.343
HDI	heavy diesel interface	0.882		0.344	
HD	heavy diesel-cut	0.894		0.453	

In Table 5.5, we highlight the final-cut specific gravity and sulfur properties that are calculated using both the conventional and improved swing-cut models. These values are then compared with actual data of a run performed on the CDU with the same total crude-oil flow and diet as well as with naphtha, kerosene and light diesel final-cuts.

Table 5.5. Specific-gravity and sulfur concentration values for both swing-cut methods.

	SG (g/cm^3)			sulfur (wppm)		
final-cuts	N	K	LD	N	K	LD
Conventional Swing-Cut (CSW)	0.719	0.800	0.849	75	600	1980
Improved Swing-Cut (ISW)	0.717	0.798	0.852	78	570	1950
Actual Plant Data	0.717	0.797	0.862	105	503	2354

From Table 5.4, the specific gravity predictions using the improved swing-cut method show marginally better agreement with the actual plant data compared with the conventional swing-cut method, although the conventional method is still within experimental error. For the sulfur predictions the data is more inconclusive in terms of which method is better. As for this example all crude oils are fixed and also for the final product demands of naphtha, kerosene and light diesel, the case is treated as a simulation because the number of variables and equations are the same, so there are no degrees of freedom. In the next example, the difference in qualities predictions for both swing-cuts models is shown in an optimization case for the operational planning considering different grades of diesel as like as hydrotreaters operation.

5.4.2. Example 2: oil-refinery planning case

Four crude oils are used, and the CDU diet is determined considering property specifications on the final products and the processing taking place in the CDU and hydrotreaters as shown in Figure 5.7. The sulfur reduction provided by the hydrotreaters is a variable controlled by their severity where the bounds are given by Equations 5.14 and 5.15.

$$0.950 \leq S_{D1HT} \leq 0.980 \tag{5.14}$$

$$0.960 \leq S_{D2HT} \leq 0.996 \tag{5.15}$$

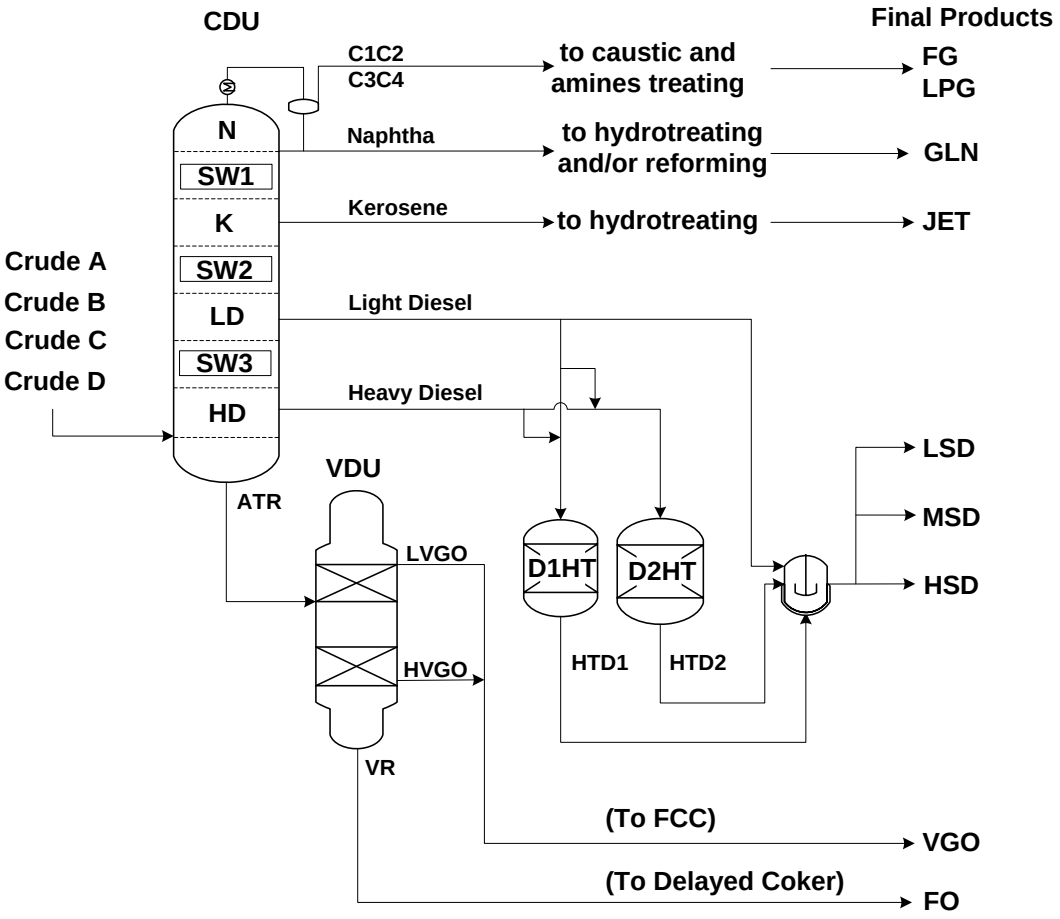

Figure 5.7. Fuels production planning case.

The final products or pooled demands are completely free or open so that the optimization problem can determine the crude-oil diet and maximize the profit considering the quality constraints for the CDU feeds and product fuels. Table 5.6 shows the results for the profit, unit throughputs, and final product amounts for the conventional (CSW) and improved (ISW) swing-cut models where the proposed model predicts an improvement in the profit of 3.3% (12.0 k US$/d or 4.380 million US$/y).

Table 5.6. Planning example results.

units (m^3/d)	CSW	ISW	lower	upper
CDU	18,000	18,000	14,000	18,000
VDU	9,960	9,960	6,000	10,000
D1HT	1,000	1,000	500	1,000
D2HT	2,200	2,200	1,000	2,200
hydrotreaters severity				
D1HT	0.950	0.950	0.920	0.950
D2HT	0.995	0.995	0.950	0.995
crude (m^3/d)			price (US$/$m^3$)	
A	2,060	2,060	720.0	
B	15,940	15,940	569.0	
C			585.0	
D			540.0	
fuels (m^3/d)			price (US$/$m^3$)	
FG	8	8		
LFG	213	213	273.0	
GLN	1,478	1,478	681.5	
JET	2,214	2,330	800.0	
LSD	1,764	1,966	708.0	
MSD	1,890	1,349	693.8	
HSD	473	697	680.0	
VGO	4,721	4,721	550.0	
FO	5,239	5,239	498.0	
profit (k US$/d)				
	367.8	379.8		

Table 5.7 and Table 5.8, the cuts (also swing-cuts) and the final pool properties explain the different production amounts for JET and the distillates using CSW and ISW methods. Because the JET has the higher price and there are only property constraints in the model, the lower light-SW2 sulfur content in the ISW model enables higher flow of this stream to the kerosene final-cut (sulfur content specification $\leq 0.030\%$) and hence a higher profit is achieved. In Table 5.8 all sulfur content specification in the products are at their maximum value, without giveaway in quality.

Table 5.7. Cuts flows and properties.

cuts	final-cuts	CSW	ISW	CSW	ISW	CSW	ISW
		cuts flows (m^3/d)		SG (g/cm^3)		sulfur (w%)	
LN	LN	1,478		0.714		0.001	
SW1L		-	-	0.765	0.756*	0.005	0.003*
SW1H	K	679	679	0.765	0.765	0.005	0.005
K		1,242		0.794		0.032	
SW2L		293	409	0.828	0.819	0.074	0.062
SW2H	LD	825	709	0.828	0.833	0.074	0.088
LD		1,490		0.848		0.148	
SW3L		-	-	0.867	0.858*	0.272	0.217*
SW3H	HD	911	911	0.867	0.867	0.272	0.272
HD		902		0.887		0.380	

*properties at the interfaces

Table 5.8. Specific-gravity and sulfur concentration in the CDU feed and final pools.

	SG (g/cm^3)		sulfur (w%)	
	CSW	ISW	CSW	ISW
CDU	0.900	0.900	0.459	0.459
JET	0.789	0.790	0.030	0.030
LSD	0.850	0.850	0.001	0.001
MSD	0.858	0.861	0.050	0.050
HSD	0.877	0.877	0.180	0.180

The size of the problem is relatively small given that we are not including the entire oil refinery, and there is only one time period that has been considered. Table 5.9 and Table 5.10 show the model sizes and also the results for the solvers CONOPT, SNOPT, and IPOPT.

Table 5.9. Models sizes.

	CSW	ISW
equations	154	194
variables	173	213
nonzeros	592	756
nonlinear	317	449

Table 5.10. Solvers results.

	CSW	ISW	CSW	ISW	CSW	ISW
	CPU (s)		iteration		profit (k US$)	
CONOPT	0.219	0.062	213	188	367.8	379.8
IPOPT	0.156	0.234	105	162	367.8	379.8
SNOPT	0.047	0.078	23	16	367.8	379.8

The modest increase in the number of extra variables, constraints, and nonzeros for the improved swing-cut method should not significantly increase the computational time when

embedded into larger planning or scheduling optimization problems. Good initial starting points for the variables can also be determined by first solving the conventional swing-cut model followed by the improved swing-cut model. In our opinion, the added accuracy afforded by the improved swing-cut method will more than offset the slight increase in solution time that may be required.

5.5. Conclusions

We have presented in this chapter a new and relatively simple improvement to the conventional swing-cut modeling found in most nonlinear planning and scheduling optimization models used to plan and schedule most of the world's oil refineries. The concept is simple, in the sense that the usual assumption that the swing-cut properties flowing from the swing-cut to the light and heavy final-cuts (or product-cuts) are the same, has been extended or modified to account for the fact that they vary according to their proportions between the light and heavy interfaces. This can be easily calculated using the bilinear equations in Equations 5.9 to 5.12. A small but representative example, taken from an actual CDU operation with eighteen crude oils and three swing-cuts (see Figure 5.3), was highlighted to demonstrate the property differences for the light and heavy swing-cut streams in both methods. Also, a planning example with different grades of diesel, including two hydrotreater operations, shows that the improved swing-cut model yields higher profit because of its higher jet fuel production, provided by the lower specific gravity value for the light-SW2 flowing to the kerosene final-cut. Conceptually, the notion that the light and heavy flows from the swing-cut to its corresponding light and heavy final-cuts have different properties is sound engineering and was shown qualitatively to be acceptable with respect to the results shown. The improved swing-cut method can choose the best solution considering the more accurate formulation, and even if the problem presented lower profit for a specific set of constraints, the improved method avoids the overestimation of the profit.

Chapter 6

in Kelly, J.D.; Menezes, B.C.; Grossmann, I.E. Distillation Blending and Cutpoint Temperature Optimization using Monotonic Interpolation. *Industrial & Engineering Chemistry Research*, 53: 15146-15156. 2014.

6. Distillation Blending and Cutpoint Temperature Optimization using Monotonic Interpolation

A novel technique using monotonic interpolation to blend and cut distillation temperatures and evaporations for petroleum fuels in an optimization environment is proposed. Blending distillation temperatures are well known in simulations whereby cumulative evaporations at specific temperatures are mixed together these data points are used in piece-wise cubic spline interpolations to revert back to the distillation temperatures. Our method replaces the splines with monotonic splines to eliminate Runge's phenomenon, and to allow the distillation curve itself to be adjusted by optimizing its initial and final boiling points known as cutpoints. By optimizing both the recipes of the blended material and its blending component distillation curves, very significant benefits can be achieved especially given the global push towards ultralow sulfur fuels (ULSF), because of the increase in natural gas plays reducing the demand for other oil distillates. Four examples are provided to highlight and demonstrate the technique.

6.1. Introduction

Oil refinement involves a series of complex manufacturing processes in which the final products (such as fuels, lubricants, and petrochemical feedstocks) are produced from crude-oil feedstocks by separation and conversion unit-operations, in coordination with tanks, blenders, and transportation vessels. To manage the processing of the hydrocarbon streams, well-known distillation curves or assays of both the crude-oil and its derivatives are decomposed or characterized into several temperature “cuts”, based on what are known as the True Boiling Point (TBP) temperature distribution or distillation curves (Riazi, 2005), and can be found in all process design simulators and crude-oil assay management programs. These curves are relatively simple and one-dimensional representations of how a complex hydrocarbon material’s yield and quality data (such as density, sulfur, and pour point) are

distributed or profiled over its TBP temperatures, where each cut is also referred to as a component, pseudo-component, or hypothetical in process simulation and optimization technology. Throughout the oil-refinery process, the full range of hydrocarbon components is transformed (blended, reacted, separated) to smaller boiling-point temperature ranges, resulting in intermediate and final products in which planning and scheduling optimization using TBP curves of the various streams can be used to effectively model these process unit-operations and predict the macroscopic (i.e., cold flow) properties of their outlet streams (Kelly, 2004). The entire refining process can be categorized into three distinct areas: crude-oil blending, refinery unit-operation processing, and product blending (Jia et al., 2004), where the focus is related to the last two areas.

Our proposed new technique is to integrate both the optimization of blending several streams' distillation curves together with also shifting or adjusting the cutpoints of one or more of the stream's initial boiling point (IBP) and/or final boiling point (FBP) in order to manipulate its TBP curve in an either offline or online environment. This shifting or adjusting of the TBP curve's IBP and FBP (front end and back end respectively) ultimately requires that the upstream unit-operation has sufficient handles or controls to allow this type of cutpoint variation, where the solution from this higher-level optimization would provide set points or targets to lower-level advanced process control systems, which are now commonplace in oil refineries. By shifting or adjusting the front end and back end of the TBP curve for one or more distillate blending streams, it allows for improved control and optimization of the final product demand quantity and quality, affording better maneuvering closer to and around downstream bottlenecks, such as tight property specifications and volatile demand flow and timing constraints.

These distillate blending streams are usually produced from divergent and multiproduct distillation towers (e.g., atmospheric and vacuum distillation columns (CDU/VDU) and fluid catalytic and hydrocracking main fractionators (FCCU/HCC)); thus, changes in the yields and properties of one stream results in changes in the adjacent streams. Physical phenomena that are related to these changes are described by molar, energy, and equilibrium balances, etc. and are significantly influenced by the tower's operating or processing conditions, such as temperature and pressure profiles, as well as its feed composition. Modeling and solving these types of phenomena would require sophisticated process design caliber and rigorous simulation software, which has its own and well-recognized set of difficulties for the type of industrial implementation used here. Instead, our

approach is simpler, whereby we adjust and interpolate actual measured data of the evaporation curves to optimize, based on downstream product blending demand flows and qualities by manipulating recipes at the blend headers and incrementally shifting initial and final cutpoints (IBP and FBP) of the upstream rundown components when required to alleviate certain bottleneck constraints encountered during the downstream blending. These new recipes and IBP/TBP cutpoints then become targets that are sent to advanced and regulatory process controllers. The benefits for such an optimization strategy can be found in a recent white paper by Honeywell (Honeywell, 2014), which has a payback of less than one-month at an European oil-refinery producing a majority of its products as diesel fuel, while similar benefits for crude-oil blend scheduling optimization can be found documented in the report by Kelly and Mann (2003a, 2003b).

6.2. Distillation Curve Overview

Hydrocarbon streams (crude oils, fuels, petrochemical feeds) are identified or characterized by distillation curves, in terms of their quantity (yield) and quality (properties) and how they vary with respect to temperature. These data are determined by experimental methods using small-scale laboratory distillation columns in which hydrocarbon fractions are collected at certain boiling-point temperatures to define their quantity and quality data or assay at each boiling temperature. These data can then be used in mathematical models, either in rigorous engineering or simplified empirical simulation and optimization environments, to determine the yields and properties of distillation, separation, or fractionation unit-operation outputs. Integrated with this can be the final product recipes necessary to match demand quantity and quality specifications such as specific gravity, sulfur, pour point, and evaporation temperatures of the fuels, so that simultaneous distillation blending and cutpoint temperature shifting or adjusting can be simulated and optimized together, as is proposed in this work.

Since obtaining TBP curve data directly from a laboratory distillation run is expensive and time-consuming, the normal procedure is to determine distillation curves by applying American Society for Testing and Material (ASTM) methods such as D86 (atmospheric) and D1160 (vacuum) or simulated distillation (SD) methods, using gas chromatography (GC) such as D2887 and D7169. These are based on reduced numbers of separation stages and can fortunately be easily interconverted to TBP data with sufficient accuracy and precision (Riazi, 2005). Figure 6.1 shows both the ASTM D86 and TBP data from the Colorado School of

Mines (2012) for a straight-run gasoline stream from a crude-oil distillation unit (CDU), plotted with volume yield percent as the ordinate and temperature as the abscissa.

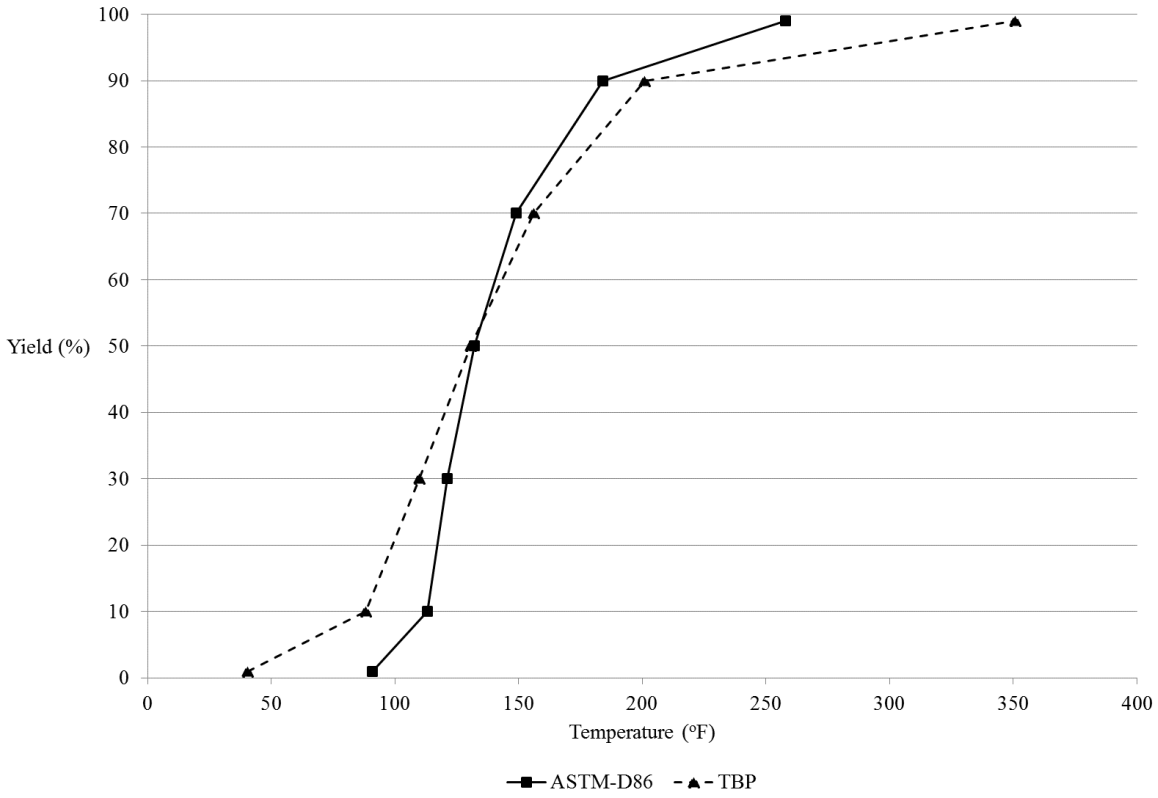

Figure 6.1. ASTM D86 and TBP volume yield percent curves.

A well-known observation, with regard to Figure 6.1, is that the ASTM D86 and TBP temperatures are near equal at their 50% yield point, whereas D86 yields are underestimated below the 50% yield and D86 yields are overestimated above the 50% yield. Equations 6.1 to 6.13 are the Riazi correlations used to convert ASTM D86 (*D01* to *D99*) to TBP (*T01* to *T99*) temperatures at conventional yield percentages of 1%, 10%, 30%, 50%, 70%, 90%, and 99%, where the same equations can be simply inverted in order to convert from TBP to ASTM D86.

$$DT1001 = 7.40120(D10 - D01)^{0.60244} \quad (6.1)$$

$$DT3010 = 4.90040(D30 - D10)^{0.71644} \quad (6.2)$$

$$DT5030 = 3.03050(D50 - D30)^{0.80076} \quad (6.3)$$

$$DT7050 = 2.52820(D70 - D50)^{0.82002} \quad (6.4)$$

$$DT9070 = 3.04190(D90 - D70)^{0.75497} \quad (6.5)$$

$$DT9990 = 0.11798(D99 - D90)^{1.66060} \quad (6.6)$$

Equations 6.1 to 6.6 use the differences between the ASTM D86 temperatures to compute TBP temperature differences at the same percent yields, where Equations 6.7 to 6.13 use the TBP temperature at 50% yield to difference backward and forward to the other TBP temperatures.

$$T01 = T50 - DT5030 - DT3010 - DT1001 \quad (6.7)$$

$$T10 = T50 - DT5030 - DT3010 \quad (6.8)$$

$$T30 = T50 - DT5030 \quad (6.9)$$

$$T50 = 0.87180\ D50^{1.02580} \quad (6.10)$$

$$T70 = T50 + DT7050 \quad (6.11)$$

$$T90 = T50 + DT7050 + DT9070 \quad (6.12)$$

$$T99 = T50 + DT7050 + DT9070 + DT9990 \quad (6.13)$$

Note that for the IBP and FBP, we use the percent evaporated at 1% and 99% instead of 0% and 100%; this is a well-known recommendation found in several sources, given then repeatability of the 1% and 99% evaporated when compared to the 0% and 100% counterparts. Other interconversion correlations can be found Riazi and Daubert (1986) and Daubert (1994). Also note that, for temperatures greater than circa 650 ºF, and at atmospheric pressure, thermal cracking may occur due to pyrolysis reactions. In these situations, ASTM D1160 should be used, which is conducted at a lower pressure (near vacuum), where its temperatures need to be corrected back to atmospheric pressure.

For product streams separated from unit-operations such as distillation columns and fractionation towers, the experimental TBP and/or ASTM distillation curves reflect the nonideal separation inside the vessels. For example, if we compare a CDU's crude-oil feed distillation curve with all of its product distillation curves, as shown in Figure 6.2, it is interesting to see what are known as overlaps between the light and heavy adjacent products; this represents what is referred to as nonsharp or nonideal fractionation (Li et al. 2005).

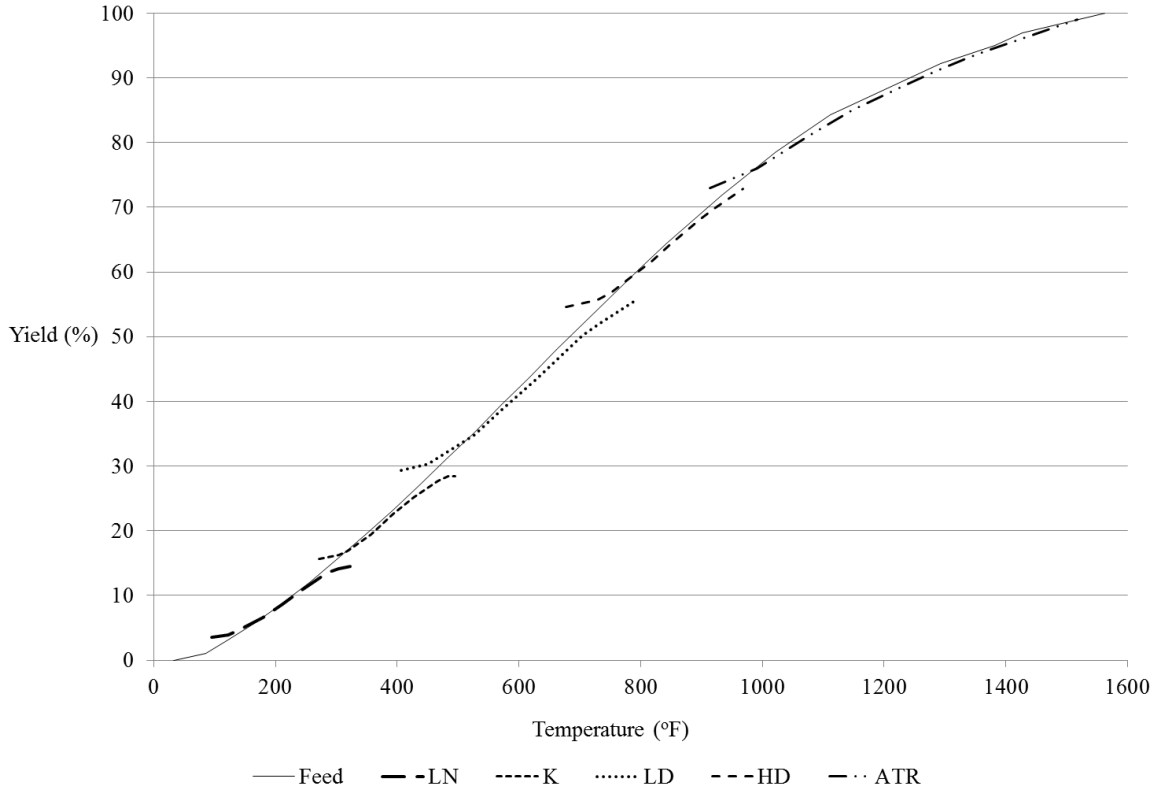

Figure 6.2. Feed and product yield curves.

These overlaps are due to the limitations in the number and efficiency of the equilibrium stages in the column, as well as the reflux ratios when operating the actual tower. In general, the separation temperature between two adjacent fractions is called the temperature cutpoint and is defined by Watkins (1979) as the midpoint of the TBP overlapping temperatures; this parameter has been used in previous studies, such as the works of Li et al. (2005), Guerra and Le Roux (2011a, 2011b), and Alattas et al. (2011, 2012).

In another study by Mahalec and Sanchez (2012), they used two models: one is a PLS model which infers product composition from some of the tray temperatures which is similar to Mejdell and Skogestad (1991), while the second model computes product yields from internal reflux and cutpoint temperatures which requires data to be generated from rigorous process simulations to develop the hybrid models.

6.3. Distillation Blending using Monotonic Interpolation

In an industrial fuels blending optimization problem, starting recipes or ingredient amounts to produce hopefully on-specification final products are based on mixing intermediate products or components with somewhat known quantity availabilities and laboratory- and/or field-analyzed qualities. However, there will be some component quantity and quality variability or uncertainty over the duration of the blend which is attenuated to some degree when dead or standing-gauge component tanks are used to decouple the upstream processing from the downstream blending (Kelly, 2006). As such, in most oil-refinery blendshops today, real-time nonlinear model-based advanced process controllers are used to control the final blended product qualities, incorporating online measurement feedback from diverse online analyzers and usually projecting one and perhaps two time periods into the future. Their manipulated variables are the recipes or ratio amounts of components directly feeding into the blender, which are transferred as set points to basic regulatory PID controllers. In this study, our focus is the off-line optimization of the initial recipes sent down to the online control strategy, although it would be straightforward to optimize in real-time provided that measurement feedback is also included similar to bias updating or moving horizon estimation employed in advanced process (Forbes and Marlin, 1994; Kelly and Zyngier, 2008).

The difficulty with blending the distillation temperatures from several component materials is that these TBP distillation temperatures do not blend linearly on a mass or volume basis. Although there is some use of what are commonly referred to as blending indices or property transforms for distillation temperatures (and used effectively for other properties such as cloud-point, pour point, viscosity, etc.), which then allow the indexed or transformed properties to be blended linearly, literature on their mathematical structure and coefficients is scarce. Instead, an acceptable approach is to convert the TBP temperatures to evaporation cumulative compositions at several pre-defined temperatures using monotonic interpolation of which linear interpolation is inherently monotonic but may not be as accurate as higher-order monotonic interpolations (Fritsch and Carlson, 1980; Fritsch and Butland, 1984; Kruger, 2002). Unfortunately, if nonmonotonic interpolation is used such as cubic splines, then oscillating behavior around the breakpoints will occur; this is well-known as Runge's phenomenon. The temperature range should be defined to span all of the expected TBP temperatures for all of the distillates included in the blend at a suitable level of resolution or

temperature discretization. After the set of evaporation components have been blended together using the recipes fractions of each component blended, the blended product's distillation temperatures at 1%, 10%, 30%, 50%, 70%, 90% and 99% evaporated, distilled or yielded are computed by again using monotonic interpolation where the evaporation components constitute the abscissa and the distillation temperatures represent the ordinate.

Monotonic interpolation is defined as a variant of cubic interpolation that preserves monotonicity of the dataset being interpolated. Monotonicity is maintained by linear interpolation but not guaranteed by cubic interpolation (Wikipedia, 2014). As observed in both Figure 6.1 and Figure 6.2, distillation curves are inherently monotonic; therefore, not using monotonic interpolation will result in unrealistic and unexpected prediction variability. Although linear interpolation will produce monotonic interpolations it does not preserve the shape of the curves. Shape-preserving cubic splines are available known as Piecewise Cubic Hermite Interpolation Polynomials (PCHIP) (Fritsch and Carlson, 1980; Fritsch and Butland, 1984; Kahaner et al., 1988; Kruger, 2002). More recently, another shape-preserving or what has been termed "constrained" cubic spline interpolation method has appeared; this method was developed based on practical arguments by Kruger (2002) and employed in the financial sector for bond yields, for example (Greeff, 2003).

To summarize, the overall calculation process of distillation blending is shown in Figure 6.3. We first interconvert from ASTM D86 to TBP temperatures, and using the TBP temperatures at their defined yields of 1%, 10%, 30%, etc., evaporations are determined by interpolating the TBP distillation curve at selected predefined TBP temperature increments. These evaporation cumulative compositions for each blending component are mixed using the ideal blending law, i.e., no excess properties and no nonlinear behavior, where, if the amounts or flows of components are fixed, then this is also called linear blending.

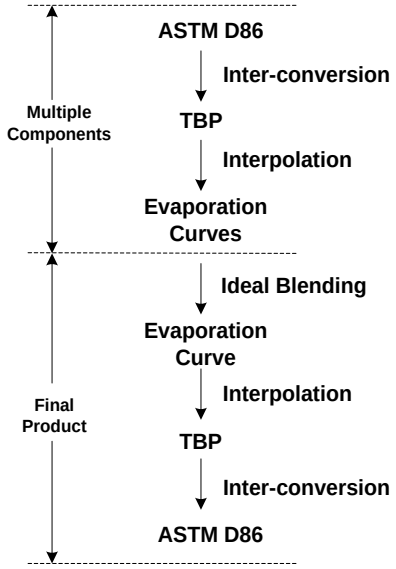

Figure 6.3. Flowchart of distillation blending calculation process.

After the blending of all of the components' evaporations, another interpolation step is used to compute the TBP temperatures of the final blended product at the defined yield values. Then, interconversion is again used to calculate the ASTM D86 temperatures, which can be downloaded to various control strategies, as mentioned.

6.4. Cutpoint Temperature Optimization

Distillation curves of petroleum products are typically plotted as TBP temperature versus relative yield percent, where we have chosen to represent the curves in the opposite way, indicating that the TBP temperature is now our independent variable or degree-of-freedom in the optimization. When yields, evaporations, or relative amounts distilled of the distillates are used as a function of temperature, the IBP (*T01*) and FBP (*T99*) can be manipulated for example to adjust or shift the distillation curve by interpolation and/or extrapolation in order to increase or decrease the front end and back end of the curves, as graphically depicted in Figure 6.4. The incremental or marginal adjustment or shifting can also be likened to fine-tuning the distillation curve, and this will ultimately translate to changing all of the relative yield values along the total or overall TBP temperature range of the distillate stream. This will have the desired effect that we can alter the evaporation amounts in the downstream blending to better control and optimize the blend quantity and quality specifications to meet market demands. However, when we manipulate the *T01* and/or *T99* for any distillate component stream, these values (interconverted to *D01* and *D99*, if required) must be sent down as targets or set points to an appropriate advanced process

control strategy on the respective upstream unit-operation such as an atmospheric crude-oil distillation column or the main fractionator tower of the fluidized bed catalytic cracking unit (FCCU). Fortunately, such strategies are available whereby reliable online analyzers measure in real-time or near-time (including sampling and analysis delays) ASTM D86 temperatures, which can be linked to pump-around heat exchanger duty and draw tray temperature controls to achieve the desired increase and/or decrease in initial and final cutpoint temperatures.

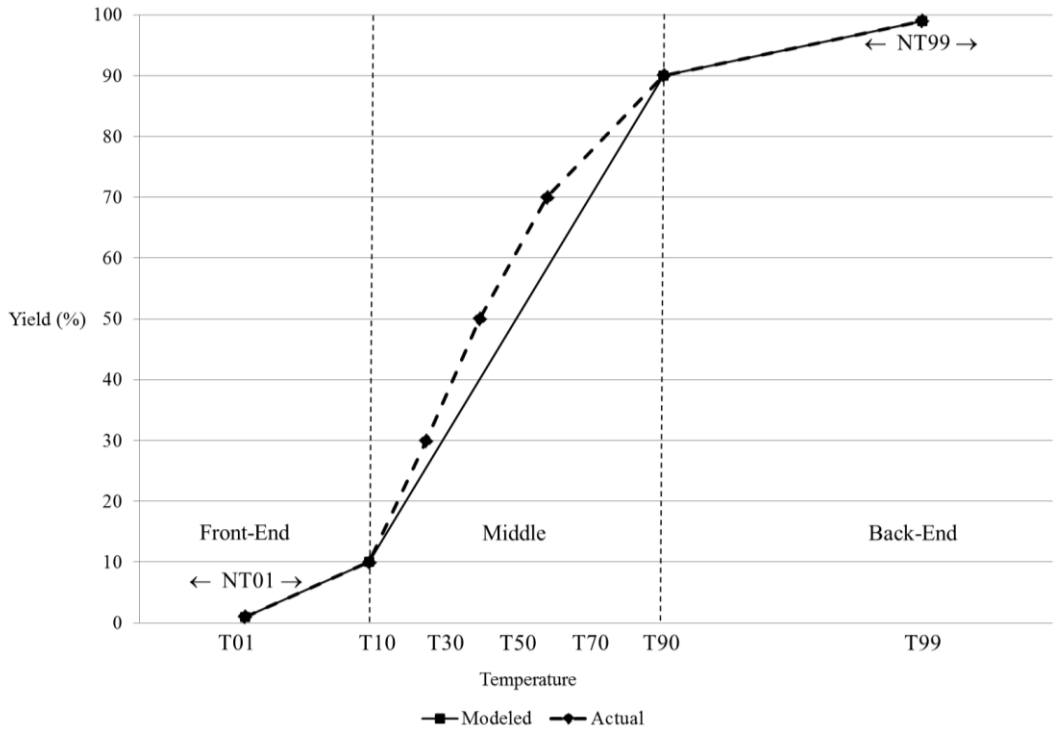

Figure 6.4. Distillation curve adjustment or shifting, as a function of TBP temperature.

Our new distillation curve adjustment or shifting technique to perform temperature cutpoint optimization is straightforward to implement mathematically. The concept is to assume that a typical distillation curve can be reasonably decomposed or partitioned into three distinct regions or parts, i.e., a front end, a middle, and a back end. The different sections can be sufficiently approximated as straight lines or piece-wise continuous from *OT01* to *OT10* for the front end, *OT10* to *OT90* for the middle, and *OT90* to *OT99* for the back end, where "O" stands for "old" and, of course, "N" stands for "new" (for the new adjusted or shifted 1% and 99% temperatures found in Equations 6.14 to 6.17, i.e, *NT01* and *NT99*).

Equations 6.14 and 6.15 model both the yield (*YNT01*) and the change or difference in the yield (*DYNT01*) when we adjust or shift *T01* from *OT01* to *NT01*, assuming a constant

slope determined from the unadjusted or unshifted old/original curve. Obviously, if *NT01* = *OT01* (no change), then *YNT01* = 0.01 and *DYNT01* = 0.0, as expected.

$$YNT01 = 0.10 - \frac{0.10 - 0.01}{OT10 - OT01}(OT10 - NT01) \tag{6.14}$$

$$DYNT01 = 0.01 - YNT01 \tag{6.15}$$

Similarly, for the back-end regime, we can model the new yield at *NT99* and its delta yield *DYNT99* in Equations 6.16 and 6.17, respectively. Morover, if *NT99* = *OT99*, then *YNT99* = 0.99 and *DYNT99* = 0.0, trivially.

$$YNT99 = 0.90 + \frac{0.99 - 0.90}{OT99 - OT90}(NT99 - OT90) \tag{6.16}$$

$$DYNT99 = YNT99 - 0.99 \tag{6.17}$$

Equation 6.18 easily models the increase or decrease in the new flow from the upstream unit-operation, depending on the amount of adjustment or shifting of the cutpoint temperature variables *NT01* and *NT99*, where *OF* denotes the old or measured flow value.

$$NF = OF(1 + DYNT01 + DYNT99) \tag{6.18}$$

A useful feature of adjusting or shifting the distillation curve, along the original front- and back-end slopes, is its ability to predict the marginal increase or decrease in the distillate stream flow directly without having to resort to a separate equation with unknown coefficients that will need to be continuously calibrated.

Given that our TBP distillation curve plots the relative yield versus temperature, we need to normalize each new yield found in Equations 6.19 to 6.25 which correspond to the temperatures *NT01*, *OT10*, *OT30*, *OT50*, *OT70*, *OT90*, and *NT99*. Again, if both *DYNT01* = *DYNT99* = 0.0, because *NT01* = *OT01* and *NT99* = *OT99*, then we are obviously left with our old or original TBP distillation curve for the upstream unit-operation component distillate stream yield profile.

$$NY01 = 0.01/(1 + DYNT99) \tag{6.19}$$

$$NY10 = (0.10 + DYNT01)/(1 + DYNT01 + DYNT99) \tag{6.20}$$

$$NY30 = (0.30 + DYNT01)/(1 + DYNT01 + DYNT99) \tag{6.21}$$

$$NY50 = (0.50 + DYNT01)/(1 + DYNT01 + DYNT99) \quad (6.22)$$

$$NY70 = (0.70 + DYNT01)/(1 + DYNT01 + DYNT99) \quad (6.23)$$

$$NY90 = (0.90 + DYNT01)/(1 + DYNT01 + DYNT99) \quad (6.24)$$

$$NY99 = (0.99 + DYNT01)/(1 + DYNT01 + DYNT99) \quad (6.25)$$

The idea for these equations is straightforward, in the sense that if we increase or decrease the front end and the back end, then given their delta yield amounts found in in Equations 6.15 and 6.17, we can easily adjust the new yields, given the old yields where the old yields are, of course, the well-defined 1%, 10%, 30%, etc. values. However, it is re-emphasized that our approach is to incrementally or marginally shift or adjust the *NT01* and *NT99* so as not to significantly disrupt the adjacent distillation streams and can be controlled by specifying acceptable bounds on *NT01* and *NT99* in the optimization.

Also, it should be pointed out that our use of the term cutpoint is somewhat different than is found, for example, in the work of Mahalec and Sanchez (2012) and chapter 5, in which a cutpoint is defined as the lower/initial and upper/final temperatures on the TPB of the entire crude oil, which hypothetically represents the crude-oil fraction distilled or evaporated from the distillation tower such as a CDU. Instead, given that the TBP curve of a CDU's crude-oil mixture is not normally available in practice, and especially if the feed is to an FCC main fractionator, which is rarely known, we use the definition commonly found in oil-refinery operations (Honeywell, 2014) of defining cutpoint temperatures as the smallest and/or largest controllable separation or fractionation temperature (i.e., IBP, 5% or 10% and 90%, 95%, or FBP) between adjacent cuts, fractions, or streams from a distillation tower.

6.5. Examples

Four examples are provided below, which are modeled and solved using IMPL (Industrial Modeling and Programming Language) from Industrial Algorithms LLC. IMPL is a problem-specific platform suitable for both discrete and nonlinear process industry optimization problems and implements monotonic interpolation as standard built-in functions, whereby all first-order partial derivatives are computed numerically but close to analytical quality (Squire and Trapp, 1998). Other modeling systems such as GAMS and AIMMS unfortunately do not provide derivatives automatically for the variables found in both the

abscissa and ordinate axes of the interpolation dataset. Another detail of the implementation in IMPL is the use of ranking, ordering, or precedence constraints to ensure that the abscissa data used in the interpolation is in ascending or increasing order, especially when the x-axis can be composed of variables. These are simple linear inequalities that enforce that the TBP temperature for, e.g, a 10% yield is less than or equal to its adjacent TBP temperature at 30%; these ranking constraints are also applied to the cumulative evaporations. Furthermore, to generate useful initial values or starting points for the optimization, IMPL also has simulation capability when the degrees-of-freedom equal zero (i.e., all component flows are fixed or known) whereby the sparse Jacobian matrix is iteratively factorized (using various LU decompositions) and successive substitution is employed to cycle to a solution. To locally solve the resulting nonlinear and nonconvex problem, IMPL employs a typical or standard successive linear programming (SLP) algorithm (Zhang and Lasdon, 1985) called SLPQPE, which is also not available in the GAMS and AIMMS but is very appropriate for these types of problems.

6.5.1. Example 1: Gasoline blending simulation

This is a gasoline or naphtha blending simulation case taken directly from a presentation on oil-refinery feedstock and product property modeling from Colorado School of Mines (2012). It is a 50:50 mixture of two gasoline components - LSR (light straight run) and MCR (midcut reformate) - with ASTM D86 (1 atm) of [(1%,91), (10%,113), (30%,121), (50%,132), (70%,149), (90%,184), (99%,258)] and [(1%,224), (10%,231), (30%,232), (50%,234), (70%,237), (90%,251), (99%,316)], respectively, where the temperatures are expressed in degrees Fahrenheit (ºF). Again, we are using their recommendation to consider the IBP and FBP temperatures to be defined at 1% and 99% instead of 0% and 100%, of course, which in practice, are difficult to measure. Converting these to TBP temperatures (also at 1 atm) using the method defined by Riazi (2005) (see pages 103-104, equations 3.20, 3.21, 3.22 and Table 3.7), we get values of [(1%,40.5), (10%,88.1), (30%,109.9), (50%,130.5), (70%,156.3), (90%,200.9), (99%,350.8)] and [(1%,200.8), (10%,224.7), (30%,229.6), (50%,234.8), (70%,241.1), (90%,263.4), (99%,384.2)], respectively, which are identical to the results from Colorado School of Mines.

When we interpolate from the interconverted TBP temperatures to evaporation cumulative fractions using the three different monotonic interpolation methods (linear,

PCHIP, and Kruger), we get the following results found in Table 6.1 and Table 6.2, along with the results from Colorado School of Mines, where Figure 6.5 plots LSR's interpolated evaporation cumulative compositions using the data from Table 6.1 and LSR's TBP curve data.

Table 6.1. Example 1's Interpolated Evaporation Fraction Results for LSR.

	Colorado	Linear	PCHIP	Kruger
E25	0.004	0.006	0.004	0.005
E50	0.017	0.028	0.017	0.017
E75	0.058	0.075	0.061	0.063
E100	0.193	0.209	0.195	0.194
E125	0.444	0.447	0.449	0.449
E150	0.654	0.651	0.659	0.659
E175	0.800	0.784	0.807	0.807
E200	0.897	0.896	0.899	0.899
E225	0.926	0.914	0.927	0.924
E250	0.948	0.929	0.948	0.944
E275	0.964	0.944	0.964	0.961
E300	0.976	0.959	0.976	0.974
E325	0.984	0.975	0.985	0.984
E350	0.990	0.990	0.990	0.990
E375	0.994	0.992	0.994	0.994
E400	0.996	0.995	0.997	0.996

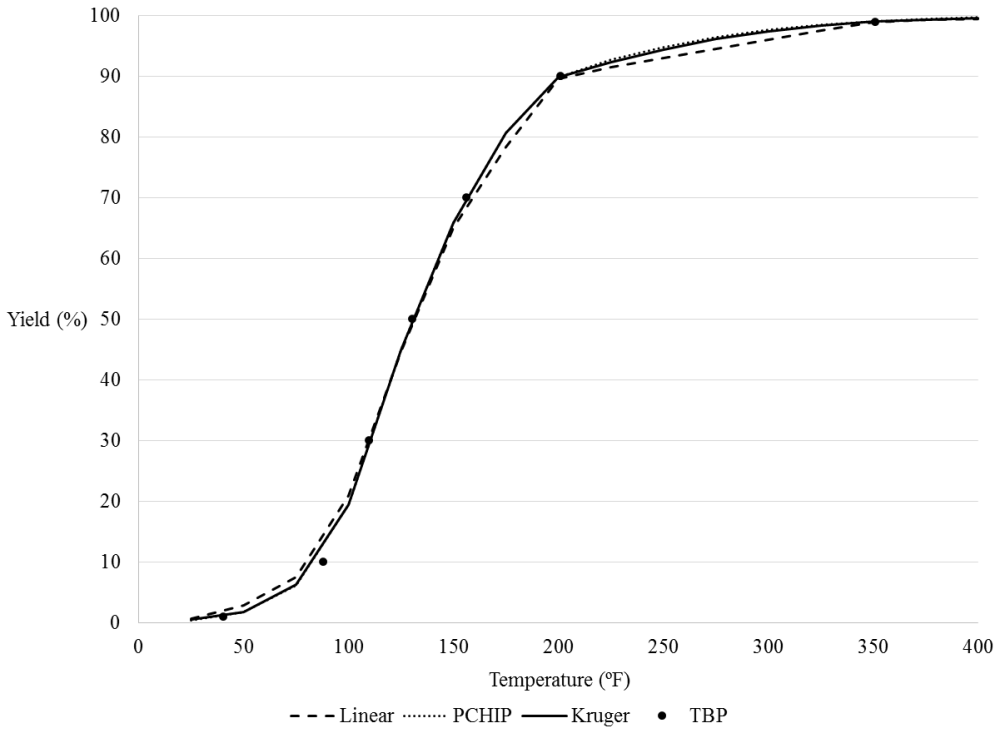

Figure 6.5. Example 1's LSR interpolated yield (%) versus TBP temperature.

It should be noted that the distillation temperature at the 10% yield point appears to be more off the curve than the others. Its deviation can be reduced by increasing the number of evaporation points used in the monotonic interpolation, although at the expense of increasing the number of points to be calculated in the simulation or optimization.

Table 6.2. Example 1's Interpolated Evaporation Fraction Results for MCR.

	Colorado	Linear	PCHIP	Kruger
E25	0.000	0.001	0.000	0.001
E50	0.000	0.002	0.003	0.001
E75	0.000	0.004	0.001	0.002
E100	0.000	0.005	0.002	0.003
E125	0.000	0.006	0.003	0.004
E150	0.000	0.007	0.005	0.006
E175	0.000	0.009	0.007	0.008
E200	0.009	0.010	0.010	0.010
E225	0.110	0.114	0.104	0.104
E250	0.796	0.780	0.817	0.813
E275	0.917	0.909	0.918	0.915
E300	0.945	0.927	0.948	0.942
E325	0.965	0.946	0.968	0.963
E350	0.979	0.965	0.980	0.978
E375	0.988	0.983	0.988	0.987
E400	0.993	0.992	0.994	0.993

After we have blended the evaporation fractions using a recipe of 50% LSR and 50% MCR, Table 6.3 shows the results using the three monotonic interpolation methods interconverting from TBP to ASTM D86 temperatures.

Table 6.3. Example 1: Interconverted ASTM D86 (TBP) Temperatures in °F.

	Colorado	Linear	PCHIP	Kruger
1%	120.5 (52.9)	109.0 (38.6)	120.0 (52.7)	118.8 (51.2)
10%	142.8 (101.0)	140.2 (97.4)	142.1 (100.5)	142.0 (100.4)
30%	163.6 (144.0)	162.6 (142.9)	161.6 (141.7)	161.4 (141.5)
50%	217.7 (218.0)	218.8 (219.2)	220.7 (221.1)	221.3 (221.8)
70%	228.6 (236.0)	230.8 (238.6)	230.4 (237.5)	230.7 (237.7)
90%	242.9 (258.7)	248.9 (265.7)	239.8 (254.0)	241.0 (255.3)
99%	305.3 (371.7)	313.2 (384.4)	303.7 (371.3)	304.9 (372.8)

Based on the temperature data, the interpolation method used by Colorado School of Mines seems to be more of a cubic spline method than a linear interpolation method, given

that they did not specify what type of interpolation method they used. The two monotonic cubic spline methods (PCHIP and Kruger) have comparable results to the first column (Colorado), especially when we consider the quoted ± 9 ºF (± 5 ºC) precision of the Riazi method (page 104) (Riazi, 2005). Therefore, we can conclude that depending on the interpolation method, different ASTM D86 interconversion temperatures can result for the same evaporation or distilled composition amounts.

Table 6.4 shows Example 1's model statistics using SLPQPE with IBM's CPLEX 12.6 as the LP subsolver on an Intel Core i7 2.2 GHz laptop computer.

Table 6.4. Example 1: Statistics.

equality constraints	107
inequality constraints	135
variables	108
equality non-zeros	672
inequality non-zeros	270

6.5.2. Example 2: Diesel blending and cutpoint temperature optimization

This case is taken, in part, from Erwin (1992), in terms of using his ASTM D86 (1 atm) temperatures for his four experimental diesel components (DC1-DC4), as shown in Table 6.5 and Figure 6.6, where the dotted line represents the final product blend distillation curve.

Table 6.5. Example 2: InterConverted TBP (ASTM D86) Temperatures in ºF.

	DC1	DC2	DC3	DC4
1%	305.2 (353)	322.2 (367)	327.0 (385)	302.4 (368)
10%	432.9 (466)	447.1 (476)	405.2 (435)	369.7 (407)
30%	521.6 (523)	507.1 (509)	457.1 (462)	441.0 (449)
50%	565.3 (551)	549.5 (536)	503.3 (492)	513.8 (502)
70%	606.4 (581)	598.4 (573)	551.1 (528)	574.3 (550)
90%	668.3 (635)	666.1 (634)	605.8 (574)	625.4 (592)
99%	715.7 (672)	757.7 (689)	647.0 (608)	655.2 (620)

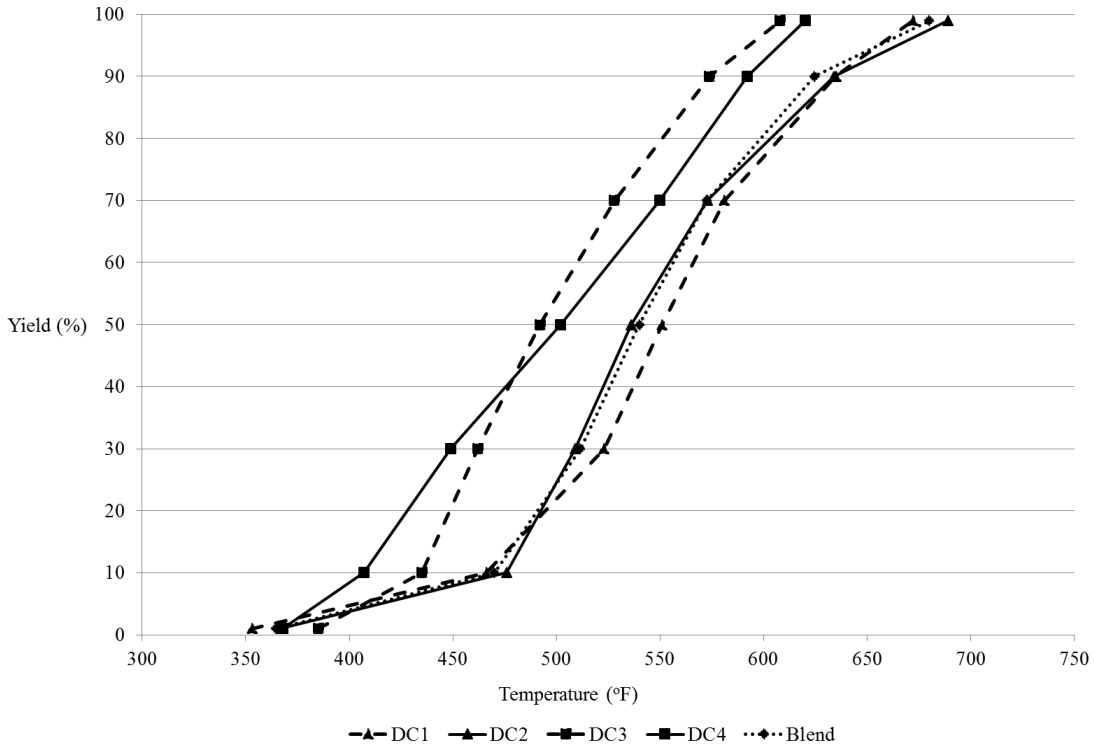

Figure 6.6. Example 2's TBP distillation curves, including the final blend.

Our blending and cutpoint temperature optimization objective function is to maximize the flow of DC1 and DC2, subject to their relative and arbitrary pricing of 0.9 for DC1 and 1.0 DC2, with lower and upper bounds of 0.0 and 100.0 each. For simplicity, we have fixed each of the flows for DC3 and DC4 to a marginal and arbitrary value of 1.0, and the total blend flow cannot exceed 100.0. The typical ASTM D86 temperature specification for international diesel sales is D10 ≤ 480, 540 ≤ D90 ≤ 640, and D99 ≤ 690 ºF. To make this problem more interesting, we have set the bounds to D10 ≤ 470, 540 ≤ D90 ≤ 630 and D99 ≤ 680. This ensures that it is not possible to satisfy the diesel blend with the most valuable DC2 component as its D10, D90, and D99 temperatures are all greater than our blended diesel's distillation temperature specification. Furthermore, it is also not possible to fill the blend with all DC1, because its D90 does not comply with the specification. As such, this forces a mixture of DC1 and DC2 and as we shall see, this also requires an adjustment or shifting to the distillation curve for DC1 where only the DC1 material is allowed to have manipulated cutpoint temperatures. At the optimized solution, *NT01* = 312.8 and *NT99* = 689.3, which are both different than their original values of *OT01* = 305.2 and *OT99* = 715.7. Since both their front- and back-end temperatures have been reduced, we expect that the new flow for DC1 is less than the old flow and it is *NF* = 37.06 and *OF* = 39.24; consequently, the flow for DC2 is

60.94 which is consistent with the total flow of 100.0. The new and optimized TBP curve for DC1 given its front- and back-end shifts is now [(1.053%,312.8), (10.015%,432.9), (31.188%,521.6), (52.361%,565.3), (73.534%,606.4), (94.707%,668.3), (98.995%,689.3)], where the new yields are computed from Equations 6.19 to 6.25.

Table 6.6 shows Example 2's model statistics solved using SLPQPE with CPLEX.

Table 6.6. Example 2: Statistics.

equality constraints	367
inequality constraints	595
variables	371
equality non-zeros	3112
inequality non-zeros	1190

6.5.3. Example 3: Gasoline blending actual versus simulated and optimized

This case is taken from an actual PETROBRAS oil-refinery's blend-shop, comparing its ASTM D86 temperatures for a blended gasoline product with three naphtha components (GC1, GC2, and GC3), as shown in Table 6.7, as well as highlighting its actual blended specific gravity (volume basis) and sulfur concentration (mass basis). The third component (GC3) is actually the heel in the product tank, which is the opening or starting material in the tank before the blending operations begin and its amount cannot be adjusted.

Table 6.7. Example 3: ASTM D86 temperature (°F), specific gravity, and sulfur content.

	GC1	GC2	GC3
1%	89.6	104.0	97.0
10%	122.9	140.0	139.6
30%	157.8	163.4	172.6
50%	206.6	197.6	243.1
70%	268.0	230.0	275.2
90%	340.9	293.0	340.3
99%	426.0	363.2	427.5
SG (g/cm^3)	0.7514	0.7008	0.7671
S (wppm)	48	57	38

The simulated quality values using the Kruger monotonic interpolation show good agreement with the actual values found in Table 6.8, where the blended component volumes and recipe amounts are found in Table 6.9. An exact match between the actual and simulated

values is difficult, given the unknown random and systemic errors that may be present in both the measured quantities and qualities.

Table 6.8. Example 3: Actual, simulated, and optimized properties and specifications.

		SG (g/cm^3)	S (wppm)	D10 (°F)	D50 (°F)	D90 (°F)
specs	min	0.7000				
	max	0.7800	65	149.0	248.0	374.0
actual		0.7290	55	131.9	206.1	320.2
simulated	linear	0.7271	51	135.4	208.8	314.9
	interpolation	0.7271	51	134.8	205.2	321.7
optimized	interpolation	0.7225	52	136.5	204.2	318.0

We have included both the “linear” and “interpolation” values for the ASTM D86 10%, 50%, and 90% results, which were the only values available from the laboratory measurements. The linear values do not use the TBP temperatures, evaporation components, or the monotonic interpolation and blend based on assuming that the ASTM D86 temperatures blend ideally or linearly by volume. As can be seen in Table 6.8, we observe that the linear ASTM D90 temperature underpredicts the actual D90 result, which is expected.

Table 6.9. Example 3's actual, simulated, and optimized volumes and prices.

	prices	actual/simulated		optimized	
	(US$/m^3)	Volume (m^3)	Recipes	(m^3)	Recipes
GC1	748.09	6465.2	26.7%	4229.1	17.5%
GC2	632.75	13066.8	53.9%	15302.9	63.2%
GC3	684.66	4692.5	19.4%	4692.5	19.4%
blend	684.66	24224.5	100.0%	24224.5	100.0%
profit (k US$)		268.3		526.1	

If we optimize the blend recipes to maximize profit (revenues minus costs) using the prices found in Table 6.9, then there seems to be significant opportunity to reduce the cost of the final blended product for a fixed quantity demanded as shown in the last row of Table 6.9, The GC1, GC2, and GC3 prices are actually costs to produce the final blend. The GC3 cost and the blend price have the same values, since GC3 is the tank heel considered in the example. The same pricing is true in the next example.

It should be noted that the recipe obtained in Table 6.9 can be considered a local optimum, given that property values in Table 6.8 are on-specification but with giveaways in the ASTM D86 that would be reduced by higher amount of the cheapest component (GC2).

Table 6.10 shows Example 3's model statistics using SLPQPE with CPLEX.

Table 6.10. Example 3: Statistics.

equality constraints	278
inequality constraints	424
variables	279
equality non-zeros	1900
inequality non-zeros	848

6.5.4. Example 4: Diesel blending actual versus simulated and optimized

Example 4 is again taken from an actual PETROBRAS oil-refinery's blend-shop, comparing its ASTM D86 temperatures for a blended product with six distillate components (DC1-DC6), shown in Table 6.11, as well as comparing its blended specific gravity and sulfur concentration, where DC6 is the tank heel.

There is also the addition of ASTM D86 85% temperature, which is required for the diesel product's quality specification limits. The TBP temperature at 85% is calculated by interpolating the standard TBP temperatures at 1%, 10%, 30%, 50%, 70%, 90%, 99% and then creating another interpolation using these TBP temperatures as the abscissa and the corresponding calculated ASTM D86 temperatures as the ordinate.

Table 6.11. Example 4: ASTM D86 temperatures (°F), specific gravity, and sulfur content.

	DC1	DC2	DC3	DC4	DC5	DC6
1%	227.5	297.1	345.4	360.1	294.3	275.9
10%	277.0	331.0	438.1	452.8	369.9	358.5
30%	309.6	344.8	492.4	515.3	412.0	426.7
50%	345.6	361.9	532.8	581.7	443.5	495.1
70%	390.4	389.7	573.8	652.3	475.7	579.0
85%	434.8	427.1	614.8	713.8	507.9	658.9
90%	454.3	443.1	634.6	741.7	524.8	693.3
99%	507.6	503.6	672.6	806.4	587.5	763.7
SG (g/cm^3)	0.7886	0.7925	0.8505	0.8773	0.8264	0.8454
S (wppm)	842	10	231	131	157	315

Presented in Table 6.12 and Table 6.13 are the volume, price, properties, and specification data used to solve both the simulated and optimized cases.

Table 6.12. Example 4: Actual, simulated, and optimized volumes and prices.

	prices	actual/simulated		optimized	
	(US$/m^3)	volume (m^3)	recipes	volume (m^3)	recipes
DC1	770.94	1598.6	10.2%	4013.6	25.6%
DC2	783.78	1274.4	8.1%	448.0	2.9%
DC3	795.65	4214.4	26.9%	1211.8	7.7%
DC4	777.14	6682.5	42.6%	7077.3	45.1%
DC5	779.48	871.9	5.6%	1891.1	12.0%
DC6	791.43	1053.8	6.7%	1053.8	6.7%
blend	791.43	15695.6	100.0%	15695.6	100.0%
profit (k US$)		130.6		204.3	

Table 6.13. Example 4's actual, simulated and optimized properties and specifications.

		SG (g/cm^3)	S (wppm)	D10 (ºF)	D50 (ºF)	D85 (ºF)	D90 (ºF)
specs	min	0.8200			473.0		
	max	0.8650	500		590.0	680.0	
actual		0.8488	311	372.6	514.9	654.6	688.1
simulated	linear	0.8492	306	410.1	513.2	620.4	644.2
	interpolation	0.8492	306	376.5	507.4	664.1	697.7
optimized	interpolation	0.8419	488	343.0	474.8	672.9	714.8

As shown in Table 6.13, again, despite inaccuracies in the actual distillate component amounts and qualities measured, there is close agreement for specific gravity, sulfur content and ASTM *D10*, *D50*, and *D90*, within experimental error, using the Kruger monotonic interpolation. The other distillation temperatures for *D01*, *D30*, *D70* and *D99* were not measured by the laboratory. However, the actual *D85* is available, although our prediction is slightly outside the ± 9 ºF error bounds. Comparing the linear blending with the actual, it significantly overestimates the *D10* temperature and underestimates both the *D85* and *D90* temperatures as expected. This confirms that unless a suitable blending index or transform is applied to the distillation temperatures or we use the method described in this chapter, then significant overpredictions and underpredictions of the front end and back ends of the distillation curves will result.

When we optimize the component recipes or volumes to maximize the profit, we notice that the sulfur concentration is pushed to its upper bound of 500 wppm, whereby less-expensive distillates are used to reduce the overall cost of the blended final product, increasing the profit by $72.6 k US$, as displayed in Table 6.12. Similar to the gasoline blend-shop example, the recipe obtained in Table 6.12 can be considered a local optimum, given that property values in Table 6.13 are on-specification but with giveaways in ASTM D86 and sulfur content that would be reduced by higher amount of the cheapest component (DC1), although the result are close to the minimum specification for D50 (473.0 ºF) and sulfur content (500 wppm) and this would allow only a little addition of DC1 because of its D50 (345.6 ºF) and sulfur content (842 wppm) values.

Table 6.14 shows example 4's model statistics using SLPQPE with CPLEX.

Table 6.14. Example 4: Statistics.

equality constraints	361
inequality constraints	527
variables	366
equality non-zeros	2614
inequality non-zeros	1054

6.6. Conclusions

In this chapter, we have presented the fine points of performing distillate blending and cutpoint temperature optimization using monotonic interpolation. The first step of the procedure is to convert from faster and less-expensive experimental methods, such as ASTM D86, to the slower and more expensive TBP temperatures, using well-established interconversion analytical expressions. These interconverted TBP temperatures are converted to cumulative evaporations similar to pseudocomponents in process design simulators using monotonic interpolation, blended linearly by mass or volume, then converted back to TBP temperatures using another monotonic interpolation. If required, these values are interconverted back to ASTM D86, and this defines the second step. The third step is to adjust or shift the front end and/or back end of one or more of the component TBP distillation curves by optimizing the *T01* (1%) and/or *T99* (99%) cutpoint temperatures, while respecting the relative yields of the adjusted or shifted distillation curves. It is the third step that, to our knowledge, has not been discussed in the literature prior to this work and if distillation blending indices are used instead of mixing, cutting, and interpolating with evaporation

components then this type of temperature cutpoint optimization is not possible. As highlighted in the Introduction, significant economic benefits can be achieved by implementing such an algorithm, especially for ultralow sulfur fuels which always require accurate prediction of key evaporation points on the final product distillation curves.

Chapter 7

7. Generalized Capital Investment Planning of Oil-Refinery Units using MILP and Sequence-Dependent Setups

Due to the complexity of oil-refinery processes, in which a mix of hydrocarbon molecules (crude-oil) is separated and converted, respectively, by physical and chemical processes, industrial-sized models integrating phenomenological (blending, processing) and procedural (sequences, setups) optimizations in planning and scheduling problems can be very difficult to solve in a full space MINLP formulation. Therefore, solution strategies such as MILP approximations, shown in this chapter, and decompositions, described in chapter 8, can be proposed to handle such complicated models with reasonable accuracy.

7.1. Introduction

To optimize process design in oil-refineries, we propose an input-output or Leontief (Leontief, 1986) modeling, also found in generalized network-flow and convergent and divergent problems, to allow all of the units, facilities, and equipment to be modeled both with multiple operations or activities and with multiple inputs and outputs interconnected both upstream and downstream forming a complex network, chain, or more appropriately an arbitrary superstructure. These can be easily represented in large-scale and sophisticated optimization problems using a new modeling and solving platform called IMPL (Industrial Modeling & Programming Language; see Appendix C) that is flowsheet, fundamentals and formula-based.

In contrast to the use of MINLP models to optimize nonlinear continuous and discrete variables in a full range space, MILP input-output models vary in a set of modes defined for parameters such as yields, rates and sizes and circumvent some of the drawbacks of the MINLP models, which includes: providing good initial values of the continuous variables to avoid infeasibilities in the nonlinear programming sub-problems and the difficulty of even solving the root NLP node when the binary or discrete variables are treated as continuous. Furthermore, given the inherent non-convexities, solving an MINLP to global optimality may become intractable for medium and large scale problems. MILP input-output approaches may not suffer from these problems, although they can vary only for the points set in the modes,

i.e., within a reduced space. Therefore, in general they provide only an approximation to the original MINLP, albeit with much greater robustness.

The proposed MILP formulation represents projects to improve or extend/enhance assets by capacity, capability or overall facilities expansion in which admissible project schedules must obey constraints such as stage dependencies, product demands, and other resource restrictions. We address the modeling of stages, activities, or tasks explicitly in order to better predict the different types of capital investment planning known as revamping, retrofitting, and repairing especially found in the petroleum, petrochemicals and oil & gas industries. We generalize or unify the modeling by combining supply-chain production and inventory planning balances with scheduling concepts of sequence-dependent setups, switchover, or changeovers (Kelly and Zyngier, 2007) to represent the construction, commission, and correction stages, in which required capital resources can be defined by product demands to be matched or limit the number of projects to be approved. The importance of the stages is that during their executions, e.g., the existing assets are totally or partially shut down, so that the plant production is modified within project time windows. This to our knowledge, has not been addressed in the conventional process design retrofitting or synthesis models found in the literature (Sahinidis et al., 1989; Liu and Sahinidis, 1996; Iyer and Grosmann, 1998; Van den Heever and Grossmann, 1999; Jackson and Grossmann, 2002).

Similar applications of the proposed approach can also be employed to what is known as production and process design synthesis, asset allocation and utilization, and turnaround and inspection scheduling. Two motivating examples describe the modeling including their IMPL's configuration and equations (see the supplementary material). A retrofit case reproduced from Jackson and Grossmann (2002) and an investment planning of an oil-refinery plant are given as examples.

In addition to the novel project execution phase using sequence-dependent setups modeling, capital and capacity of the units are regarded as flows or amounts as in a scheduling environment that, to our knowledge, has not been addressed in this way in the literature prior to this work. The problem includes expansion/extension of existing and installation of new units or equipment modeled in a non-aggregated framework, i.e., in an actual or real plant configuration. In this case, considering also a multiperiod formulation, the model size gives rise to large-scale MINLP problems in which the input-output approximation

using sequence-dependent setups modeling is proposed for solving industrial-sized problems in an MILP model.

7.2. Sequence-dependent setup modeling of stages

Here we describe the sequence-dependent setups, changeover, or switchover discrete-time modeling (Kelly & Zyngier, 2007) to optimize projects and their stages in the capital investment planning problem. Unlike conventional approaches, such as the full space (Sahinidis et al., 1989; Liu and Sahinidis, 1996), the bi-level decomposition (Iyer and Grosmann, 1998; You, Grossmann, and Wassick, 2011; Corsano et al., 2014), and the generalized disjunctive programming formulation (Van den Heever and Grossmann, 1999; Jackson and Grossmann, 2002), we address explicitly the project setup and startup over time by modeling it essentially as a scheduling problem. When complex process frameworks like those found in the oil-refining industry are modeled, project life time must be included to better assess capital resource predictions and production discounts in the NPV function. In this sense, the conventional capital investment planning approaches are more suitable for repair or retrofit problems, where disregarding project execution time and related production changes has little influence in the decisions because of the lower capital investment involved and lower project impacts in the production. In the end, any kind of improvement in the reproduction of project scheduling and staging within the oil-refining industry can potentially save millions, if not billions of U.S. dollars, from the shorter term repair types of projects to the longer term revamps and installations of process units.

We introduce staging or phasing as variation of the sequence-dependent changeover problem (Kelly and Zyngier, 2007, Balas et. al., 2008) except that the sequencing, cycling, or phasing is assumed to be fixed as opposed to being variable or free. Phasing allows for the implementation of what is known in the specialty chemicals and consumer goods industries as a product-wheel, and also known as blocking in other industries where the cost of sequence-dependent changeovers is significant such as in the paper and bottling industries. A product-wheel forces product A to be followed by product B then followed by product C and so on. In this way, the sequence-dependency is fixed or forced, i.e., it is essentially pre-defined, as opposed to variable or free sequence-dependent switchovers, requiring more variables and constraints to be modeled and more solution time when solving or searching for solutions. Hence, the advantage of phasing is that it can be used to find solutions quicker at the expense

of being less flexible in terms of handling more disruptions or disturbances with respect to supply, demand, investment, maintenance, and other production-order scenarios.

The other three sequence-dependent changeover modeling types are purging, prohibiting, and postponing. Purging requires a repetitive maintenance task to be configured between two production or process operations involving cleaning activities that may or may not require the consumption and/or production of resources, which in the capital investment planning case can be considered the configuration or re-configuration task (correction, commission, and construction). Prohibiting forbids or disallows certain sequences of operations from ever being scheduled or occurring like as in a multi-product pipeline or blender in which certain sequence of products are strictly not allowed to avoid or decrease product contamination. Postponing implements sequence-dependent and sequence-independent down-times between certain operations, modes, or stages of a unit.

7.2.1. Types of capital investment planning

Considering the projects with stages or phases in a capital investment planning (CIP), the types of projects can be classified as revamping (facilities planning), retrofitting (capacity/capability planning), and repairing (maintenance/turnaround planning). We denote the proposed model as the generalized capital investment planning (GCIP) problem extending the conventional capital investment planning (CCIP), and specifically for the retrofit problem as discussed in Sahinidis et al. (1989) and Liu and Sahinidis (1996). CCIP is the optimization problem where it is desired to expand the capacity and/or extend the capability (conversion) of either the expansion of an existing unit or the installation of a new unit (Jackson and Grossmann, 2002).

Figure 7.1 shows the three types of CIP problems with its capital cost and time scales.

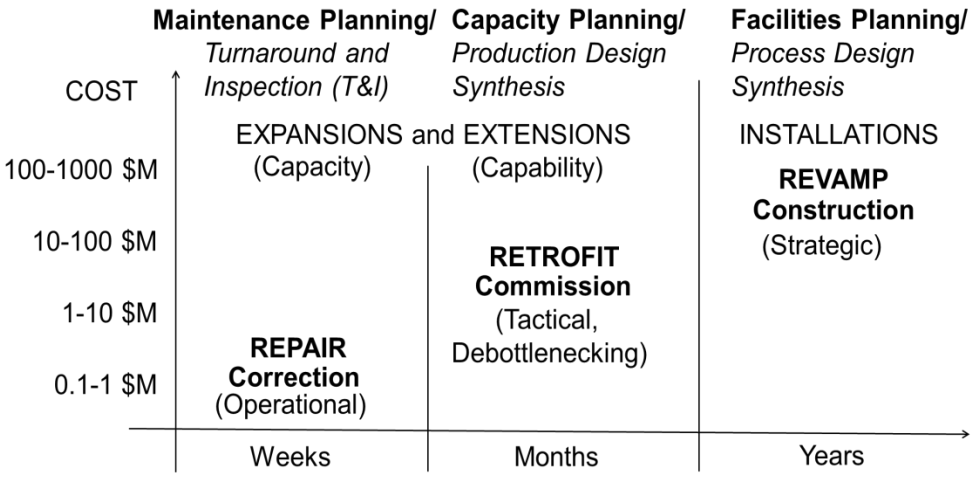

Figure 7.1. Three types of capital investment planning problems.

The shortest CIP problem is the repair problem, which is typically referred to as maintenance planning or turnaround and inspection (T&I) planning, and has a correction stage that is placed in between the existing unit before the correction and the improved unit after the correction. For repair problems, the correction stage is in general in-series and is the stage that implements the turnaround & inspection operations such as de-fouling or cleaning heat exchangers, etc. In this case, the existing process can be totally or partially shut-down during the corrections.

The medium term CIP problem is the retrofit problem (i.e., replacing or refitting new or enhanced equipment after it is already been constructed and in production) and is often referred to as capacity planning or production design synthesis and has a commission stage that is placed in between the existing unit before the commission and the expanded/extended capacity/capability of the unit after the commission. For retrofit problems, there can be a construction stage in-parallel to the existing stage, and the commission stage is in-series similar to a cleaning/purging (or repetitive maintenance) operation, activity, or task in sequence-dependent setup, changeover, or switchover problems. The existing process can be partially or totally shut down during the commission stage.

The longest CIP problem is the revamp problem, which is sometimes referred to as facilities planning and process design synthesis, and has a construction stage that is placed in between the existing unit before the construction and the expanded/extended capacity/capability of the unit after the construction. If the unit does not previously exist, then this is an installation versus an expansion/extension. For revamp problems, the construction stage is in-series and is the stage that installs the expanded or extended equipment. The

existing process is totally shut down during the construction or revamp stage. For an installed new unit, a commission phase can be placed between the construction and installed stages, in which, as example, parts of the new process unit are started up before its full implementation. To accommodate multiple expansions within the same planning horizon, multiple pre-preparation, commission, and expansion operations need to be configured, where sequence-dependent setups or switchovers can only occur from a previously expanded operation through a commission operation to the next expanded operation as a phasing sequence.

To the best of our knowledge, this is the first time a connection between the different types of CIP problems has been made, i.e., repair/correction (operational), retrofit/commission (tactical/debottlenecking), and revamp/construction (strategic). There are two other salient aspects of our general CIP formulation that sets our formulation apart from all other formulations found in the literature. The first is the modeling of sequence-dependent setups, switchovers, or changeovers to manage the realistic situation that a correction, commission, or construction stage, activity, or task must be planned or scheduled in between the existing and expanded/extended capacity/capability of the units. This is handled using the appropriate variables and constraints found in Kelly and Zyngier (2007), which albeit intended for discrete-time scheduling problems with repetitive maintenance, can be easily applied to CIP problems that are also modeled in discrete-time given the longer term decision-making framework. The second aspect is the modeling of capacity (and capability) and capital as flows or quantities. This is the notion that the correction, commission, and construction stages actually produce or create capacity and/or capability, which can then be used or consumed by the unit in subsequent time-periods, yet there is, of course, a charge for the capacity/capability known as the capital cost expenditure. Net present value (NPV) adjustments due to inflationary or deflationary trends over time can be applied to the cost of capital, and is simply reflected as a modification to the cost weights in the objective function. A specific NPV representation for an MINLP process design synthesis of oil-refinery units in Brazil can be found in chapter 4. An extensive review on retrofit design of processes can be found in Grossmann et al. (1987), where different types of redesign decisions such as throughput or conversion increase, product quality improvement, new feedstock processing, among others are explored to indicate the possible alterations (equipment expansion, extension, installation, etc.) to achieve the goals. The authors outline the strategies for design problems as (i) optimize the process using operating and performance models, (ii) identify subset of equipment for removal, expansion, installation to improve the process, (iii) develop primal

and dual bounding information in decomposed models, (iv) establish and evaluate alternative configurations using existing equipment where needed.

7.2.2. Sequence-dependent setup formulation

To model the sequence-dependent transitioning of stages in our formulation, we use the concept of "memory" variables first described in Kelly and Zyngier (2007). This is a key notion because it tracks the temporal unit-operation events or activities occurring for each unit within the time horizon, thus allowing us to know the last production operation or state that was active for the unit. It is important to note that the repetitive maintenance or non-productive operation does not have a memory variable.

The sequence-dependency of the unit-operation-time setup variable $y_{i,t}$ for each production mode i representing the initial, intermediate, or final state of a unit rely on four dependent transition variables: the startup of an operation $su_{i,t}$, its shutdown $sd_{i,t}$, switch-over-to-itself $sw_{i,i,t}$, and the memory $yy_{i,t}$ of the last operation performed. These dependent variables are relaxed within the interval [0,1] by considering them as continuous variables, so that we do not need to explicitly declare them as binary variables in the global search of the MILP (i.e., in the branch-and-bound). To enable this, an additional relationship is necessary to preserve the integrality of $su_{i,t}$ and $sd_{i,t}$ to prevent the linear program from setting both $su_{i,t}$ and $sd_{i,t}$ to 0.5 in the LP nodes of the branch-and-bound search (see Equation 3 in Kelly and Zyngier, 2007).

The sequence-dependent setup, changeover, or switchover relationship between different operations (phasing, purging, prohibiting, and postponing) on the same unit can be derived from these dependent variables, whereby intermediate operations can be activated and placed in between the mode operations such as the project execution phases proposed in this work, i.e., the correction, commission, or construction stages. The mode-operation setup variable $y_{i,t}$, in the proposed GCIP model are defined as ("Existing", "Non-Existing") and ("Expanded", "Extended", "Installed") stages of a capacity investment planning problem in which the input-output yields, rates, etc., for each operation on the same unit can have different values. Increasing the number of project stages between the initial and final project state can improve the accuracy of the problem.

The memory and sequence-dependent setup constraints to manage the project staging are shown in Equations 7.1, 7.2, 7.3, and 7.4, respectively (Kelly and Zyngier, 2007).

$$\sum_i yy_{i,t} = 1 \quad \forall \; t \tag{7.1}$$

$$y_{i,t} - yy_{i,t} \leq 0 \quad \forall \; i,t \tag{7.2}$$

$$yy_{i,t} - yy_{i,t-1} - su_{i,t} \leq 0 \quad \forall \; i,t \tag{7.3}$$

or

$$yy_{i,t-1} - yy_{i,t} - sd_{i,t} \leq 0 \quad \forall \quad i,t \tag{7.4}$$

By Equation 7.1, if even any operation i is not being performed in the unit, the information on the last productive operation is preserved by the memory variables $yy_{i,t}$. This is a single-use or unary-resource or commitment constraint that states that one and only one production operation must be active or setup on the unit in any given time-period. In Equation 7.2, when a unit is performing a particular production operation, the appropriate memory variables $yy_{i,t}$ are activated. Equations 7.3 and 7.4 propagate the memory of the productive operation when the unit is completely shut-down or inactive during the productive to the non-productive transitions and vice-and-versa. Equation 7.3 is when the unit goes from the non-productive to the productive state, so it is a startup $su_{i,t}$. Equation 7.4 is when the unit goes from the productive to the non-productive state, so it is a shutdown $sd_{i,t}$. Equations 7.1-7.4 are applied even for units that always have an operation active throughout the horizon such as a storage unit (tank), given that sequence-dependent switchovers from one operation to another must be properly tracked, in this case, the unit-operation is in a switchover-to-itself, $sw_{i,i,t}$. Figure 7.2a shows the stages of two batches and the profiles of the independent variable ($y_{i,t}$) and the four dependent variables ($su_{i,t}$, $sd_{i,t}$, $sw_{i,i,t}$, and $yy_{i,t}$) extracted from Kelly and Zyngier (2007). For the capital investment planning case (Figure 7.2b), the startup, shutdown and switchover-to-itself variables are disregarded, only the setup and the memory variables are defined to control the project scheduling and staging. In our project scheduling case, the time-duration of the dependent startup and shutdown transitions are covered by the intermediate stages (correction, commission, or construction).

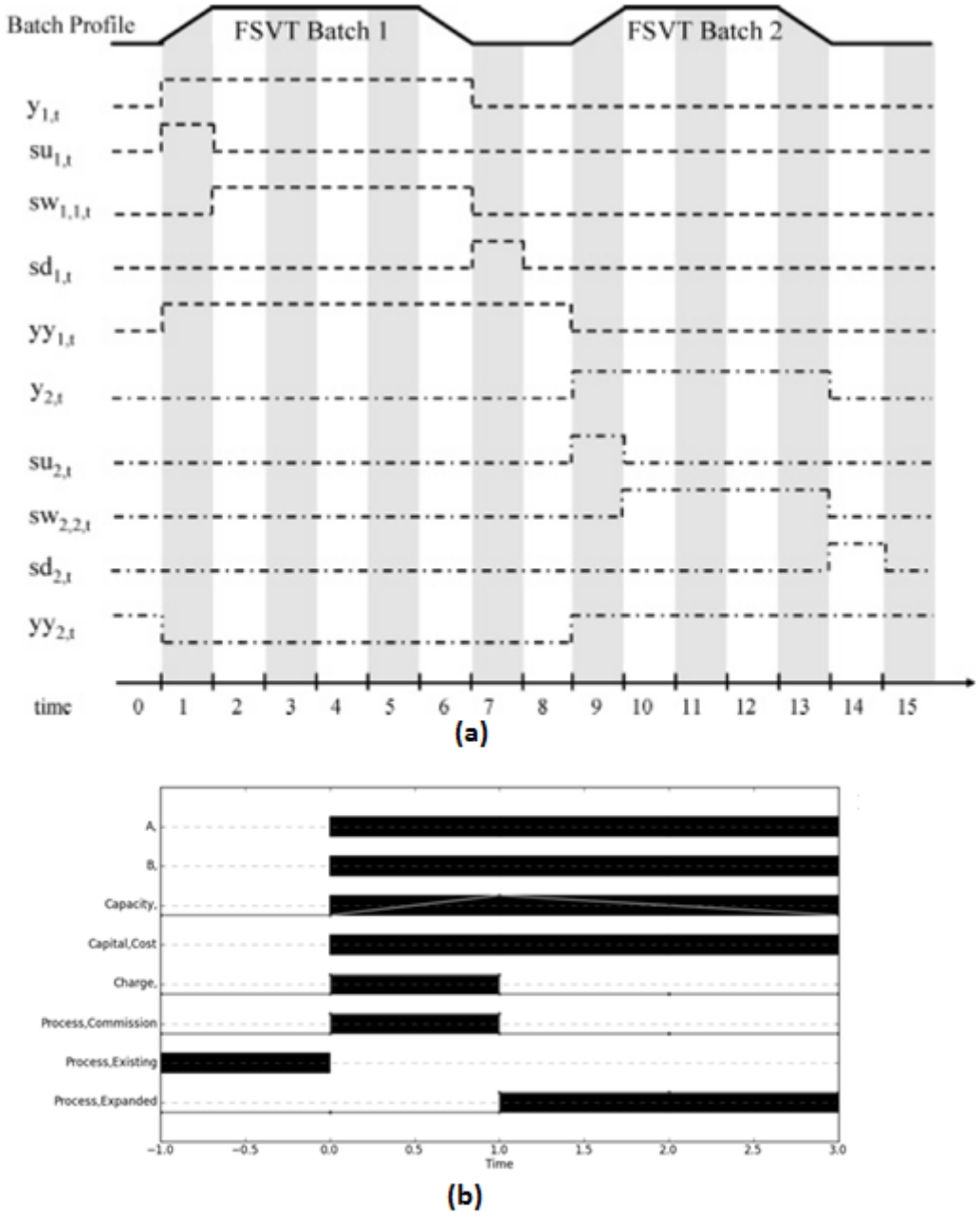

Figure 7.2. Scheduling stages in a batch process and in our project investment problem.

In order to activate a specific maintenance, non-productive, intermediate operation on a unit before a spatial switchover occurs from operation *i* in some time-period in the past to *j*, then Equation 7.5 must be used, where *i* is the from/previous operation or operation-group; *j* is the to/next operation or operation-group, and *m* is the repetitive-maintenance-intermediate, which represents in the generalized capital investment planning (GCIP) problem the project stage (correction, commission, and construction). In this equation we expect that the startup of

j and the shutdown of m take place in the same time-period, i.e., they are temporally coincident.

$$\left(yy_{i,t} + yy_{i,t-1} - 1\right) + su_{j,t} - sd_{m,t} \leq 1 \quad \forall \quad i, j, m, t \tag{7.5}$$

This equation allows to understand when the Existing or Non-Existing operation occurs on the unit, and then we can insert the Commission or Construction stage for example before the Expanded or Installed operations or stages; this is the core idea in GCIP with the explicit Commission and Construction stages activated in between the Existing/Non-Existing and the Expanded/Installed operations or stages.

Other project scheduling types of problems in both discrete and continuous time can be found in for example Kopanos et al. (2014) to address the resource-constrained project scheduling problem (RCPSP), in which renewable resources fully retrieve the occupied resource amount after the completion of each activity, while the total duration of the project (the makespan) is minimized satisfying precedence and resource constraints. The problem consists of finding a schedule of minimal duration by assigning a start time to each activity in which the precedence relations and the resource availabilities are respected. Several planning and process level decision problems can be reduced to the RCPSP (Varma et al., 2004), such as in high scale projects management in software development, plants building, and military industry (Pinedo and Chao, 1999), and in highly regulated industries where a large number of possible new products are subject to a series of tests for certification (Shah, 2004), such as in pharmaceutical and agrochemical industries.

7.3. Generalized capital investment planning (GCIP) model using sequence-dependent setups

The network of the generalized approach for capital investment planning is implicitly represented in the flowsheet-based superstructure shown in Figure 7.3 by using the unit-operation-port-state superstructure (UOPSS) described in Kelly (2004), Kelly (2005), and Zyngier and Kelly (2012). The comparative formulation with the conventional approach will be given in the motivating example 1.

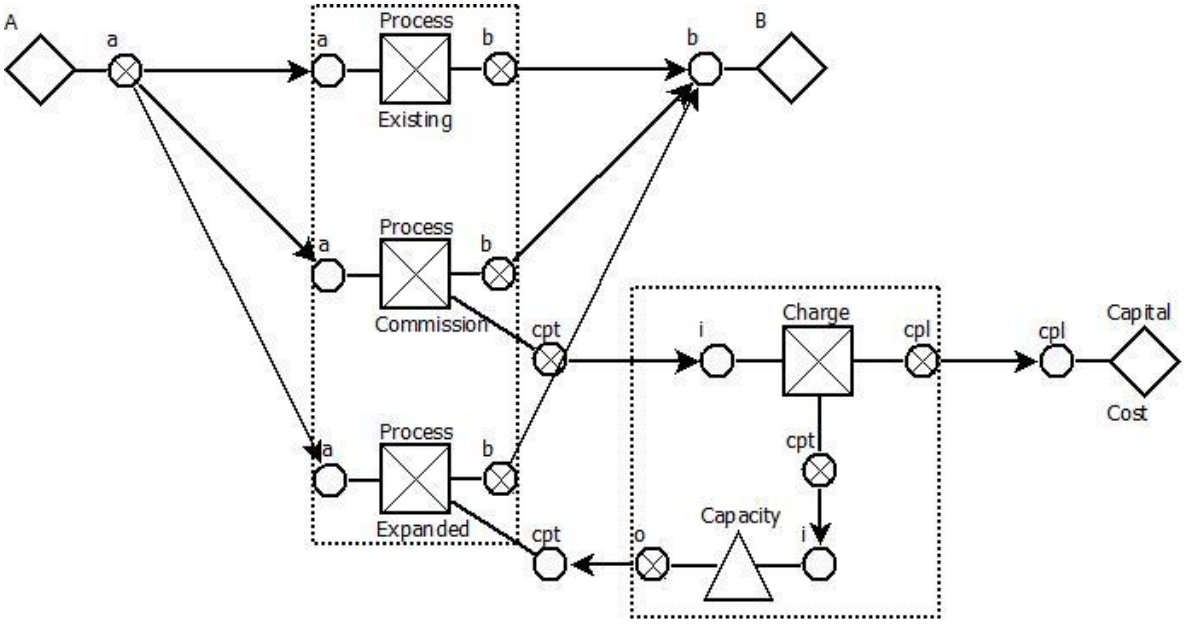

Figure 7.3. Motivating example 1: small GCIP flowsheet for expansion.

In Figure 7.3, the diamond shapes or objects are the perimeter unit-operations where they consume material A (source) and produce material B (sink), i.e., in- and out-bound resources. We have just one process unit with three operations of Existing, Commission, and Expanded as shown by the square boxes with an "x" through it indicating it is a continuous-process type (⊠). The first dotted line box highlights that only one unit-operation can be active or setup at a time, i.e., a unary resource or the unit commitment constraint. The small circles are the in-ports (○) and out-ports (⊗), where these ports have the attributed lower and upper yields available similar to the modeling of generalized network-flow problems, i.e., having the previously mentioned Leontief input-output models with intensities, bill-of-material, or transfer coefficients. The port-states allow flow into and out of a unit and can be considered as flow-interfaces similar to ports on a computer, e.g., nozzles, spouts, spigots. Port-states also provide an unambiguous description of the flowsheet or superstructure in terms of specifically what type of materials or resources are being consumed and produced by the unit-operation. Port-states can also represent utilities (steam, power), utensils (operators, tools) as well as signals such as data, time, tasks, etc. In-ports and out-ports can be compared to the mixers and splitters found in Moro and Pinto (1998) formulation, but including the concept port-state, which is symmetric with unit-operation.

Each of the two perimeters, A and B, can have tanks available for storage, and is a requirement when balancing the production-side and transportation-side supply and demand of the value-chain. Finally, the lines or arcs between the unit-operations and port-states and

across an upstream unit-operation-port-state to a downstream unit-operation-port-state correspond to flows as one would except to code given that the superstructure is ultimately composed of a network, graph, or diagram of nodes/vertices and arcs/edges (directed).

Each unit-operation and external stream have both a quantity and a logic variable assigned or available, and represent either a flow or holdup if quantity and either a setup or startup if logic. Batch-processes have holdups and startups, continuous-processes have flows and setups, pools have holdups and setups, and perimeters only have a logic setup variable. The internal streams have neither explicit/independent flow nor setup variables given that their flows are uniquely determined by the aggregation of the appropriate external streams (arrows between in- and out-ports), and their setups are taken from the setup variables on the unit-operation they are attached to. The network material balance is given by the flowsheet connectivity between the elements or shapes (units, tank, in-ports, out-ports, etc.).

The case in Figure 7.3 shows the expansion of an existing process unit (Process), which is initially in the Existing mode. For a completely grass-roots or green-field installation, the operations or states are the Construction and the Installed modes, which are equivalent to the Commission and Expanded modes in Figure 7.3. However, to control the sequence of stages, a NonExisting mode should be included for the installation case that is equivalent to the Existing mode in an expansion. Each of the expansion or installation unit-operations represented by commission/construction stages, have a capacity port-state *cpt* connected to the unit-operation named Charge to transfer this capacity to the Capacity tank, where the Expanded or Installed unit can have an increase in capacity by the new additional charge-size from the tank. In the Charge unit, the capital port-state *cpl* carries the NPV cash-flow to the perimeter named Capital (diamond shaped). This is the non-material or non-stock flow of a financial resource.

The existing or non-existing unit selection is based on the economic viability with respect to its expected expanded or installed cost and projected revenue of the products, which in the example in Figure 7.3, is the perimeter B. The inlet port-state of this unit-operation will have a time-varying NPV cash-flow lower and upper bound to constrain the expansions and/or installations according to the expected cash-flow profiles in the future. An additional restriction required, sometimes referred to as a side-constraint, is the fact that if an expansion/installation unit-operation is selected in some future time-period, then it must be setup for the rest of the time-horizon. This can be modeled using the up-time logic constraint,

where a lower or minimum up-time is configured as the time-horizon length of the problem (Wolsey, 1998, Kelly and Zyngier, 2007 and Zyngier and Kelly, 2009). Up-time is also known as a run or campaign-length, and essentially restricts a shutdown of the unit-operation for a specified number of time-periods in the future.

7.3.1. Motivating example 1

At this point we explore further the solution to the small retrofit generalized CIP problem fully defined in Fig. 3. The future planning time-horizon is arbitrarily configured as three months and with one month time-periods. The existing or old capacity of the process is 1.0 quantity-units per month and the new capacity can be 1.5. The capital cost is computed with α= 0.5 ($ per quantity-units) and β= 0.5 ($ per setup-units). All of these data are declared in the 'Calculation Data (Parameters)' frame in the supplementary material. By simplification, the cost for material A is $0.0 per quantity-unit and the price for B is $1.0 per quantity-unit and we do not apply any NPV given the relatively short horizon. The costs are defined in the 'Cost Data (Pricing)' frame in the supplementary material, where the IMPL configuration of the motivating example 1 is presented, as well as the final equations formed from this configuration and the 'Construction Data' frame given by the flowsheet connectivity shown in Fig. 3.

The operations of Commission and Expanded each have a special out-port and in-port labeled as *cpt*, which stands for the outflow and inflow of capacity, respectively. There is a Charge unit-operation, which will only be setup if the Commission unit-operation is active, and its purpose is to convert the variable capacity to a variable and fixed capital cost. It is represented as 'Charge,,cpl,,alpha,alpha,beta-alpha*oldcapacity' in the 'Capacity Data (Prototypes)' frame (see supplementary material), where the α (alpha) coefficient or parameter is applied to the incremental or delta capacity change, and the β (beta) is applied to the setup variable if the Charge unit-operation is on or open. The out-port on the Charge unit-operation labeled *cpt* is the flow of capacity charged or dispatched to the Capacity pool unit-operation (triangle shape). During the one time-period when the Charge unit-operation is active, the flow of capacity to the Capacity pool must have enough capacity to operate the Expand operation for as many time-periods left in the planning time-horizon. For example, if we have a three time-period future horizon and the Commission operation starts in time-period, one then enough capacity must be fed or sent to the Capacity pool unit-operation for

time-periods two and three (END). In this way, the capacity to be expanded or installed, an extensive amount, is approximated as an intensive value. As example, for the first period, it is represented as ‘Charge,,cpt,,1.0*(END-1.0),1.0*(END-1.0),,0.0,1.0’ in the ‘Command Data (Future Provisos)’ frame (see supplementary material).

The *cpt* in-port on the Expanded operation will draw only up to the maximum allowable or upper limit of the expanded capacity allowed from the Capacity pool, and this will control the capacity charge-size, throughput, or flow through the unit-operation for the Expanded operation. In order to do this, the lower yield bound on the *cpt* in-port is configured as one and the upper yield bound as infinity or some large number. This will regulate the capacity of the Expanded unit-operation as in ‘Process,Expanded,cpt,,1.0,large’ in the ‘Capacity Data (Prototypes)’ frame (see supplementary material).

The problem is solved using MILP with a provably optimal objective function of $3.25. If we apply no expansion, then the profit would be $3.0 since the existing capacity is 1.0 for three time-periods. Since the profit is $0.25 more than $3.0, then there has been an expansion where the Commission operation is setup or started in time-period one. To perform an expansion of 1.5 – 1.0 = 0.5 quantity-units then, the capital cost required is 0.5 * 0.5 + 0.5 = $0.75. Given the timing of the Commission stage, this implies that the Expanded stage occurs in time-periods two and three, which is enforced by the sequence-dependent setup modeling, i.e., after the Commission stage only the Expanded stage can be setup for the rest of the horizon. With an expansion capital cost of $0.75 and a revenue for the sale of material B of 1.0 + 1.5 + 1.5 = $4.0 for the three planning periods, this leaves a profit of $4.0 - $0.75 = $3.25, which is the same value found by the MILP. The Gantt chart for this example is found in Figure 7.4. In this case, we are considering the Commission mode with the same capacity as in the existing to permit production during this stage, since an interruption of this production in the first time period can impede the expansion.

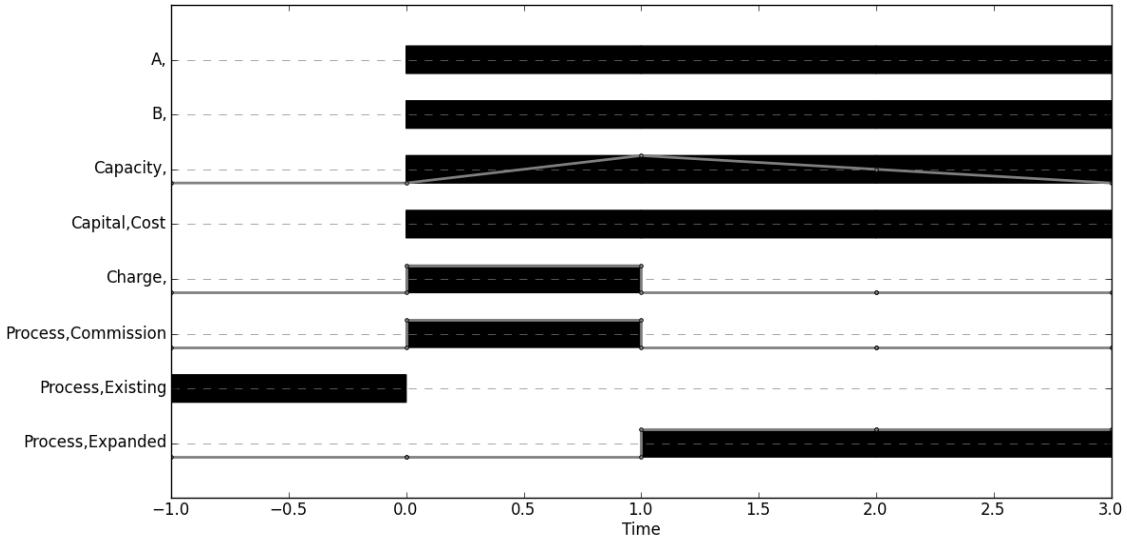

Figure 7.4. Gantt chart for expansion of a generalized CIP example.

From the Gantt chart in Figure 7.4 we can verify the timing for the Commission and Expanded unit-operation on the Process unit. The interesting detail is the Capacity pool holdup or inventory trend of capacity, which is shown as the grey line inside the black horizon bar. We can see a charge of capacity in time-period one, and a continuous draw or dispatch out in time-periods two and three. The black horizon bar means that the binary variable of the shape is active.

7.3.2. Motivating example 2

An installation structure similar to the expansion in Figure 7.3 is added to the motivating example 2. The Existing, Commission, and Expanded modes or stages in the installation case is changed to NonExisting, Construction, and Installed modes as shown in Figure 7.5.

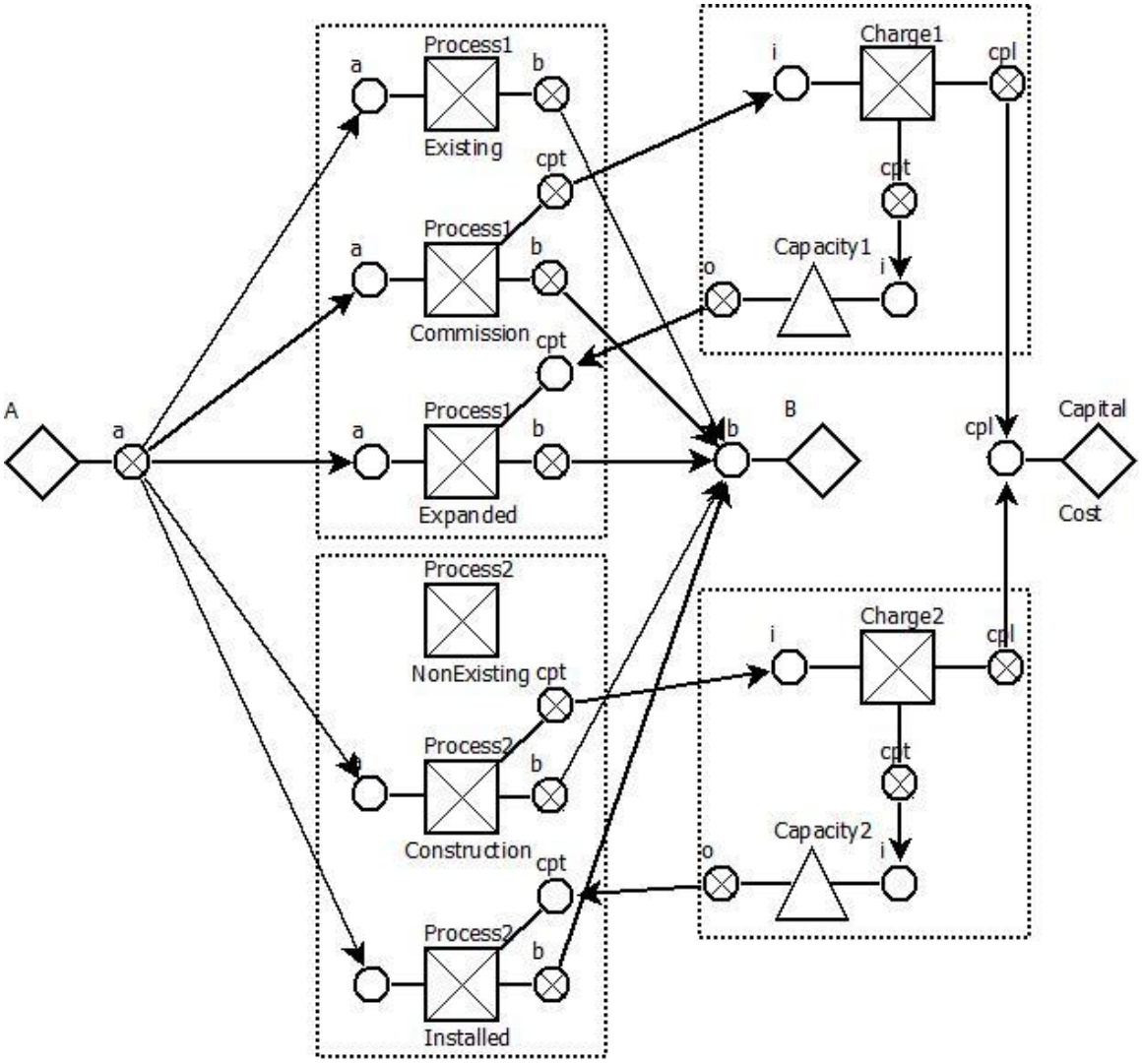

Figure 7.5. Motivating example 2: small GCIP flowsheet for expansion and installation.

The problem is solved using MILP with a provably optimal objective function of \$5.00. If we apply no expansion or installation then the profit would be \$3.0 since the existing capacity is 1.0 for three time-periods. To perform an expansion, we have the same as the in motivating example 1. To perform an installation of the same 1.5 quantity-units, the capital cost required is 1.5 * 0.5 + 0.5 = \$1.25. Given the timing of the Construction stage, this implies that the Installed stage occurs in time-periods two and three which is enforced by the sequence-dependent setup modeling, i.e., after the Construction stage only the Installed can be setup for the rest of the horizon. Different from the expansion cost evaluation, there is no existing capacity for an installation (NonExisting mode), so the alpha*oldcapacity is not discounted in the beta cost. The production from the Construction stage was disregarded by considering the out-port linked to the product perimeter B with zero yield. With an expansion capital cost of \$0.75 and an installation capital cost of \$1.25, a revenue for the sale of material

B of 1.0 + 1.5 + 1.5 = $4.0 from the expanded existing unit and 0.0 + 1.5 + 1.5 = $3.0 from the installed non-existing unit for the three planning periods. This leaves a profit of $4.0 + $3.0 - $0.75 - $1.25 = $5.0, which is the same value found by the MILP. The Gantt chart for this example is found in Figure 7.6. Also, the commission mode has the same capacity as in the existing to permit production during this stage.

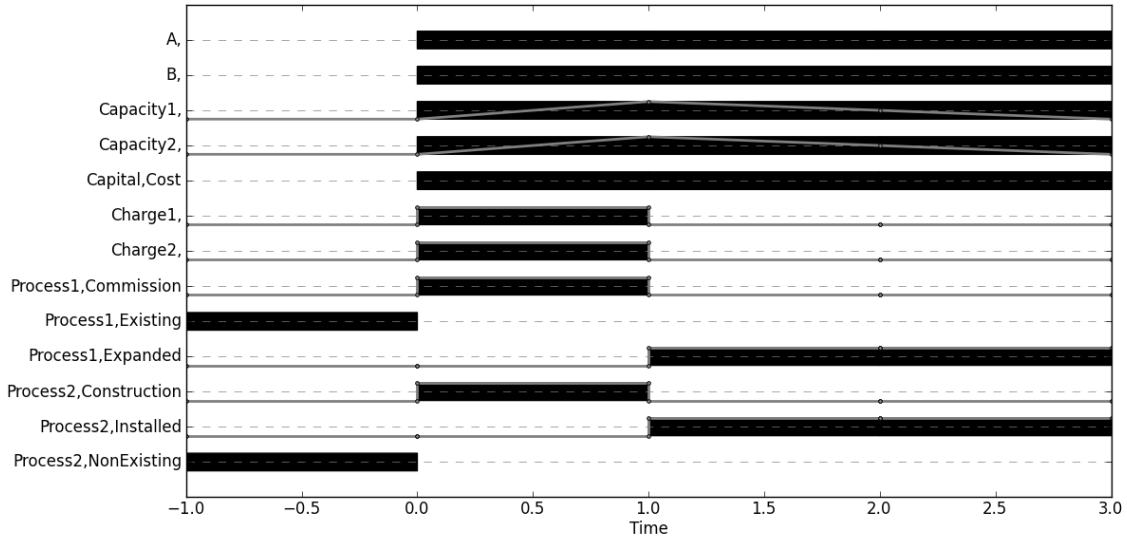

Figure 7.6. Gantt chart for expansion and installation of a generalized CIP example.

7.4. Examples

The capital investment planning examples presented in the following include (i) a retrofit problem for process unit expansion and extension with fixed investment costs, as the transformations are pre-defined as fixed values, and (ii) an expansion and installation problem on an integrated oil-refinery with variable costs, since the size of the revamped (expanded or installed) capacity can vary. The examples were modeled using Industrial Algorithm's IMPL and solved using IBM's CPLEX 12.6.

7.4.1. Retrofit planning of a small process network

Our illustrative example is taken from Jackson & Grossmann (2002). There are 3 feeds and 2 product materials (A,B,C,D,E) with 3 processes (Figure 7.7) that can be either expanded (capacity increase) or extended (conversion increase) or both, considering fixed values as the transformations. A total of three time periods is considered.

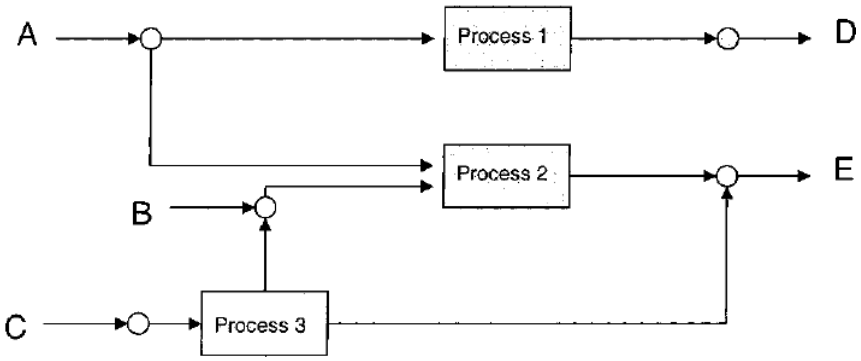

Figure 7.7. Retrofit example for capacity (expansion) and capability (extension) projects.

In Figure 7.8 is our new flowsheet representation with the Existing, Commission, and Expanded (or Extended) stages shown explicitly where M denotes the flow of money (investment costs). The associated MILP model using our approach in IMPL includes 403 constraints, 114 continuous variables, and 154 binary variables, and was solved with CPLEX in less than 0.25-seconds to provably optimal. The convex hull MILP formulation proposed in Jackson & Grossmann (2002) has 394 constraints, 244 continuous variables, and 36 discrete variables. They also modeled the problem using conventional big-M constraints to reformulate the GDP into an MILP more compact with 328 constraints, 124 continuous variables, and 36 discrete variables.

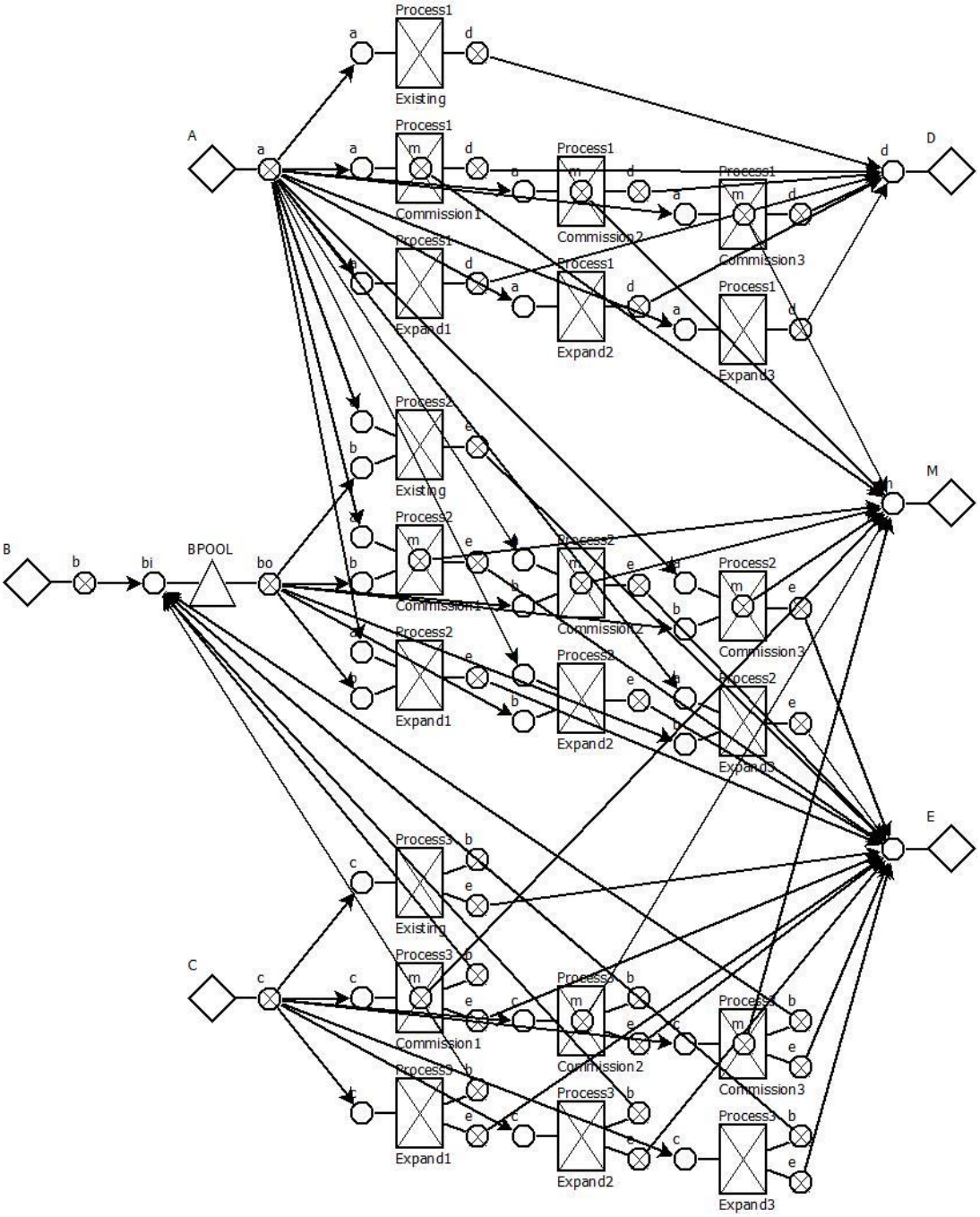

Figure 7.8. UOPSS flowsheet for Jackson and Grossmann (2002) example.

The two Gantt charts shown in Figure 7.9 have the same solution with an NPV = 11.841 M$ over three one-year time-periods, where Process 1 has its capacity expanded, Process 2 is unchanged, and Process 3 is conversion (capability) extended. The commission throughputs and yields are considered the same as in the expanded or extended modes in order to compare with the Jackson and Grossmann (2002) example, where the project staging is disregarded.

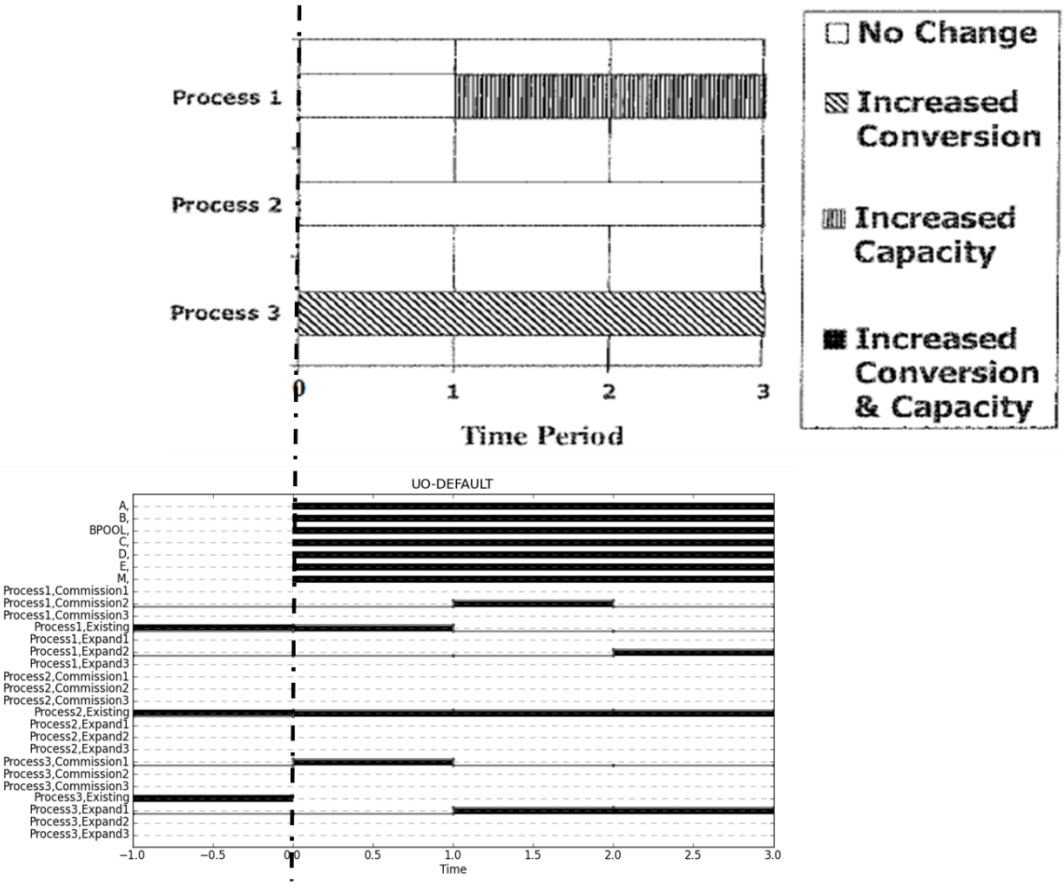

Figure 7.9. Gantt chart for Jackson and Grossmann (2002) example.

It should be noted that the results of the example are different than the ones reported in Jackson and Grossmann (2002), since these authors reported incorrect numbers in their Figure 3, although their original GAMS file was correct and is in fact the one we have used in this chapter in Figure 7.9.

7.4.2. Oil-refinery process design synthesis

The oil-refinery example in Figure 7.10 represents a complete plant with expansions and installations permitted only for the crude and vacuum distillation units (CDU and VDU) over three time periods. The capacity upper bound for the other units is considered a large number to avoid bottlenecks. The commission/expanded and the construction/installed structures or shapes for the CDU and VDU are not depicted. They are constructed similarly to the motivating examples.

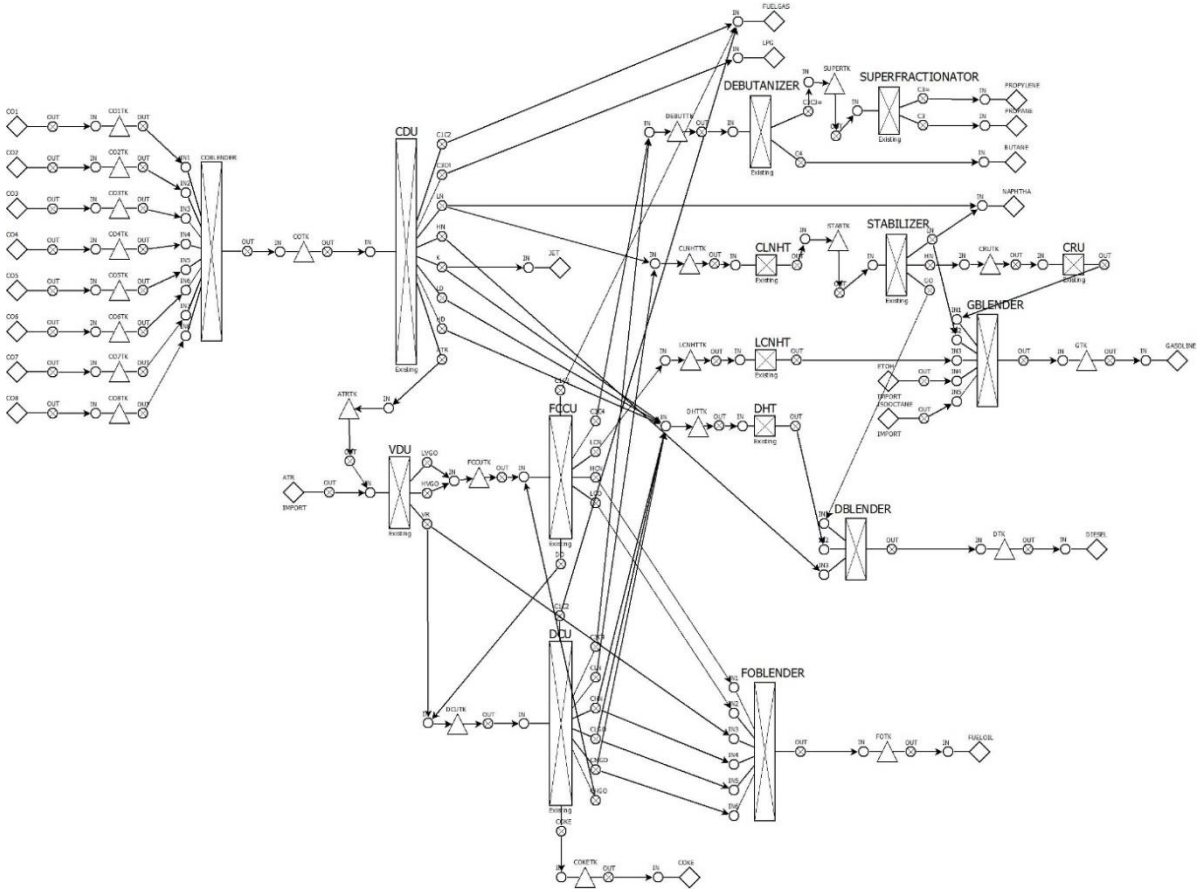

Figure 7.10. Oil-refinery example flowsheet.

The considered MILP model includes 722 constraints, 170 continuous variables, and 200 binary variables, and was solved with CPLEX in 0.5-seconds, and solved to optimality yielding a NPV = 732.94 M$**.**

In Fig. 11, CDU and VDU labels represent the expansions and the CDU2 and VDU2 the installations. As we now consider the commission stage in the expansions with zero production, the problem only set up installation projects (CDU2 and VDU2). The charges of these projects occur together with the constructions as well as the capacity tank filling. After the constructions, the capacity of the new installed modes is continuously maintained as shown in Figure 7.11.

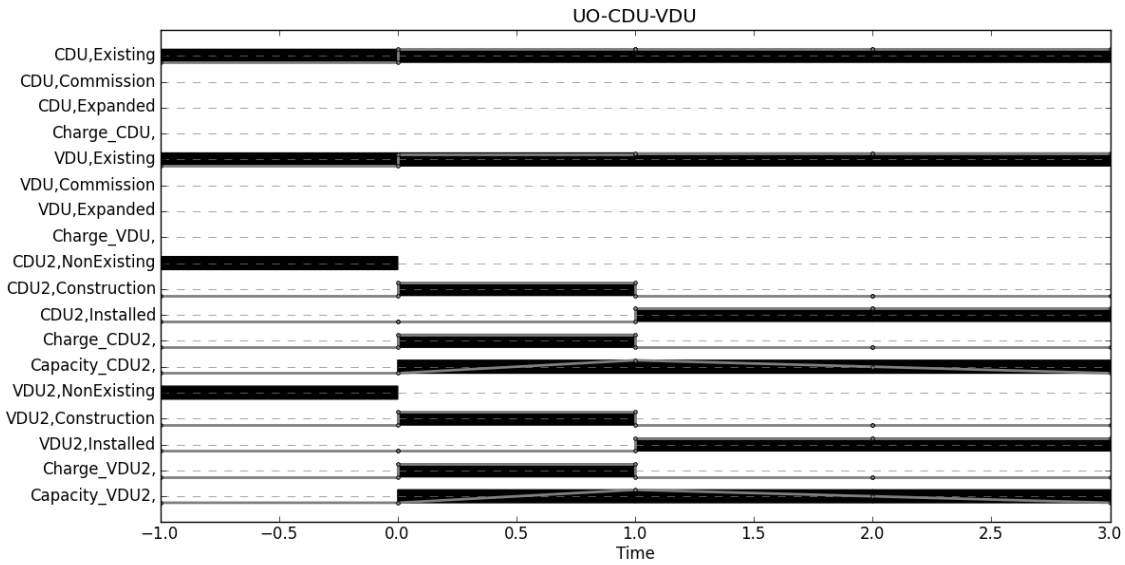

Figure 7.11. Gantt chart for the CDU and VDU installations.

7.5. Conclusion

In summary, we have proposed a generalized network-flow MILP model using setups approach to model and solve a typical capital investment planning problem considering intermediate stages between the existing state (existing unit or new unit) and the final state after the repair, retrofit, or revamp (expansion, extension and installation) projects. We have applied the concepts of sequence-dependent setups to manage the project scheduling by considering phasing (from one state to another) and the project execution similar to the maintenance or purging stage as normally found in scheduling sequence-dependent changeover problems. A unique and novel way is used to formulate the CIP problem using capacity/capability and capital as flows in a scheduling environment. The problems are relatively easy to implement without having to explicitly code the sets, parameters, variables and constraints required in algebraic modeling languages such as AIMMS, AMPL, GAMS, LINGO, MPL, MOSEL, OPL, etc. Instead, the modeling platform IMPL allows the modeler or user the ability to configure the problem using semantic variables such as flows, holdups, yields and setups, startups, etc. which is more intuitive and natural. Finally, our generalized CIP formulation can be straightforwardly applied to any CIP problem found in many process industries including such specific applications as shale-gas well startup and ore mining and extraction planning which require more scheduling details to be considered.

Chapter 8

8. Phenomenological Decomposition Heuristic for Production Synthesis of Oil-Refinery Units

The processing of a raw material is a phenomenon that varies its quantity and quality along a specific network and logics to transform it into final products. To capture the production framework in a mathematical programming model, a full space formulation integrating discrete design variables and quantity-quality relations gives rise to large scale non-convex mixed-integer nonlinear models often difficult to solve. In order to overcome this problem, we propose a phenomenological decomposition heuristic to solve separately in a first stage the quantity and logic variables in a mixed-integer linear model, and in a second stage the quantity and quality variables in a nonlinear programming formulation. By considering different fuel demand scenarios, the problem becomes a two-stage stochastic programming model, where nonlinear models for each demand scenario are iteratively restricted by the process design results. Three examples demonstrate the tailor-made decomposition scheme to construct the complex oil-refinery process design in a quantitative manner.

8.1. Introduction

Production optimization relating quantity and quality variables in processing (blending, reacting, and separating) constraints are sufficient to describe planning and scheduling problems for a given process design, sequence of operation, selection of tasks, etc. On the other hand, for full-designed mixed-integer models, in spite of being necessary, quantity-quality relationships solely are insufficient, because these problems must also be able to deal with discrete decisions such as investment setup, project scheduling, plant shutdown, assignment, sequencing, etc. The combination of quantity, quality and logic variables in a single model results in a mixed-integer nonlinear programming (MINLP) model that is non-convex due to, at the very least, the bilinear terms associated with quantity times quality variables, but also due to the either-or logic decisions. While significant advances have been recently made in MINLP solution efficiency (Belotti et al., 2013), a robust commercial software tool is still not available for solving non-convex MINLP industrial-sized problems.

Hence, alternative and heuristic methods are proposed in order to solve such large-scale MINLP problems.

A decomposition solution method, denoted here as the phenomenological decomposition heuristic (PDH), is proposed to avoid the full space MINLP model, which is decomposed, partitioned, or separated into two simpler sub models namely logistics (quantity and logic) and quality (quantity and quality) optimization sub problems. The logistics model solves a problem with quantity and logic variables subject to quantity and logic balances and constraints (Kelly and Mann, 2003; Kelly, 2004a; Kelly, 2006; Zyngier and Kelly, 2009). Quality optimization solves for quantity and quality variables subject to quantity and quality balances and constraints (Kelly, 2003; Kelly, 2004a; Kelly, 2004b) after the logic variables have been fixed at the values obtained from the solution of the logistics optimization.

The proposed PDH methodology is applied to solve the strategic investment planning problem in a two-stage stochastic programming model for different demand scenarios. The goal is to maximize the net present value (NPV) to determine project setups and their related new capacities by expansion and installation of units, which are scenario-independent in the MILP master or high-level problem (first stage), so they are the linking variables over the different scenarios. In this stage, fuel production, material flows, yields and other types of variables for each scenario are modeled in a linear manner within the operational layer of the MILP problem. The operational scenarios have the same discrete probability, so this value is simply a coefficient in the scenarios' operational amounts (gains and costs) taken into account in the NPV objective function.

In the second stage, the NLP operational slave or lower-level problems are solved for each scenario considering the process design found in the MILP problem, and new yields and crude-oil diet compositions are updated in the next MILP iteration until both the MILP and NLP solutions convergence on the objective function and variable solution values. The combinatorial enumeration of projects within the MILP problem takes into account two groups of binary constraints to reduce the tree search, the first considers investment decisions in expansion and installation of process units and the second addresses process unit sequence-dependency based on the possible connectivity in the oil-refinery framework, network, or process design found among the worldwide sites included in this work.

This work is organized as follows. In section 8.2, the phenomenological decomposition heuristic to construct the complex oil-refinery network is presented. Section 8.3 establishes the problem statement as well as the oil-refinery framework and groups of

units considered. The strategic investment problem is shown in section 8.4 with both the conventional capital investment planning in an MILP formulation and the integer constraints addressed in this work. Besides, the NLP formulation references for the operational layer problem are presented in this section. In section 8.5, two examples are highlighted, the first is a motivating example to better discuss the decomposition algorithm workflow using the conventional and the generalized capital investment planning models (CCIP and GCIP) without considering scenarios. The CCIP model is defined in this work and the GCIP model is found in chapter 7. The second example uses the CCIP modeling for one oil-refinery site. Conclusions and future work are presented in section 8.6.

8.2. Phenomenological decomposition heuristic

8.2.1. Partitioning (decomposition) and positioning of models

Partitioned or decomposed models demand more coding and calculation (Kallarath, 2011), and there is always a price or cost to be paid for their modularization with repeated calculations, instead of solving the monolithic or full space problem directly (Conejo et al., 2006). Partitioning is the notion of decomposing the problem into smaller sub problems along its hierarchical (Kelly and Zyngier, 2008), structural or spatial (Kelly and Mann, 2004), operational (Kelly, 2006), temporal (Kelly, 2002) and now phenomenological (Kelly, 2003, Kelly and Mann, 2003, Kelly and Zyngier, 2015) dimensions. Positioning is the ability to configure the lower and upper hard bounds and target soft bounds for any time-period over the future time-horizon within the sub problem and is especially useful to fix variables (i.e., its lower and upper bounds are set equal), which will ultimately remove or exclude these variables from the solver's model or matrix.

Figure 8.1 highlights the partitioning along the phenomenological dimension of the MINLP into two sub problems we call the quality and logistics sub problems as previously mentioned, which is a rational break-down of the quantity, logic, and quality phenomena (QLQP) or qualogistics and allows to iteratively and sequentially solve industrial-sized, -scaled, and -scoped MINLP problems found in the process industries using what is considered to be a natural and intuitive decomposition heuristic, strategy or algorithm.

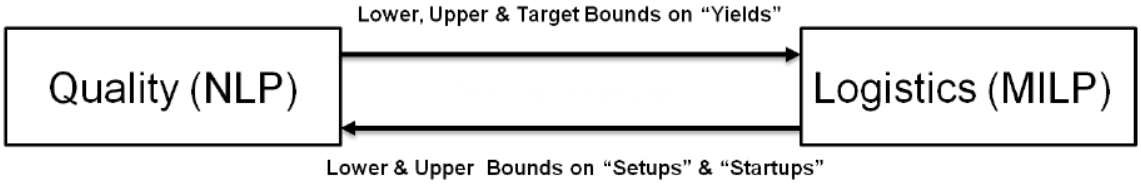

Figure 8.1. Partitioning and positioning conjunction variables

The variables that connect, coordinate, match, transfer, or link, etc. one sub problem to another are called the conjunction variables. Semantically the conjunction variables are primarily intensive (do not scale with size as opposed to extensive variables which scale with size) such as yields and setups/startups, although any QLQP variable can be a candidate such as flows, holdups, switchovers, shutdowns, properties, and conditions. The proposed solution procedure is relatively simple and first starts with a single or mono-period quality sub problem (NLP) (partitioning) to generate starting or initial yields, which are then used as input (positioning) to the multi-period logistics sub problem (MILP). Once an acceptably good MILP solution is found then the values for the setup binary variables can be used to solve a multiperiod quality sub problem and the solution process repeats between the two multiperiod sub problems until a reasonable convergence between the NLP and MILP sub problem objective functions (or other common variable) is found.

Similar to the depth-first with backtracking search found in Kelly (2002), this same technique can also be employed here whereby each sub problem, due to its inherent non-convexity, will most likely exhibit multiple local solutions. By retaining then recovering these solutions using unformatted binary files for example and applying a systematic search mechanism similar to branch-and-bound, multiple solution paths can be circumscribed where the goal is to find the best overall or combined solution with the highest profit, best performance and/or least amount of penalties, i.e., the combination of both MILP and NLP sub problem solutions making up the MINLP problem.

In previous works, an MINLP crude-oil scheduling problem using priority-slot based continuous-time formulation (Mouret et al., 2009) compares the full space solution and its decomposed MILP-NLP problem by neglecting the pooling or blending nonlinear constraints in the MILP model, and then re-composing the model in an NLP problem by relating quantity and quality variables for the binary results found in the MILP model. In their work the full space solution becomes intractable for industrial-sized examples, but they are solved in MILP-NLP decomposition with an objective function gap between both solutions lower than

4%. Only a small example considering a low number of time slots is solved using the MINLP formulation, which yields the same result found in the decomposed solution, but with higher computational expense.

The proposed phenomenological decomposition heuristic resembles the well-studied approach suggested in Benders decomposition where “complicating” variables (in this case, binary) are fixed such that a simpler problem may be solved which are later freed again for the next iteration (Geoffrion, 1972). A similar method has also been applied for a different purpose, namely that of integrating decentralized decision-making systems through a hierarchical decomposition heuristic (HDH) (Kelly and Zyngier, 2008). In the context of the integration between logistics and quality problems, the coordinator (logistics MILP sub problem) would send what we call “logic pole-offers” to the cooperator (quality NLP sub problem), which in turn would send back logic pole-offsets to the coordinator. This procedure continues until convergence is achieved, hopefully providing at least a globally feasible MINLP solution.

Other decomposition approaches include bi-level (Iyer and Grossmann, 1998) and Lagrangean decomposition (Karuppiah and Grossmann, 2008). Similar to Benders decomposition, the bi-level approach is based on the idea that some complicating variables e.g., investment decisions or assignment variables, are withdrawn to solve an easier sub model and then included in a further step fixing some results from the previous model. In their NPV-based capital investment planning example with two sets of binary variables (selection and expansion of process unit), the design master problem does not contain binary variables associated with capacity expansion decisions. It only contains binary variables representing the selection of a process over the entire planning horizon, so the high-level or design problem is combinatorially less complex and selects a subset of processes for design. Following the algorithm, the lower level planning problem is solved for the selected set of processes to define the capacity expansion. Bounding information is used over the algorithm based on specific relaxations that under and overestimate the investment costs in the NPV maximization.

On the other hand, in the Lagrangean decomposition a set of hard constraints is violated by addition of a penalty term into the objective function to form an easier problem, the dual problem, although it may require excessive computation for even small problems by the additional Lagrangean multipliers determination usually through subgradient optimization. Large-scale process industry problems including multi-entity relationship by integrating the

production and distribution supply chain problems (You et al., 2011; Corsano et al., 2014) showed that the bi-level decomposition (Iyer and Grossmann, 1998) requires smaller computational times leading to solutions that are much closer to the global optimum when compared to the full space solution and to Lagrangean decomposition (Guignard and Kim, 1987).

8.2.2. PDH algorithm for oil-refinery design synthesis

The proposed two-stage stochastic program scheme (Birge and Louveaux, 2011) displayed in Figure 8.2 where the investment decisions are the first-stage variables (here-and-now) considering scenario probabilities in a logistics (logic and quantity) problem and all operational decisions modeling the necessary quantity and quality balances (quality problem) are the second-stage decisions (wait-and-see) according to the demand realizations of the scenarios. Considering the proposed modeling, the second-stage variables do not contain discrete decisions related to the modes of operation and associated sequencing, transitions or other logic relation, which would make the resulting two-stage stochastic programming problem hard to solve.

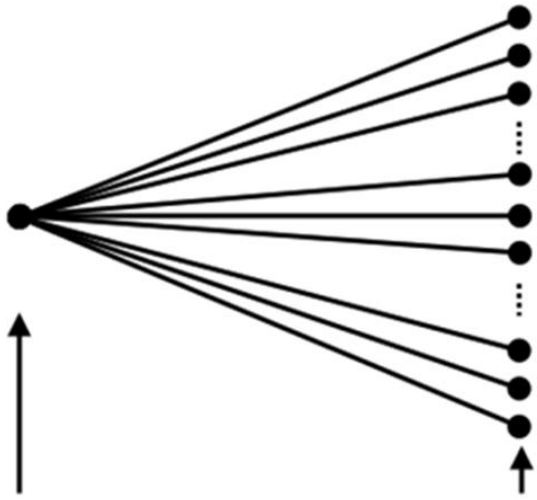

1st stage: Investment decisions (here-and-now)
(for all time periods t with investment allowed)
- New process unit (*yi*)
- Revamp of the existing unit (*ye*)

2nd stage: Operational decisions (wait-and-see)
(for all time periods *t* and product scenario *s*)
- Production levels
- Yields
- Properties

Figure 8.2. Two-stage stochastic programming strategy.

The applied PDH algorithm flowchart is presented in Figure 8.3. Before to perform the first stage problem, one quality optimization finds continuous variables *x* initial-values for all

demand scenarios *sc* considering the existing process units in a single-period operational planning calculation based on profit, as the hot-start or warm-start phase. Then, taking into account the NPV maximization as goal, the PDH method solves the logistics optimization in which the selection of binary decisions *y* for installation and expansion of process units over time occurs. In the MILP stage, the results of each scenario from the warm-start phase are used for the existing units. For new units are considered given values. In this first step, all parameters and initial-values for each demand scenario are considered the same throughout the periods under consideration.

After the logistics optimization, the multi-period NLP quality optimization validates or composes the MILP results considering the new production framework found by fixing the binary variables from the MILP problem, and then an iterative process is used to converge both multiperiod models. For the second or later multi-period MILP-NLP iteration, the initial points, unit yields, and the crude-oil diet are taken from the past multi-period NLP or quality optimization results, that brings crude-oil and processing changes into the MILP problem. This flexibility is referred to as recourse and is one of the most attractive features of stochastic programming (Goel, 2005).

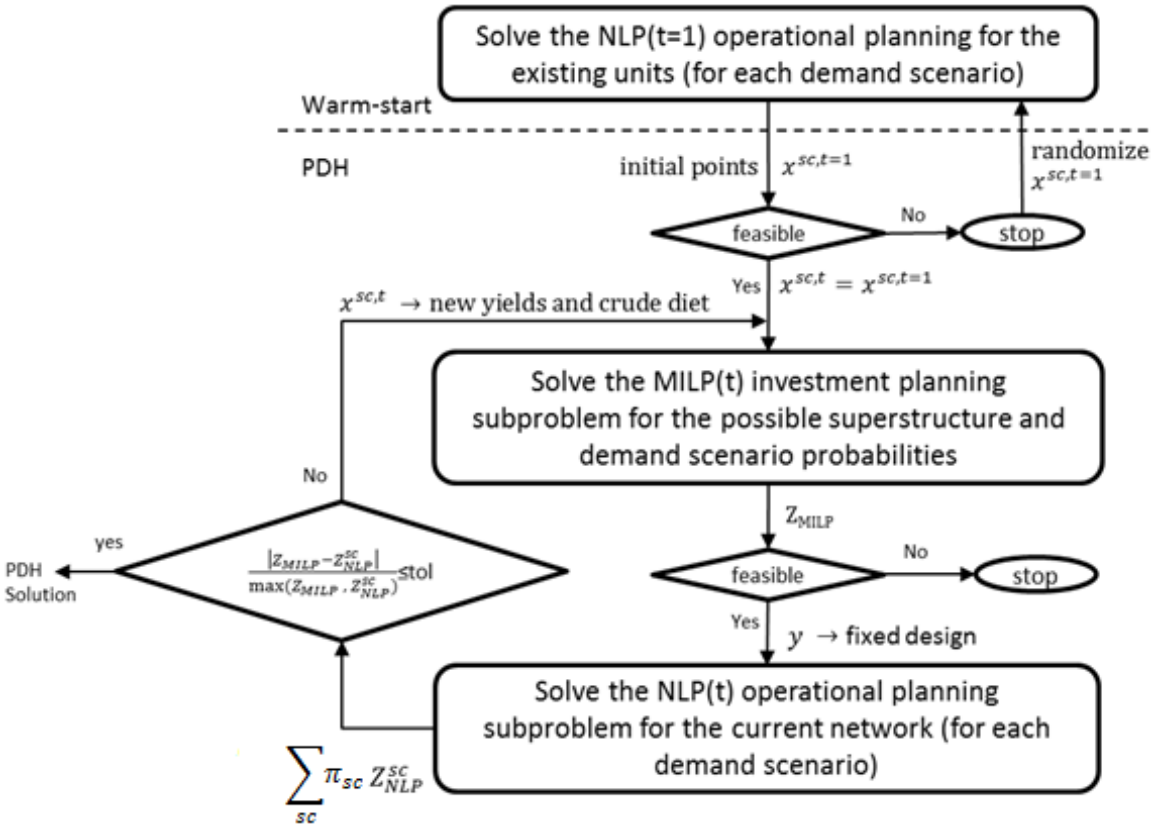

Figure 8.3. PDH algorithm flowchart.

Although the MILP sub problem uses a global search technique (branch-and-bound) to find its best or globally optimal solution, the NLP sub problem does not, unless it is a global nonlinear optimizer itself. Given that most, if not all, of industrial optimization problems are non-convex, one simple solution would be to re-run the NLP using multiple randomized re-starts for example and then to choose the best solution from this set of runs before proceeding again to the MILP sub solver. This could help to improve the solution quality of the heuristic in a straightforward manner.

When compared with the MINLP solutions, we should note that one of the advantages of the PDH is that each sub problem is individually exposed in the algorithm, i.e., we solve separate single-period NLP (like a root-relaxation), and the multi-period MILP and NLP models iteratively. For industrial models, solving each sub problem individually provides a useful intelligent problem-solving approach given that in MINLP solvers such as DICOPT, if the root, MILP or NLP fails (infeasible, unconverted) there is no easy way to dissect and diagnose it to locate the defects, faults, inconsistencies, etc. The PDH method decomposes MINLP models into a logistics optimization or quantity-logic (QL) MILP master or high-level problem and in a quality optimization or quantity-quality (QQ) NLP slave or lower-level problem. Both sub problems are completely and independently solved and then their results are used to integrate each other.

8.3. Problem Statement

The specific problem addressed in this paper can be stated as follows. Given future demand scenarios *sc*, the decomposed MINLP based on our phenomenological decomposition heuristic consists of determining the expansion of existing units and installation of new units in petroleum refineries. The expansions and installations have investments costs defined by varying and fixed terms. The parameter α_u represents the investment varying cost related to the size of the unit u and β_u for the fixed cost related of the decision to invest or not in its capacity at a certain time, which is the binary selection or investment setup. More details about the investment cost curves and coefficients determination can be found in Appendix B. These investment costs can take into account certain rules as depreciation, salvage value, working capital or any governmental, environmental and/or company specific expenditures. A review on the NPV investment cost or coefficient evaluation for oil-refinery units can be

found in Appendix D and the investment costs per type of oil-refinery unit considered in this work can be found in Table 4.1

The problem's time horizon comprises investment t and operational t_0 time periods as seen in Figure 8.4, although the problem is only performed over each time-period t. The shorter time-period t_0 is only shown to understand how the MILP and NLP objective functions are formulated. The operational layer in both linear and nonlinear formulation, the former in the MILP problem and the latter in the NLP sub problems, calculates the annual profit based on daily operations. After projects execution over each t, the new production framework is considered within the following time periods to determine a new operational profit that counts within the following periods.

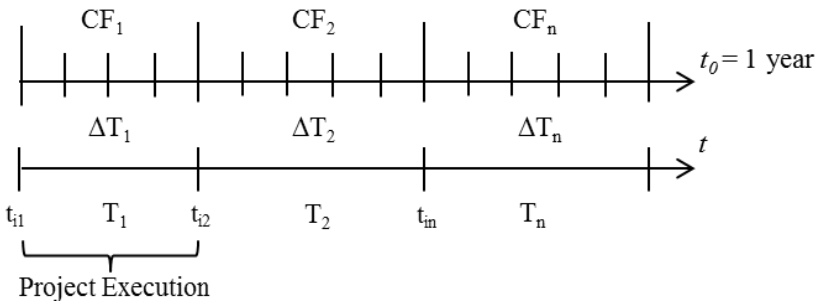

Figure 8.4. Investment t and operational t_0 time-periods.

The model considers unchangeable the operational variables within the investment time t, although the operational cash inflows $CF_{op}(x,sc,t_0)$ for each scenario with probability π_{sc} vary annually (over t_0) by price increase. These annual operational gains are brought back to the initial time t_i (t_{i1}, t_{i2},…; see Figure 8.4) after every each t_0 using constant interest rate ir to reflect the correction suffered by the future gains when it is considered at the present as shown in Equation 8.1. The investment cash outflows $CF_{in}(x,y,t)$ are withdrawn at the beginning of the time-period t with investment under consideration for expansion and installation of the new capacities over time taking into account the framework superstructure, given by the possible projects. The objective function calculation evaluates the potential gains from the operational activities within the following time periods to decide whether the discrete decisions to approve the projects at the beginning of each investment period are

made. As we consider that the project execution occurs within the time interval ΔT with several years, the investment is only allowed until the next-to-last time period ($t < t_{end}$).

$$\max \quad NPV_{MILP} = \sum_{t} \left(\sum_{t_0=t_i}^{t_0=t_f} \left(\sum_{sc} \frac{\pi_{sc} CF_{op}(x, sc, t_0)}{(1+ir)^{t_0}} \right) - \frac{CF_{in}(x, y, t)}{(1+ir)^{t-1}} \right) \tag{8.1}$$

A particular NPV formula for investment in oil-refineries is shown in chapter 4 to find the required expansion in oil-refinery capacity for the future oil products market in Brazil. The details about the deflationary NPV discounts are given in Appendix D.

Within the NLP operational sub problems, the objective function of each scenario *sc* is given by Equation 8.2. The investment costs $\overline{CF}_{in}(x, y, t)$ are considered constant by fixing the setups (projects approved) and their new capacities. For non-approved projects, their constraints and variables are eliminated from the possible framework superstructure within the NLP operational problems (second stage), and they are again included when the solution returns to the MILP investment problem iteration (first stage) (see in Figure 8.3 to understand the solution workflow).

$$\max \quad NPV_{NLP}^{sc} = \sum_{t} \left(\sum_{t_0=t_i}^{t_0=t_f} \left(\frac{CF_{op}(x, sc, t_0)}{(1+ir)^{t_0}} \right) - \frac{\overline{CF}_{in}(x, y, t)}{(1+ir)^{t-1}} \right) \quad \forall \quad \text{sc} \tag{8.2}$$

Two examples are shown to demonstrate the tailored decomposition scheme:

1-) a motivating example to better access the decomposition algorithm workflow considering expansion and installation of hydrotreating units using both the conventional and the generalized capital investment planning models (CCIP and GCIP) without considering demand scenarios. The CCIP model is defined in the following section and the GCIP model is found in chapter 7.

2-) two industrial examples using the CCIP modeling considering one and four oil-refinery sites with demand scenarios.

To formulate the multisite industrial-sized problem, the possible superstructure of projects for investing must be known a priori to control models' elements (equations, variables, etc.) formation throughout the PDH algorithm, where is considered the network in Figure 8.5 and the groups of units in Table 8.1. To generate the binary variables and their

linked variables along the PDH algorithm workflow, we consider at most four units *u* of the same type within one refinery site.

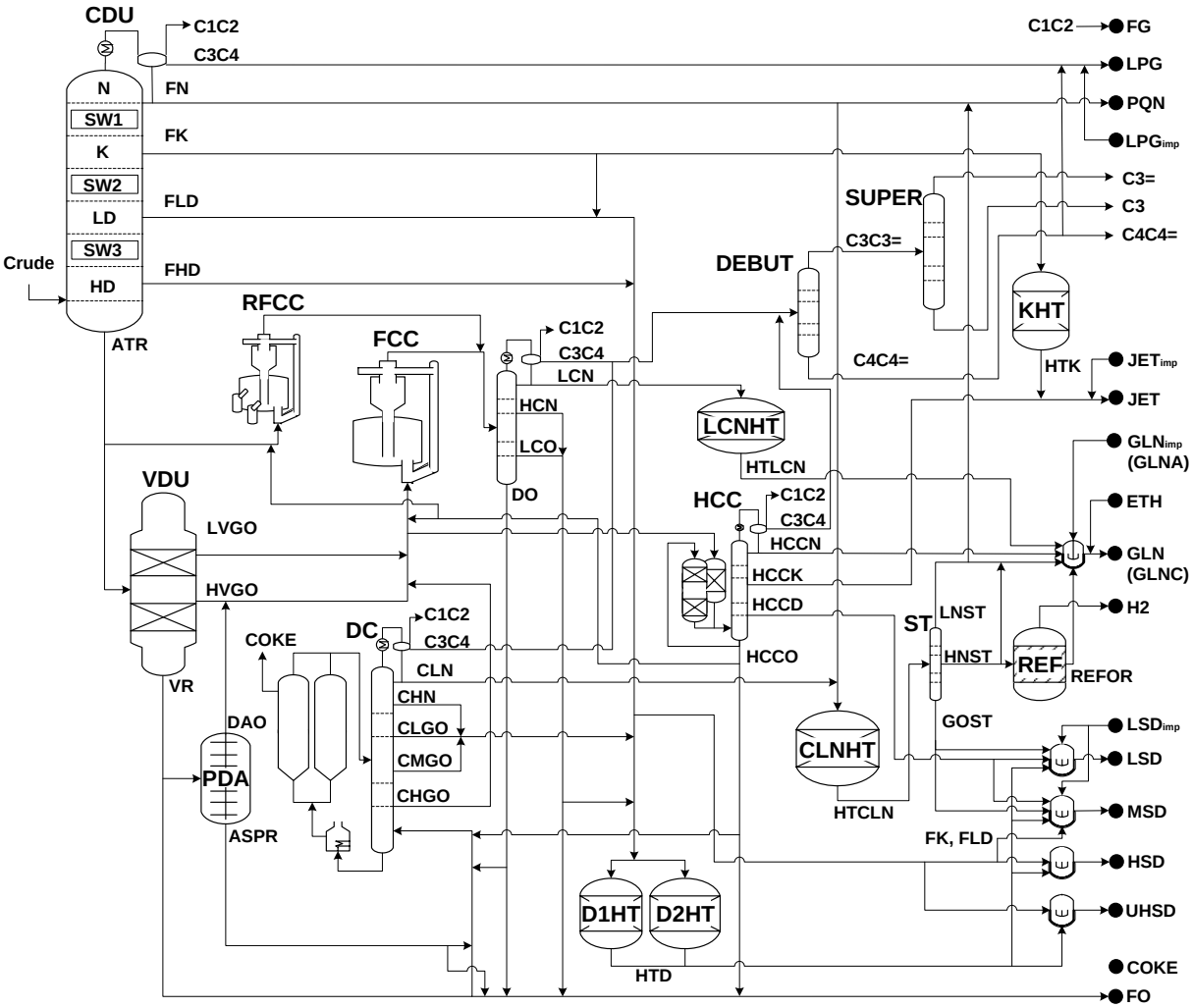

Figure 8.5. Oil-refinery processing network example.

Table 8.1. Groups of units to build the superstructure.

Group	Type	Unit	Name
Crude-oil consumer	Crude-oil distillation	CDU	Crude-oil distillation unit
ATR consumer	reduced crude distillation	VDU	vacuum distillation unit
	catalytic cracking	RFCC	residue fluid catalytic cracking
VGO consumer	catalytic cracking	FCC	fluid catalytic cracking
	catalytic hydrocracking	MHC	medium hydrocracking
	catalytic hydrocracking	HCC	hydrocracking

VR consumer	Extraction	PDA	propane/butane deasphalting
	delayed thermal cracking	DCU	delayed coker unit
	thermal cracking	TCU	thermal cracking unit
Hydrotreater (HT)	Hydrotreating	LCNHT	light cracked naphtha HT
	Hydrotreating	CLNHT	coker light naphtha HT
	Hydrotreating	KHT	kerosene HT
	Hydrotreating	DHT	diesel HT
Octane booster	chain cycling	REF	reformer
	chain isomerization	ISO	isomerization
	C3 to C5 combination	ALK	alkylation
Fractionator	C3 and C4 distillation	DEBUT	debutanizer
	C3 and C3= distillation	SUPER	superfractionator (C3 + C3=)
	naphtha separation	ST	stabilizer

In the PDH model, the three optimization areas within the oil-refinery boundaries are integrated. The first is the crude-oil diet determination using the improved swing-cut modeling considering pseudocomponents, hypotheticals, or micro-cuts distribution as in chapter 5. The second area of optimization covers oil-refinery unit processing transformations to vary quantity and quality variables in hydrotreaters, fluid catalytic cracking units (FCC and RFCC), and propane desasphalting. In the third area, intermediate and final blends are optimized considering quality specifications.

Within the MILP design problem, the aforementioned oil-refinery optimization areas are adapted to avoid nonlinearities. The distillate streams only include yield determination given by Equations 5.1-5.3 in improved swing-cut modeling addressed in chapter 5. The processing transformations are linear considering input-output yield models, conversions or rates given by the last nonlinear iteration. And the blending correlations are neglected or linear related by fixing the qualities from the last nonlinear iteration.

8.4. Process design synthesis of multisite refineries formulation

In each processing center or refinery *r*, the investment layer problem controls the capacity $QC_{r,u,n,t}$ of each nth-unit *u,n* over the investment time *t*. Only for the selected

investments ($y_{r,u,n,t}$ = 1) are the installations $QI_{r,u,n,t}$ and expansions $QE_{r,u,n,t}$ allowed. At each *t*, the unit throughput $QF_{r,u,n,sc,t}$, regardless of the demand scenario *sc*, cannot exceed the unit capacity as shown in Equation 8.3. Only in the following period the unit capacities under expansion or installation are started up after their project execution within ΔT.

$$QF_{r,u,n,sc,t} \leq QC_{r,u,n,t} \quad \forall \quad r,u,n,sc,t \tag{8.3}$$

8.4.1. MILP investment planning model

Moro et al. (1998), Pinto et al. (2000) and Neiro and Pinto (2004) modeled operational planning and scheduling cases for oil-refinery units considering a network whose streams are linked to them by mixers and splitters as shown in Figure 8.6. The scenario index *sc* was omitted for the sake of simplicity.

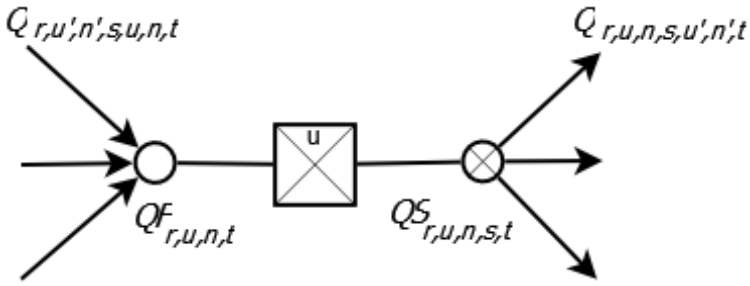

Figure 8.6. Material balance in *u*.

Equation 8.4 represents the mixer concentrating upstream streams *up*, and Equation 8.5 represents the splitter distributing downstream streams *do*.

$$\sum_{(u',n',s)_{up}} Q_{r,u',n',s,u,n,sc,t} = QF_{r,u,n,sc,t} \quad \forall \; r,u,n,sc,t \tag{8.4}$$

$$QS_{r,u,n,s,sc,t} = \sum_{(u',n')_{do}} Q_{r,u,n,s,u',n',sc,t} \quad \forall\, r,u,n,s,sc,t \tag{8.5}$$

Product yields of the units can be considered fixed values, as in the MILP problem, or they can vary throughout the processing network, as in the NLP sub problems for some units, and in this case a nonlinear constraint is formed by the quantity-quality variation. These yields $Y_{r,u,n,s,sc,t}$ are given as a unit throughput ratio for each stream *s*, as seen in Equation 8.6. In the MILP problem, they are generated by the previous NLP problems either in the warm-start or

in last multiperiod NLP operational planning sub problem solved. For the new units or installations, the unit yields are given in the first MILP step. Distillate yields can vary in the MILP problem in a linear formulation by using the swing-cut methodology in chapter 5.

$$QS_{r,u,n,s,sc,t} = Y_{r,u,n,s,sc,t} QF_{r,u,n,sc,t} \quad \forall \quad r,u,n,s,sc,t \tag{8.6}$$

The unit capacities within an oil-refinery *r* can be updated after the project execution to expand existing or install new assets. The capacity expansion $QE_{r,u,n,t}$ and installation $QI_{r,u,n,t}$ of a unit in a certain time ($t < t_{end}$) are active by the constrains 8.7 and 8.8. When an oil-refinery process unit is revamped, the reasonable minimum capacity expansion is around 10% of its current capacity. The maximum reaches around 30% depending on the unit equipment complexity. For higher capacity requirements a new unit is installed.

$$ye_{r,u,n,t} QE^{L}_{r,u,n,t} \leq QE_{r,u,n,t} \leq ye_{r,u,n,t} QE^{U}_{r,u,n,t} \quad \forall \quad r,(u,n)_e,t < t_{end} \tag{8.7}$$

$$yi_{r,u,n,t} QI^{L}_{r,u,n,t} \leq QI_{r,u,n,t} \leq yi_{r,u,n,t} QI^{U}_{r,u,n,t} \quad \forall \quad r,(u,n)_i,t < t_{end} \tag{8.8}$$

In the first investment time period, the operational gains derive from the existing units and their initial capacities are given by $EXCAP_{r,u,n,t=1}$. After the project execution intervals, a new capacity can be added to the unit and another profit is found in the operational layer for the following investment time period if the project is approved, as shown in Equations 8.9 and 8.10.

$$QC_{r,u,n,t} = EXCAP_{r,u,n,t=1} + QC_{r,u,n,t-1} + QE_{r,u,n,t-1} \quad \forall \quad r,(u,n)_e,t \tag{8.9}$$

$$QC_{r,u,n,t} = 0 + QC_{r,u,n,t-1} + QI_{r,u,n,t-1} \quad \forall \quad r,(u,n)_i,t \tag{8.10}$$

With respect to the capital amount available in each investment time *t*, the liquid cash expenses to build the units is lower than the limit capital for investment LCI_t as seen in Equation 8.11.

$$\sum_{r,(u,n)_e} \left(\alpha^{e}_{u,t} QE_{r,u,n,t} + \beta^{e}_{u,t} ye_{r,u,n,t}\right) + \sum_{r,(u,n)_i} \left(\alpha^{i}_{u,t} QI_{r,u,n,t} + \beta^{i}_{u,t} yi_{r,u,n,t}\right) \leq LCI_t \quad \forall\, t < t_{end} \tag{8.11}$$

8.4.2. Integer constraints for investment

Equations 8.12-8.15 are introduced to control the investment logic. Equations 8.12 and 8.13 permit the expansion (*ye*) and installation (*yi*) occurrence of a specific unit *u* only once over all time periods with investment under consideration ($t < t_{end}$). Some refining units such as CDU can have more than one expansion and its life-time, but in this work all units have only one. Equations 8.12 and 8.13 must be active over all periods with investment under consideration to maintain the MILP investment planning approach functionality as defined in this work.

$$\sum_{t<t_{end}} ye_{r,u,n,t} \leq 1 \quad \forall\, r,u,n \tag{8.12}$$

$$\sum_{t<t_{end}} yi_{r,u,n,t} \leq 1 \quad \forall\, r,u,n \tag{8.13}$$

The integer constraints defined in Equations 8.14-8.19 can be added or excluded in the MILP solution. The first group, Equations 8.14 and 8.15, is related to investment logic when expansion of existing units and installation of new ones are being modeled. Equation 8.14 allows only one investment (expansion or installation) per type of unit to avoid investing in more than one unit of the same type at the same time. Equation 8.15 is similar to Equation 8.14, excepting that the types of unit are arranged by groups considering their functionality, like those units responsible for the octane number boosting such as reformer (REF), alkylation (ALK) and isomerization (ISO) or unit consuming the same type of feed such as vacuum distillation unit (VDU) and residuum fluid catalytic cracking (RFCC), both atmospheric residuum consumers (ATRC). Again, both Equations 8.14 and 8.15 can be withdrawn from the model once they only reduce the binary search tree to prevent different project for the same process needs. It is preferred to invest in one larger process unit than two or three small ones.

$$\sum_{n} \left(ye_{r,u,n,t} + yi_{r,u,n,t}\right) \leq 1 \;\; \forall \;\; r,u,t < t_{end} \tag{8.14}$$

$$\sum_{U_G} \sum_{n} \left(ye_{r,u,n,t} + yi_{r,u,n,t}\right) \leq 1 \quad \forall \quad r,t < t_{end} \tag{8.15}$$

8.4.3. Integer constraints for framework sequence-dependency

The second group of binary constraints, Equations 8.16-8.19, is related to the oil-refinery processing framework precedency. It means that sequence-dependency logic exists to invest in a certain type of unit if another investment is set up. The proposed disjunction to manage the quantity transformations throughout the oil-refinery network is given in QTD, where *y* means investment in projects by expansion or installation of capacity. The indices for refinery *r*, number of unit *n*, and time *t* were excluded from QTD for the sake of simplicity. GOC and VRC are gasoil and vacuum residue consumers, respectively.

$$\left[\begin{array}{c} y_{CDU} \\ \left[\begin{array}{c} y_{VDU} \\ \uparrow GO + VR \\ GOC \\ VRC \end{array}\right] \vee \left[\begin{array}{c} \neg y_{VDU} \\ \uparrow ATR \\ ATRC \end{array}\right] \end{array}\right] \vee \left[\begin{array}{c} \neg y_{CDU} \\ VRC \end{array}\right] \qquad \text{(QTD)}$$

In refineries with high production of fuel oil streams (≥ 15% of the CDU feed), the investment in VRC unit can be a profitable choice since it converts low value streams to light and medium products such as gasoline and diesel and requires less investment in downstream units when compared with CDU investments. In high fuel oil production, the first disjunction ($y_{CDU} \vee \neg y_{CDU}$) in Equation 8.16 is true, meaning CDU or no CDU, and decides about the oil-refinery production growth by considering capacity increase in (i) crude distillation unit (CDU) by feeding the whole refinery with higher throughputs or in (ii) VRC units such as delayed coker unit (DC), propane deasphalting (PDA), and thermal cracking unit (TC), that is the no CDU condition.

$$y_{CDU} \vee \neg y_{CDU}(y_{VRC})$$

$$\sum_{n}\left(ye_{r,CDU,n,t} + yi_{r,CDU,n,t}\right) + \sum_{U_{VRC}}\sum_{n}\left(ye_{r,u,n,t} + yi_{r,un,t}\right) \leq 1 \quad \forall\, r, t < t_{end} \qquad (8.16)$$

The disjunction in the second level ($y_{VDU} \vee \neg y_{VDU}$) decide about the consumption of the atmospheric residue (ATR) formed by the CDU investment, so it implies in $y_{CDU} \Rightarrow y_{VDU} \vee \neg y_{VDU}$. In the common oil-refinery network, ATR is the VDU feed, where vacuum gasoil (VGO) and vacuum residue (VR) are produced. If the VDU unit is not invested ($\neg y_{VDU}$), the alternative is to increase the capacity of ART consumer units (ATRC) such as RFCC. Equation 8.17 represents the second disjunction with the previous implication of the CDU

investment due to the consequent increase in ATR. As seen, only one type of project to consume ATR within the refinery *r* in each time *t* is permitted, if the CDU investment occurs. The possibilities are expansion or installation of VDU or other ATRC units.

$$y_{CDU} \Rightarrow y_{VDU} \vee \neg y_{VDU}(y_{ATRC})$$

$$\sum_{n}\left(ye_{r,VDU,n,t} + yi_{r,VDU,n,t}\right) + \sum_{U_{ATRC}}\sum_{n}\left(ye_{r,u,n,t} + yi_{r,un,t}\right) \leq \sum_{n}\left[\left(ye_{r,CDU,n,t} + yi_{r,CDU,n,t}\right)\right] \quad \forall\, r, t < t_{end} \tag{8.17}$$

A straightforward VDU investment consequence is the implication of capacity addition of vacuum gasoil and residue consumer units (GOC and VRC) to convert the VDU streams (GO and VR) into light and medium streams. The main GOC units are fluid catalytic cracking (FCC) and medium and high severity hydrocracking (MHC and HCC). The VRC units are DC and TC by thermal cracking or PDA by solvent extraction. Equation 8.18 represents the $y_{VDU} \Rightarrow y_{GOC}$ implication and Equation 8.19 the $y_{VDU} \Rightarrow y_{VRC}$.

$$y_{VDU} \Longrightarrow y_{GOC} \wedge y_{VRC}$$

$$\sum_{U_{GOC}}\sum_{n}\left(ye_{r,u,n,t} + yi_{r,un,t}\right) \leq \sum_{n}\left[\left(ye_{r,VDU,n,t} + yi_{r,VDU,n,t}\right)\right] \quad \forall\, r, t < t_{end} \tag{8.18}$$

$$\sum_{U_{VRC}}\sum_{n}\left(ye_{r,u,n,t} + yi_{r,un,t}\right) \leq \sum_{n}\left[\left(ye_{r,VDU,n,t} + yi_{r,VDU,n,t}\right)\right] \quad \forall\, r, t < t_{end} \tag{8.19}$$

Other sequence-dependent logic to complete the oil-refinery network are disregarded because gas, light, or medium streams formed by CDU, ATRC, GOC, and VRC units can be dispatched to several downstream units such as fractionators, hydrotreaters, reformers, etc., that can have some idling capacity, so the new amounts of the intermediate streams formed by the units addressed in the quantity disjunction QTD will determine the capacity needs for their downstream units.

8.4.4. NLP operational planning model

The processing nonlinearities are related to the CDU/VDU, PDA, FCC, and hydrotreater (HT) outputs. For CDU/VDU is considered the improved swing-cut modeling (chapter 5) to calculate the quantity and quality variations (yields and properties) of the

distillate streams. The crude-oil diet or basket are found considering this improved swing-cut NLP model by treating the crude as micro-cuts, psedocomponents, or hypotheticals pieces of hydrocarbon material discretized within 10ºC, from pentane to heavy fractions up to 850ºC. The FCC is configured with the delta-based model from Moro et al. (1998) to predict yields variation based on Conradson carbon residue in feed and reactor and feed temperature deviation. The PDA modeling simply considers the operational variable extraction factor as the de-asphalted oil yield. The HT main transformation is the sulfur concentration reduction, but the consequent specific gravity and octane number reductions are also regarded. All streams with fixed yields and properties are given in the supporting information.

All blending equations are given in chapter 3. The properties being considered are the volume-based (specific gravity, olefin, and aromatic content), the mass-based (sulfur content, acidity, and Conradson carbon residue) and the ad-hoc octane number (research octane number, and motor octane number).

8.5. Results and discussion

8.5.1. Motivating example

The motivating example is solved using the conventional and the generalized capital investment planning (CCIP and GCIP) formulations without considering NPV deflation and uncertainties from scenarios. The CCIP model is developed in GAMS (Brooke et al., 1992) and the GCIP in IMPL. In the example depicted in Figure 8.7, the hydrotreater DHT1 produces 50 wppm sulfur diesel (D50) from a source containing 1000 wppm of sulfur (D1000), wppm is ppm in weight basis. As the severity of the DHT1 varies between 0.90 and 0.95, the unit is not able to reduce the sulfur content to 15 wppm S (D15) as required in a future scenario, so a new hydrotreater with higher severity must be installed. The severity of the new unit DHT2 is between 0.90 and 0.99 and there is no explicit consumption of hydrogen shown given that it is not perceived as a bottleneck or active constraint.

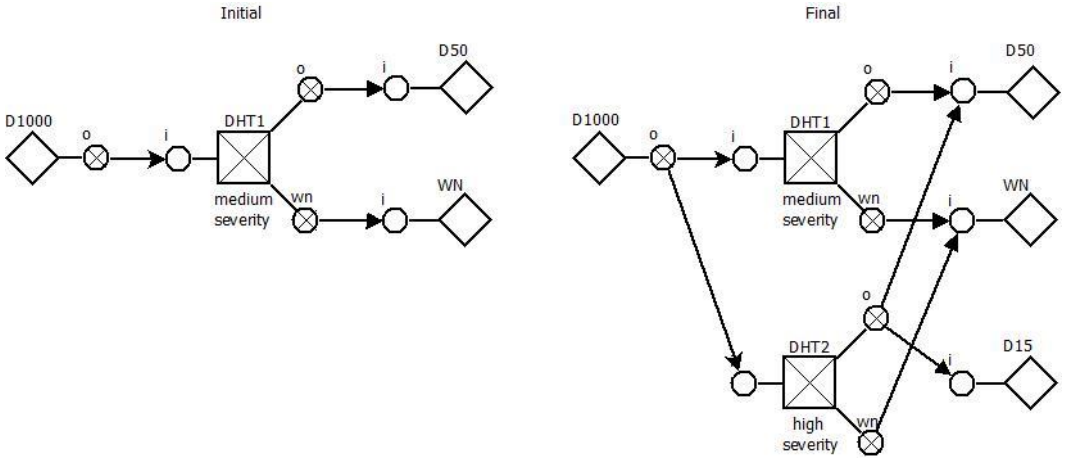

Figure 8.7. Initial and final network for 50 and 15 wwpm S diesel.

This is an MINLP problem given that all flows are variable as well as the specific gravities and sulfur contents including the severity times sulfur thus resulting in bi-linear and tri-linear terms with plus and minus coefficients making the NLP quality sub problem non-convex. Due to the setup logic variables for the expansion and/or installation logic decisions we have the integer or discrete (binary) variables resulting in the MINLP and more appropriately a non-convex MINLP problem.

In the hydrotreating process, there is a trade-off between the sulfur content reduction and the amount of hydrotreated stream lost as naphtha, which is inevitably produced by cracking side reactions in the carbon chain. The H_2S formed by the sulfur removing at high pressure of H_2 and high temperature are recovered in a fractionation tower after the reactor bed and its upper stream is known as wild naphtha, a mix of naphtha and H_2S. The correlation considered to calculate the yields for *o* and *wn*, respectively, the hydrotreated stream and the wild naphtha, are $o = (1 - (sev-0.90)/2)$ and $wn = (sev-0.90)/2$. In the severity lower bound scenario ($sev=0.90$), the *wn* formation is zero in both hydrotreaters. In the severity upper bound ($sev = 0.95$ for DHT1 and $sev = 0.99$ for DHT2) the *wn* formation is 2.5% for DHT1 and 4.5% for DHT2.

To give more degrees of freedom to the motivating example, the DHT2 output *o* can flow to D50 and D15 sinks of diesel on-specification. Considering the proposed PDH algorithm the sequence of problems to be solved is 1-) the single-period NLP problem to generate optimal initial values and unit yields (warm-start), 2-) the multiperiod MILP model to find the new process design by expansion and installation of unit, and 3-) the multiperiod NLP model to find new yields considering the new process design. In the multiperiod models,

there are three periods considered and the iteration between the steps 3 to 2 is performed while the multiperiod MILP and NLP objective functions are within a 1% relative gap. The warm-start can be neglected by using given numbers for initial values and upper and lower bounds in the MILP problem.

The density is required to perform the mass-basis sulfur balances, although we considered it a fixed number without any changing in the process. There is no cost applied to the supply of diesel nor is there a price for wild naphtha. However, the D50 product has a price of 1.0 and the price for D15 is 1.2, which implies that it is more economical to produce a lower sulfur diesel material especially when there is no raw material or operating costs currently modeled, although there is loss of diesel to wild naphtha with the severity increase. In the design problem, the initial capacity of the DHT1 is 1.0 and the expansion is permitted at most at 50% of the existing capacity. For the installed DHT2, the maximum capacity is 1.5. The variable and fixed costs of the installation are equal 0.5 $/volume and 0.5 $ respectively. The expansion is 60% of the installation costs. The initial value of the DHT2 considers zero formation of wild naphtha, meaning that if the severity of the new hydrotreater has been modeled in the MILP, it would be considered 0.90, without loss of hydrotreated stream *o* to *wn*. In this case, the DHT2 would not be able to produce diesel with 15 wppm of sulfur if it was taken into account in the MILP problem.

8.5.1.1. CCIP modeling results

Using the conventional capital investment planning (CCIP) formulation as defined in this work, equations 8.12 and 8.13 are needed to avoid more than one investment in the same unit. The results of the 3 steps are shown in Table 8.2. The problem is performed in the GAMS modeling language, version 23.9.3, on an Intel Core 2 Duo (3.00 GHz, 16.0 GB of RAM). As we can see, both expansion of DHT1 at 1.5 and installation of 1.5 of DHT2 occurred.

In the first MILP iteration, the objective function resulted in 5.800 $. When the new process design scenario is used in the first iteration of the multiperiod NLP problem, with DHT1 capacity expanded from 1 to 1.5 and DHT2 installed with 1.5 of capacity, the DHT2 produces diesel at 15 wppm and its severity resulted in 0.985 to avoid more less of DHT2 output as *wn*. The MILP and NLP problems in the second iteration have the same yields as in the $NLP_{(ite=1)}$ as seen in Table 8.3, converging both problems to the same results. The NLP

solvers used is CONOPT, IPOPT and SNOPT, which converged in less than 0.01 seconds in all cases, and the MILP solver is CPLEX with less than 0.01 seconds of solution.

Table 8.2. Motivating example results of the warm-start and the first PDH iteration

		$NLP_{(t=1)}$	$MILP_{(ite=1)}$			$NLP_{(ite=1)}$		
objective function		0.975		5.800			5.647	
			t1	t2	t3	t1	t2	t3
yield	DHT1.o	0.9750	0.9750	0.9750	0.9750	0.9750	0.9750	0.9750
	DHT1.wn	0.0250	0.0250	0.0250	0.0250	0.0250	0.0250	0.0250
	DHT2.o			1.0000	1.0000		0.9575	0.9575
	DHT2.wn			0.0000	0.0000		0.0425	0.0425
capacity	DHT1	1.0	1.0	1.5	1.5	1.0	1.5	1.5
	DHT2			1.5	1.5		1.5	1.5
severity	DHT1	0.950				0.950	0.950	0.950
	DHT2						0.985	0.985

Table 8.3. Motivating example results for the second PDH iteration.

		$MILP_{(ite=2)}$			$NLP_{(ite=2)}$		
objective function			5.647			5.647	
		t1	t2	t3	t1	t2	t3
yield	DHT1.o	0.9750	0.9750	0.9750	0.9750	0.9750	0.9750
	DHT1.wn	0.0250	0.0250	0.0250	0.0250	0.0250	0.0250
	DHT2.o		0.9575	0.9575		0.9575	0.9575
	DHT2.wn		0.0425	0.0425		0.0425	0.0425
capacity	DHT1	1.0	1.5	1.5	1.0	1.5	1.5
	DHT2		1.5	1.5		1.5	1.5
severity	DHT1				0.950	0.950	0.950
	DHT2					0.985	0.985

8.5.1.2. GCIP modeling results

Figure 8.8 shows the unit-operation-port-state superstructure (UOPSS) or flowsheet using the generalized capital investment planning (GCIP) modeling (chapter 7) where the UOPSS shapes can be found in Kelly (2004), Kelly (2005), Zyngier and Kelly (2009), and Zyngier and Kelly (2012). This problem is formulated whereby both the capacity and capital cost for the expansion and installation of the diesel hydrotreating units (DHT1 and DHT2 respectively) are modeled as flows in a scheduling environment with project staging. Diamond shapes are perimeters which indicate where material or even money and other necessary resources can flow into or out of the problem. The square shapes with an "x" through them are continuous-processes and the triangle shapes are pools or inventory/storage

unit-operations. The circles are ports where an “x” inside is an out-port and without an “x” is in-port and the lines connected to ports and units are what we call “internal streams”. Lines with arrow-heads connecting out-ports to in-ports are called “external streams” and these along with the unit-operations have setup and startup logic variables created as well as switchovers and shutdown logic variables if up-times and/or down-times are configured to manage the temporal transitions (Kelly and Zyngier, 2007 and Zyngier and Kelly, 2009).

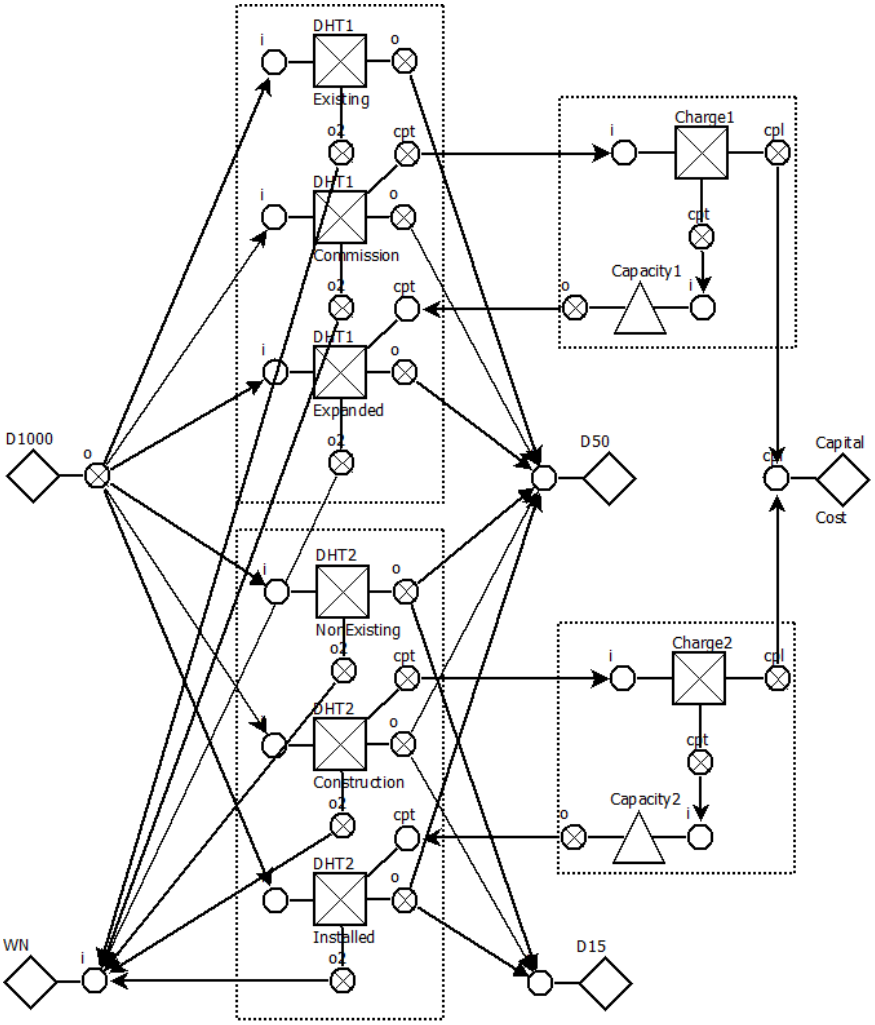

Figure 8.8. Partitioning and positioning GCIP example UOPSS flowsheet.

The scope of this problem is to decide if the existing unit DHT1 should be expanded via the commission-stage operation or not and to decide if the non-existing unit DHT2 should be installed via the construction-stage operation or not. If so then there is a capital cost during the commission and construction-stages for the capacity expansion and installation using a variable and fixed cost linear expression of capital cost = alpha * (capacity_new – capacity_old) + beta * setup, where if an installation, the old capacity is of course 0 (zero). A more detailed description of this modeling can be found in chapter 7.

When we solve the $NLP_{(t=1)}$ (temporal relaxation) sub problem using SLPQPE, with either CPLEX, COINMP, GLPK, or LPSOLVE as the LP solvers, we get an objective function value of 0.975 currency-units given that we have only allowed the existing DHT1 and non-existing DHT2 unit-operations to be active during the mono-period time-horizon in order to provide starting, initial, or default yields to the multiperiod MILP, i.e., no capital costs incurred. The 0.975 value corresponds to the fact that only flow from the DHT1,Existing,o out-port to the D50,i in-port is active in the amount of 0.975 flow-units. Upon solving the multiperiod MILP using CPLEX, COINMP, GLPK, or LPSOLVE we get an objective function value of 5.800 currency-units which corresponds to the profit of performing the DHT1 commission-stage in time-period 1 and DHT2 construction-stage also in time-period 1. This allows two time-periods for expanded capacity for DHT1 and also two time-periods for newly installed and extended capacity and capability for DHT2, i.e., the DHT2 unit can produce both D50 and D15 due to its extended conversion. The Gantt chart in Figure 8.9 displays the setup logic variables in black horizontal bars for all unit-operations.

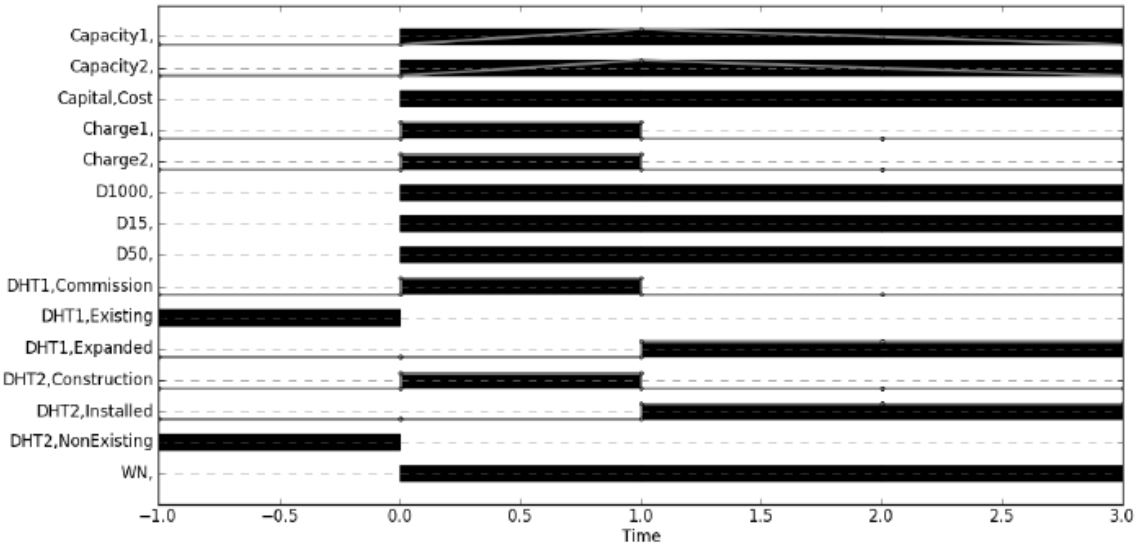

Figure 8.9. Gantt Chart with 1-period and 3-period Past and Future Horizons for the multiperiod MILP.

Using the fixed setups from the multiperiod MILP for both the unit-operations and the unit-operation-port-state to unit-operation-port-state external streams, we get a profit of 5.647 currency-units from the multiperiod NLP sub problem solution. Solving again the MILP with the new fixed/finite yields from the NLP we converge on an objective function value of 5.647, that is the same result found in the CCIP example. In this GCIP model, the production in the commission phase for the expansion is considered the same as its existing mode in order to compare both CCIP and GCIP results.

8.5.2. Oil-refinery design synthesis

8.5.2.1. REVAP Investment Planning

The example is performed for two time-periods and two demand scenarios considering the existing units at REVAP refinery (Figure 8.10). As seen in Table 8.4, the problem converged after 4 iterations when the results (objective function, new capacities, etc.) stop to change. We can see that after the 1st iteration the CDU investment changed from expansion to installation and the CDU and VDU new capacities are modified until their stabilization in the 4th iteration. Although the gap between the MILP and the average value of the NLP sub problems (considering the scenarios) has increased after the 1st iteration, it still continues within 5%.

Figure 8.10. São Paulo state supply chain and Brazilian refineries.

Table 8.5 shows the statistics of the problem. The number of variables and equations change from the 1st to the 2nd iteration because of the CDU installation in the 2nd iteration that it different from the 1st iteration, where the investment in CDU was expansion of an existing unit. Also, we notice reduction in time of execution along the iterations. The NLP solver used is CONOPT and the MILP solver is CPLEX. The full space MINLP problem was tested, but it could not be solved even in the root relaxation due to infeasibilities.

Table 8.4. Capacity expansions (exp) and installations (ins) in REVAP.

capacity [=] k m^3/d			Iteration							
			1		2		3		4	
u	n	EXCAP	exp	ins	exp	ins	exp	ins	exp	ins
CDU	1	40.0	9.6							
VDU	1	20.0	4.5		4.2		4.0		4.0	
FCC	1	14.0								
DC	1	5.0								
LCNHT	1	7.0								
CLNHT	1	4.0								
ST	1	4.0								
KHT	1	3.0								
KHT	2	3.5								
DHT	1	6.0								
DHT	2	6.5								
REF	1	1.5								
CDU	2					9.7		9.4		9.4
ST	2			5.1		5.1		5.1		5.1
DC	2			8.7		8.7		8.7		8.7
CLNHT	2			5.1		5.1		5.1		5.1
KHT	3			2.0		2.0		2.0		2.0

Z [=] billions of U.S. dollars					
Z_{MILP}		3.164	3.166	3.189	3.189
MILP GAP (%)		0.072	0.244	0.979	0.979
Z_{NLP}	sc=1	3.135	3.052	3.058	3.058
	sc=2	3.080	2.997	3.003	3.003
Avg(Z_{NLP})		3.108	3.025	3.030	3.030
Z_{MILP}-Avg(Z_{NLP}) (%)		1.782	4.464	4.985	4.985

Table 8.5. REVAP example: Statistics.

		Iteration							
		1		2		3		4	
		MILP	NLP	MILP	NLP	MILP	NLP	MILP	NLP
equations		1,911	954	1,911	1,100	1,911	1,100	1,911	1,100
variables		2,558	1,050	2,558	1,210	2,558	1,210	2,558	1,210
binaries		93		93		93		93	
non-zeros		7,026	3,614	7,026	4,339	7,026	4,339	7,026	4,339
non-linear			2,109		2,607		2,607		2,607
CPU(s)	sc	0.235		0.110		0.032		0.078	
	sc=1		0.406		0.250		0.047		0.047
	sc=2		0.296		0.219		0.016		0.093

8.5.2.2. São Paulo Supply Chain Refineries Investment Planning

Table 8.6 shows the capacity planning for the multisite refineries in São Paulo Supply Chain. For the sake of simplicity, only the results in the 1st and 4th iterations are shown. The existing capacity (EXCAP) and demands for each scenario are in Table S8.1 and Table S8.2. The investment amount in the 1st iteration is 19 billions of U.S. dollars in the 4th is 21.5 billions. Table 8.7 and Table 8.8 show the MILP and NLP solutions and model statistics of

the problem. Similar to the REVAP example, the decomposition solution converged after 4 iterations and within a 5% gap between the MILP and average-NLP solutions. The NLP solver used is CONOPT and the MILP solver is CPLEX. The full space MINLP problem was tested, but it could not be solved even in the root relaxation due to infeasibilities.

Table 8.6. Capacity expansions (exp) and installations (ins) in São Paulo refineries.

			iteration			
			1		4	
r	u	n	exp	ins	exp	ins
REPLAN	CDU	1	9.7			
	CDU	2			5.5	
	VDU	1			2.0	
	VDU	2	6.6			
	FCC	1				
	CLNHT	1	1.1		1.1	
	ST	2		5.1		5.1
	DC	3		10.0		10.0
	REF	2		1.3		1.3
REVAP	CDU	1	12.0		12.0	
	VDU	1	5.4		6.0	
	FCC	1	2.5		3.9	
	DC	2		7.5		5.7
	KHT	3		2.0		2.0
	LCNHT	2	2.1			2.8
	CLNHT	2		4.3		3.0
	ST	2				3.0
	REF	2		1.4		1.0
RPBC	CDU	1	4.0		4.0	
	VDU	1		2.9	2.9	
	VDU	3		6.2		
	DEBUT	2		2.0		2.0
	FCC	2		18.9		12.7
	LCNHT	2		9.5		6.4
	CLNHT	2		2.0		2.7
	ST	2		2.0		2.7
	REF	2			0.6	
	ALK	1		0.8		
RECAP	SUPER	2		2.0		2.0

Table 8.7. São Paulo refineries example: MILP and NLP Solutions.

		Iteration			
		1	2	3	4
Z_{MILP}		8,063	7,812	7,893	7,934
MILP GAP (%)		0.9573	0.9937	0.9982	0.9914
Z_{NLP}	sc=1	6,722	8,429	7,856	7,866
	sc=2	6,567	8,287	7,719	7,730
	sc=3	6,099	7,777	7,099	7,139
$Avg(Z_{NLP})$		6,462	8,164	7,558	7,578
Z_{MILP}-$Avg(Z_{NLP})$ (%		19.9	4.5	4.2	4.5

Table 8.8. São Paulo refineries example: Statistics.

	Iteration							
	1		2		3		4	
	MILP	NLP	MILP	NLP	MILP	NLP	MILP	NLP
equations	10,076	5,406	10,076	5,347	10,076	5,378	10,076	5,349
variables	13,782	5,932	13,782	5,870	13,782	5,899	13,782	5,870
binaries	213		213		213		213	
non-zeros	36,950	24,825	36,950	25,515	36,950	24,606	36,950	24,547
non-linear		16,842		16,652		16,673		16,682
CPU(s) sc	2.969		4.281		3.375		3.407	
sc=1		17.484		5.468		3.515		3.657
sc=2		20.718		0.219		4.235		4.203
sc=3		20.609		0.219		4.078		4.297

8.6. Conclusion

In summary, we have described how to iteratively solve a *qualogistics* or MINLP capital investment problem using MILP and NLP sub-solvers configured in a coordinated manner. This same technique can be applied to any advanced planning and scheduling MINLP problem found in the process industries given our assertion that these types of problems can be phenomenologically modeled using the QLQP attributes to concatenate the sub problems. The major advantage of the partitioning and positioning approach is that each sub problem can be independently and individually isolated and thoroughly investigated and interrogated to troubleshoot and debug inconsistencies and unexpected solutions when they exist. Existing MINLP and global optimizers are treated as black-boxes and if reliable and relevant solutions are not obtained which is usually the case in practice, then little insight and analysis is afforded back to the development and/or deployment user.

The integration between logistics and quality sub problems was implemented in a complete oil-refinery investment planning problem to design new process frameworks as well as to determine new process capacities. The processing uncertainties are intended to decrease by more detailed formulation in crude dieting, process transformation and blending as a type of preventative uncertainty management. Even though it is well recognized that the decomposed procedure may generate merely sub-optimal feasible solutions, these are both logistics and quality consistent, and the procedure is therefore significantly better than other alternative usually employing manual trial and error simulation. It is important to highlight that hopefully sometime in the near future, the pragmatic decomposition of the MINLP into two simpler sub problems (logistics and quality) will not be required given the expected evolution of MINLP solver technology. Yet, from an intelligent problem solving perspective, dissecting a large problem into smaller sub problems (divide-and-conquer) can be a very effective way of detecting, identifying and eliminating defects in the model and data supplied.

Chapter 9

9. Conclusion and Future Work

In this thesis, we have described models and solution methods for the operational and strategic decision-making of oil-refinery processes in a quantitative manner. In chapter 3, we developed a model for the optimal nonlinear production planning of oil-refinery processes and applied it to the Brazil's oil-refining industry considering the hypothetical large refinery REBRA to approximate the national multisite refineries production. In chapter 4, we described a model for the optimal mixed-integer nonlinear strategic investment planning of oil-refinery processes to determine overall capacity expansions per type of oil-refinery unit considering the aggregated refinery REBRA. In chapter 5, we improved the swing-cut modeling for better predicting quantity and quality values of distillate streams using a property-based interfacial linear interpolation considering micro-cuts, hypotheticals, or pseudocomponents distribution. We developed in chapter 6 a model that integrates distillate stream cutpoints (initial and final boiling point temperatures) and fuel recipes optimization by taking into account product evaporation data (ASTM) and its interconversion to TBP (and vice-and-versa) to formulate the method using both monotonic interpolation. In chapter 7, a generalized capital investment planning model that can be applied to small, medium, and large size types of projects (repair, retrofit, revamps) formulates project setups and phases using sequence-dependent setups in a scheduling environment. Finally, in chapter 8, we outlined the phenomenological decomposition heuristic algorithm to solve the quantity-logic-quality or *qualogistics* problem in a two-stage stochastic programming formulation with a quantity-logic or mixed-integer problem in the first-stage defining the binary variables (project setups) and NLP sub problems in the second-stage for the continuous variables determination including quantity and quality balances.

9.1. Nonlinear Production Planning of Oil-Refinery Units for the Future Fuel Market in Brazil: Process Design Scenario-Based Model.

In chapter 3, nonlinear operational planning model of oil-refinery processes defines the production and import figures for Brazil's future oil products market. The national refineries are aggregated in a hypothetical large refinery to calculate overall volume balances using as baseline the existing refineries and national data in 2013. The refineries under construction and those in conceptual phases, starting up in 2016 and in 2020 respectively, are

added to the hypothetical large refinery (REBRA) to predict overall capacity increase to match four different market demand scenarios.

The results for the 2013 scenario presented good precision with the national data accumulated in the past 12 months until October, 2013 considering the gasoline and ethanol for fueling market stabilization (GLNC scenario, see Figure 3.4). Crude import dependence to yield more medium distillates is confirmed in around 12%, which is commonly ultralight African oil, without including the crude imports for lubricant production of around 6%, mostly from the Middle East. The $GLNC_{ETH}$ scenario in 2013, discounting the ethanol to gasoline market shift, demonstrates that before this move the country was free of gasoline imports. The cause of this market shift was the ethanol price surge since 2009 that started as conjectural situation related to sugar cane harvesting problems, due to droughts, and sugar demand increase overseas, and it was intensified and is maintained by structural modification in gasoline demands considering the economy increase from 2009 to 2012 in Brazil. As ethanol is part of the retail gasoline between 18-25%, any further demand in gasoline directly causes more demands for ethanol in the retail gasoline mix (GLNC).

In the baseline calculation for the existing refineries in 2013, higher prices for gasoline and diesel are considered to yield a minimal margin of 0.5 US$/barrel. As seen in Table 3.7, the current prices of these fuels are consuming around 14 million US$/d from PETROBRAS' resources because of the import price differences when compared with the national Brazilian market price.

By adding the refineries under construction (RNEST and COMPERJ-1) in the large refinery REBRA in 2016, fuel imports (LPG, gasoline, jet fuel, and diesel) are minimized, mainly diesel. RNEST production yields around 70% of diesel and a small increase in gasoline and jet fuel production is from COMPERJ-1, basically from the first hydrocraking unit to be installed in Brazil. Only in lower demand cases (4.2% p.a.) with investments in projects to start up in 2020, jet fuel and diesel imports are reduced to zero, and the external dependence of gasoline ceases in the investment cases only in the minimum import scenario (4.2% p.a. and $GLNC_{ETH}$) with the conceptual projects performed with refitting.

In all demand scenarios with the conceptual phase projects built in 2020, the total size of planned capacities of most units needs refitting. As example, for the overall planned CDU capacity in 2020 (538 k m^3/d), the throughputs idling figure of ~30−40 k m^3/d, suggesting that

a new site could be withdrawn from the future investment portfolio, given the expected demand scenarios.

9.2. Mixed-Integer Nonlinear Production Planning of Oil-Refinery Units for the Future Fuel Market in Brazil: Process Design Synthesis Model

Despite the importance of process design synthesis optimization within the oil-refinery industry due to the intensive capital amount and complex processes involved, most methodologies to determine facilities expansion of physical separation and chemical reaction equipment in oil-refineries are based on a trial-and-error procedure. The oil-refinery process design is manually tested to avoid mixed-integer models and they are usually formulated as linear by considering crude oil diet, fuel recipe, and intermediate product quality as fixed values, and the processing transformations are mostly delta-based formulae ($f(x) = ax+b$, a and b as constant), all demanding continuous effort to update the overall parameter data in order to maintain the accuracy of the simpler model. In chapter 3, the Brazil's current and future fuel production profiles are reproduced for fixed process design, in which a profit-based approach for different fuel market scenarios considering the national crude oil production by groups, fuel production, and imports of both crude and fuel is solved.

Alternatively, in the framework optimization-based approach presented in chapter 4, a discrete optimization model finds the optimal process design creating a combinatorial enumeration of setup variables to be explored by branch-and-bound methods. Continuous variables are combined with these setup variables to evaluate the size of the projects by using semi-continuous constraints, i.e., a continuous variable is zero or between bounds by the appropriate selection of its respective binary variable. In the chapter, an MINLP model determines the overall capacity expansion of existing units for the Brazilian large refinery REBRA based on setup and sizing of projects in a multiperiod case. Similar to the results found in chapter 3 for the 2020 scenarios, when the refineries under conceptual phase are considered on-stream, the results in chapter 4 indicate the need to reevaluate the strategic decisions considering the possible variation on future fuel demands.

In terms of modeling, comparing the results in 2020 from both NLP and the MINLP methodologies, the former, considering a large number for unit throughput upper bounds, results in unrealistic process design by decreasing the capacity of separation units (CDU and VDU) and increasing the capacity of cracking units (HCC and DC). Unlike the NPV-based MINLP methodology, the NLP problem does not take into account the investment constraints

in the profit-based maximization, so that larger profits are obtained with higher capacity of low-to-high stream value units (HCC and DC), despite their more expensive investment costs.

Simplifications for considering five groups of crude, same cuts, and swing-cuts for all CDU and VDU units, aggregated capacity per type of unit, averaged values for currency, prices, demands, etc., all of them may influence the quality of the results. However, for the national strategic planning level, the aggregated model and other simplifications addressed in chapters 3 and 4 are sufficient for predicting the overall capacity expansion per type of oil-refinery unit required to match the country's future fuel demands and prevent the solution of very large models by including all the refineries. The NLP operational planning formulation (chapter 3) is used in a full space model integrated with the binary problem (chapter 4), which can be solved in the aggregated approach instead of solving the multisite problem with 12 to 16 refineries considering the existing and new oil-refinery sites.

In both aggregated approaches, the NLP operational planning (chapter 3) and the MINLP strategic planning (chapter 4) models, the future plans around the refining assets expansion in Brazil cannot prevent the country's fuel import in 2020, except in the lowest fuel demand case ($GLCN_{ETH}$ and 4.2% p.a.). Considering the country's economy growth in the past recent years, the retail gasoline/ethanol for fueling market steady-state, and the uncertainties related to the national light crude production expansion from the new presalt fields, the national oil-refining industry are reconfiguring proposed projects, as discussed in Appendix A, and the approaches developed and the results obtained in chapters 3 and 4 may guide investment decisions in the country.

9.3. Improved Swing-Cut Modeling for Planning and Scheduling of Oil-Refinery Distillation Units

In chapter 5, we outlined an improvement to the conventional swing-cut modeling by taking into account that the swing-cut fractions flowing to the light and heavy final-cuts, distillates, or product-cuts have different properties that varies according to their proportions between the light and heavy hypothetical interfaces (light-cut/swing-cut and swing-cut/heavy-cut). The novel quality variation prediction for the light and heavy swing-cuts uses pseudocomponents, hypotheticals or micro-cuts discretized into 10ºC increments of the crude (crude-oil assay distribution curves) in a interfacial property-based linear interpolation. Additional nonlinear relations (Equations 5.9 to 5.12) consider light and heavy swing-cut

amounts and properties of the hypothetical interfaces and the whole swing-cut (bulk properties) to determine the different light and heavy swing-cut qualities.

An actual CDU operation with eighteen crude oils and three swing-cuts (see Figure 5.3) demonstrates property differences for final distillates in both the conventional and improved swing-cut methods. The results show that the proposed improvement better predicts specific gravity than sulfur content (see Figure 5.5 and Figure 5.6). This should be due to the more nonlinear behavior in sulfur content, which is not well-captured in the linear interpolation used. Although the small differences between the distillate qualities found in both methods, when intensive values of the distillates, such as specific gravity and sulfur content, are used in blend-shops and downstream units (such as hydrotreaters), these small differences can avoid under or overestimation in operational settings when these intensive values are extended considering stream volumes in pipelines or tanks.

In the planning example for production of different grades of diesel, the improved swing-cut model yields higher profit if compared with the conventional method because of its higher jet fuel production, which is provided by the lower specific gravity value for the light-SW2 flowing to the kerosene final-cut (see Table 5.7 and Table 5.8). This difference represented 3.3% in profit increase, which indicates 12.0 k US$/d or 4.380 million US$/y.

9.4. Distillation Blending and Cutpoint Temperature Optimization using Monotonic Interpolation

Cutpoint optimization for distillation models in planning and scheduling problems commonly use crude assay data considering simplifications in distillation process without considering the thermodynamic and equilibrium relationships. In the swing-cut model, the cutpoint optimization is approximated by amounts of light and heavy swing-cuts to determine distillate flows with a given flexibility, which are used in rigorous process simulators to define distillate temperature cutpoints (initial and final boiling points – IBP and FBP). These points are defined as that temperature on the whole crude TBP that represents the limits (upper and lower) of a fraction to be produced (Jones and Pujado, 2006), although simple methods define cutpoint as the midpoint temperature between two adjacent “tails” (100% of the lighter cut and 0% of the heavier cut).

The distillation blending and cutpoint optimization addressed in chapter 6 integrates two major areas inside the oil-refineries, which is the distillate cutpoints (IBP and FBP) and

final blending recipes optimization. By interpolating experimental evaporation curves of the distillate streams compounding the final blending pools, a novel adjustment or shifting modeling modifies the distillate amounts and the whole evaporation curves to match quantity and quality demands in fuel recipes optimization. The proposed methodology converts evaporation curves from ASTM D86 to TBP temperatures and these points are converted to cumulative evaporations using monotonic interpolation, where blending components are linearly mixed in mass or volume basis to determine blended qualities such as evaporations. These blended evaporations need to be converted back to TBP temperatures using another monotonic interpolation, which is interconverted back to ASTM D86 to match fuel specification (see Figure 6.3).

The illustrative example 6.1 represents a small optimization case (only 1 degree of freedom) to compare three interpolation (linear, PCHP, Kruger) methods and to better understand the interconversions of the distillation blending methodology. As seen, Kruger's, also known as constrained interpolation (Kruger, 2014), is more accurate with experimental data, so this interpolation is used to reproduce all other examples in the chapter. Actual PETROBRAS oil-refinery's blend-shops comparing ASTM D86 temperatures for gasoline and diesel products, examples 6.3 and 6.4 respectively, demonstrate that the proposed methodology has better prediction than assuming ASTM D86 temperatures linearly blended by volume (see Table 6.8 and Table 6.13). For the middle point (50% evaporation), the ASTM D86 linear blending and the proposed distillation blending methodology are similar, but for lower points (< 50%), the linear blending model overestimates the final blend values, and for higher points (> 50%), they are underestimated.

In example 6.2, the distillation blending and cutpoint optimization case is demonstrated by considering the distillate stream as a blending component to optimize the front end, IBP, or *T01* (1%) and/or back end, FBP, or *T99* (99%) of the component TBP distillation curves, updating the relative yields for other points of the adjusted or shifted distillation curves. Physical phenomena that describe the behavior of the distillation towers are captured in the experimental curves, which is a result of crude assays and fractionation inside the towers. The model implies that the properties of the streams can be adjusted without including the equations that describe the separation in a given distillation tower, although the results must be used in further steps in rigorous process simulators to verify that

the modification is possible considering the actual tower operation. The results can also be used as initial points in on-line optimization strategies.

Finally, in the diesel blending example, we can notice the addition of the ASTM D86 85% temperature which is required for the diesel product's quality specification limits. As there is no correlation to convert ASTM D86 85% to its respective TBP, this point is calculated by interpolating the standard TBP temperatures at 1%, 10%, 30%, 50%, 70%, 90%, 99% and then creating another interpolation using these TBP temperatures as the abscissa and the corresponding calculated ASTM D86 temperatures as the ordinate. The built-in interpolation functions and the possibility to have their derivatives calculated automatically, techniques found in IMPL (Industrial Modeling & Programming Language), becomes the interconversions and interpolation quite easy to handle, which would be impossible or extremely hard to implement by using other modeling languages in the market.

9.5. A General Approach for Capital Investment Planning using MILP and Sequence-Dependent Setups

In chapter 7, a generalized model for capital investment planning of oil-refineries using MILP is developed from a more realistic framework by considering project phases or stages. The novel idea is to use sequence-dependent switchover modeling to represent the construction, commission, and correction stages of the revamp, retrofit, and repair problem as repetitive maintenance tasks or activities that are inserted between the "existing" and "expanded" unit-operations. This allows generalizing the popular retrofit design synthesis problem as a usual sequence-dependent changeover production planning or scheduling problem including inventory and logistics details such as operating modes, run-lengths, capacity expansions, conversion extensions, etc.

Although the addressed logic variables determine setups for installation and expansion of oil-refinery units, this can be extended to procedures or tasks of units, pipelines, tanks, or blenders. The project scheduling or investment analysis proposed is concerned with temporal coordination for setups over time or startups of projects, in which admissible project schedules must obey constraints such as precedence relations (investment, or tasks if included production scheduling, cannot start unless another have been selected) and resource restrictions (crude, capital, etc., scarce resources with limited capacities) (Wiesemann et al., 2010).

The capital investment planning (CIP) is reformulated using capacity/capability and capital as flows in a scheduling environment. The generalized CIP formulation can be applied to any CIP problem found in the process industries which may require more scheduling details to be considered. It can be easily modeled using the modeling and solving platform IMPL, which is based on the superstructure shown in Figure 9.1 allowing the modeler or user the ability to configure the problem using semantic variables such as flows, holdups, yields and setups, startups, etc. without having to explicitly code the sets, parameters, variables, and constraints required in all other algebraic modeling languages in the market. In the UOPSS scheme, all links between the ports and the units have a binary variable to turn on or off the existence of the shapes (units, ports, and streams) over time. This idea permits to solve industrial-sized optimization problems in both planning and scheduling environments in which the UOPSS shapes and procedures (each one having their own meaning) are integrated over space and time considering renewable (units) and/or non-renewable resources (states).

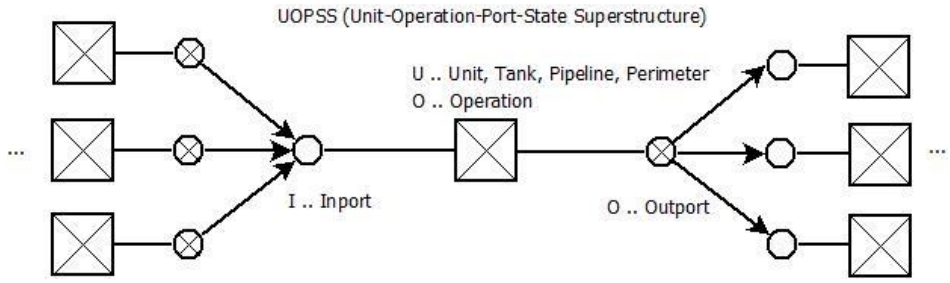

Figure 9.1. UOPSS scheme.

In the motivating examples (expansion and installation of a unit) and in the oil-refinery case for investments in CDU and VDU considering both expansion and installation, the investment costs consider fixed and varying terms, in which capital and capacity are treated using holdups, flows, tanks, etc. However, in the example taken from Jackson & Grossmann (2002) with 3 feeds (A,B,C) and 2 product materials (D,E) with 3 processes (Figure 7.7), expanded (capacity increase) or extended (conversion increase) or both projects can be performed with fixed capacity/capability and costs. In a total of three time periods, 36 binary variables are necessary to formulate the problem in both big-M and convex-hull approaches, although 154 binary variables are necessary in our proposed approach, which was solved with CPLEX in less than 0.25-seconds to provably optimal.

9.6. Phenomenological Decomposition Heuristic for Process Design Synthesis of Oil-Refinery Units

The full space MINLP or quantity-logic-quality (QLQ) models are still challenging for industrial-sized problems, because considering all three types of QLQ variables and constraints simultaneously results in both a discrete and nonlinear formulation due to the binary and integer nature of the logic variables and the multilinear terms of quantity times quality. Fortunately, first solving the problem for *logistics* and then for *quality* is actually somewhat intuitive and natural given that if the quantity and logic details are not feasible (or consistent) then the quantity and quality details will also not be feasible, and even immaterial. Hence, this provides some level of intelligent problem solving structure by allowing for a staged or progressive workflow when making production or manufacturing decisions.

The alternative but heuristic approach proposed in chapter 8 is to successively solve the logistics (quantity and logic) MILP sub problem first, fix the logic variables at their solution values and then solve the quality (quantity and quality) NLP sub problem second. After this solution is found, the quality variables can be fixed and/or updated yields (recipes, ratios, recoveries, etc.) can be computed and the logistics problem resolved. This procedure can be repeated until acceptable convergence is achieved or it is locally or globally infeasible.

The proposed two-stage stochastic programming framework, which is appropriate for the integration of the NLP operational and MILP strategic decision-making, reduces uncertainties related to the process with recourse in crude-oil diet and yields, which are updated in the strategic decision after their determination in the NLP operational sub problems for each demand scenario. The phenomenological decomposition method can be applied to any quantity-logic-quality MINLP model to segregate it in two solutions. As we propose, the nonlinearities from the processing and blending equations are solved separately from the logic equations, so that the quantity-quality nonlinearity or phenomena is decomposed to solve the quantity and logic optimization and then the quantity and quality problem.

The oil-refinery example considers REVAP's existing units in order to determine expansion and installation of units as seen in Table 8.4. Although the gap between the MILP and the average value of the NLP sub problems (considering the scenarios) is within 5% since the 1st iteration, the problem converged after 4 iterations when the results (objective function, new capacities, etc.) stop to change. The CDU investment after the 1st iteration

moved from expansion to installation and the new capacities for CDU and VDU converged in the 4th iteration.

9.7. Contributions of the Thesis

The main contributions of the thesis are summarized as follows:

1. An NLP formulation for operational planning of oil-refinery processes. The formulation is proposed in chapter 3 and has been applied to calculate fuel production in Brazil's oil-refining industry considering the national existing refineries in 2013 aggregated in the hypothetical large refinery REBRA, where the future refineries were added to determine the required overall unit throughputs in 2020 to match different market scenarios.

2. An MINLP formulation for strategic planning of oil-refinery processes integrating the operational and strategic layers in a full space model. A discrete formulation defines the types of units to invest and the overall size of the new capacities for the Brazil's oil-refining industry considering nonlinearities from processing and blending constraints.

3. An improved swing-cut model by taking into account that the light and heavy swing-cut fractions have different qualities. The novel approach uses micro-cuts, hypotheticals, or pseudocomponents to infer the quality distribution along the whole swing-cut. The additional correlations to predict the light and heavy swing-cut properties consider swing-cut bulk properties, light and heavy swing-cut amounts, and properties in the hypothetical interfaces between the swing-cut and its lighter (upper) and heavier (lower) adjacent cut streams

4. A novel technique to optimize distillate stream cutpoints (initial and final boiling points) integrated with fuel recipes optimization. Experimental data of evaporation curves is interpolated in monotonic interpolation and a new adjustment or shifting modeling is addressed to modify the distillation curves considering distillates' initial and final boiling point temperature changes.

5. A generalized capital investment planning introduces a novel modeling for optimization of project setups and phases using sequence-dependent logic, where capital and capacity are treated as flows in a scheduling environment.

6. A tailored decomposition scheme to solve the process design or logistics problem in a stochastic MILP approach considering probabilities over demand scenarios (first stage) from where the defined process design is validated in NLP sub problems for each scenario (second

stage), with recourse in crude-oil diet and unit yields which are updated in the MILP problem every each MILP-NLP iteration.

9.8. Recommendations for Future Work

9.8.1. Modeling of operational decision-making

1. In chapter 3, we used a complete oil-refinery network to determine production amounts considering modeling in processing and blending. Development of processing models to predict product quantity and quality variations for types of units unaddressed in this work such as delayed coker, reformer, and hydrocracker units would be interesting to increase the accuracy of the production. Evaluation around the computational efforts over processing and blending models, each one added step-by-step in a problem, may guide one to define the best set of models to include considering their solution burdens.

2. In chapter 5, improving the distillate predictions, the conventional swing-cut method is reformulated to include quality variation in the light and heavy swing-cut fractions using pseudocomponents or micro-cuts distribution of the crude. The approach mixes the micro-cuts of each crude oil to form cuts and swing-cuts inside the towers considering known their temperature cut ranges. Then, these internals are blended to yield final cuts or distillates. Other approach that firstly mixes the micro-cuts from the crude pool, creating large blended micro-cuts and then cutting them to form the internal cuts and swing-cuts, can also be explored. The internals (cuts and swing-cuts) modeling can be avoided by creating micro-swing-cuts that mix with their adjacent micro-cuts to form the final cuts directly. These micro-cuts, pseudocomponents or hypos (hypothetical species) can also be used either in interpolation or in regressed data models using cumulative distributive functions (CDF), which demands temperature cutpoint determination instead of swing-cut amounts to approximate the distillate variation. All mentioned models are depicted in Figure 9.2.

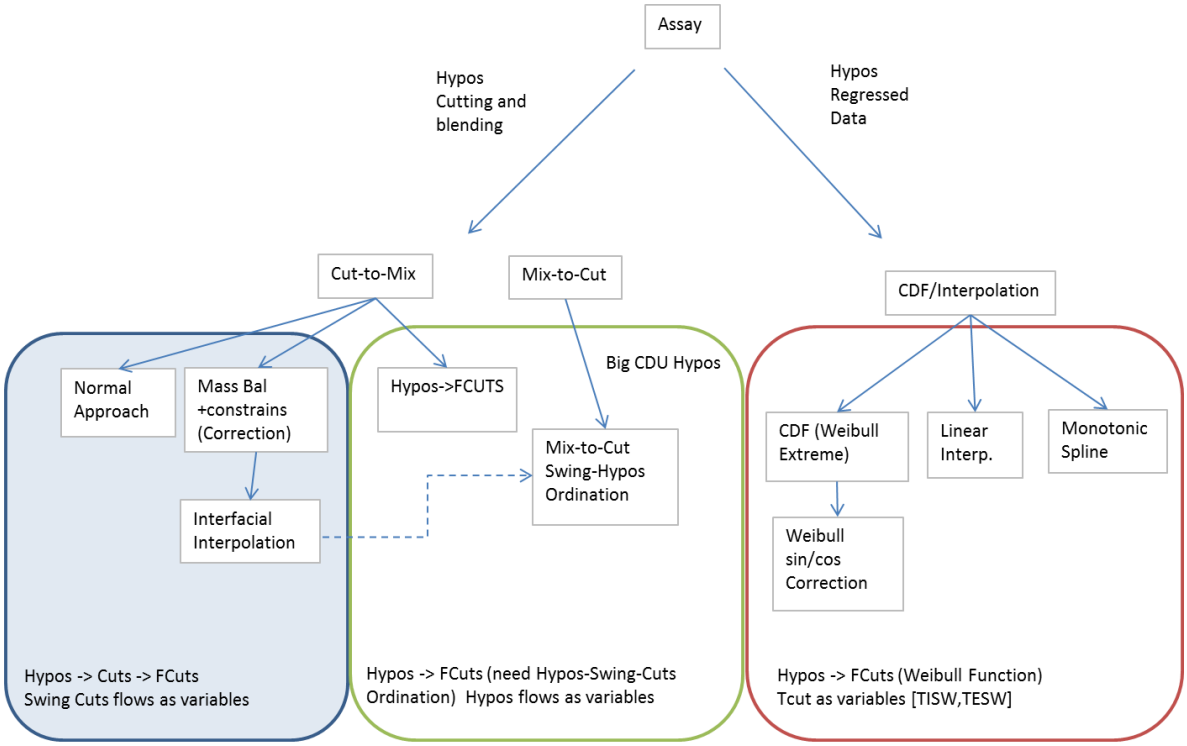

Figure 9.2. Micro-cuts, hypos (hypothetical species), or pseudocomponents modeling in distillation problems.

3. In chapter 6, distillation temperature cutpoints and blending recipes are optimized together by converting experimental distillation curves from ASTM to TBP and then in monotonic interpolation to be used in a novel adjustment and shifting modeling considering initial and final boiling points (IBP and FBP) temperatures of the distillates. Three regions are modeled in the evaporation curves (front end: 1% to 10%; middle: 10% to 90%; and back end: 90% to 99%), although it can be detailed in more regions to better assess the nonlinearities of the curves (see Figure 6.4). Also, the modeling can be extended to FCC and DC main fractionators and as well as to hydrotreaters.

4. In chapter 6, the properties of the streams leaving the upstream units cannot be adjusted for one stream independently of the other streams. Large portion of these streams are produced by multi-product distillation towers (e.g. atmospheric distillation or FCC main fractionator), so changing properties of one stream results in changes of the properties of the remaining streams which are produced by the same tower. So, integration of two adjacent distillate streams would be interesting to model.

5. In chapter 6, the cutpoint optimization is simply based on properties that would be the most advantageous from the blending viewpoint. Such optimization is always a trade-off between

energy consumed to accomplish given separation and the incremental benefits accomplished by changing the stream properties, which is not included in the proposed optimization model. Even if one argues that the incremental energy costs are always lower than the benefits from producing incremental amounts of better quality blending streams, one ends up with an "overshoot" since the cost of incremental energy is treated as zero. So, a robust solution would be the integration of energy balances in the problem.

6. The operational planning formulation used throughout the thesis is considered as a pre-scheduling problem due to its material balance calculation in cubic meter per day, but it is modeled in LP or NLP approaches without including scheduling operations. Discrete optimization over these operations can be included to account selection of tasks and their transitions in tanks, blenders or pipelines. This scheduling operation addition may not influence in the strategic evaluation or gains, but at least validates the production feasibility.

7. Extending the production by including logistics movements inside and outside the refinery boundaries can improve the overall modeling by integrating crude distribution, crude processing, and fuels distribution, which are the productive related branches in between the commercial segments (crude purchasing and fuel sales).

9.8.2. Modeling of strategic decision-making

1. The strategic and operational decision-making addressed in chapter 8 (PDH) can be extended to the case with all 12 existing refineries in Brazil in order to compare with the planned capacity for the new sites, considering the refineries under construction and in conceptual phase. In these large examples would be necessary other types of decomposition such as in time and space.

2. The strategic decision-making can be extended to the entire supply chain as in the operational problem. Decisions on which units, tanks, pipelines, blenders, etc. to expand or newly build can be included to consider the restructuring for a set of sites (refineries, terminals, etc.).

3. The strategic decision-making can be extended to determine new sites such as refineries and terminals by adding the possible units, tanks, and pipelines in the superstructure. Regional differences in terms of taxes, environmental constraints, and logistics costs, considering crude and fuel distribution, may be valuable information to include before a new site determination.

4. The power-law formula for equipment cost versus size can be linearized in three regions (initial, middle, and final) (see Appendix B), where the middle region is considered in the calculations. Considering the investment coefficients (alpha and beta) differences related to the size of the new capacity, these numbers can be updated every each MILP-NLP iteration after the capacity determination within the MILP problem.

5. For simplification, in the strategic planning models in chapters 4 and 8, an investment time interval of several years is considered for the calculation without taking into account the annual projects approving as commonly performed within the oil-refining companies. A reformulation considering annual project approving may be explored, although the increase in the number of binary variables will elevate the computational burden.

6. Considering that some companies have oil-refineries around the world such as Exxon, Shell and Total, an oil-refining investment world map might guide the companies to choose the best countries for investing in oil refinement. It can be done using the GCIP (chapter 7) and PDH (chapter 8) models, and considering investment cost profile per region, national information on oil production, refining capacity, oil product demands, transportation costs, etc. An example to reproduce would be the KNPC (Kuwait oil company) refineries, where process details of their 3 refineries can be found in their website.

7. Another kind of uncertainty such as in project startup schedule, crude oil production, and investment resources can be addressed. The risk measurement as applied in the financial strategy studies in PETROBRAS today would allow the introduction of risk measure concepts like Value at Risk (VaR) or Conditional Value at Risk (CVaR) to the strategic problem.

8. An optimization strategy for integration of strategic, tactical, and operational decision-making levels in vertical (multi-level) and horizontal (multi-entity) realms (Figure 9.3) would be explored to address an industrial solution covering these areas that is still missing the world.

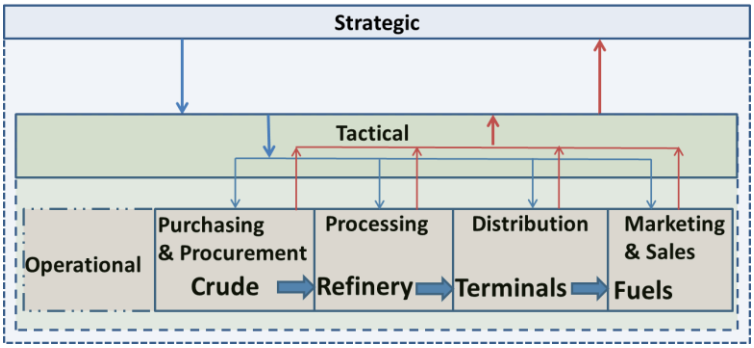

Figure 9.3. Strategic, tactical and, operational decision-making levels.

Appendix A: Investment Strategies for the Future Fuel Market in Brazil

Oil industry investments in Brazil are growing at an unprecedented pace. New oil reserves, significant increases in fuel demands, and new and more stringent fuel specifications have accounted for US$ 300 billion in investments over the past 10 years. The progress of the oil and fuel production as result of these investments is analyzed considering the current and proposed alternatives to match both quantity and quality demands for the future fuel market in Brazil. Today, two grassroots refineries under construction and more three additional sites in conceptual phase are planned to prevent deficit in crude-oil derivatives of around 30% in 2020, as recent estimate in the country. However, the future perspectives about the national oil refining capacity expansion deal with uncertainties around government policies, oil production, gasoline-ethanol costumer preference, and fuel demands, which are leading to investment reanalysis. Additionally, the economic logic may postpone investments in downstream to raise capital to higher project returns in upstream, and may the persistent economic world crisis started in 2008 and the unconventional Brazilian fuel policies change business expectations. As will be seen, half of the capital planned in downstream in the next cycle of investments, US$ 20.6 billion, is being reevaluated in several segments.

A1.Introduction

The economic growth in Brazil over the past 10 years, has led the country to critical levels in terms of fuel demands. Analyzing this situation in progress, Tavares et al. (2005) proposed market scenario simulation considering oil refining assets or facilities expansion criteria in the country, which indicate that the investments required for the Brazilian oil refining sector are over and above those allocated. In their work, the national oil refining expansion strategies consider (1) energy security by reducing imports and vulnerability of key products (e.g., gasoline, jet fuel, and diesel), (2) profit maximization by boosting the output of higher value oil products (e.g., jet fuel, and diesel), (3) national oil processing priority by reducing exports of heavy acid oil (e.g., metallurgic protection in crude distillation units, and new delayed coker units), and (4) petrochemical integration (e.g., integrated refinery and petrochemical complex projects). They concluded that the decision to invest in the oil refining sector in Brazil depends on local infrastructure conditions, environmental constraints, fuel specifications, companies' strategies, steady growth in fuel demands and the definition of government policies that eases institutional risks.

Facilities planning alternatives for the Brazilian oil refining industry is shown in chapters 3 and 4, where are proposed simulation- and optimization-based methodologies to expand the overall oil-refinery capacity in the country. In these modeling, the national refineries are aggregated in one hypothetical large refinery to evaluate the overall capacity expansion per type of process unit using mathematical programming approaches. Both methodologies indicate alterations in the country's oil-refining investment plans and outline new required capacity expansion for 12 different types of process unit.

This work analyzes the development of the oil refining industry in Brazil from its historical evolution as well as the future perspectives for investments in this sector in the country. In section 2, the past and future of the Brazil's oil industry investments are interconnected to the oil production and processing growth in terms of both quantity and quality. In section 3, the capital amounts being reevaluated by downstream segments as a consequence of the new national oil industry scenario, and the deleterious gasoline and diesel controlled pricing policy are shown. In section 4, the economic and political scenarios currently faced by the nation and by the national oil and energy company PETROBRAS are highlighted. In addition, the needs to develop high performance strategic investment decision-making models to handle with uncertainties, nonlinearities from oil-refining processes, and the unusual fuel market in terms of pricing and flex-fuel fleet market in Brazil are remarked. Final comments and policy implications are presented in section 5.

A2. Brazilian Oil Industry: Past, Present and Future

A2.1. Oil industry investments in Brazil

Founded in 1953, Brazil's national oil company, PETROBRAS, monopolized the oil industry (with the exception of fuels retailing), until the "market flexibilization" in 1997, when the country became open to non-governmental activities in the sector. As a consequence of the lack of oil resources and small-sized fuel market, national oil investments (mainly in downstream) stood below US$ 2 billion per year until 1977, when the investments in upstream arose as a result of the Second Oil Crisis in the aftermath of the War between Iran and Iraq. After this period, the expense with oil imports increased more than ten times and reached US$ 10 billion in 1981. To overcome this unbalanced situation, investments in upstream activities were expanded and concentrated in the Campos Basin exploration, discovered in 1977, thereby switching the investments priority from the downstream to the upstream sector - a trend that endures to this day. The national oil production expanded from

167 kbpd in 1979 to 630 kbpd in 1990, and the expense with oil imports decreased to US$ 3 billion per year in 1990 (PETROBRAS, 2013a). Additionally, governmental programs to substitute gasoline with ethanol appeared as an option to reduce the external oil dependence since that time, ethanol has become an important compound in the country's fuel scenario.

After the market flexibilization, the increase of nonpublic investments, both national and foreign, to compete in any oil activity promoted a surge in investments in the oil sector. Over the past 10 years, PETROBRAS itself expanded its investments from US$ 5 to almost US$ 45 billion per year, as shown in Figure A1, which, to the best of our knowledge, can be considered a growth in capital for investments never-before-seen in any company worldwide. In this period (2002-2012), investments ensured significant deep water fields exploration and expanded the oil-refining assets in order to accomplish the first cycle of investments after the flexibilization of the market. Investments in downstream accounted for more than 35% of the entire amount by the end of the period, which is a significant departure from the historical trend, with upstream representing more than 60%. The second cycle (2013-2020) focuses both on the downstream required projects, which includes the startup of new refineries, and, primarily, on expanding the exploration of new fields recently discovered in the so-called presalt reserves. Within the next five years (2014-2018), PETROBRAS plans to invest US$ 220.6 billion, an average of US$ 44.12 billion per year with 70% in upstream and 18% in downstream (PETROBRAS, 2014a).

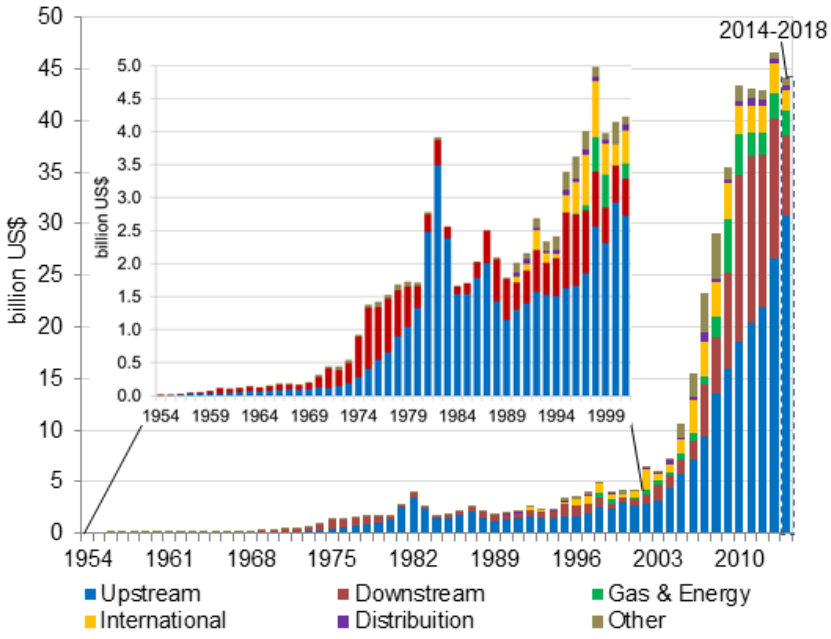

Figure A1. Historical and future investments in PETROBRAS (PETROBRAS, 2014a,2014b).

Despite the current and probably even with the future fuel deficit in the country, the upstream sector emerges as a definite priority in the investment portfolio due to the lack of enough capital to be invested in all necessary projects throughout all sectors and also due to the fact that the upstream margins are considerably higher than the downstream ones.

The oil-refining assets or facilities expansion performed in the first cycle and those in executions or in the conceptual phases in the second cycle aim to supply the growing fuel demands and to increase the processing of domestic oil, both of which contribute to a reduction in imports. Additionally, new specifications for gasoline and diesel, mainly related to the reduction of their sulfur concentration, demand an extension of the investment expenses without adding any quantity of fuels, since this only guarantees their new qualities specifications. In the existing refineries, investment projects revamped and installed several units. Around thirty-two new units were installed such as delayed cokers to convert fuel oil into higher value products, hydrotreaters to reduce sulfur concentration in gasoline and diesel, and reforming units to guarantee the gasoline octane number specification (PETROBRAS, 2009). For the next few years, the fuels market scenario in Brazil demands new projects to prevent a deficit in crude-oil derivatives (fuels and lubricants) of around 30% in 2020 as shown is Figure 3.1. The downstream investments portfolio includes new refineries adding 1,595 kbpd to the 2,103 kbpd attained in 2013 by the existing ones, considering crude distillation capacity.

A2.2. National oil production and processing evolution

The historical evolution of the national oil production can be segmented into four phases: onshore, flat water, deep water and Pre-Salt. Oil production began on onshore fields in the Brazilian northeast region known as Reconcavo Baiano and the production was modest until the deep water Campos Basin discovery even with the flat water fields along the east coast. Only after the Albacora production startup in 1990 and later with other huge fields such as Roncador, Barracuda and especially Marlim, all of them in deep waters, did oil production grow significantly from 1994 until its stabilization in 2.1 million bpd in 2010 as seen in Figure A2. The last phase brought huge expectations when in 2006 the discovery of an enormous offshore oil basin, known as presalt, was reported. This basin lies over deeper than the deep water fields, that is, around 6-8 km below the ocean floor, and already accounted for 14% of all national oil production in 2012 (PETROBRAS, 2013c).

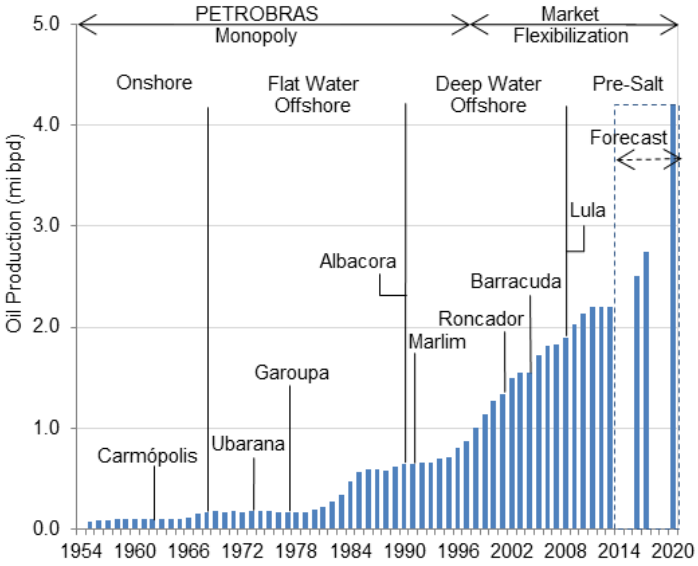

Figure A2. National oil production (ANP, 2013; PETROBRAS, 2013c (forecast)).

In terms of oil quality, the deep water fields in Campos Basin present a significant naphthenic acidity and low ºAPI (around 22), which represents a challenge to be processed by the national refineries. Metallurgic modifications in distillation units and foreign light oil blending allowed the processing of part of these acid and heavy national oils, creating opportunity to export oil even with the national oil deficit until 2008, when the oil produced and processed in the country became equivalent in terms of quantity. Between 1990 and 2012, the national oil processing more than doubled, totalizing 1.6 million bpd in 2012, which represents around 80% of the total processed oil. During this period, the stabilization of the total processed oil ºAPI was strongly dependent on light-oil imports. Investments in upstream increased the national oil production and, consequently, led to a decrease in oil imports and national and total processed oil ºAPI reduction. This situation created the necessity to import even lighter oil, with ºAPI between 45 and 35, to diminish in short and medium terms the deviation between the national oil quality and the national refineries' complexity. Figure A3 shows the national oil production and the national, imported and total processed oil in Brazilian refineries.

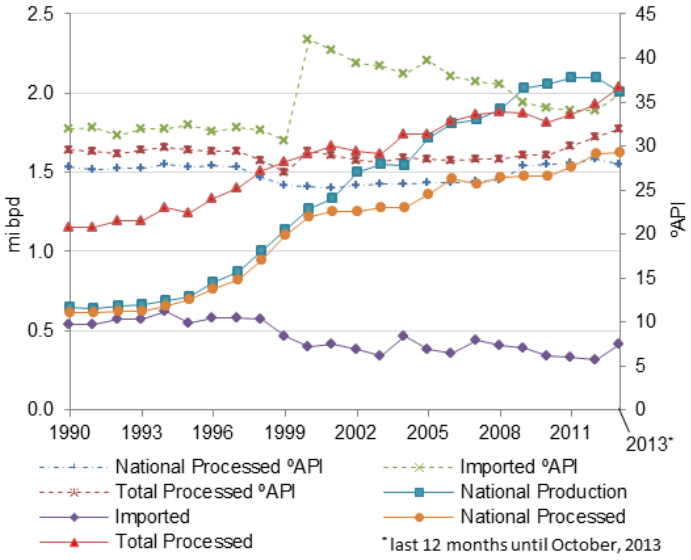

Figure A3. National oil production and national, imported and total oil processed and their ºAPI (ANP, 2013).

The first cycle of investments in the downstream sector after the flexibilization of the market projected the refining assets modifications considering the ºAPI decrease scenario, based on Campos Basin crudes production. But after the light-oil discovery in the oceanic sub-salt layer along the Brazilian southeast coast, the national oil ºAPI projection increased. The Pre-Salt fields gave way to a new scenario in Brazil, not only due to the expected rise in oil production, but also because the new fields are compounded by crude-oils lighter than the oils in the Campus Basin (around 32 ºAPI) creating the opportunity to reduce or even cease oil imports altogether in the future.

A2.3. Fuel quantity and quality improvements

As a consequence of historical and recent situation, the needs for higher quantity and better quality of fuel drove huge investments in the downstream sector in the past 10 years in Brazil. Considering the main fuels, the historical deficit in LPG (Liquid Petroleum Gas) and diesel (DSL) have structural reasons. LPG imports are the result of low natural gas reserves and a deficient pipeline infrastructure, made worse by the existence of distant countryside regions in a continental country like Brazil. The diesel deficit has its origins in past political decisions, whereby road transportation was given priority throughout the country. Today, this deficit prevents the market from producing small and medium cars fueled by diesel.

Jet fuel (JET) and gasoline imports increase started as a conjectural situation that seems to have led to a structural problem. Growing domestic and international tourism increased the demands for jet fuel, which are expected to reach critical levels or even

bottleneck flight expansion. For retailed gasoline (GLNC), after the 2009-2010 summer driven-season in the country, demand overcame the production and increased from 25 to 40 10^6 m^3 per year during the 2009-2012 period (11.8% p.a.) because of two reasons. First, a decade of programs against poverty and mainly after the 2008-2009 global economic crises, with the increase of political practices to inject money in the country, the Brazil's economy grew and the middle class went from representing 30% to 50% of the Brazilian population, creating a surge in fuel demands. Secondly, the GLNC demand increase within 2009-2012 was influenced by the ethanol for fueling (ETH) to GLNC shift drove by flex-fleet costumer preference because of the ethanol price surge due to national sugar cane harvesting problems in 2009 and to sugar demand escalation overseas, both molding the current fueling ethanol-gasoline preference. Additionally, as the refined gasoline (GLNA) is mixed with ethanol at a percentage ranging from 25 to 18% to produce the retailed gasoline (GLNC), the higher demands of gasoline for fueling since 2009 push the ethanol demands to continue high and then the prices of ethanol for fueling, which price relation ETH/GLNC cannot return to 0.7 or less to revert the customer preference.

Figure A4 shows fuel demands and production in Brazil since 2000, including the fuels percentage increase in the 2009-2012 period. $GLNC_{ETH}$ represents retailed gasoline increase without considering the flex-fuel fleet shift, if the ethanol for fueling decrease is discounted from the GLNC demand increase. This consideration yields an increase of 7.2% p.a. for $GLNC_{ETH}$. A full discussion about the Brazilian future fuel market scenarios and the flex-fuel fleet costumers' preference between GLNC and ETH can be found in chapter 3.

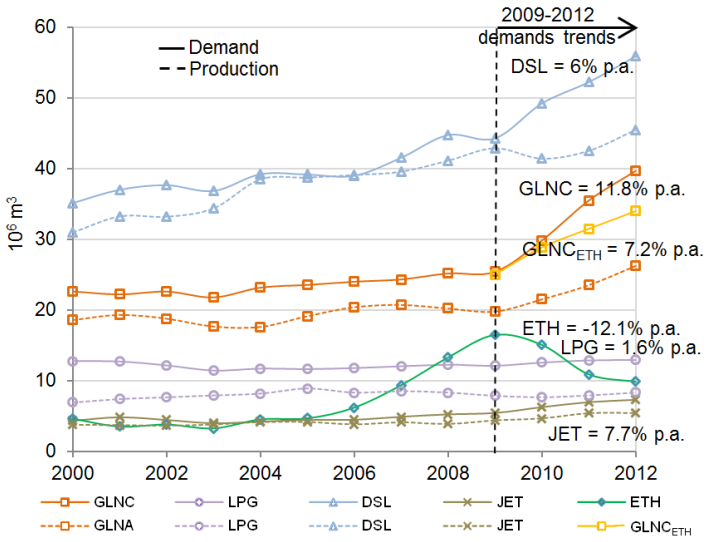

Figure A4. Fuel demands and production in the country (ANP, 2013).

In terms of fuel quality, in 1986 the Brazilian Environmental Agency established a national program to control air pollution from automobiles. This government program focuses on gradually reducing automobiles emission with exhaust gases mitigation in new fleets, more efficient motor combustion and fuel quality improvements to decrease sulfur and nitrogen contaminants, which form, respectively, SOx and NOx. Because of the lower sulfur concentration particulates reduction is also achieved. The national program for diesel is shifting the S1800 (1800 ppm of sulfur in weight) market to S500 and S10 (10 and 500 wppm, respectively), as shown in Figure A5. The lower sulfur grades of diesel S10 and S500 will represent 80.37% of the market. After 2014, the S1800 diesel will be fueling only engines used in so-called off-road transport, like tractor and train fleets. Additionally, the gasoline specification after 2014 will be changed from 1000 to 50 wppm in sulfur, which demands the installation of new hydrotreaters for distilled, coker and cracked naphtha.

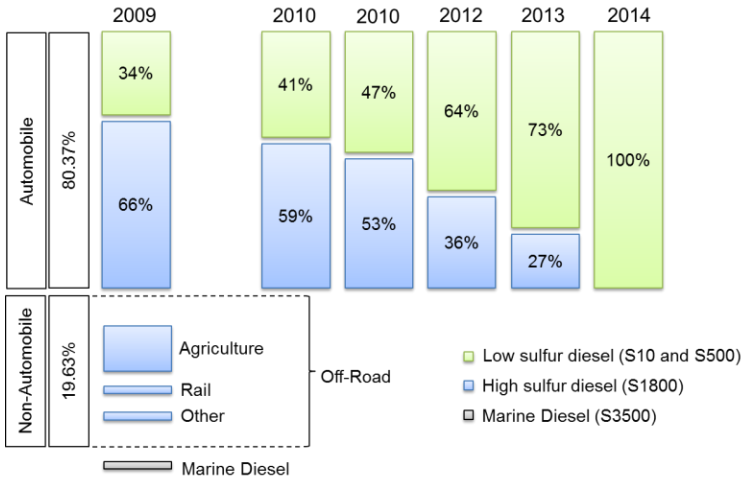

Figure A5. Diesel grades evolution (MPF, 2013).

In addition to altering the refining process to produce ultra-low sulfur diesel (S10), there will be investments in logistics for the new diesel grades. The pipelines and tanks handling S10 should be dedicated exclusively to this service in order to prevent sulfur contamination from other grades. Other specifications are also changing like specific gravity and distillation temperature, both to reduce heavy fractions on ultra-low sulfur diesel. Other diesel variant, the S50 (50 wppm S), was discontinued to avoid investments in two logistics assets for diesel variants so close (S10 and S50). The S50 initial existence came from the necessity to produce low sulfur diesel compatible with the refining assets in 2009. It was obtained with operational adjustments and improvements in hydrotreaters efficiency using

catalyst bed with higher activities, lower spatial velocity and feed management. Only with the new hydrotreating units the refineries will be able to produce S10 demanded by the country, because of their higher severity in dealing with higher pressure and temperature, which demanded higher investments to build hydrotreaters with large thickness and metallurgy and reactors more specialized.

The future refining scenario needs to complete the investments to increase fuels supply and to satisfy the gasoline and diesel new specifications mainly related to the sulfur reduction. Other tendencies like to reduce the nitrogen content in jet fuel and to increase the octane number in gasoline may demand more investments in the sector. Changes in premises in the second cycle (started in 2013) consider the future national oil to be produced lighter than in the first cycle because of the presalt reserves. Also, the market stabilization considering the gasoline-ethanol costumer dynamics and the boosting demands throughout the fuels are leading to projects reanalyzes.

A3. National Strategies and Pricing Policy for Fuels

A3.1. Downstream investments reevaluation

The refineries currently under construction, RNEST and COMPERJ-1, were projected to privilege diesel production. Exogenously, its higher price in comparison with jet fuel and gasoline, and endogenously, the road-based transport predominance in the country, accounted for the diesel preference when it came to investment decisions. However, considering the boost in other fuel demands due to the Brazilian economic growth and the ethanol for fueling to retail gasoline market shift, doubts have been raised concerning the application of the same emphasis on diesel production in the projects in conceptual phase (Premium I, Premium II and COMPERJ-2). Additionally, the presalt production may change the refining design outline, replacing the African ultra-light and Middle East paraffinic crudes, currently used to provide higher yields in medium distillates and lubricants, respectively. Figure A6 shows the foreseen investments for the period 2013-2017 in PETROBRAS' downstream sector. As shown, about 50% of total capital planned for the projects is being reevaluated.

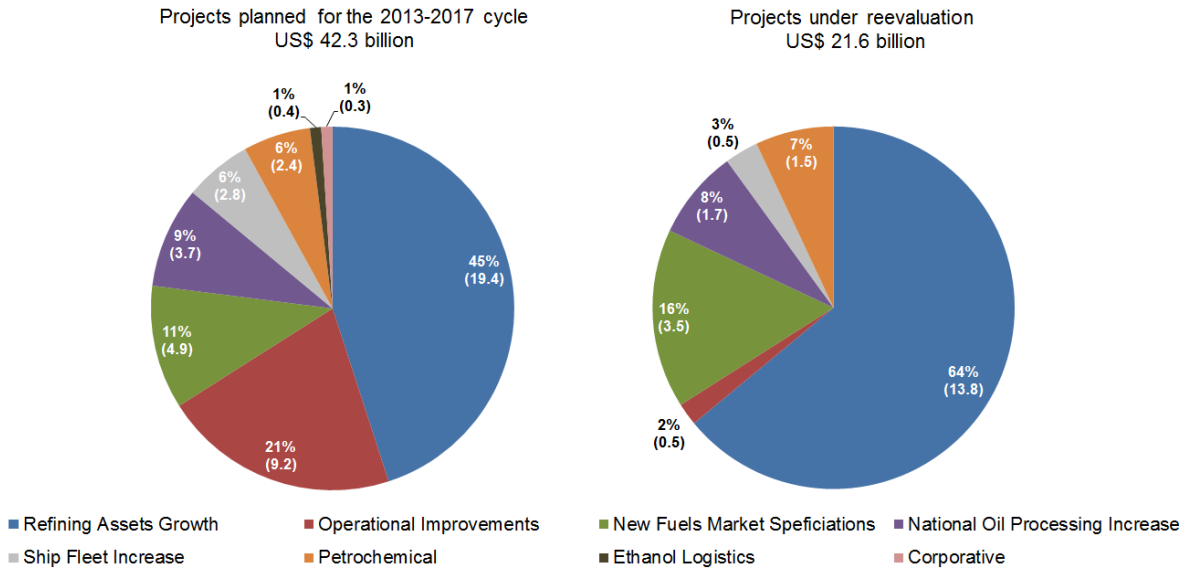

Figure A6. Downstream investment portfolio reevaluation in Brazil (PETROBRAS, 2013a).

The refining assets growth amount under reevaluation represents a large and complex refinery in Brazil. The operational improvements to increase the efficiency of obsolete equipment and operational debottlenecking in on-site and off-site assets proceed essentially as planned. The investments related to fuel market specifications are mandatory and possibly the projects in this segment related to the reduced asset expansion are being reevaluated. Other segments in reevaluation are associated with Brazilian peculiarities. The investments to increase the national crude processing percentage are related to the Brazilian crude's most difficult characteristic, its acidity. Possibly, the new perspective about the increase of national light oil from the presalt reserves is restraining investments in this topic. On the other hand, investments in the ship fleet and in ethanol logistics, priorities aiming at reducing foreign fleet contracts and supporting the gasoline-ethanol market expansion respectively, may have a residual reduction as well as the investments related to operational improvements, since the current logistics bottlenecks in Brazil threaten companies' profitability.

Finally, the petrochemical disinvestments are likely to be accomplished, since this is part of PETROBRAS' new strategy. Despite that, the high import levels of petrochemicals can be considered a national problem, and estimates of required investments in the 2011-2020 period reach figures of around US$ 87-167 billion for petrochemicals to face the current situation and the expected increase in demand, which came to 29% in 2009-2010 (Pinto, 2012). PETROBRAS' prior experience in petrochemicals was based on the purchase of assets and minority participations in petrochemical companies. The strategic decision to build

COMPERJ-2 as a petrochemical complex could not be sustained due to lack of capital to simultaneously invest in the necessary and more profitable downstream and upstream portfolios, respectively.

A3.2. Gasoline and Diesel Pricing Policies

The Brazilian state has been rolling an intensive interventionism policy for fuel pricing with the excuse that the weight of gasoline and diesel in the national inflation calculation is significant. Since the flexibilization of the market in 1997, state intervention in fuel pricing was being reduced directly, although the major control of the national oil and energy company PETROBRAS by the 50.2% ordinary state-owned stocks indirectly maintain the state interventionism. As a consequence of this, the refining activity in Brazil today is not being lucrative. This is a well-known situation due to the national gasoline and diesel producer lower price in comparison with import prices. Although the LPG and jet fuel imports in the country, they do not damage the company's profitability because in Brazil the controlled LPG price is similar to the international practices and the jet fuel prices are not controlled by the country. However, for gasoline and diesel the difference between the national producer prices and the imports is absorbed by PETROBRAS. The Brazilian Center of Infrastructure estimates losses of 2.2 billions of U.S. dollars from January to May, 2013 (14.379 million US$/d) considering the difference between the producer prices for gasoline and diesel in US Gulf Coast and Brazil (Globo, 2013). In chapter 3, the proposed calculation estimates losses of 16.702 million US$/d considering the pricing scenario of the past 12 months until October, 2013.

In Figure A7 the price percentage for gasoline and diesel in Brazil and US are compared in terms of distribution & marketing, taxes and producer amounts. In both countries, the percentage for distribution & marketing are similar, but the taxes in Brazil in comparison to US is almost a double for gasoline and more than double for diesel. In Brazil the taxes on these fuels are split between national and state taxes, representing, respectively, 7% and 28% of gasoline price and 6% and 14% of diesel price (PETROBRAS, 2014b). In Brazil the producer percentage for gasoline is compound by ethanol mixed at 25% with refined gasoline, and for diesel is compound by biodiesel mixed at 6% with refined diesel, so the total producer amount for gasoline is 48% and for diesel is 65% of their final price percentage. In the US, the producer percentage for gasoline and diesel is 76% and 77%, respectively (EIA, 2014). This unusual controlled prices situation inside the oil-refining

industry in Brazil threatens companies' sustainability. Today, the new pricing policy announced on November 29, 2013 increased the retail gasoline prices by 4% and diesel by 8%, but this move has not sufficient the overcome the current daily losses of 13.786 million US$/d by PETROBRAS as found in chapter 3. The authors consider price increase of 15% for retailed gasoline and 20% for diesel in its different grades to yield a positive gain of 1.068 million US$/d in the national refineries. This price increase is evaluated by the market as the demanded pricing policy to avoid losses and to get a minimal expected margin returns of around 0.5 US$/barrel in the country.

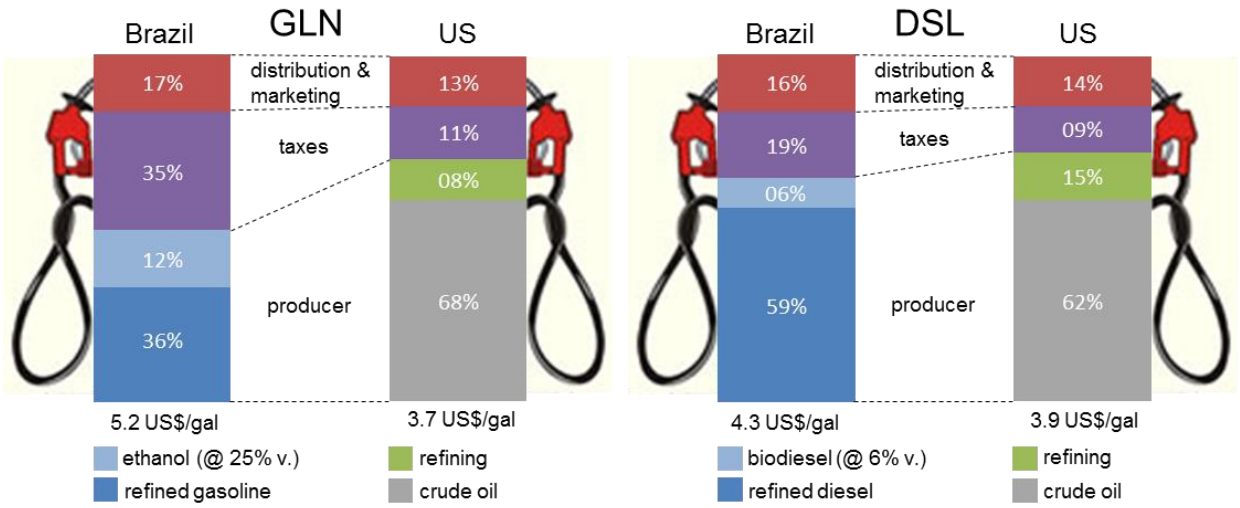

Figure A7. Gasoline (GLN) and diesel (DSL) price distribution in Brazil (PETROBRAS, 2014b) and US (US EIA, 2014).

As seen in Figure A7, the price of gasoline and diesel in Brazil in comparison with US is 40% higher for gasoline and 10% for diesel. Nevertheless, the octane number specification in Brazil is 82, versus the minimum of 87 found in US, and the ethanol content in retail gasoline is currently in 25% in Brazil, but at most 10% in US retail. In Figure A7, the price of gasoline with ethanol in US is not considered because it is not an obligation as in Brazil. The ethanol energy content is around 33% less than refined gasoline and only flex-fuel vehicles can be fueled by gasoline with ethanol content higher than 15% in US and higher than 25% in Brazil.

A5. Final remarks

The fast-growing demand for fuels – a result of the national economic growth in the last decade –, new fuels specifications and the presalt discovery drove even further the structural and technological developments in the oil refining industry. In this new context, more efficient strategic investment planning models capable of discerning the best

investments portfolio, are being developed in the country. It has transpired not only due to the monopoly being broken and the consequent investments surge, but also as a result of the need to adequately refit the existing refining and logistics structures to avoid unnecessary expenses, especially to maintain the company's competitiveness. Investments in production and logistics facilities considering the new fuel consumption rate and the unpredictable gasoline-ethanol demand shift driven by the flex-fuel consumers is necessary to provide the future fuel market needs and the required supply chain structure in the country. Additional challenges to produce different diesel grades in terms of sulfur concentration should be considered in the overall expenses as well as the needs to operate diesel and gasoline blenders.

The decision to invest in the refining segment in Brazil depends on the demanded capital diagram equilibrium in upstream and downstream sectors, which, concerns in a company like PETROBRAS, dealing with cash flow constraints and investments around 45 billion dollars per year, must be huge. Additionally to this, tanks and pipelines in terminals and refineries demands crucial investments to solve the logistics bottlenecks, creating an infrastructure lack that accounts today for a considerable incremental price in the country's final goods, especially in fuels. The estimation is that the logistics costs in Brazil reach around 18% of the final goods prices (CNI, 2012), more than a double when compared with the world average percentage in around 8%.

The unusual behavior of the national market, in which gasoline and diesel prices are controlled by the government, may drive back foreign investments, but initiatives to update the national fuels producer gains in consonance with international business are being structured at this moment in the country (PETROBRAS, 2013d). The today's fuel weight over the inflation control in Brazil threatens PETROBRAS sustainability. The recent negative results in PETROBRAS related with low profits and dangerous debt situation decrease the level of confidence in the company. The future perspectives about the expansion capacity for the refining assets in Brazil do not decrease the fuels imports in a short or medium-term, and doubts to this aspect are emerged for a long-term due to the future projects reanalyzes. The economic logic may lead the country to postpone the investments in downstream to invest in higher returns projects in upstream. At present, technical and economic efforts to develop projects related to the presalt reserves have become the country's number one priority. The current estimate is that it will cost around 1 trillion dollars to explore the whole presalt

reserves in the coming decades. To find the best set of investments conjugated with a good balance of imports and exports is the goal of any thoughtful investment plan.

Appendix B: Investment costs of oil-refinery units

The investment costs in process equipment is well known to have essentially two parts, a fixed and a variable cost where the fixed cost is applied to the binary or logic variable determining the existence of the expansion or installation (i.e., its setup or startup logic) and the variable cost is applied to its capacity. When known power-law relationships of capital cost versus capacity for oil-refinery units are available such as found in Gary and Handwerk (1994), Johnston (1996), and Kaiser and Gary (2007), simple linear regression can be applied to convert these to approximated fixed+variable coefficients (Liu et. al. 1996; Kelly 2004a) that can be easily used inside mixed-integer formulations such as that presented here. The power-law relation $capacity/capacity^o = (cost/cost^o)^{0.6}$ considers parameters for each type of unit for a known or standard capacity and cost (capacity^o and cost^o). When these nonlinear curves are linearized, the slope and linear coefficients α_u and β_u, respectively, are determined in which the linear coefficient β_u is the binary variable $y_{u,t}$ coefficient in millions of U.S. dollars and the slope α_u is the expansion or installation continuous variables ($QE_{u,t}$ and $QI_{u,t}$) coefficient in millions of U.S. dollars per 1000 m^3, as shown for delayed coker (DC) and fluid catalytic cracking (FCC) in Figure A8.

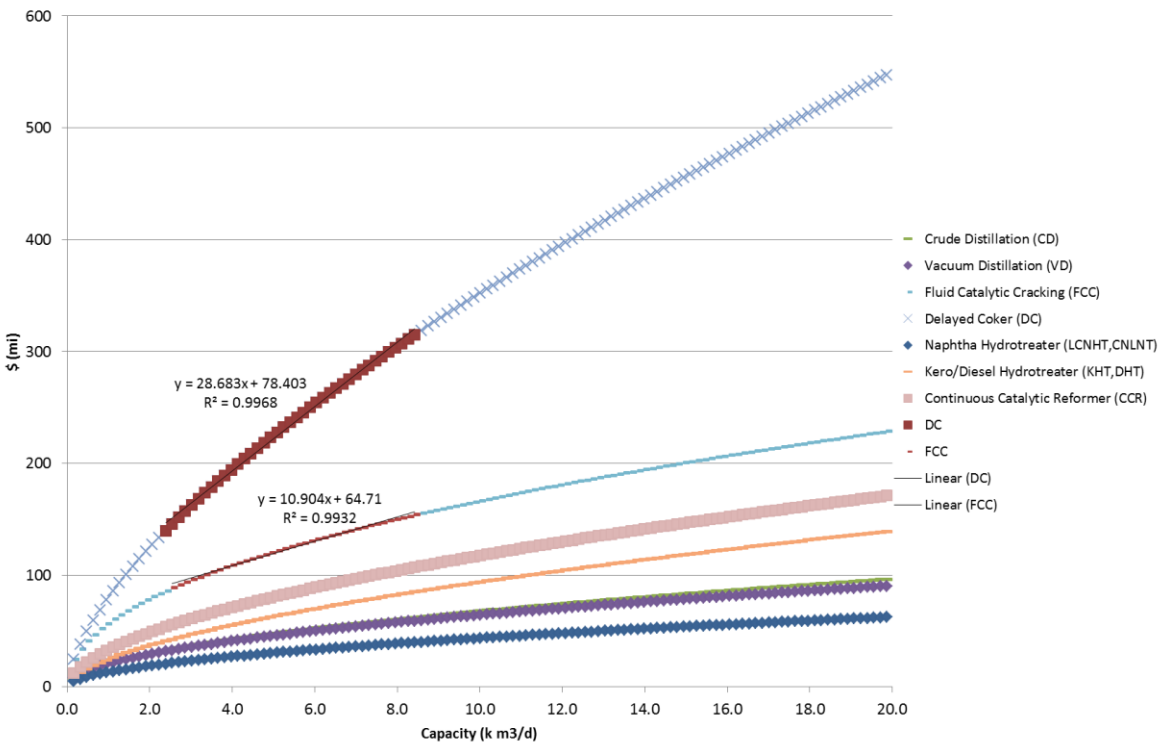

Figure A8. DC and FCC plots to find their fixed and variable investment costs.

Clearly, the unit investment costs have three distinct regions to be linearized. The initial between 0.8 and 2.4 m^3/d, the intermediate between 2.4 and 9 m^3/d (as represented for DC and FCC), and the final region for unit with capacity bigger than 9 m^3/d. As they need to be known a priori before the capacity size determination, these parameters or costs can be updated after each MILP-NLP iteration considering the capacity increment size found the last MILP problem performed.

Appendix C: IMPL's configuration and equations formed for the motivating example 1

```
 i M P l (c)

 Copyright and Property of i n d u s t r I A L g o r i t h m s LLC.

!!!!!!!!!!!!!!!!!!!!!!!!!!!!!!!!!!!!!!!!!!!!!!!!!!!!!!!!!!!!!!!!!!!!!!!!!!!!!!!!

! Calculation Data (Parameters)

!!!!!!!!!!!!!!!!!!!!!!!!!!!!!!!!!!!!!!!!!!!!!!!!!!!!!!!!!!!!!!!!!!!!!!!!!!!!!!!!

&sCalc,@sValue

START,-1.0

BEGIN,0.0

END,3.0

PERIOD,1.0

LARGE,10000.0

ALPHA,0.5

BETA,0.5

OLDCAPACITY,1.0

NEWCAPACITY,1.5

&sCalc,@sValue

!!!!!!!!!!!!!!!!!!!!!!!!!!!!!!!!!!!!!!!!!!!!!!!!!!!!!!!!!!!!!!!!!!!!!!!!!!!!!!!!

! Chronological Data (Periods)

!!!!!!!!!!!!!!!!!!!!!!!!!!!!!!!!!!!!!!!!!!!!!!!!!!!!!!!!!!!!!!!!!!!!!!!!!!!!!!!!

@rPastTHD,@rFutureTHD,@rTPD

START,END,PERIOD

@rPastTHD,@rFutureTHD,@rTPD

!!!!!!!!!!!!!!!!!!!!!!!!!!!!!!!!!!!!!!!!!!!!!!!!!!!!!!!!!!!!!!!!!!!!!!!!!!!!!!!!

! Construction Data (Pointers)

!!!!!!!!!!!!!!!!!!!!!!!!!!!!!!!!!!!!!!!!!!!!!!!!!!!!!!!!!!!!!!!!!!!!!!!!!!!!!!!!

&sUnit,&sOperation,@sType,@sSubtype,@sUse

A,,perimeter,,

B,,perimeter,,

Capacity,,pool,,

Capital,Cost,perimeter,,

Charge,,processc,,

Process,Commission,processc,,

Process,Existing,processc,,

Process,Expand,processc,,

&sUnit,&sOperation,@sType,@sSubtype,@sUse

&sUnit,&sOperation,&sPort,&sState,@sType,@sSubtype

A,,a,,out,

B,,b,,in,

Capacity,,i,,in,
```

```
Capacity,,o,,out,
Capital,Cost,cpl,,in,
Charge,,cpl,,out,
Charge,,cpt,,out,
Charge,,i,,in,
Process,Commission,a,,in,
Process,Commission,b,,out,
Process,Commission,cpt,,out,
Process,Existing,a,,in,
Process,Existing,b,,out,
Process,Expand,a,,in,
Process,Expand,b,,out,
Process,Expand,cpt,,in,
&sUnit,&sOperation,&sPort,&sState,@sType,@sSubtype
&sUnit,&sOperation,&sPort,&sState,&sUnit,&sOperation,&sPort,&sState
A,,a,,Process,Commission,a,
A,,a,,Process,Existing,a,
A,,a,,Process,Expand,a,
Capacity,,o,,Process,Expand,cpt,
Charge,,cpl,,Capital,Cost,cpl,
Charge,,cpt,,Capacity,,i,
Process,Commission,b,,B,,b,
Process,Commission,cpt,,Charge,,i,
Process,Existing,b,,B,,b,
Process,Expand,b,,B,,b,
&sUnit,&sOperation,&sPort,&sState,&sUnit,&sOperation,&sPort,&sState
!!!!!!!!!!!!!!!!!!!!!!!!!!!!!!!!!!!!!!!!!!!!!!!!!!!!!!!!!!!!!!!!!!!!!!!!!!!!!!!!
! Capacity Data (Prototypes)
!!!!!!!!!!!!!!!!!!!!!!!!!!!!!!!!!!!!!!!!!!!!!!!!!!!!!!!!!!!!!!!!!!!!!!!!!!!!!!!!
&sUnit,&sOperation,@rRate_Lower,@rRate_Upper
Process,Existing,0.0,OLDCAPACITY
Process,Commission,0.0,OLDCAPACITY
Process,Expand,0.0,LARGE
Charge,,0.0,NEWCAPACITY
&sUnit,&sOperation,@rRate_Lower,@rRate_Upper
&sUnit,&sOperation,@rHoldup_Lower,@rHoldup_Upper
Capacity,,0.0,NEWCAPACITY*END
&sUnit,&sOperation,@rHoldup_Lower,@rHoldup_Upper
&sUnit,&sOperation,&sPort,&sState,@rTotalRate_Lower,@rTotalRate_Upper
ALLINPORTS,0.0,LARGE
ALLOUTPORTS,0.0,LARGE
&sUnit,&sOperation,&sPort,&sState,@rTotalRate_Lower,@rTotalRate_Upper
```

```
&sUnit,&sOperation,&sPort,&sState,@rTeeRate_Lower,@rTeeRate_Upper

ALLINPORTS,0.0,LARGE

ALLOUTPORTS,0.0,LARGE

Process,Expand,cpt,,0.0,NEWCAPACITY

&sUnit,&sOperation,&sPort,&sState,@rTeeRate_Lower,@rTeeRate_Upper

&sUnit,&sOperation,&sPort,&sState,@rYield_Lower,@rYield_Upper,@rYield_Fixed

Process,Existing,a,,1.0,1.0,

Process,Existing,b,,1.0,1.0,

Process,Commission,a,,1.0,1.0,

Process,Commission,b,,1.0,1.0,

Process,Commission,cpt,,0.0,LARGE,

Process,Expand,a,,1.0,1.0,

Process,Expand,b,,1.0,1.0,

Charge,,i,,1.0,1.0

Charge,,cpl,,ALPHA,ALPHA,BETA-ALPHA*OLDCAPACITY

Charge,,cpt,,0.0,0.0

Process,Expand,cpt,,1.0,LARGE,

&sUnit,&sOperation,&sPort,&sState,@rYield_Lower,@rYield_Upper,@rYield_Fixed

!!!!!!!!!!!!!!!!!!!!!!!!!!!!!!!!!!!!!!!!!!!!!!!!!!!!!!!!!!!!!!!!!!!!!!!!!!!!!!!

! Constriction Data (Practices/Policies)

!!!!!!!!!!!!!!!!!!!!!!!!!!!!!!!!!!!!!!!!!!!!!!!!!!!!!!!!!!!!!!!!!!!!!!!!!!!!!!!

&sUnit,&sOperation,@rUpTiming_Lower,@rUpTiming_Upper

Process,Commission,1.0,1.0

Process,Expand,END,

&sUnit,&sOperation,@rUpTiming_Lower,@rUpTiming_Upper

!!!!!!!!!!!!!!!!!!!!!!!!!!!!!!!!!!!!!!!!!!!!!!!!!!!!!!!!!!!!!!!!!!!!!!!!!!!!!!!

! Consolidation Data (Partitioning)

!!!!!!!!!!!!!!!!!!!!!!!!!!!!!!!!!!!!!!!!!!!!!!!!!!!!!!!!!!!!!!!!!!!!!!!!!!!!!!!

&sUnit,&sOperation,&sOperationGroup

Process,Existing,ExistingGroup

Process,Expand,ExpandGroup

&sUnit,&sOperation,&sOperationGroup

!!!!!!!!!!!!!!!!!!!!!!!!!!!!!!!!!!!!!!!!!!!!!!!!!!!!!!!!!!!!!!!!!!!!!!!!!!!!!!!

! Compatibility Data (Phasing, Prohibiting, Purging, Postponing)

!!!!!!!!!!!!!!!!!!!!!!!!!!!!!!!!!!!!!!!!!!!!!!!!!!!!!!!!!!!!!!!!!!!!!!!!!!!!!!!

&sUnit,&sOperationGroup,&sOperationGroup,@sOperation

Process,ExistingGroup,ExpandGroup,Commission

&sUnit,&sOperationGroup,&sOperationGroup,@sOperation

!!!!!!!!!!!!!!!!!!!!!!!!!!!!!!!!!!!!!!!!!!!!!!!!!!!!!!!!!!!!!!!!!!!!!!!!!!!!!!!

! Cost Data (Pricing)

!!!!!!!!!!!!!!!!!!!!!!!!!!!!!!!!!!!!!!!!!!!!!!!!!!!!!!!!!!!!!!!!!!!!!!!!!!!!!!!

&sUnit,&sOperation,&sPort,&sState,@rFlowPro_Weight,@rFlowPer1_Weight,@rFlowPer2_Weight,@rFlowPen_Weight
```

```
A,,a,,0.0

B,,b,,1.0

Capital,Cost,cpl,,-1.0

&sUnit,&sOperation,&sPort,&sState,@rFlowPro_Weight,@rFlowPer1_Weight,@rFlowPer2_Weight,@rFlowPen_Weight

!!!!!!!!!!!!!!!!!!!!!!!!!!!!!!!!!!!!!!!!!!!!!!!!!!!!!!!!!!!!!!!!!!!!!!!!!!!!!!!!!!!

! Content Data (Past, Present Provisos)

!!!!!!!!!!!!!!!!!!!!!!!!!!!!!!!!!!!!!!!!!!!!!!!!!!!!!!!!!!!!!!!!!!!!!!!!!!!!!!!!!!!

&sUnit,&sOperation,@rHoldup_Value,@rStart_Time

Capacity,,0.0,0.0

&sUnit,&sOperation,@rHoldup_Value,@rStart_Time

&sUnit,&sOperation,@rSetup_Value,@rStart_Time

Process,Existing,1,START

&sUnit,&sOperation,@rSetup_Value,@rStart_Time

!!!!!!!!!!!!!!!!!!!!!!!!!!!!!!!!!!!!!!!!!!!!!!!!!!!!!!!!!!!!!!!!!!!!!!!!!!!!!!!!!!!

! Command Data (Future Provisos)

!!!!!!!!!!!!!!!!!!!!!!!!!!!!!!!!!!!!!!!!!!!!!!!!!!!!!!!!!!!!!!!!!!!!!!!!!!!!!!!!!!!

&sUnit,&sOperation,@rSetup_Lower,@rSetup_Upper,@rBegin_Time,@rEnd_Time

ALLPARTS,0,1,BEGIN,END

&sUnit,&sOperation,@rSetup_Lower,@rSetup_Upper,@rBegin_Time,@rEnd_Time

&sUnit,&sOperation,&sPort,&sState,&sUnit,&sOperation,&sPort,&sState,@rSetup_Lower,@rSetup_Upper,@rBegin_Time,@rEnd_Time

ALLPATHS,0,1,BEGIN,END

&sUnit,&sOperation,&sPort,&sState,&sUnit,&sOperation,&sPort,&sState,@rSetup_Lower,@rSetup_Upper,@rBegin_Time,@rEnd_Time

&sUnit,&sOperation,&sPort,&sState,@rYield_Lower,@rYield_Upper,@rYield_Target,@rBegin_Time,@rEnd_Time

Charge,,cpt,,1.0*(END-1.0),1.0*(END-1.0),,0.0,1.0

Charge,,cpt,,1.0*(END-2.0),1.0*(END-2.0),,1.0,2.0

Charge,,cpt,,1.0*(END-3.0),1.0*(END-3.0),,2.0,3.0

&sUnit,&sOperation,&sPort,&sState,@rYield_Lower,@rYield_Upper,@rYield_Target,@rBegin_Time,@rEnd_Time
```

Index Names:

```
1..U: units.

1..M: unit-operations.

1..I: unit-operation-port-states (in).

1..J: unit-operation-port-states (out).

1..SG: unit-operation sequence-groups.

1..NTPF: time-periods in both the past and future time-horizons.

1..NTF: time-periods in both the future time-horizon.
```

Variable Names:

```
v2r_ymsu(1..M,1..NTPF): unit-operation (M) setup variable.

v3r_yjisu(1..J,1..I,1..NTPF): unit-operation-port-state-unit-operation-port-state (JI) setup variable.

v2r_xmf(1..M,1..NTPF): unit-operation (M) flow variable.

v2r_xmh(1..M,1..NTPF): unit-operation (M) holdup variable.

v3r_xjif(1..J,1..I,1..NTPF): unit-operation-port-state-unit-operation-port-state (JI) flow variable.
```

v2r_zmsu(1..M,1..NTPF): unit-operation (M) startup variable.

v2r_zmsv(1..M,1..NTPF): unit-operation (M) switchover-to-itself variable.

v2r_zmsd(1..M,1..NTPF): unit-operation (M) shutdown variable.

v2r_zysgsu(1..SG,1..NTF): unit-operation sequence-group (SG) memory setup variable.

Constraint Names:

c2r_xmflower(1..M,1..NTF): unit-operation (M) flow lower semi-continuous constraint.

c2r_xmfupper(1..M,1..NTF): unit-operation (M) flow upper semi-continuous constraint.

c3r_xjifupper(1..J,1..I,1..NTF): unit-operation-port-state-unit-operation-port-state (JI) upper flow constraint.

c2r_xjyupper(1..J,1..NTF): unit-operation-port-state (J) upper yield constraint.

c2r_xuhbalance(1..U,1..NTF): unit (U) holdup balance constraint.

c2r_yumultiuseupper(1..U,1..NTF): unit (U) upper multi-use setup constraint.

c2r_yumultiusesos1(1..U,1..NTF): unit (U) multi-use setup special-order-set-one (SOS1).

c3r_yjistructuraltrans(1..J,1..I,1..NTF): unit-operation-port-state-unit-operation-port-state (JI) structural transition constraint.

c2r_zmsutemporaltrans(1..M,1..NTF): unit-operation (M) setup temporal transition constraint.

c2r_zmsdtemporaltrans(1..M,1..NTF): unit-operation (M) shutdown temporal transition constraint.

c2r_zmsvtemporaltrans(1..M,1..NTF): unit-operation (M) switchover-to-itself temporal transition constraint.

c2r_zmsvtemporaltranssos1(1..M,1..NTF): unit-operation (M) switch-over-to-itself temporal transition special-ordered-set-one (SOS1).

c2r_ymuptimelower(1..M,1..NTF): unit-operation (M) lower uptime constraint.

c2r_ymuptimeupper(1..M,1..NTF): unit-operation (M) upper uptime constraint.

c2r_ymuptime(1..M,1..NTF): unit-operation (M) uptime temporal aggregation cut constraint.

c2r_zyusingleuse(1..U,1..NTF): unit (U) memory setup single-use constraint.

c2r_zyusingleusesos1(1..U,1..NTF): unit (U) memory setup single-use special-ordered-set-one (sos1).

c2r_zysgsu1(1..SG,1..NTF): unit-operation sequence-group (SG) memory setup constraint one.

c2r_zysgsu2(1..SG,1..NTF): unit-operation sequence-group (SG) memory setup constraint two.

c3r_zsgswseqdeptemporal3(1..SG,1..SG,1..NTF): unit-operation sequence-group (SG) switchover-to-others sequence-dependent temporal constraint three.

c1_gprofitterm(1): profit term constraint.

c1_totalobjfun(1): total objective function constraint.

Constraints and Bounds:

c2r_xmflower(5,1) <= 1.000000000000000E-004 v2r_ymsu(5,1) -1 v2r_xmf(5,1)

c2r_xmflower(5,2) <= 1.000000000000000E-004 v2r_ymsu(5,2) -1 v2r_xmf(5,2)

c2r_xmflower(5,3) <= 1.000000000000000E-004 v2r_ymsu(5,3) -1 v2r_xmf(5,3)

c2r_xmfupper(7,1) <= 1 v2r_xmf(7,1) -1 v2r_ymsu(7,1)

c2r_xmfupper(7,2) <= 1 v2r_xmf(7,2) -1 v2r_ymsu(7,2)

c2r_xmfupper(7,3) <= 1 v2r_xmf(7,3) -1 v2r_ymsu(7,3)

c2r_xmfupper(6,1) <= 1 v2r_xmf(6,1) -1 v2r_ymsu(6,1)

c2r_xmfupper(6,2) <= 1 v2r_xmf(6,2) -1 v2r_ymsu(6,2)

c2r_xmfupper(6,3) <= 1 v2r_xmf(6,3) -1 v2r_ymsu(6,3)

c2r_xmfupper(8,1) <= 1 v2r_xmf(8,1) -10000 v2r_ymsu(8,1)

c2r_xmfupper(8,2) <= 1 v2r_xmf(8,2) -10000 v2r_ymsu(8,2)

c2r_xmfupper(8,3) <= 1 v2r_xmf(8,3) -10000 v2r_ymsu(8,3)

```
c2r_xmfupper(5,1) <=  1 v2r_xmf(5,1)   -1.50000000000000      v2r_ymsu(5,1)

c2r_xmfupper(5,2) <=  1 v2r_xmf(5,2)   -1.50000000000000      v2r_ymsu(5,2)

c2r_xmfupper(5,3) <=  1 v2r_xmf(5,3)   -1.50000000000000      v2r_ymsu(5,3)

c2r_xifupper(1,1) <=  1 v3r_xjif(5,1,1) 1 v3r_xjif(7,1,1) 1 v3r_xjif(8,1,1) -10000 v2r_ymsu(2,1)

c2r_xifupper(1,2) <=  1 v3r_xjif(5,1,2) 1 v3r_xjif(7,1,2) 1 v3r_xjif(8,1,2) -10000 v2r_ymsu(2,2)

c2r_xifupper(1,3) <=  1 v3r_xjif(5,1,3) 1 v3r_xjif(7,1,3) 1 v3r_xjif(8,1,3) -10000 v2r_ymsu(2,3)

c2r_xifupper(3,1) <=  1 v3r_xjif(3,3,1) -10000 v2r_ymsu(4,1)

c2r_xifupper(3,2) <=  1 v3r_xjif(3,3,2) -10000 v2r_ymsu(4,2)

c2r_xifupper(3,3) <=  1 v3r_xjif(3,3,3) -10000 v2r_ymsu(4,3)

c2r_xjfupper(1,1) <=  1 v3r_xjif(1,5,1) 1 v3r_xjif(1,6,1) 1 v3r_xjif(1,7,1) -10000 v2r_ymsu(1,1)

c2r_xjfupper(1,2) <=  1 v3r_xjif(1,5,2) 1 v3r_xjif(1,6,2) 1 v3r_xjif(1,7,2) -10000 v2r_ymsu(1,2)

c2r_xjfupper(1,3) <=  1 v3r_xjif(1,5,3) 1 v3r_xjif(1,6,3) 1 v3r_xjif(1,7,3) -10000 v2r_ymsu(1,3)

c3r_xjifupper(1,5,1) <=  1 v3r_xjif(1,5,1) -10000 v3r_yjisu(1,5,1)

c3r_xjifupper(1,5,2) <=  1 v3r_xjif(1,5,2) -10000 v3r_yjisu(1,5,2)

c3r_xjifupper(1,5,3) <=  1 v3r_xjif(1,5,3) -10000 v3r_yjisu(1,5,3)

c3r_xjifupper(1,6,1) <=  1 v3r_xjif(1,6,1) -10000 v3r_yjisu(1,6,1)

c3r_xjifupper(1,6,2) <=  1 v3r_xjif(1,6,2) -10000 v3r_yjisu(1,6,2)

c3r_xjifupper(1,6,3) <=  1 v3r_xjif(1,6,3) -10000 v3r_yjisu(1,6,3)

c3r_xjifupper(1,7,1) <=  1 v3r_xjif(1,7,1) -10000 v3r_yjisu(1,7,1)

c3r_xjifupper(1,7,2) <=  1 v3r_xjif(1,7,2) -10000 v3r_yjisu(1,7,2)

c3r_xjifupper(1,7,3) <=  1 v3r_xjif(1,7,3) -10000 v3r_yjisu(1,7,3)

c3r_xjifupper(2,8,1) <=  1 v3r_xjif(2,8,1)   -1.50000000000000      v3r_yjisu(2,8,1)

c3r_xjifupper(2,8,2) <=  1 v3r_xjif(2,8,2)   -1.50000000000000      v3r_yjisu(2,8,2)

c3r_xjifupper(2,8,3) <=  1 v3r_xjif(2,8,3)   -1.50000000000000      v3r_yjisu(2,8,3)

c3r_xjifupper(3,3,1) <=  1 v3r_xjif(3,3,1) -10000 v3r_yjisu(3,3,1)

c3r_xjifupper(3,3,2) <=  1 v3r_xjif(3,3,2) -10000 v3r_yjisu(3,3,2)

c3r_xjifupper(3,3,3) <=  1 v3r_xjif(3,3,3) -10000 v3r_yjisu(3,3,3)

c3r_xjifupper(4,2,1) <=  1 v3r_xjif(4,2,1) -10000 v3r_yjisu(4,2,1)

c3r_xjifupper(4,2,2) <=  1 v3r_xjif(4,2,2) -10000 v3r_yjisu(4,2,2)

c3r_xjifupper(5,1,1) <=  1 v3r_xjif(5,1,1) -10000 v3r_yjisu(5,1,1)

c3r_xjifupper(5,1,2) <=  1 v3r_xjif(5,1,2) -10000 v3r_yjisu(5,1,2)

c3r_xjifupper(5,1,3) <=  1 v3r_xjif(5,1,3) -10000 v3r_yjisu(5,1,3)

c3r_xjifupper(6,4,1) <=  1 v3r_xjif(6,4,1) -10000 v3r_yjisu(6,4,1)

c3r_xjifupper(6,4,2) <=  1 v3r_xjif(6,4,2) -10000 v3r_yjisu(6,4,2)

c3r_xjifupper(6,4,3) <=  1 v3r_xjif(6,4,3) -10000 v3r_yjisu(6,4,3)

c3r_xjifupper(7,1,1) <=  1 v3r_xjif(7,1,1) -10000 v3r_yjisu(7,1,1)

c3r_xjifupper(7,1,2) <=  1 v3r_xjif(7,1,2) -10000 v3r_yjisu(7,1,2)

c3r_xjifupper(7,1,3) <=  1 v3r_xjif(7,1,3) -10000 v3r_yjisu(7,1,3)

c3r_xjifupper(8,1,1) <=  1 v3r_xjif(8,1,1) -10000 v3r_yjisu(8,1,1)

c3r_xjifupper(8,1,2) <=  1 v3r_xjif(8,1,2) -10000 v3r_yjisu(8,1,2)

c3r_xjifupper(8,1,3) <=  1 v3r_xjif(8,1,3) -10000 v3r_yjisu(8,1,3)

c2r_xiylower(4,1) =   1 v2r_xmf(5,1) -1 v3r_xjif(6,4,1)
```

```
c2r_xiylower(4,2) =   1 v2r_xmf(5,2) -1 v3r_xjif(6,4,2)

c2r_xiylower(4,3) =   1 v2r_xmf(5,3) -1 v3r_xjif(6,4,3)

c2r_xiylower(5,1) =   1 v2r_xmf(6,1) -1 v3r_xjif(1,5,1)

c2r_xiylower(5,2) =   1 v2r_xmf(6,2) -1 v3r_xjif(1,5,2)

c2r_xiylower(5,3) =   1 v2r_xmf(6,3) -1 v3r_xjif(1,5,3)

c2r_xiylower(6,1) =   1 v2r_xmf(7,1) -1 v3r_xjif(1,6,1)

c2r_xiylower(6,2) =   1 v2r_xmf(7,2) -1 v3r_xjif(1,6,2)

c2r_xiylower(6,3) =   1 v2r_xmf(7,3) -1 v3r_xjif(1,6,3)

c2r_xiylower(7,1) =   1 v2r_xmf(8,1) -1 v3r_xjif(1,7,1)

c2r_xiylower(7,2) =   1 v2r_xmf(8,2) -1 v3r_xjif(1,7,2)

c2r_xiylower(7,3) =   1 v2r_xmf(8,3) -1 v3r_xjif(1,7,3)

c2r_xiylower(8,1) <=  1 v2r_xmf(8,1) -1 v3r_xjif(2,8,1)

c2r_xiylower(8,2) <=  1 v2r_xmf(8,2) -1 v3r_xjif(2,8,2)

c2r_xiylower(8,3) <=  1 v2r_xmf(8,3) -1 v3r_xjif(2,8,3)

c2r_xiyupper(8,1) <=  1 v3r_xjif(2,8,1) -10000 v2r_xmf(8,1)

c2r_xiyupper(8,2) <=  1 v3r_xjif(2,8,2) -10000 v2r_xmf(8,2)

c2r_xiyupper(8,3) <=  1 v3r_xjif(2,8,3) -10000 v2r_xmf(8,3)

c2r_xjylower(3,1) =     0.500000000000000      v2r_xmf(5,1) -1 v3r_xjif(3,3,1)

c2r_xjylower(3,2) =     0.500000000000000      v2r_xmf(5,2) -1 v3r_xjif(3,3,2)

c2r_xjylower(3,3) =     0.500000000000000      v2r_xmf(5,3) -1 v3r_xjif(3,3,3)

c2r_xjylower(4,1) =   2 v2r_xmf(5,1) -1 v3r_xjif(4,2,1)

c2r_xjylower(4,2) =   1 v2r_xmf(5,2) -1 v3r_xjif(4,2,2)

c2r_xjylower(5,1) =   1 v2r_xmf(6,1) -1 v3r_xjif(5,1,1)

c2r_xjylower(5,2) =   1 v2r_xmf(6,2) -1 v3r_xjif(5,1,2)

c2r_xjylower(5,3) =   1 v2r_xmf(6,3) -1 v3r_xjif(5,1,3)

c2r_xjylower(7,1) =   1 v2r_xmf(7,1) -1 v3r_xjif(7,1,1)

c2r_xjylower(7,2) =   1 v2r_xmf(7,2) -1 v3r_xjif(7,1,2)

c2r_xjylower(7,3) =   1 v2r_xmf(7,3) -1 v3r_xjif(7,1,3)

c2r_xjylower(8,1) =   1 v2r_xmf(8,1) -1 v3r_xjif(8,1,1)

c2r_xjylower(8,2) =   1 v2r_xmf(8,2) -1 v3r_xjif(8,1,2)

c2r_xjylower(8,3) =   1 v2r_xmf(8,3) -1 v3r_xjif(8,1,3)

c2r_xjyupper(6,1) <=  1 v3r_xjif(6,4,1) -10000 v2r_xmf(6,1)

c2r_xjyupper(6,2) <=  1 v3r_xjif(6,4,2) -10000 v2r_xmf(6,2)

c2r_xjyupper(6,3) <=  1 v3r_xjif(6,4,3) -10000 v2r_xmf(6,3)

c2r_xuhbalance(3,1) =   -1 v2r_xmh(3,1) 1 v3r_xjif(4,2,1) -1 v3r_xjif(2,8,1)

c2r_xuhbalance(3,2) =   1 v2r_xmh(3,1) -1 v2r_xmh(3,2) 1 v3r_xjif(4,2,2) -1 v3r_xjif(2,8,2)

c2r_xuhbalance(3,3) =   1 v2r_xmh(3,2) -1 v2r_xmh(3,3) -1 v3r_xjif(2,8,3)

c2r_yumultiuseupper(6,1) <=  1 v2r_ymsu(6,1) 1 v2r_ymsu(7,1) 1 v2r_ymsu(8,1)  -1.000000000000000

c2r_yumultiuseupper(6,2) <=  1 v2r_ymsu(6,2) 1 v2r_ymsu(7,2) 1 v2r_ymsu(8,2)  -1.000000000000000

c2r_yumultiuseupper(6,3) <=  1 v2r_ymsu(6,3) 1 v2r_ymsu(7,3) 1 v2r_ymsu(8,3)  -1.000000000000000

c2r_yumultiusesos1(6,1) 1 v2r_ymsu(6,1) 2 v2r_ymsu(7,1) 3 v2r_ymsu(8,1)

c2r_yumultiusesos1(6,2) 1 v2r_ymsu(6,2) 2 v2r_ymsu(7,2) 3 v2r_ymsu(8,2)
```

```
c2r_yumultiusesos1(6,3) 1 v2r_ymsu(6,3) 2 v2r_ymsu(7,3) 3 v2r_ymsu(8,3)

c3r_yjistructuraltrans(1,5,1) <=  2 v3r_yjisu(1,5,1) -1 v2r_ymsu(1,1) -1 v2r_ymsu(6,1)

c3r_yjistructuraltrans(1,5,2) <=  2 v3r_yjisu(1,5,2) -1 v2r_ymsu(1,2) -1 v2r_ymsu(6,2)

c3r_yjistructuraltrans(1,5,3) <=  2 v3r_yjisu(1,5,3) -1 v2r_ymsu(1,3) -1 v2r_ymsu(6,3)

c3r_yjistructuraltrans(1,6,1) <=  2 v3r_yjisu(1,6,1) -1 v2r_ymsu(1,1) -1 v2r_ymsu(7,1)

c3r_yjistructuraltrans(1,6,2) <=  2 v3r_yjisu(1,6,2) -1 v2r_ymsu(1,2) -1 v2r_ymsu(7,2)

c3r_yjistructuraltrans(1,6,3) <=  2 v3r_yjisu(1,6,3) -1 v2r_ymsu(1,3) -1 v2r_ymsu(7,3)

c3r_yjistructuraltrans(1,7,1) <=  2 v3r_yjisu(1,7,1) -1 v2r_ymsu(1,1) -1 v2r_ymsu(8,1)

c3r_yjistructuraltrans(1,7,2) <=  2 v3r_yjisu(1,7,2) -1 v2r_ymsu(1,2) -1 v2r_ymsu(8,2)

c3r_yjistructuraltrans(1,7,3) <=  2 v3r_yjisu(1,7,3) -1 v2r_ymsu(1,3) -1 v2r_ymsu(8,3)

c3r_yjistructuraltrans(2,8,1) <=  2 v3r_yjisu(2,8,1) -1 v2r_ymsu(8,1)  -1.000000000000000

c3r_yjistructuraltrans(2,8,2) <=  2 v3r_yjisu(2,8,2) -1 v2r_ymsu(8,2)  -1.000000000000000

c3r_yjistructuraltrans(2,8,3) <=  2 v3r_yjisu(2,8,3) -1 v2r_ymsu(8,3)  -1.000000000000000

c3r_yjistructuraltrans(3,3,1) <=  2 v3r_yjisu(3,3,1) -1 v2r_ymsu(5,1) -1 v2r_ymsu(4,1)

c3r_yjistructuraltrans(3,3,2) <=  2 v3r_yjisu(3,3,2) -1 v2r_ymsu(5,2) -1 v2r_ymsu(4,2)

c3r_yjistructuraltrans(3,3,3) <=  2 v3r_yjisu(3,3,3) -1 v2r_ymsu(5,3) -1 v2r_ymsu(4,3)

c3r_yjistructuraltrans(4,2,1) <=  2 v3r_yjisu(4,2,1) -1 v2r_ymsu(5,1)  -1.000000000000000

c3r_yjistructuraltrans(4,2,2) <=  2 v3r_yjisu(4,2,2) -1 v2r_ymsu(5,2)  -1.000000000000000

c3r_yjistructuraltrans(4,2,3) <=  2 v3r_yjisu(4,2,3) -1 v2r_ymsu(5,3)  -1.000000000000000

c3r_yjistructuraltrans(5,1,1) <=  2 v3r_yjisu(5,1,1) -1 v2r_ymsu(6,1) -1 v2r_ymsu(2,1)

c3r_yjistructuraltrans(5,1,2) <=  2 v3r_yjisu(5,1,2) -1 v2r_ymsu(6,2) -1 v2r_ymsu(2,2)

c3r_yjistructuraltrans(5,1,3) <=  2 v3r_yjisu(5,1,3) -1 v2r_ymsu(6,3) -1 v2r_ymsu(2,3)

c3r_yjistructuraltrans(6,4,1) <=  2 v3r_yjisu(6,4,1) -1 v2r_ymsu(6,1) -1 v2r_ymsu(5,1)

c3r_yjistructuraltrans(6,4,2) <=  2 v3r_yjisu(6,4,2) -1 v2r_ymsu(6,2) -1 v2r_ymsu(5,2)

c3r_yjistructuraltrans(6,4,3) <=  2 v3r_yjisu(6,4,3) -1 v2r_ymsu(6,3) -1 v2r_ymsu(5,3)

c3r_yjistructuraltrans(7,1,1) <=  2 v3r_yjisu(7,1,1) -1 v2r_ymsu(7,1) -1 v2r_ymsu(2,1)

c3r_yjistructuraltrans(7,1,2) <=  2 v3r_yjisu(7,1,2) -1 v2r_ymsu(7,2) -1 v2r_ymsu(2,2)

c3r_yjistructuraltrans(7,1,3) <=  2 v3r_yjisu(7,1,3) -1 v2r_ymsu(7,3) -1 v2r_ymsu(2,3)

c3r_yjistructuraltrans(8,1,1) <=  2 v3r_yjisu(8,1,1) -1 v2r_ymsu(8,1) -1 v2r_ymsu(2,1)

c3r_yjistructuraltrans(8,1,2) <=  2 v3r_yjisu(8,1,2) -1 v2r_ymsu(8,2) -1 v2r_ymsu(2,2)

c3r_yjistructuraltrans(8,1,3) <=  2 v3r_yjisu(8,1,3) -1 v2r_ymsu(8,3) -1 v2r_ymsu(2,3)

c2r_zmsutemporaltrans(6,1) =   1 v2r_ymsu(6,1) -1 v2r_zmsu(6,1) 1 v2r_zmsd(6,1)

c2r_zmsutemporaltrans(6,2) =   1 v2r_ymsu(6,2) -1 v2r_ymsu(6,1) -1 v2r_zmsu(6,2) 1 v2r_zmsd(6,2)

c2r_zmsutemporaltrans(6,3) =   1 v2r_ymsu(6,3) -1 v2r_ymsu(6,2) -1 v2r_zmsu(6,3) 1 v2r_zmsd(6,3)

c2r_zmsutemporaltrans(8,1) =   1 v2r_ymsu(8,1) -1 v2r_zmsu(8,1) 1 v2r_zmsd(8,1)

c2r_zmsutemporaltrans(8,2) =   1 v2r_ymsu(8,2) -1 v2r_ymsu(8,1) -1 v2r_zmsu(8,2) 1 v2r_zmsd(8,2)

c2r_zmsutemporaltrans(8,3) =   1 v2r_ymsu(8,3) -1 v2r_ymsu(8,2) -1 v2r_zmsu(8,3) 1 v2r_zmsd(8,3)

c2r_zmsdtemporaltrans(6,1) =   1 v2r_ymsu(6,1) -1 v2r_zmsu(6,1) -1 v2r_zmsd(6,1) -2 v2r_zmsv(6,1)

c2r_zmsdtemporaltrans(6,2) =   1 v2r_ymsu(6,2) 1 v2r_ymsu(6,1) -1 v2r_zmsu(6,2) -1 v2r_zmsd(6,2)
                -2 v2r_zmsv(6,2)

c2r_zmsdtemporaltrans(6,3) =   1 v2r_ymsu(6,3) 1 v2r_ymsu(6,2) -1 v2r_zmsu(6,3) -1 v2r_zmsd(6,3)
                -2 v2r_zmsv(6,3)
```

```
c2r_zmsdtemporaltrans(8,1) =   1 v2r_ymsu(8,1) -1 v2r_zmsu(8,1) -1 v2r_zmsd(8,1) -2 v2r_zmsv(8,1)

c2r_zmsdtemporaltrans(8,2) =   1 v2r_ymsu(8,2) 1 v2r_ymsu(8,1) -1 v2r_zmsu(8,2) -1 v2r_zmsd(8,2)

                -2 v2r_zmsv(8,2)

c2r_zmsdtemporaltrans(8,3) =   1 v2r_ymsu(8,3) 1 v2r_ymsu(8,2) -1 v2r_zmsu(8,3) -1 v2r_zmsd(8,3)

                -2 v2r_zmsv(8,3)

c2r_zmsvtemporaltrans(6,1) <=  1 v2r_zmsu(6,1) 1 v2r_zmsd(6,1) 1 v2r_zmsv(6,1)  -1.000000000000000

c2r_zmsvtemporaltrans(6,2) <=  1 v2r_zmsu(6,2) 1 v2r_zmsd(6,2) 1 v2r_zmsv(6,2)  -1.000000000000000

c2r_zmsvtemporaltrans(6,3) <=  1 v2r_zmsu(6,3) 1 v2r_zmsd(6,3) 1 v2r_zmsv(6,3)  -1.000000000000000

c2r_zmsvtemporaltrans(8,1) <=  1 v2r_zmsu(8,1) 1 v2r_zmsd(8,1) 1 v2r_zmsv(8,1)  -1.000000000000000

c2r_zmsvtemporaltrans(8,2) <=  1 v2r_zmsu(8,2) 1 v2r_zmsd(8,2) 1 v2r_zmsv(8,2)  -1.000000000000000

c2r_zmsvtemporaltrans(8,3) <=  1 v2r_zmsu(8,3) 1 v2r_zmsd(8,3) 1 v2r_zmsv(8,3)  -1.000000000000000

c2r_zmsvtemporaltranssos1(6,1) 1 v2r_zmsu(6,1) 2 v2r_zmsd(6,1) 3 v2r_zmsv(6,1)

c2r_zmsvtemporaltranssos1(6,2) 1 v2r_zmsu(6,2) 2 v2r_zmsd(6,2) 3 v2r_zmsv(6,2)

c2r_zmsvtemporaltranssos1(6,3) 1 v2r_zmsu(6,3) 2 v2r_zmsd(6,3) 3 v2r_zmsv(6,3)

c2r_zmsvtemporaltranssos1(8,1) 1 v2r_zmsu(8,1) 2 v2r_zmsd(8,1) 3 v2r_zmsv(8,1)

c2r_zmsvtemporaltranssos1(8,2) 1 v2r_zmsu(8,2) 2 v2r_zmsd(8,2) 3 v2r_zmsv(8,2)

c2r_zmsvtemporaltranssos1(8,3) 1 v2r_zmsu(8,3) 2 v2r_zmsd(8,3) 3 v2r_zmsv(8,3)

c2r_ymuptimelower(8,2) <=  1 v2r_zmsu(8,1) -1 v2r_ymsu(8,2)

c2r_ymuptimelower(8,3) <=  1 v2r_zmsu(8,2) 1 v2r_zmsu(8,1) -1 v2r_ymsu(8,3)

c2r_ymuptimeupper(6,1) <=  1 v2r_ymsu(6,1) 1 v2r_ymsu(6,2) 1 v2r_ymsu(6,3)   -2.00000000000000

c1_ymuptime(8,1) <=  3 v2r_zmsu(8,1) 3 v2r_zmsu(8,2) 3 v2r_zmsu(8,3)   -3.00000000000000

c2r_zyusingleuse(6,1) =   1 v2r_zysgsu(1,1) 1 v2r_zysgsu(2,1)  -1.000000000000000

c2r_zyusingleuse(6,2) =   1 v2r_zysgsu(1,2) 1 v2r_zysgsu(2,2)  -1.000000000000000

c2r_zyusingleuse(6,3) =   1 v2r_zysgsu(1,3) 1 v2r_zysgsu(2,3)  -1.000000000000000

c2r_zyusingleusesos1(6,1) 1 v2r_zysgsu(1,1) 2 v2r_zysgsu(2,1)

c2r_zyusingleusesos1(6,2) 1 v2r_zysgsu(1,2) 2 v2r_zysgsu(2,2)

c2r_zyusingleusesos1(6,3) 1 v2r_zysgsu(1,3) 2 v2r_zysgsu(2,3)

c2r_zysgsu1(1,1) <=  1 v2r_ymsu(7,1) -1 v2r_zysgsu(1,1)

c2r_zysgsu1(1,2) <=  1 v2r_ymsu(7,2) -1 v2r_zysgsu(1,2)

c2r_zysgsu1(1,3) <=  1 v2r_ymsu(7,3) -1 v2r_zysgsu(1,3)

c2r_zysgsu1(2,1) <=  1 v2r_ymsu(8,1) -1 v2r_zysgsu(2,1)

c2r_zysgsu1(2,2) <=  1 v2r_ymsu(8,2) -1 v2r_zysgsu(2,2)

c2r_zysgsu1(2,3) <=  1 v2r_ymsu(8,3) -1 v2r_zysgsu(2,3)

c2r_zysgsu2(1,2) <=  1 v2r_zysgsu(1,2) -1 v2r_zysgsu(1,1)

c2r_zysgsu2(1,3) <=  1 v2r_zysgsu(1,3) -1 v2r_zysgsu(1,2)

c2r_zysgsu2(2,1) <=  1 v2r_zysgsu(2,1) -1 v2r_zmsu(8,1)

c2r_zysgsu2(2,2) <=  1 v2r_zysgsu(2,2) -1 v2r_zysgsu(2,1) -1 v2r_zmsu(8,2)

c2r_zysgsu2(2,3) <=  1 v2r_zysgsu(2,3) -1 v2r_zysgsu(2,2) -1 v2r_zmsu(8,3)

c3r_zsgswseqdeptemporal3(1,2,1) <=  1 v2r_zysgsu(2,1) 1 v2r_zmsu(8,1) -1 v2r_zmsd(6,1)  -1.000000000000000

c3r_zsgswseqdeptemporal3(1,2,2) <=  1 v2r_zysgsu(2,2) 1 v2r_zysgsu(1,1) 1 v2r_zmsu(8,2)

                -1 v2r_zmsd(6,2)   -2.00000000000000

c3r_zsgswseqdeptemporal3(1,2,3) <=  1 v2r_zysgsu(2,3) 1 v2r_zysgsu(1,2) 1 v2r_zmsu(8,3)
```

```
                -1 v2r_zmsd(6,3)   -2.00000000000000

c1_gprofitterm(1,1) =   1 v1_gprofitterm(1,1) 1 v3r_xjif(3,3,1) 1 v3r_xjif(3,3,2)

                1 v3r_xjif(3,3,3) -1 v3r_xjif(5,1,1) -1 v3r_xjif(5,1,2) -1 v3r_xjif(5,1,3) -1 v3r_xjif(7,1,1)

                -1 v3r_xjif(7,1,2) -1 v3r_xjif(7,1,3) -1 v3r_xjif(8,1,1) -1 v3r_xjif(8,1,2) -1 v3r_xjif(8,1,3)

c1_totalobjfun(5,1) =   1 v1_totalobjfun(5,1) -1 v1_gprofitterm(1,1)


0 <= v2r_ymsu(1,1) <= 1

0 <= v2r_ymsu(1,2) <= 1

0 <= v2r_ymsu(1,3) <= 1

0 <= v2r_ymsu(2,1) <= 1

0 <= v2r_ymsu(2,2) <= 1

0 <= v2r_ymsu(2,3) <= 1

0 <= v2r_ymsu(4,1) <= 1

0 <= v2r_ymsu(4,2) <= 1

0 <= v2r_ymsu(4,3) <= 1

0 <= v2r_ymsu(5,1) <= 1

0 <= v2r_ymsu(5,2) <= 1

0 <= v2r_ymsu(5,3) <= 1

0 <= v2r_ymsu(6,1) <= 1

0 <= v2r_ymsu(6,2) <= 1

0 <= v2r_ymsu(6,3) <= 1

0 <= v2r_ymsu(7,1) <= 1

0 <= v2r_ymsu(7,2) <= 1

0 <= v2r_ymsu(7,3) <= 1

0 <= v2r_ymsu(8,1) <= 1

0 <= v2r_ymsu(8,2) <= 1

0 <= v2r_ymsu(8,3) <= 1

0 <= v3r_yjisu(1,5,1) <= 1

0 <= v3r_yjisu(1,5,2) <= 1

0 <= v3r_yjisu(1,5,3) <= 1

0 <= v3r_yjisu(1,6,1) <= 1

0 <= v3r_yjisu(1,6,2) <= 1

0 <= v3r_yjisu(1,6,3) <= 1

0 <= v3r_yjisu(1,7,1) <= 1

0 <= v3r_yjisu(1,7,2) <= 1

0 <= v3r_yjisu(1,7,3) <= 1

0 <= v3r_yjisu(2,8,1) <= 1

0 <= v3r_yjisu(2,8,2) <= 1

0 <= v3r_yjisu(2,8,3) <= 1

0 <= v3r_yjisu(3,3,1) <= 1

0 <= v3r_yjisu(3,3,2) <= 1

0 <= v3r_yjisu(3,3,3) <= 1
```

0 <= v3r_yjisu(4,2,1) <= 1

0 <= v3r_yjisu(4,2,2) <= 1

0 <= v3r_yjisu(4,2,3) <= 1

0 <= v3r_yjisu(5,1,1) <= 1

0 <= v3r_yjisu(5,1,2) <= 1

0 <= v3r_yjisu(5,1,3) <= 1

0 <= v3r_yjisu(6,4,1) <= 1

0 <= v3r_yjisu(6,4,2) <= 1

0 <= v3r_yjisu(6,4,3) <= 1

0 <= v3r_yjisu(7,1,1) <= 1

0 <= v3r_yjisu(7,1,2) <= 1

0 <= v3r_yjisu(7,1,3) <= 1

0 <= v3r_yjisu(8,1,1) <= 1

0 <= v3r_yjisu(8,1,2) <= 1

0 <= v3r_yjisu(8,1,3) <= 1

0 <= v2r_xmf(7,1) <= 1

0 <= v2r_xmf(7,2) <= 1

0 <= v2r_xmf(7,3) <= 1

0 <= v2r_xmf(6,1) <= 1

0 <= v2r_xmf(6,2) <= 1

0 <= v2r_xmf(6,3) <= 1

0 <= v2r_xmf(8,1) <= 1.50000000000000

0 <= v2r_xmf(8,2) <= 1.50000000000000

0 <= v2r_xmf(8,3) <= 1.50000000000000

0 <= v2r_xmf(5,1) <= 1.50000000000000

0 <= v2r_xmf(5,2) <= 1.50000000000000

0 <= v2r_xmf(5,3) <= 1.50000000000000

0 <= v2r_xmh(3,1) <= 3

0 <= v2r_xmh(3,2) <= 4.50000000000000

0 <= v2r_xmh(3,3) <= 4.50000000000000

0 <= v3r_xjif(1,5,1) <= 1

0 <= v3r_xjif(1,5,2) <= 1

0 <= v3r_xjif(1,5,3) <= 1

0 <= v3r_xjif(1,6,1) <= 1

0 <= v3r_xjif(1,6,2) <= 1

0 <= v3r_xjif(1,6,3) <= 1

0 <= v3r_xjif(1,7,1) <= 1.50000000000000

0 <= v3r_xjif(1,7,2) <= 1.50000000000000

0 <= v3r_xjif(1,7,3) <= 1.50000000000000

0 <= v3r_xjif(2,8,1) <= 1.50000000000000

0 <= v3r_xjif(2,8,2) <= 1.50000000000000

0 <= v3r_xjif(2,8,3) <= 1.50000000000000

```
0 <= v3r_xjif(3,3,1) <= 0.750000000000000

0 <= v3r_xjif(3,3,2) <= 0.750000000000000

0 <= v3r_xjif(3,3,3) <= 0.750000000000000

0 <= v3r_xjif(4,2,1) <= 3

0 <= v3r_xjif(4,2,2) <= 1.50000000000000

0 <= v3r_xjif(5,1,1) <= 1

0 <= v3r_xjif(5,1,2) <= 1

0 <= v3r_xjif(5,1,3) <= 1

0 <= v3r_xjif(6,4,1) <= 1.50000000000000

0 <= v3r_xjif(6,4,2) <= 1.50000000000000

0 <= v3r_xjif(6,4,3) <= 1.50000000000000

0 <= v3r_xjif(7,1,1) <= 1

0 <= v3r_xjif(7,1,2) <= 1

0 <= v3r_xjif(7,1,3) <= 1

0 <= v3r_xjif(8,1,1) <= 1.50000000000000

0 <= v3r_xjif(8,1,2) <= 1.50000000000000

0 <= v3r_xjif(8,1,3) <= 1.50000000000000

0 <= v2r_zmsu(6,1) <= 1

0 <= v2r_zmsu(6,2) <= 1

0 <= v2r_zmsu(6,3) <= 1

0 <= v2r_zmsu(8,1) <= 1

0 <= v2r_zmsu(8,2) <= 1

0 <= v2r_zmsu(8,3) <= 1

0 <= v2r_zmsv(6,1) <= 0.500000000000000

0 <= v2r_zmsv(6,2) <= 1

0 <= v2r_zmsv(6,3) <= 1

0 <= v2r_zmsv(8,1) <= 0.500000000000000

0 <= v2r_zmsv(8,2) <= 1

0 <= v2r_zmsv(8,3) <= 1

0 <= v2r_zmsd(6,1) <= 1

0 <= v2r_zmsd(6,2) <= 1

0 <= v2r_zmsd(6,3) <= 1

0 <= v2r_zmsd(8,1) <= 1

0 <= v2r_zmsd(8,2) <= 1

0 <= v2r_zmsd(8,3) <= 1

0 <= v2r_zysgsu(1,1) <= 1

0 <= v2r_zysgsu(1,2) <= 1

0 <= v2r_zysgsu(1,3) <= 1

0 <= v2r_zysgsu(2,1) <= 1

0 <= v2r_zysgsu(2,2) <= 1

0 <= v2r_zysgsu(2,3) <= 1

-1.000000000000000E+020 <= v1_gprofitterm(1,1) <= 1.000000000000000E+020
```

-1.000000000000000E+020 <= v1_totalobjfun(5,1) <= 1.000000000000000E+020

Appendix D: Net Present Value Formulation for Investment of Oil-Refinery Units

Net present value (NPV) is the main objective to predict capacity increment of process units in investment or facilities planning analysis. This is a virtual value meaning how present decisions can be evaluated regarding future perspectives around possible revenues. In mathematical programming model, rather than simply production frameworks simulation, high performance NPV calculation is based on mixed-integer models to install new units or expand existing ones creating a combinatorial tree to be explored in an optimization environment to obtain better results. Considerations over work capital, depreciation, and salvage value must be included in the NPV cost coefficients because it can affect company's decisions. The first is the demanded capital to maintain the production, and the second and third are related to investment cost discounts.

Besides NPV calculation, the company's profitability is also an important investment qualifier configuring as a quick and easy way to judge the overall production performance. However, the profit evaluated from the operational gains not actually reflect the income acquired with the present investment decisions as expected in a strategic decision-making model for a long-term period, even more dealing with assets like in the oil-refining industry, in which revamp and installation investments can reach billions of dollars. In real, operational, investments and financial activities determine the cash in and out to be considered for the projects evaluations in an accounting perspective formulation as proposed here.

The cash generation source is the operational gains with the current and possible future assets. On the other hand, cash outflows can be separated in project investments and work capital expenditures. The capital investment *CI* expenses in the projects are compound by construction, property, equipment, labor, detailed project, investment securities, etc. The work capital *WC* guarantees the company's earnings maintenance, affording sufficient cash to cover ongoing debits. In general *WC* is supposed to be proportional to *CI*. In this work $WC=0.0517CI$.

Financial transactions can also be included in the cash flow. Continuously the companies' borrows, debits, and equity can influence the cash flow, but financial transitions are not being considered here. Amortization, also not included in the model, is the deduction with specific expenses over a time period, for example, non-drilling costs sustained while

developing the reserves. Expenses with wells from developed reserves should be amortized, because by definition, those are the reserves that will be produced as a result of the costs already incurred. The remaining proved reserves but still underdeveloped are excluded (Wright and Gallun, 2008).

NPV is evaluated accordingly applicable rules (depreciation), legislation (taxes), market expectative, monetary policy, company's specifics, etc. (Guillén et al., 2005). In general, this is the main objective in a strategic planning model and evaluates the capital amount gained at the moment of decision in having or not a project. So that a discrete, binary, or setup variable should be included in an investment model to predict the overall capacity planning for the oil-refinery units as we propose. NPV is an open formula calculated as the summation of the cash flows balance in each time interval CF_t like in Equation A1.

$$NPV = \sum_{t} \frac{CF_t}{(1+ir)^{t-1}} \qquad (A1)$$

As proposed here, the time horizon is divided in investment t and operational t_o time periods. The NLP operational model calculates the daily profit to be extended to annual gains. Only after the project execution the productive scenario is modified within the following time periods recalculating the operational profit. The operational cash flow along the time is corrected annually by the factor Cop_{to} to reflect the deflation suffered by the future annual gains when it is considered at the present as shown in Equation A2. The interest rate ir considered is fixed in 10% for the Brazilian market (Trading Economics, 2013).

$$Cop_{to} = \frac{1}{(1+ir)^{to}} \qquad (A2)$$

The investments expenses when evaluated at once at the moment of decision lessen by equipment depreciation DEP and salvage value SV deductions. SV is the equipment realized selling price at the end of its useful life. The value is used to determine depreciation amounts to deduct taxes. Depreciation in an accounting problem is considered the costs to maintain the unit production in compliance with safety requirements along its useful lifetime. Usually the depreciation method is set by the company's policy and should be in accordance with regulatory bodies about how and when the deduction may be taken based on what the asset is and how long it will last. Typically after 25 years, various studies need to be done to determine options for extending a refining unit useful life, reaching its final salvage value. So,

considering the equipment realized value components as discussed, the investment costs for each discrete decision to approve the projects are defined in Equation A3.

$$[costs_t]_{investment} = CI_t + WC_t - DEP_t - SV_t = CI_t Cinv_t \quad \text{(A3)}$$

CI_t is the liquid cash or project capital investment clamed to build the asset. WC_t is the work capital demanded to maintain the company's activities. After the total time period considered for the NPV calculation, the WC_t is withdrawn. Deductions from depreciation DEP_t and salvage value SV_t reflect the projects no-cash weight to be included in the discrete variable decision.

To evaluate the realized investment costs along the NPV investigation time $Cinv_t$, Equations A4 and A5 are needed to find the investment costs deductions related to the WC cash back, the depreciation tax refunds, and the salvage amount recovered. The model uses the initial point and the interval of a project execution to determine the economical evaluation of an asset. $Tcur_t$ is the investment time begging in which the discrete decisions are made. The project execution interval ΔT_t can vary for each unit, but by the sake of simplicity all units have the same project execution, but the model is ready for different investment intervals.

$$Tcur_t = \sum_{t=1}^{t} \Delta T_t - \Delta T_t \quad (A4)$$

$$T_{end} = \sum_{t=1}^{t=T_n} \Delta T_t \quad (A5)$$

As the model allows investment decision in a multiperiod formulation the costs for the units to be invested in each t considering their NPV are given by Equation A6. The direct costs represent the project and work capital expenditures. The work capital factor WC_F is a percentage of the project capital. This cash is ultimately given back at the investment end time t_{end}. The depreciation deduction is a linear tax refund ratio based on the difference between the capital to be invested in the equipment and its final salvage value. For oil-refinery units the useful lifetime considered is t_{dep} = 25 years. Finally the cash gained with the possible equipment selling is calculated taking in account the salvage value factor (SV_F) which is considered 5% for all units. It means that after 25 years the value for a unit is 5% of its startup value. The startup value considered here is the CI_t for a unit deflated by the interval to have it

built. Also the deflation is applied when the non-cash inflows are return to the present. Only after the projects execution intervals ΔT_t the depreciation refunds and salvage value can be applied.

$$CI_t = \frac{1}{(1+ir)^{Tcur_t}} + WC_F\left(\frac{1}{(1+ir)^{Tcur_t}} - \frac{1}{(1+ir)^{Tend}}\right) - \left(\frac{Tdep - (Tcur_t + \Delta T_t)}{Tdep}\right)\frac{(1-SV_F)tr}{Tdep}\sum_{t_o=Tcur_t+\Delta T_t}^{t_o=Tend}\frac{1}{(1+ir)^{t_o}} - \left(\frac{Tdep}{Tcur_t+\Delta T_t}\right)\frac{SV_F}{(1+ir)^{Tend}} \quad (A6)$$

For future projects starting in further intervals, the liquid cash granted at the moment of decision should return to the present deflating as shown in the equation (S6) for the CI and the WC expenses. The CI and WC amounts defined for the projects in the first period are withdrawn at the moment of decision, so that the interest rate correction is not applied ($Tcur_1=0$) . As mentioned, the WC is rescued at the portfolio evaluation end time reducing the overall project costs. The other non-cash deductions are related with the equipment existence along the time. The liquid cash invested in a project is converted in the current asset which during its life demands capital to maintain its integrity and safety. This expense is discounted as a tax refund so-called depreciation (DEP). As the refunds are collected within the total investment period in evaluation t_{end}, maybe shorter than the useful lifetime, the depreciation discount is deflated at every year after the unit startup until t_{end}. An annual straight-line depreciation ratio determines the total amount refund for each project until the final time studied by the investment portfolio investigation. Finally, the last term in equation (S6) is related with the current salvage value (SV) held by the equipment built. As like for depreciation, an annual linear reduction along the unit useful lifetime compute the amount lost after its startup, but its deflation is accounted only at the end time period when its current SV is realized at the moment of decision.

Supporting Information

Table S3.1. Crude-oil assay yields, $Y_{cr,c}$ (%).

Crude		C1C2	C3C4	N	SW1	K	SW2	LD	SW3	HD	ATR	LVGO	HVGO	VR
National	Light	0.01	1.06	6.72	4.85	13.64	11.91	17.38	9.17	7.78	27.48	18.81	2.38	6.30
	Pre-Salt	0.09	1.02	8.72	5.02	6.89	5.55	6.91	4.24	4.46	57.11	21.81	5.30	29.99
	Medium	0.12	0.90	7.20	3.50	6.30	5.58	7.34	4.71	4.78	59.58	20.96	5.41	33.20
	Heavy	0.08	0.44	4.50	2.05	4.46	5.10	9.20	6.11	5.77	62.28	19.71	4.97	37.61
Imported	Ultra Light	0.06	3.38	19.82	8.86	12.35	9.87	12.57	7.40	6.25	19.43	13.59	1.51	4.34

Table S3.2. Crude-oil assay specific gravity, $G_{cr,c}$ (g/cm^3).

Crude		N	SW1	K	SW2	LD	SW3	HD	ATR	LVGO	HVGO	VR
National	Light	0.722	0.779	0.806	0.843	0.861	0.868	0.880	0.936	0.916	0.948	0.994
	Pre-Salt	0.701	0.753	0.789	0.819	0.840	0.853	0.867	0.944	0.903	0.935	0.976
	Medium	0.698	0.763	0.798	0.829	0.850	0.865	0.883	0.969	0.920	0.944	1.004
	Heavy	0.726	0.776	0.804	0.832	0.860	0.882	0.906	0.986	0.940	0.956	1.015
Imported	Ultra Light	0.713	0.756	0.780	0.804	0.823	0.833	0.845	0.916	0.886	0.937	1.004

Table S3.3. Crude-oil assay sulfur content, $S_{cr,c}$ (w%).

Crude		N	SW1	K	SW2	LD	SW3	HD	ATR	LVGO	HVGO	VR
National	Light	0.001	0.007	0.017	0.032	0.056	0.081	0.109	0.196	0.150	0.208	0.316
	Pre-Salt	0.032	0.037	0.056	0.076	0.112	0.175	0.227	0.501	0.312	0.423	0.642
	Medium	0.001	0.007	0.045	0.093	0.187	0.325	0.372	0.723	0.539	0.613	0.855
	Heavy	0.002	0.025	0.105	0.232	0.400	0.503	0.638	0.746	0.676	0.709	0.785
Imported	Ultra Light	0.003	0.003	0.005	0.013	0.026	0.039	0.057	0.161	0.098	0.172	0.332

Table S3.4. Crude-oil assay acidity, $A_{cr,c}$ (mgKOH/g).

Crude		N	SW1	K	SW2	LD	SW3	HD	ATR	LVGO	HVGO	VR
National	Light	0.010	0.036	0.060	0.066	0.072	0.095	0.188	0.573	0.588	0.543	0.543
	Pre-Salt	0.124	0.118	0.168	0.207	0.270	0.293	0.266	0.291	0.250	0.227	0.329
	Medium	0.026	0.030	0.053	0.111	0.250	0.378	0.532	0.196	0.362	0.294	0.084
	Heavy	0.015	0.033	0.054	0.133	0.339	0.776	1.432	1.276	1.743	1.696	0.997
Imported	Ultra Light	0.007	0.021	0.039	0.060	0.084	0.105	0.118	0.249	0.163	0.527	0.395

Table S3.5. Products yields and properties for other oil-refinery units.

Unit (u)	Stream (s)	$Y_{u,s}$ (%)	$G_{u,s}$ (g/cm^3)	$S_{u,s}$ (w%)	$MON_{u,s}$	$RON_{u,s}$	$ARO_{u,s}$	$OLE_{u,s}$
RFCC	C1C2	5						
	C3C4	11						
	LCN	54	0.758	0.098	80.00	92.00	45.00	29.00
	HCN	5	0.857	0.120				
	LCO	7	0.901	0.343				
	DO	18	0.956	0.453				
FCC	C1C2	4						
	C3C4	10						
	LCN	54	0.758	0.098	81.78	94.05	45.00	29.00
	HCN	7	0.857	0.120				
	LCO	10	0.901	0.343				
	DO	15	0.956	0.453				
HCC	C1C2	3						
	C3C4	7						
	HCCN	15	0.758	0.001	69.00	76.00	2.00	1.00
	HCCK	18	0.770	0.001				
	HCCD	25	0.850	0.001				
	HCCO	32	0.900	0.001				
PDA	DAO	54	0.929	0.748				
	ASFR	46	1.090	0.857				
DC	C1C2	4						
	C3C4	8						
	CLN	15	0.750	0.427	65.88	68.96	10.69	4.00
	CHN	12	0.786	0.537				
	CLGO	12	0.845	0.597				
	CMGO	8	0.925	0.679				
	CHGO	13	0.967	0.759				
	COKE	28						
KHT	HTK	100	G_{KHT}	S_{KHT}				
D1HT	HTD	98	G_{D1HT}	S_{D1HT}				
D2HT	HTD	96	G_{D2HT}	S_{D2HT}				
LCNHT	HTLCN	100	G_{LCNHT}	S_{LCNHT}	MON_{LCNHT}	RON_{LCNHT}	ARO_{LCNHT}	OLE_{LCNHT}
CLNHT	HTCLN	100	G_{CLNHT}	S_{CLNHT}	MON_{CLNHT}	RON_{CLNHT}	ARO_{CLNHT}	OLE_{CLNHT}
ST	LNST	40	0.710	S_{CLNHT}	65.0	75.0		
	HNST	50	0.790	S_{CLNHT}	65.0	75.0		
	GOST	10	0.855	S_{CLNHT}				
REF	H2	12						
	REFOR	88	0.850	0.005	92.00	100.00	50.00	1.00
ETH_{imp}	ETH	100	0.789	0.000	90.00	109.00		
GLN_{imp}	GIMP	100	0.758	0.005	81.78	94.05	20.00	5.00
JET_{imp}	KIMP	100	0.800	0.030				
LSD_{imp}	DIMP	100	0.830	0.001				

Table S3.6. Parameter for RON and MON blend values.

	Parameter	
RON	a	0.01929
	b	0.00043
	c	0.00144
	d	0.00165
MON	e	0.04450
	f	0.00081
	g	0.000000645

Table S8.1. Existing capacity (EXCAP) of the São Paulo refineries in k m^3/d.

REPLAN			REVAP			RPBC			RECAP		
u	n	EXCAP	u	n	EXCAP	u	n	EXCAP	u	n	EXCAP
CDU	1	33.0	CDU	1	40.0	CDU	1	13.5	CDU	1	8.5
CDU	2	36.0	VDU	1	20.0	CDU	2	9.7	DEBUT	1	0.5
VDU	1	20.0	DEBUT	1	1.5	CDU	3	5.2	SUPER	1	0.6
VDU	2	22.0	SUPER	1	0.8	VDU	1	9.7	RFCC	1	3.7
DEBUT	1	3.0	ST	1	4.0	VDU	2	3.2	DHT	1	4.0
SUPER	1	1.5	PDA	1	6.8	DEBUT	1	1.0	LCNHT	1	2.0
ST	1	6.0	FCC	1	14.0	ST	1	2.5			
FCC	1	8.5	DC	1	5.0	FCC	1	10.0			
FCC	2	7.5	KHT	1	3.5	DC	1	2.5			
DC	1	6.0	KHT	2	3.0	DC	2	2.8			
DC	2	6.0	DHT	1	6.0	DHT	1	6.0			
DHT	1	6.0	DHT	2	6.5	DHT	2	10.0			
DHT	2	6.0	LCNHT	1	7.0	ALK	1	0.5			
DHT	3	10.0	CLNHT	1	4.0	LCNHT	1	5.0			
LCNHT	1	5.0	REF	1	1.5	CLNHT	1	2.5			
LCNHT	2	5.0				REF	1	2.0			
CLNHT	1	10.0									
REF	1	2.6									

Table S8.2. Demand of the scenario sc=1 in k m^3/d (sc=2 is 5% higher and sc=3 is 10%).

r	u	n	sc	t=1	t=2
REPLAN	PLPG	1	1	4.00	4.72
	PPQN	1	1		
	PGLN	1	1	17.60	20.75
	PJFUEL	1	1		
	PDFC	1	1	18.00	19.48
	PDME	1	1	10.00	11.79
	PDIN	1	1	2.00	2.36
	PDMA	1	1	1.00	1.18
RPBC	PLPG	1	1	1.40	1.65
	PPQN	1	1		
	PGLN	1	1	12.00	14.15
	PDFC	1	1	4.00	4.72
	PDME	1	1	12.00	14.15
	PDIN	1	1	1.00	1.18
	PDMA	1	1	1.00	1.18
RECAP	PLPG	1	1	0.85	1.00
	PPQN	1	1		
	PGLN	1	1	2.20	2.59
	PDFC	1	1	4.00	4.72
	PDME	1	1	0.20	0.24
	PDIN	1	1	0.10	0.12
	PDMA	1	1	0.10	0.12
REVAP	PLPG	1	1	1.80	2.12
	PPQN	1	1		
	PGLN	1	1	16.00	18.86
	PJFUEL	1	1	7.00	8.25
	PDFC	1	1	10.00	11.79
	PDME	1	1	5.00	5.89
	PDIN	1	1	2.00	2.36
	PDMA	1	1	1.00	1.18

References

[1] Agencia T1. Preço de querosene de aviação ainda pesa nas passagens aéreas Home Page. http://www.agenciat1.com.br/preco-de-querosene-de-aviacao-ainda-pesa-nas-passagens-areas (Access Apr 30, 2013).

[2] Alattas, A.M.; Grossmann, I.E.; Palou-Rivera, I. Integration of Nonlinear Crude Distillation Unit Models in Refinery Planning Optimization. *Industrial & Engineering Chemistry Research,* 50, 6860-6870, 2011.

[3] Alattas, A.M.; Grossmann, I.E.; Palou-Rivera, I. Refinery Production Planning-Multiperiod MINLP with Nonlinear CDU Model. *Industrial & Engineering Chemistry Research*, 2012, 50, 6860-6870, 2012.

[4] ANP Petroleum National Agency. Brazilian Annual Oil Statistic 2012 Home Page. http://www.anp.gov.br/?pg=62463&m=&t1=&t2=&t3=&t4=&ar=&ps=&cachebust=1371 79937518 (Access Nov 30, 2013).

[5] ANP Petroleum National Agency. Fuels and Derivatives Market Evolution 2000-2012. Available on line at www.anp.gov.br/?dw=64307 (Access Sep 29 2013).

[6] ANP Petroleum National Agency. Price System Survey Home Page. http://www.anp.gov.br/preco/prc/Resumo_Mensal_Index.asp (Access Nov 30, 2013).

[7] Aronofsky, J.S; Dutton, J.M; Tayyabkhan, M.T. *Managerial Planning with Linear Programming*. Wiley & Sons: New York, NY, 1978.

[8] Balas, E. Disjunctive Programming and a Hierarchy of Relaxations for Discrete Optimization Problems, *SIAM Journal on Applied Mathematics*, 6, 466-486, 1985.

[9] Barsamian, A. *Gasoline and Diesel Blending: Technology, Operations, Economics*. Refinery Automation Institute, LLC, 2007.

[10] Bazaraa, M.S.; Sheraly, H.D.; Shetty, C.M. *Nonlinear Programming, Theory and Applications.* Wiley & Sons: New York, NY, 1993.

[11] Belotti, P.; Kirches, C.; Leyffer S.; Linderoth, J.; Luedtke, J; Mahajan. A. Mixed-Integer Nonlinear Optimization. *Acta Numerica,* 22, 1-131, 2013.

[12] Benders J.F., Partitioning Procedures for Solving Mixed Variables Programming Problems. *Numerical Mathematics*, 4, 238-252, 1962.

[13] Bixby, B. Solving Real-World Linear Programs: A Decade and More of Progress. *Operations Research*, 50, 3–15, 2002.

[14] Bixby, R.; Rothberg, E. Progress in Computational Mixed Integer Program-Ming: A Look Back from the Other Side of the Tipping Point. *Annals of Operations Research*, 149(1), 37–41, 2007.

[15] Brooke A.; Kendrick D.; Meeraus A. GAMS - A User's Guide (Release 2.25): The Scientific Press. San Francisco, CA, 1992.

[16] Brooks, R.W.; Van Walsem, F.D.; Drury, J. Choosing Cut-points to Optimize Product Yields. *Hydrocarbon Processing*, 78(11), 53-60, 1999.

[17] CNI Industry National Confederation 2012. Available on line at http://www.cni.empauta.com (Access Oct 20 2013).

[18] Colorado School of Mines. Refinery Feedstocks and Products - Properties & Specifications.http://home.comcast.net/~jjechura/CHEN409/02_Feedstocks_&_Products.pdf (Access Jan 25, 2014).

[19] Conejo, A.J.; Castillo, E.; Mínguez R.; García-Bertrand R. *Decomposition Techniques in Mathematical Programming.* Springer: New York, NY, 2006.

[20] Corsano, G.; Guillén-Gosálbez G.; Montagna J. Computational Methods for the Simultaneous Strategic Planning of Supply Chain and Batch Chemical Manufacturing Sites. *Computer & Chemical Engineering*, 60, 154-171, 2014.

[21] Dantzig, G. Linear Programming and Extension. Princeton University Press: New Jersey. 1963

[22] Daubert, T.E. Petroleum Fraction Distillation Interconversion. *Hydrocarbon Processing*, 73(9), 75-78, 1994.

[23] DiVita, V.B. *White Paper on the Development of the Liquids Fuels Market Module* (LFMM). Jacobs Consultancy, Houston, TX, 2009.

[24] Drud, A. CONOPT: A GRG Code for Large Sparse Dynamic Nonlinear Optimization Problems. *Mathematical Programming*, 31 (2), 153-191, 1985.

[25] Duran, M.A.; Grossmann, I.E. An Outer Approximation Algorithm for a Class of Mixed-Integer Nonlinear Programs. *Mathematical Programming*, 36, 307–339, 1986.

[26] EIA Energy Information Administration. Performance Profiles of Major Energy Producers 2009 Home Page. http://www.eia.gov/cfapps/frs/frstables.cfm?tableNumber=28 (Access Jun 10, 2013).

[27] EIA Energy Information Administration. Spot Prices for Crude Oil and Petroleum Products Home Page. http://www.eia.gov/dnav/pet/pet_pri_spt_s1_d.htm (Access Nov 30, 2013).

[28] EIA Energy Information Administration. Gasoline and Diesel Fuel Update. http://www.eia.gov/petroleum/gasdiesel (accessed Mar 20, 2014).

[29] Erwin, J. Assay of Diesel Fuel Components Properties and Performance. Symposium of Processing and Product Selectivity of Synthetic Fuels. *American Chemical Society*: Washington, DC, August 1992.

[30] Floudas, C.A., Lin, X. Continuous-time Versus Discrete-time Approaches for Scheduling of Chemical Processes: A Review. *Computers & Chemical Engineering*, 28, 2109–2129, 2004.

[31] Forbes, J.F.; Marlin, T.E. Model Accuracy for Economic Optimizing Controllers: The Bias Update Case. *Industrial & Engineering Chemistry Research*, 33, 1919, 1994.

[32] Fritsch, F.N.; Carlson, R.E. Monotone Piecewise Cubic Interpolation. *SIAM Journal on Numerical Analysis*, 17, 238-246, 1980.

[33] Fritsch, F.N.; Butland, J. A Method for Constructing Local Monotone Piecewise Interpolants. *SIAM Journal on Scientific and Statistical Computing*, 5, 300-304, 1984.

[34] Gary, J.H.; Handwerk, G.E. Petroleum refining technology and economics. New York: Marcel Dekker; 1994.

[35] Geoffrion, A.M. Generalized Benders Decomposition, *Journal of Optimization Theory and Application*, 10 (4), 237-260, 1972.

[36] Gill, P.E.; Murray, W.; Saunders, M. SNOPT: An SQP Algorithm for Large-Scale Constrained Optimization. *SIAM Journal on Optimization*, 12 (4), 979-1006, 2002.

[37] Greeff, P. Applying Constrained Cubic Splines to Yield Curves. RisCura's ThinkNotes, October, 2003.

[38] Guignard, M.; Kim, S. Lagrangean Decomposition: A Model Yielding Stronger Lagrangean Bounds. *Mathematical Programming*, 39, 215–228, 1987.

[39] Goetschalckx M. Supply chain engineering. *International Series in Operations Research & Management Science*, vol. 161. Springer US, 2011.

[40] Grossmann, I.E. Review of Nonlinear Mixed-Integer and Disjunctive Programming Techniques. *Optimization & Engineering*, 3, 227–252, 2002.

[41] Grossmann, I.E. Enterprise-wide Optimization: A New Frontier in Process Systems Engineering. *AIChE Journal*, 51:1846–1857, 2005.

[42] Grossmann, I.E. Advances in Mathematical Programming Models for Enterprisewide Optimization. *Computers & Chemical Engineering*, 47:2–18, 2012.

[43] Grossmann, I.E.; Caballero, J.A.; Yeomans, H. Mathematical Programming Approaches to The Synthesis of Chemical Process Systems. *Korean Journal of Chemical Engineering*, 16(4), 407-426, 1999.

[44] Grossmann, I.E.; Westerberg, A.W.; Biegler, L.T. Retrofit design of processes. Research showcase at Carnegie Mellon University. Department of Chemical Engineering. Paper 110 (http://repository.cmu.edu/cheme/110), 1987.

[45] Grossmann, I. E.; Van den Heever, S.A.; Harjunkoski, I. Discrete Optimization Methods and their Role in the Integration of Planning and Scheduling. *AIChE Symposium Series*, 98, 150, 2002.

[46] Guerra, O.J.; Le Roux, A.C. Improvements in Petroleum Refinery Planning: 1. Formulation of Process models. *Industrial & Engineering Chemistry Research*, 2011a, 50, 13403-13418.

[47] Guerra, O.J.; Le Roux, A.C. Improvements in Petroleum Refinery Planning: 2. Case studies. *Industrial & Engineering Chemistry Research*, 2011b, 50, 13419-13426.

[48] Harjunkoski, I.; Maravelias, C.; Bongers, P.; Castro, P.; Engell, S.; Grossmann, I.E., Hooker, J.; Mendez, C.; Sand, G.; Wassick, J. Scope for Industrial Applications of Production Scheduling Models and Solution Methods, *Computer and Chemical Engineering*, 62, 161-193, 2014.

[49] Honeywell Process Solutions. Distillate Blending Optimization. https://www.honeywellprocess.com/library/marketing/whitepapers/WP-13-11-ENG-AdvSol-BMM-DieselBlending.pdf (accessed Apr 29, 2014).

[50] Iachan, R. A Brazilian Experience: 40 Years Using Operations Research. *International Transactions in Operational Research*, 16, 585-593, 2009.

[51] Iyer, R.R.; Grossmann, I.E. A Bilevel Decomposition Algorithm for Long-range Planning of Process Networks. *Industrial & Engineering Chemistry Research*, 37(2), 474–48, 1998.

[52] Jackson, R.J.; Grossmann, I.E. High-Level Optimization Model for the Retrofit Planning of Process Networks. *Industrial & Engineering Chemistry Research*, 41, 3762–3770, 2002.

[53] Jia, Z.; Ierapetritou, M.; Kelly, J.D. Refinery Short Term Scheduling Using Continuous Time Formulation: Crude-Oil Operations. *Industrial & Engineering Chemistry Research*, 42, 3087-3097, 2004.

[54] Johnston, D. Complexity index indicates refinery capability and value. *Oil & Gas Journal*, 94 (12), 1996.

[55] Johnson, E.L.; Nemhauser, G.L.; Savelsbergh, M.W.P. Progress in Linear Programming-Based Algorithms for Integer Programming: An Exposition. *INFORMS Journal on Computing*, 12(1), 2–23, 2000.

[56] Jones, D.S.J.; Pujado, P.P. *Handbook of Petroleum Processing*. Springer, 2006.

[57] Kaiser, M.J.; Gary, J.H. Study updates refinery investment cost curves. *Oil & Gas Journal*, 105, 82, 2007.

[58] Kahaner, D.; Moler, C.; Nash, S. Numerical Methods and Software. Prentice Hall. 1988.

[59] Kallrath, J. Planning and Scheduling in the Process Industry. *OR Spektrum*, 24, 219–250, 2002.

[60] Kallrath, J. Combined Strategic Design and Operative Planning in the Process Industry. *Computers & Chemical Engineering*, 33:1983–1993, 2009.

[61] Kallrath, J. Polylithic Modeling and Solution Approaches Using Algebraic Modeling Systems, *Optimization Letters*, 5, 453-466, 2011.

[62] Karmarkar, N. A New Polynomial-time Algorithm for Linear Programming. *Combinatorica*, 4, 373-395, 1984.

[63] Karuppiah, R.; Grossmann, I.E. A Lagrangean Based Branch-and-Cut Algorithm for Global Optimization of Nonconvex Mixed-Integer Nonlinear Programs with Decomposable Structures. *Journal of Global Optimization*, 41, 163-186, 2008.

[64] Kelly, J.D. Chronological Decomposition Heuristic for Scheduling: Divide and Conquer Method. *Aiche Journal*, 48(12), 2995-2999, 2002.

[65] Kelly, J.D. Next Generation Refinery Scheduling Technology. NPRA Plant Automation and Decision Support, San Antonio, 2003.

[66] Kelly, J.D. Formulating Production Planning Models. *Chemical Engineering Progress.* March, 43-50, 2004a.

[67] Kelly, J.D. Production modeling for multimodal operations. *Chemical Engineering Progress*, 44, 2004b.

[68] Kelly, J.D. Formulating Large-Scale Quantity-Quality Bilinear Data Reconciliation Problems. *Computer and Chemical Engineering*, 28 (3), 357-366, 2004c.

[69] Kelly, J.D. The Unit-Operation-Stock Superstructure (UOSS) and the Quantity-Logic-Quality Paradigm (QLQP) for Production Scheduling in the Process Industries, MISTA Conference Proceedings, 327, 2005.

[70] Kelly, J.D. Logistics: The Missing Link in Blend Scheduling Optimization, *Hydrocarbon Processioning*. June, 45-51, 2006.

[71] Kelly, J.D.; Zyngier, D. Continuously Improve the Performance of Planning and Scheduling Models with Parameter Feedback. *FOCAPO 2008 – Foundations of Computer Aided*: Boston, MA, June 2008.

[72] Kelly, J.D.; Mann, J.L. Crude-Oil Blend Scheduling: An Application with Multimillion Dollar Benefits: Part I. *Hydrocarbon Processing*, June, 47-53, 2003.

[73] Kelly, J.D.; Mann, J.L. Crude-Oil Blend Scheduling: An Application with Multimillion Dollar Benefits: Part II. *Hydrocarbon Processing*, July, 72-79, 2003.

[74] Kelly, J.D.; Zyngier, D. An Improved MILP Modeling of Sequence-Dependent Switchovers for Discrete-Time Scheduling Problems, *Industrial & Engineering Chemistry Research*, 46, 4964, 2007.

[75] Kelly, J.D.; Zyngier, D. Hierarchical Decomposition Heuristic for Scheduling: Coordinated Reasoning for Decentralized and Distributed Decision-Making Problems. *Computer and Chemical Engineering*, 32, 2684–2705, 2008.

[76] Kelly, J.D., Zyngier, D. Unit Operation Nonlinear Modeling for Planning and Scheduling Applications. K.C. Furnam et. al. (eds.), Optimization and Analytics in the Oil & Gas Industries, Springer Science. 2015.

[77] Kopanos, G.M.; Kyriakidis, T.S.; Georgiadis, M.C. New continuous-time and discrete-time mathematical formulations for resource-constrained project scheduling problems. *Computer and Chemical Engineering*, 68: 96-106, 2014.

[78] Kruger, C.J.C. Constrained Cubic Spline Interpolation for Chemical Engineering Applications. www.korf.co.uk./spline.pdf (accessed Jan 15, 2014).

[79] Leontief, W.W. *Input-Output Economics*. 2nd ed., New York: Oxford University Press, 1986.

[80] Geddes, R.L. A General Index of Fractional Distillation Power for Hydrocarbon Mixtures. *AIChE Journal*, 4, 389-392, 1958.

[81] Guillén, G.; Mele, F.D.; Bagajewicz, M.J.; Espuña, A.; Puigjaner, L. Multiobjective Supply Chain Design under Uncertainty. *Chemical Engineering Science*, 60, 1535-1553, 2005.

[82] Land, A.H.; Doig, A. G. An Automatic Method of Solving Discrete Programming Problems. *Econometrica*, 28(3), 497–520, 1960.

[83] Li, W.; Hui C.; Li, A. Integrating CDU, FCC and Blending Models into Refinery Planning. *Computer and Chemical Engineering*, 29, 2010-2028, 2005.

[84] Liu, M., and Sahinidis, N. V. Long range Planning in the Process Industries: a Projection Approach. *Computers & Operational Research*, 23(3), 237–253, 1996.

[85] Maravelias, C.T.; Sung, C. Integration of Production Planning and Scheduling: Overview, Challenges and Opportunities. *Computer and Chemical Engineering*, 33, 1919-1930, 2008.

[86] Mahalec, V.; Sanchez, Y. Inferential Monitoring and Optimization of Crude Separation Units via Hybrid Models. *Computer and Chemical Engineering*, 45, 15-26, 2012.

[87] Méndez, C.A.; Grossmann, I.E.; Harjunkoski, I.; Kabore, P. A Simultaneous Optimization Approach for Off-Line Blending and Scheduling of Oil-Refinery Operations. *Computers & Chemical Engineering*, 30, 614–634, 2006.

[88] Mejdell, T.; Skogestad, S. Estimation of Distillation Compositions from Multiple Temperature Measurements Using Partial – Least – Squares Regression. *Industrial & Engineering Chemistry Research*, 30, 2543–2555, 1991.

[89] Mitra, S.; Garcia-Herreros, P.; Grossmann I.E. A Novel Cross-decomposition Multi-cut Scheme for Two-Stage Stochastic Programming. *Computer Aided Chemical Engineering*, 33, 241-246, 2014.

[90] Mitra, S.; Pinto, J.M.; Grossmann, I.E. Optimal Multi-Scale Capacity Planning for Power-Intensive Continuous Processes Under Time-Sensitive Electricity Prices and Demand Uncertainty. Part I: Modeling. *Computer and Chemical Engineering*, 65, 89-101, 2014.

[91] Mitra, S.; Pinto, J.M.; Grossmann, I.E. Optimal Multi-Scale Capacity Planning for Power-Intensive Continuous Processes Under Time-Sensitive Electricity Prices and Demand Uncertainty. Part I: Enhanced hybrid bi-level decomposition. *Computer and Chemical Engineering*, 65, 102-111, 2014.

[92] Moro, L.F.L.; Zanin, A.C.; Pinto, J.M. A Planning Model for Refinery Diesel Production. *Computer and Chemical Engineering*, 22(1), 1039-1042, 1998.

[93] Mouret, S.; Grossmann, I.E.; Pestiaux, P. A Novel Priority-Slot Based Continuous-Time Formulation for Crude-Oil Scheduling Problems. *Industrial & Engineering Chemistry Research*, 48, 8515-8528, 2009.

[94] MPF. Diesel and Gasoline Agreement for Sulfur Reduction Home Page. http://s.conjur.com.br/dl/acordo_diesel.pdf (Access Apr 14, 2013).

[95] National Agency of Petroleum, Natural Gas and Biofuels (ANP). Brazilian Annual Oil Statistic 2012 Home Page. http://www.anp.gov.br/?pg=62463&m=&t1=&t2=&t3=&t4=&ar=&ps=&cachebust=1371479937518 (Access Nov 30, 2013).

[96] Neiro, S.M.S.; Pinto, J.M. A General Modeling Framework for the Operational Planning the Petroleum Supply Chain. *Computer and Chemical Engineering*, 28, 871-896.

[97] Nemhauser, G.L.; Wolsey, L.A. *Integer and Combinatorial Optimization*. NewYork: Wiley, 1988.

[98] O Globo. Economy: Brazilian Center of Infrastructure Data. http://oglobo.globo.com/economia/petrobras-acumula-perda-de-22-bi-com-venda-de-combustiveis-diz-cbie-9041250 (Access Nov 30, 2013).

[99] Papageorgiou, L.G. Supply Chain Optimization for the Process Industries: Advances and Opportunities. *Computer and Chemical Engineering*, 33, 1931-1938, 2009.

[100] Pelham, R.; Pharris, C. Refinery operation and control: a future vision. *Hydrocarbon Processing*, 75(7), 89-94, 1996.

[101] Perrisé, J.B. Oil-Refining Evolution in Brazil. M.D. Thesis, State University of Rio de Janeiro, August 2007.

[102] PETROBRAS Petróleo Brasileiro. Business Plan 2009-2013. Rio de Janeiro, January 2009.

[103] PETROBRAS, Petróleo Brasileiro. Our History. Available on line at http:// http://www.petrobras.com.br/pt/quem-somos/nossa-historia (Access Apr 10, 2013a).

[104] PETROBRAS Petróleo Brasilieiro. Business Plan 2013–2017. Rio de Janeiro, March 2013b.

[105] PETROBRAS Petróleo Brasileiro. Esclarecimentos sobre metodologia de precificação. Available on line at http://fatosedados.blogspetrobras.com.br/2013/10/30/esclarecimento-sobre-metodologia-de-precificacao (Access Oct 30, 2013c).

[106] PETROBRAS Petróleo Brasilieiro. Products: Price Composition Home Page. http://www.petrobras.com.br/pt/produtos/composicao-de-precos (Access Nov 30, 2013d).

[107] PETROBRAS Petróleo Brasilieiro. Business Plan 2014-2018; Rio de Janeiro, February 2014a.

[108] PETROBRAS Petróleo Brasilieiro. Investidor Relationship Home Page. http://www.investidorpetrobras.com.br/pt/home.htm (Access Mar 5, 2014b).

[109] Pinto, J.M.. Challenges and perspectives on the chemical industry in Brazil. *AIChE*, Global Outlook, 57-61. 2011

[110] Pinto, J.M.; Joly, M.; Moro, L.F.L. Planning and Scheduling Models for Refinery Operations. *Computer and Chemical Engineering*, 24(9-10), 2259–2276, 2000.

[111] Pinedo M.; Chao, X. Operations scheduling and applications in manufacturing, algorithms and systems. Prentice Hall: New York, Second Edition, 1999.

[112] Pochet, Y., Wolsey, L.A. *Production Planning by Mixed Integer Programming*. New York: Springer, 2006.

[113] Raman, R.; Grossmann, I.E. Modeling and Computational Techniques for Logic Based Integer Programming. *Computer and Chemical Engineering*, 18, 563-578, 1994.

[114] Reklaitis, G.V. Overview of Planning and Scheduling Technologies. *Latin American Applied Research*, 30, 285, 2000.

[115] Refinery Technology Petroleum Chemicals Division. The Ethyl Technique of Octane Prediction. Ethyl Corporation. October, 1981.

[116] Riazi, M.R. Characterization and Properties of Petroleum Fractions. American Society for Testing and Materials, 2005.

[117] Riazi, M.R.; Daubert, T.E. Analytical Correlations Interconvert Distillation Curve Types. *Oil & Gas Journal*, 84, 50-57, 1986.

[118] Ryu, J.; Pistikopoulos, E. Design and operation of enterprise-wide process network using operation policies. *Industrial and Engineering Chemistry Research*, 44, 2174-2182, 2005.

[119] Sahebi, H.; Mickel, S.; Asheyeri, J. Strategic and Tactical Mathematical Programming Models within the Crude Oil Supply Chain Context—A Review. *Computer and Chemical Engineering*, 13(9), 1049-1063, 2014.

[120] Sahinidis, N.V.; Grossmann, I.E.; Fornari, R.E.; Chathrathi, M., Optimization Model for Long Range Planning in the Chemical Industry. *Computer and Chemical Engineering*, 13(9), 1049-1063, 1989.

[121] Sahinidis, N. BARON: A General Purpose Global Optimization Software Package. *Journal of Global Optimization*. 8(2), 201–205, 1996.

[122] Shah, N. Process industry supply chains: advances and challenges. Computers and *Computer and Chemical Engineering*, 29, 1225-1235, 2005.

[123] Shah, N. Pharmaceutical Supply Chains: Key Issues and Strategies for Optimisation. *Computer and Chemical Engineering*, 28, 929–941, 2004.

[124] Shapiro, J.F. *Modeling the Supply Chain*. Duxbury Press: New York, 2001.

[125] Shapiro, J.F. Challenges of Strategic Supply Chain Planning and Modeling. *Computer and Chemical Engineering*, 28, 855–861, 2004.

[126] Sousa, R.; Shah, N.; Papageorgiou, L.G. Supply Chain Design and Multilevel Planning - An Industrial Case. *Computers & Chemical Engineering*, 32, 2643–2663, 2008.

[127] Squire, W.; Trapp, G. Using Complex Variables to Estimate Derivatives of Real Functions, *SIAM Journal*, 40(1), 110-112, 1998.

[128] Stadtler, H. Supply Chain Management and Advanced Planning—Basics, Overview and Challenges. *European Journal of Operational Research*, 163, 575, 2005.

[129] Symonds, G. *Linear Programming: The Solution of Refinery Problems*. Esso Standard Oil Company: New York, NY, 1955.

[130] Tavares, M.E.E.; Szklo, A.S.; Machado, G.V.; Schaeffer, R.; Mariano, J.B.; Sala, J.F. Oil refining expansion criteria for Brazil. *Energy Policy*, 34, 3027-3040, 2006.

[131] Trade Economics. Brazilian Interest Rate. http://www.tradingeconomics.com/brazil/interest-rate (Access Nov 30, 2013).

[132] UNICA. Sugar Cane Industry Union. http://www.unicadata.com.br/preco-ao-produtor.php?idMn=42&tipoHistorico=7&acao=visualizar&idTabela=1505&produto=Anhydrous+Fuel+Ethanol&frequencia=Monthly&estado=S%C3%A3o+Paulo (Access Nov 30, 2013).

[133] Van den Heever, S.; Grossmann, I.E. Disjunctive Multi-period Optimization Methods for Design and Planning of Chemical Process Systems. *Computer and Chemical Engineering*, 23, 1075-1095,1999.

[134] Varma, V.A.; Reklaitis, G.V.; Blau, G.E.; Pekny, J.F. Enterprise-wide Modeling & Optimisation—An Overview of Emerging Research Challenges and Opportunities. *Computer and Chemical Engineering*, 31, 692, 2007.

[135] Viswanathan J.; Grossmann, I.E. A combined Penalty Function and Outer Approximation Method for MINLP Optimization, *Computer and Chemical Engineering*, 14, 769–782, 1990.

[136] Wächter, A.; Biegler, L.T. On the Implementation of an Interior-Point Filter Line-Search Algorithm for Large-Scale Nonlinear Programming. *Mathematical Programming*. 106 (1), 25-57. 2006.

[137] Watkins, R.N. *Petroleum Refinery Distillation.* 2nd Edition, Gulf Publishing Co.: Houton, TX, 1979.

[138] Westerlund, T., Pettersson, F. An Extended Cutting Plane Method for Solving Convex MINLP Problems. *Computers & Chemical Engineering*, 19(Suppl.), S131–S136, 1995.

[139] Winston, W.L. Operations research: applications and algorithms. Wadsworth Publishing Company for Duxbury Press, Belmont, California, CA; 1994.

[140] Wiesemann, W.; Kuhn, D.; Rustem, B. Maximizing the Net Present Value of a Project under Uncertainty. *European Journal of Operational Research*, 202, 356-367, 2010.

[141] Wright, C.J.; Gallun, R.A. *Fundamentals of Oil and Gas Accounting*. Pennwell Books 5th edition, 2008.

[142] Wolsey, L.A. *Integer programming*. Wiley-Interscience, New York, 1998.

[143] You, F.; Grossmann, I.E. Design of Responsive Supply Chains under Demand Uncertainty. *Computer and Chemical Engineering*, 32 (12), 2839–3274, 2008.

[144] You, F.; Grossmann, I. E.; Wassick, J. Multisite Capacity, Production, and Distribution Planning with Reactor Modifications: MILP Model, Bi-level Decomposition Algorithm versus Lagrangean Decomposition Scheme. *Industrial and Engineering Chemistry Research*, 50, 4831–4849, 2011.

[145] Zhang, J.; Kim, N-H.; Ladson, L. An Improved Successive Linear Programming Algorithm. *Management Science*, 31, 1312-1331, 1985.

[146] Zhang, J.; Zhu, X.X.; Towler, G.P. A Level-by-Level Debottlenecking Approach in Refinery Operation. *Industrial & Engineering Chemistry Research*, 40, 1528-1540, 2001.

[147] Zyngier, D.; Kelly, J.D. Multi-Product Inventory Logistics Modeling in the Process Industries. *Optimization and Logistics Challenges in the Enterprise*. Springer Optimization and Its Applications, 30, Part 1, p. 61-95, DOI: 10.1007/978-0-387-88617-6_2. 2009.

[148] Zyngier, D.; Kelly, J.D. UOPSS: A New Paradigm for Modeling Production Planning and Scheduling Systems. ESCAPE 22, June, 2012.